



National Library
of Canada

Acquisitions and
Bibliographic Services Branch

395 Wellington Street
Ottawa, Ontario
K1A 0N4

Bibliothèque nationale
du Canada

Direction des acquisitions et
des services bibliographiques

395, rue Wellington
Ottawa (Ontario)
K1A 0N4

You file - Votre référence

Quelque - Notre référence

NOTICE

AVIS

The quality of this microform is heavily dependent upon the quality of the original thesis submitted for microfilming. Every effort has been made to ensure the highest quality of reproduction possible.

If pages are missing, contact the university which granted the degree.

Some pages may have indistinct print especially if the original pages were typed with a poor typewriter ribbon or if the university sent us an inferior photocopy.

Reproduction in full or in part of this microform is governed by the Canadian Copyright Act, R.S.C. 1970, c. C-30, and subsequent amendments.

La qualité de cette microforme dépend grandement de la qualité de la thèse soumise au microfilmage. Nous avons tout fait pour assurer une qualité supérieure de reproduction.

S'il manque des pages, veuillez communiquer avec l'université qui a conféré le grade.

La qualité d'impression de certaines pages peut laisser à désirer, surtout si les pages originales ont été dactylographiées à l'aide d'un ruban usé ou si l'université nous a fait parvenir une photocopie de qualité inférieure.

La reproduction, même partielle, de cette microforme est soumise à la Loi canadienne sur le droit d'auteur, SRC 1970, c. C-30, et ses amendements subséquents.

THE UNIVERSITY OF ALBERTA

**TRANSMISSION OF HIGH-STRENGTH CONCRETE COLUMN LOADS
THROUGH CONCRETE SLABS**

BY

CARLOS EMILIO OSPINA



**A THESIS
SUBMITTED TO THE FACULTY OF GRADUATE STUDIES AND RESEARCH IN
PARTIAL FULFILLMENT OF THE REQUIREMENTS FOR THE DEGREE OF
MASTER OF SCIENCE
IN STRUCTURAL ENGINEERING**

DEPARTMENT OF CIVIL ENGINEERING

Edmonton, Alberta

Spring 1996



National Library
of Canada

Acquisitions and
Bibliographic Services Branch

395 Wellington Street
Ottawa, Ontario
K1A 0N4

Bibliothèque nationale
du Canada

Direction des acquisitions et
des services bibliographiques

395, rue Wellington
Ottawa (Ontario)
K1A 0N4

Veuillez noter : Votre référence

Veuillez noter : Votre référence

The author has granted an irrevocable non-exclusive licence allowing the National Library of Canada to reproduce, loan, distribute or sell copies of his/her thesis by any means and in any form or format, making this thesis available to interested persons.

L'auteur a accordé une licence irrévocable et non exclusive permettant à la Bibliothèque nationale du Canada de reproduire, prêter, distribuer ou vendre des copies de sa thèse de quelque manière et sous quelque forme que ce soit pour mettre des exemplaires de cette thèse à la disposition des personnes intéressées.

The author retains ownership of the copyright in his/her thesis. Neither the thesis nor substantial extracts from it may be printed or otherwise reproduced without his/her permission.

L'auteur conserve la propriété du droit d'auteur qui protège sa thèse. Ni la thèse ni des extraits substantiels de celle-ci ne doivent être imprimés ou autrement reproduits sans son autorisation.

ISBN 0-612-10743-4

Canada

UNIVERSITY OF ALBERTA

Library Release Form

NAME OF AUTHOR: Carlos Emilio Ospina

TITLE OF THESIS: Transmission of High-Strength Concrete Column Loads through
Concrete Slabs

DEGREE: Master of Science

YEAR OF DEGREE GRANTED: 1996

Permission is hereby granted to the University of Alberta Library to reproduce single copies of this thesis and to lend or sell such copies for private, scholarly or scientific research purposes only.

The author reserves all other publication and other rights in association with the copyright in the thesis, and except as hereinbefore provided, neither the thesis nor any substantial portion thereof may be printed or otherwise reproduced in any material form whatever without the author's prior written permission.



Carlos Emilio Ospina
P.O. Box 60101
Edmonton, AB T6G 2S4
Canada

Date: Dec. 13, 1995

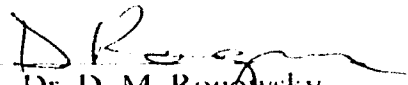
UNIVERSITY OF ALBERTA

FACULTY OF GRADUATE STUDIES AND RESEARCH

The undersigned certify that they have read, and recommend to the Faculty of Graduate Studies and Research for acceptance, a thesis entitled Transmission of High-Strength Concrete Column Loads through Concrete Slabs submitted by Carlos Emilio Ospina in partial fulfillment of the requirements for the degree of Master of Science in Structural Engineering.



Dr. S. D. B. Alexander



Dr. D. M. Rogovsky



Dr. M/G. Faulkner

Date: Dec. 13, 1995

**To Rochy, Coqui, Luces, MBOG, JCOG and Lia
for his endless patience and unrestricted support**

ABSTRACT

For economic reasons columns in multistorey reinforced concrete buildings are built with high-strength concrete whereas slabs are built with concrete of weaker strength. In the preferred method of construction, the columns are cast up to the slab soffit and the slab concrete is cast continuous through the columns. As a result, the axial load that is transmitted from the column above the floor must pass through a layer of weaker concrete before reaching the column below the floor. A design question arises as to what compressive strength should be used in the design of the column. Current North American code provisions evaluating the effective strength of columns intersected by concrete slabs are based on tests on slab-column connection specimens subjected to column loads but without slab loads. This consideration may lead to unsafe designs. It is imperative to evaluate the effect that both the slab loads and the column and slab dimensions may have on the axial load capacity of slab-column connections and to develop design guidelines which account for these two effects.

ACKNOWLEDGMENTS

The author would like to express his sincere gratitude to his research supervisor, Dr. Scott D. B. Alexander for his priceless guidance and support throughout this research work. His patience, interest and innovative suggestions are deeply appreciated.

The author gratefully acknowledges the financial assistance received from the Concrete Canada Network through Dr. Scott D. B. Alexander and Dr. James G. MacGregor. The financial support received from the Department of Civil Engineering of the University of Alberta is greatly appreciated. The author also wishes to thank Dr. D. J. Laurie Kennedy for his exemplary counsel throughout the academic program.

The impeccable technical assistance and always kind cooperation of Richard Helfrich and Larry Burden at the I. F. Morrison Structural Engineering Laboratory is greatly appreciated. Thanks are extensive to Dr. Hisham Ibrahim and Chris Jordan for the testing of the edge sandwich plates.

Likewise the Pulp Fiction script, all of the acknowledgments to my family and friends are stated randomly in order to avoid hierarchical mistakes. I do not know if Canadian hockey players behave the way I will but Colombian cyclists thank everyone just after finishing a bicycle race. I am not an exception to this rule.

Two and a half years ago the idea of coming to Canada looked like an utopia for me. Right after the sun threatened to set forever a friend of mine offered me the sort of support believed by many to be extinct: The unselfish support of a friend! I am endlessly thankful to Miguel-Angel Pando for his support and tolerance (You don't know me).

To you Mother, I would like to express my veneration. Words escape me to say how much I admire your courage and inner strength. I will always thank your love and kindness. To you Father, I have no words to express my acknowledgments for your unbelievable support and encouragement. I want you both to know that you are my pride.

I would like to express my affection to you Lucas. "Mild-mannered" CarlosE feels very proud of you. I would also like to thank Maria Beatriz and Juan Camilo for their sincere support and hard-to-believe patience. Kai Kai Kai! Glomm! Ta pocketa pocketa! Tzoing!

I would like to dedicate this thesis to you Lia. God bless your love and that of Licho, Mary, Enri and all of their children towards me (including especially the guy with the 350 mm long chest scar).

And at last but not the least, I would like to thank my family and to express my gratitude to Andrew Boucher (Emerald and cleaning expert), Hector "You are very good" GuMierrez, Leo Piccolli, Marccello Marelli, Selena, Jurgen Villamilk, Juancho "Alligator" Sanchez and my pals in Structures for their unforgettable companion during the Edmontonian years.

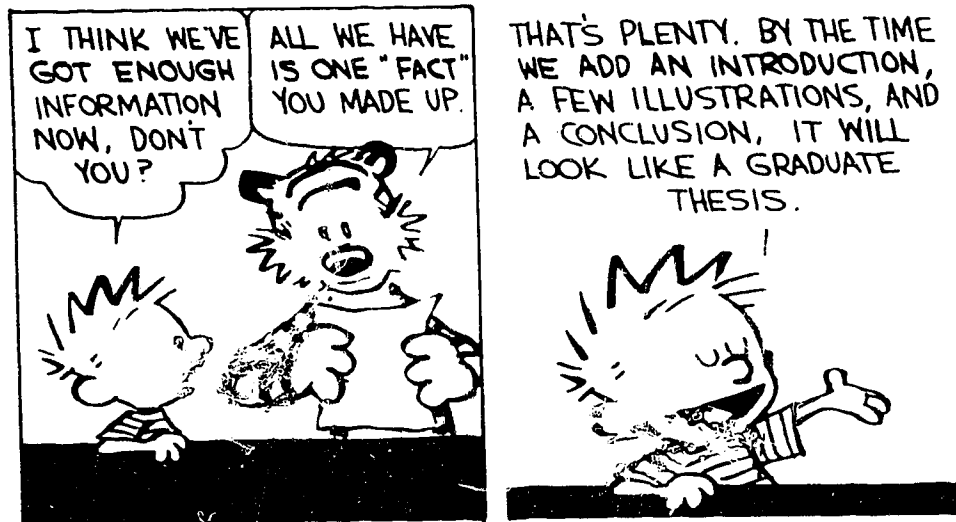


TABLE OF CONTENTS

Chapter	Page
1. Introduction	1
1.1 Description of the problem	1
1.2 Objectives and Scope	2
1.3 Organization of the Thesis	2
2. Background	4
2.1 Introduction	4
2.2 Literature Survey	4
2.2.1 General	4
2.2.2 Chronological report of published test results and Code provisions	5
2.2.2.1 Bianchini, Woods and Kesler (1960)	5
2.2.2.2 CSA A23.3-M84 and ACI 318-89	6
2.2.2.3 Gamble and Klinar (1991)	7
2.2.2.4 Shu and Hawkins (1992)	9
2.2.2.5 Kayani (1992)	10
2.2.2.6 CSA A23.3-94	11
2.3 Discussion of test results and code design provisions	12
2.3.1 Effect of slab loading	12
2.3.2 Effect of the aspect ratio h/c	14
2.3.3 Discussion of other provisions found in the Codes	15
3. Experimental Program	23
3.1 Objectives of Testing	23
3.2 Experimental Program	23
3.3 Design of the experiments	23
3.3.1 Series A specimens (Interior sandwich plates)	23
3.3.2 Series B specimens (Interior sandwich plates)	24

3.3.2.1	Analysis of prototype connections and test specimens	25
3.3.3	Series C specimens (Edge sandwich plates)	26
3.3.4	Series D specimens (Sandwich columns)	26
3.4	Materials	27
3.4.1	High-strength concrete	27
3.4.2	Normal-strength concrete	27
3.4.3	Reinforcement	28
3.5	Fabrication of specimens	29
3.5.1	Mixing, casting and curing procedures	29
3.5.1.1	Interior and edge sandwich plates	29
3.5.1.2	Sandwich column specimens	29
3.6	Testing	29
3.6.1	Test set-up	29
3.6.1.1	Sandwich plate specimens	29
3.6.1.2	Sandwich column specimens	30
3.6.2	Instrumentation	30
3.6.2.1	Linear variable-differential transformers (LVDT's)	30
3.6.2.2	Strain gauges	31
3.6.2.3	Load Cells	31
3.6.3	Calculation of the column strain through the slab thickness	31
3.6.4	Test Procedure	32
3.6.4.1	Interior and edge sandwich plate specimens	32
3.6.4.2	Sandwich column specimens	33
4.	Test results and Observations	56
4.1	General	56
4.2	General behaviour of the test specimens	56
4.2.1	Interior sandwich plate specimens	57
4.2.1.1	Interior specimens with loaded slabs	57
4.2.1.2	Interior specimens with unloaded slabs	58

4.2.2	Edge sandwich plate specimens	59
4.2.2.1	Edge specimens with loaded slabs	59
4.2.2.2	Edge specimens with unloaded slabs	60
4.2.3	Sandwich column specimens	61
4.3	Effect of slab loading	61
4.4	Effect of the h/c ratio	63
4.5	Effect of column rectangularity	63
4.6	Effect of high-strength concrete core at the joint region	63
5.	Effect of test variables	82
5.1	General	82
5.2	Effect of slab loading	82
5.3	Effect of the h/c ratio	84
5.4	Effect of column rectangularity	85
5.5	Effect of high-strength concrete core at the joint region	86
5.6	Evaluation of the effective strength, f'_{ce} , in light of CSA A23.3-94	86
6.	Proposed design provisions	98
6.1	General	98
6.2	Design provisions	98
6.2.1	Interior columns	98
6.2.2	Edge Columns	99
6.2.3	Corner columns and unconfined joints	99
7.	Summary, Conclusions and Recommendations	103
7.1	Summary	103
7.2	Conclusions	104
7.2.1	Conclusions from testing	104
7.2.2	Conclusions regarding code provisions	104
7.3	Recommendations	104

List of References	106
Appendix A	108
Appendix B	124

LIST OF TABLES

Table		Page
2.1	Description of test specimens found in the literature	17
3.1	Description of Test specimens	34
3.2	Dimensions and analysis results of specimen and prototype slabs	35
3.3	Slab Loads	36
3.4	Concrete Mix proportions	37
3.5	Properties of reinforcement steel	37
4.1	Test results	65
5.1	Evaluation of the effective compressive strength in accordance to CSA A23.3-94	89
6.1	Ratios of test to predicted column effective strength	100

LIST OF FIGURES

Figure	Page
2.1 Interior sandwich plate specimen	18
2.2 Edge sandwich plate specimen	18
2.3 Corner sandwich plate specimen	19
2.4 Sandwich column specimen	19
2.5 Stresses at joint region (specimens with unloaded slabs)	20
2.6 Stresses at joint region (specimens with loaded slabs)	20
2.7 Existing design provisions for interior columns	21
2.8 Existing design provisions for edge columns	21
2.9 Existing design provisions for corner columns	22
3.1 Geometry of interior sandwich plate specimens	38
3.2 Geometry of edge sandwich plate specimens	39
3.3 Geometry of sandwich column specimens	40
3.4 Prototype flat plate structure (series B specimens)	40
3.5 Flexural moments from SAP90 analyses ($h/c=0.60$)	41
3.6 Flexural Moments from SAP90 analyses ($h/c=1.00$)	41
3.7 Prototype flat plate structure (series C specimens)	42
3.8 Column reinforcement layout (series A specimens)	42
3.9 Column reinforcement and strain gauge layout (series B specimens)	43
3.10 Column reinforcement layout (series C specimens)	43
3.11 Column reinforcement and strain gauge layout (series D specimens)	44
3.12 Slab reinforcement and strain gauge layouts (series A specimens)	45
3.13 Slab reinforcement and strain gauge layouts (series B specimens)	46
3.14 Slab reinforcement and strain gauge layouts (series C specimens)	47
3.15 Stress-strain curve for high-strength concrete cylinder	48
3.16 Stress-strain curve for normal-strength concrete cylinder	48
3.17 Stress-strain curve for No. 15 M bar	49
3.18 Stress-strain curve for No. 10 M bar	49

3.19	Test set-up for interior sandwich plate specimens	50
3.20	Test set-up for edge sandwich plate specimens	50
3.21	Test set-up for sandwich column specimens	51
3.22	LVDT set-up for series A specimens	52
3.23	LVDT set-up for series B square column specimens	52
3.24	LVDT set-up for series B rectangular column specimens	53
3.25	LVDT set-up for series C specimens	53
3.26	LVDT set-up for series D specimens	54
3.27	Parameters to calculate the column strain through the slab thickness	54
3.28	Relationship between the column strain through the slab thickness and the LVDT strain readings	55
4.1	Schematic stress-strain curve (interior plates with loaded slabs)	66
4.2	Schematic stress-strain curve (interior plates with unloaded slabs)	66
4.3	Schematic stress-strain curve (edge plates)	67
4.4	Schematic stress-strain curve (sandwich columns)	67
4.5	Testing of interior sandwich plate with slab loads ($h/c=1.0$)	68
4.6	Testing of interior sandwich plate with slab loads ($h/c=0.6$)	68
4.7	Cracking pattern (Specimen B-1)	69
4.8	Cracking pattern (Specimen B-2)	69
4.9	Square hoop behaviour of interior sandwich plate with unloaded slab	70
4.10	Deep beam behaviour of interior sandwich plate specimen with unloaded slab	70
4.11	Testing of interior sandwich plate without slab loads	71
4.12	Detail of specimen B-4 after failure	71
4.13	Cracking pattern (specimen B-4)	72
4.14	System of forces acting within an edge slab-column joint with slab loads	72
4.15	Testing of edge sandwich plate with slab loads	73
4.16	Cracking pattern (Specimen C2-C)	73
4.17	Testing of edge sandwich plate without slab loads	74
4.18	Cracking pattern (Specimen C2-A)	74
4.19	Testing of sandwich column specimens	75

4.20	Sandwich column specimens after testing	75
4.21	Cracking pattern (Specimen D-SC1)	76
4.22	Effect of slab loading (ISP)	77
4.23	Effect of slab loading (ISP)	77
4.24	Effect of slab loading (ESP)	78
4.25	Slab loading effect on joint transverse strain	78
4.26	Triaxial state of stresses at joint region (Interior plates with loaded slabs)	79
4.27	Triaxial state of stresses at joint region (Interior plates with unloaded slabs)	79
4.28	Effect of the h/c ratio (ISP)	80
4.29	Effect of the h/c ratio (SC)	80
4.30	Effect of column rectangularity	81
4.31	Effect of HSC core within joint region	81
5.1	Test results of interior sandwich plates	90
5.2	Test results of edge sandwich plates	90
5.3	Test results on sandwich columns	91
5.4	Tests of slab-unloaded interior plates	91
5.5	Tests of slab-unloaded edge sandwich plates	92
5.6	Slab load effect on interior joint strength	92
5.7	Slab load effect on edge joint strength	93
5.8	Effect of h/c on interior joint strength	93
5.9	Test results on corner and sandwich columns	94
5.10	Correction factors for cylinder and cube test	94
5.11	Comparison of tests on sandwich columns	95
5.12	Effect of column rectangularity (ISP)	95
5.13	Effect of HSC core on interior joint strength	96
5.14	Test results of ISP according to A23.3-94	96
5.15	Test results of ESP according to A23.3-94	97
5.16	Test results of sandwich and corner columns according to A23.3-94	97
6.1	Proposed design curves for interior columns	101

6.2	Design curves and test results	101
6.3	Proposed design curve for edge columns	102
6.4	Proposed design curve for corner columns	102

NOTATION

A_g	Column gross area
A_{st}	Total area of column longitudinal reinforcement
c	Column dimension
CSP	Corner sandwich plate
ESP	Edge sandwich plate
f'_c	Specified compressive strength of concrete
f'_{cc}	Cylinder strength of column concrete at time of testing
f'_{cs}	Cylinder strength of slab concrete at time of testing
f_{ce}	Compressive stress applied to the column
f'_{ce}	Effective compressive strength of concrete in column
f_y	Yield strength of steel reinforcement
h	Slab or joint concrete thickness
ISP	Interior sandwich plate
m	Distance between the column threaded rods closer to the slab and the slab top and bottom levels
P_{col}	Applied column load
P_{ro}	Factored axial load resistance of a short tied column
P_{s1}	Slab load (applied to both interior and edge sandwich plates)
P_{s2}	Slab load (applied only to the edge sandwich plates)
SC	Sandwich column specimen
α_1	Ratio of average stress in rectangular compression block to the specified concrete compressive strength
ϵ_{col}	Column longitudinal strain outside the joint region
ϵ_{II}	Column longitudinal strain through slab thickness
ϵ_{mid}	Column longitudinal strain at specimen mid-height (includes contribution from ϵ_{col} and ϵ_{II})
ϕ_c	Resistance factor for concrete
ϕ_s	Resistance factor for steel reinforcing bars

ρ_{col}	Column flexural reinforcement ratio
ρ_{slab}	Slab flexural reinforcement ratio

1. INTRODUCTION

1.1 Description of the problem

In multistorey reinforced concrete building construction, significant economy may be achieved by building the columns with high-strength concrete and the floors with a concrete of lower strength. With an increase in concrete strength a column of smaller dimensions would carry the load that a larger normal-strength concrete column would sustain. A reduction in the column cross-sectional dimensions increases the amount of rentable space and is beneficial when architectural considerations restrict the size of the columns.

Use of concrete higher than 80 MPa in multistorey building columns is becoming prevalent in modern construction. For example, column concrete reaching 124 MPa was reported for the Pacific First Center building in Seattle (Randall and Foot (1992)). Column concrete strength of 96.5 MPa was used for the 58-storey Two Union Square building in Seattle (Howard and Leatham (1992)). Columns made of 82.7 MPa high-strength concrete were reported for the world's tallest structural concrete building -311 South Wacker Drive Tower- in Chicago. Column concrete of 117 MPa was reported by Moreno (1992) for the 31 storey 225 West Wacker Drive building, also in Chicago. Column strengths of 80 MPa have been reported for the Kuala Lumpur City Centre twin towers which at the time of completion will rank as the highest buildings in the world (CEB Bulletin d'Information No. 222, 1994).

In the construction of multistorey reinforced concrete buildings it has become accepted practice to cast the columns up to the bottom level of the slab they will support and then to cast the slab concrete continuous through the columns. Then, next storey columns are cast all the way up to the next floor level. This results in the slab concrete intersecting the high-strength concrete columns at each floor level. In other words, the axial load that is transmitted from the column above the floor must traverse a layer of weaker concrete before reaching the column immediately below the floor. A design question arises as to what compressive strength should be used in the design of the column.

Existing design provisions in the Canadian standard CSA A23.3-M84 (Clause 10.13) and in the American standard ACI 318-89 (Clause 10.13) are based on the experimental work carried out by Bianchini et al. in 1960. Test results reported by Bianchini et al. correspond to slab-column connection specimens wherein only column load was applied. There is a need to extend the work of Bianchini et al. for slab-column connection specimens subjected to both column and slab loading. It is also important to study the effect that column and slab dimensions may have on the column strength. Range of column strength should also be extended bearing in mind that column concrete strengths used in current practice greatly exceed those used three decades ago.

1.2 Objectives and Scope

In general, three design options are used to determine what compressive strength should be used to design a column intersected by concrete floors. The first consists of placing column concrete within the joint region and designing the connection based on the column concrete cylinder strength. According to the second provision, the design of the column may be based on the floor concrete strength with the addition of dowels or spirals, as required. The third guideline provides for a design equation to evaluate the effective strength of the slab portion of the column as a weighted average of the column and slab concrete cylinder strengths. Of these three design guidelines the first two are frequently adopted. Selection of any of these two design solutions may lead to a substantial increase in construction costs.

This investigation will mainly deal with the third design option. The primary objective of this research work is the development of design provisions to determine the effective strength of interior, edge and corner columns intersected by concrete slabs. Study of beam/slab-column connections is not considered in this investigation.

The main variables taken in this research program are the amount of slab loading applied to the specimens and the ratio of slab thickness to column width, h/c .

Two types of test specimens were adopted throughout the experimental program. The first type of specimen consisted of two high-strength reinforced concrete column stubs framing into a normal-strength concrete slab segment. These specimens modelled both interior and exterior slab-column connections. Specimen dimensions representative of both flat plate and flat slab systems were tested. Column loads were applied to all of the specimens. Different levels of slab loading were also applied.

The second type of specimen consisted of two high-strength reinforced concrete column stubs sandwiching a layer of normal strength concrete with same cross-sectional dimensions than the framing column ends. No segment of normal-strength concrete was cast around the joint. These specimens were subjected to column load only and were intended to study the behaviour of unconfined joints.

This experimental program reports column concrete compressive strengths similar to those reported in current building construction practice and higher than those presented by researchers in the past.

1.3 Organization of the Thesis

Chapter 2 presents a literature survey. It outlines the work reported by previous researchers and critically reviews their recommendations and existing design procedures. Chapter 3 presents a detailed description of the specimens tested throughout this experimental program. It also contains a description of the fabrication, instrumentation and testing procedures that were followed. Test results, observations and a comprehensive

description of the specimen behaviour are presented in chapter 4. In Chapter 5, the analysis of test results is presented by describing the effect that slab loading and the slab thickness-to-column width ratio, h/c , have on the strength of high-strength concrete columns intersected by normal-strength concrete slabs. Chapter 6 presents the development of design provisions for interior, edge and corner columns and finally, a summary and relevant conclusions of the research work are reported in chapter 7.

2. BACKGROUND

2.1 Introduction

In the design of interior columns intersected by weaker slab concrete, the joint concrete is assumed to be fully confined, and therefore capable of carrying compressive stresses in excess of the cylinder strength of the slab concrete. This increased strength, which can be defined as an *effective* compressive strength, results from the lateral restraint provided by stresses acting in the plane of the slab. It can be also inferred that restraint conditions will vary according to the type of connection, either interior, edge, or corner.

Past researchers (Bianchini et al. (1960), Gamble and Klinar (1991), Shu and Hawkins (1992), and Kayani (1992) have attributed this restraint to the reinforced concrete slab around the joint periphery and to the high-strength column ends framing into the joint. Their test observations lead to the following description of the joint behaviour.

Under the column compressive load the joint concrete shortens longitudinally and, due to Poisson's ratio, expands laterally. Across its height, the joint lateral expansion is resisted by the top and bottom slab reinforcing bars passing through the joint and by the surrounding floor concrete.

The joint is also restrained at the top and bottom levels by the column ends framing into the connection. The high-strength column ends restrain the joint concrete in the same way that testing machine platens restrain a concrete cylinder. In a concrete cylinder or core test, the compressive strength of the specimen depends on the specimen aspect ratio, defined as the ratio of the specimen height to its diameter (cylinder) or to its width (core). As this aspect ratio increases, the strength reduces due to the loss of lateral constraint of the ends of the specimen by the platens of the testing machine. In a connection specimen, the joint may be viewed as a concrete prism being pressed between two stronger column ends. It is likely that the aspect ratio of this concrete prism affects the compressive strength of the connection. This suggests that the aspect ratio of the connection, defined as the slab thickness relative to the column side, h/c , may be important in evaluating the effective compressive strength of columns intersected by concrete floors.

2.2 Literature Survey

2.2.1 General

Sketches of test specimens simulating slab-column connections tested in the past are presented in figures 2.1 through 2.4 .

A typical slab-column connection specimen consists of two high-strength concrete column stubs framing into a segment of slab concrete. Figures 2.1, 2.2 and 2.3 illustrate typical interior, edge and corner specimens. In this report, a slab-column connection specimen will be referred to as a *sandwich plate* since this type of connection may be viewed as a

concrete plate sandwiched by the column ends framing into the joint. When the intervening floor system consists of concrete slab and beams framing into the joint, the connection is referred to as a slab/beam-column connection. No test results nor discussion of research work carried out on specimens simulating this type of connection are reported in this thesis.

Figure 2.4 illustrates a typical *sandwich column* specimen. It consists of a high-strength column intersected by a layer of floor concrete at the column mid-height. No slab segment is cast around the joint faces. In effect, the slab concrete is cut off at the joint periphery.

2.2.2 Chronological report of published test results and Code provisions

2.2.2.1 Bianchini, Woods and Kesler (1960)

Bianchini et al. tested 29 sandwich plate specimens. Of these, there were 11 interior, 9 edge and 9 corner connections. They also tested 4 sandwich column specimens. The objectives of testing were to define how large a ratio of column concrete to slab concrete strength, f'_{cc}/f'_{cs} , could be tolerated without reducing the axial load capacity of high-strength columns, and to determine the effective column axial load capacity when this limiting value was exceeded.

The major variables were the ratio of the column concrete strength to the slab concrete strength, f'_{cc}/f'_{cs} , and the joint type, either interior, edge or corner. The slab thickness, column size and amount of column reinforcement were kept constant. Type and dimensions of the test specimens are reported in table 2.1 .

Column cylinder strengths, f'_{cc} , ranged between 15.8 to 56 MPa whereas slab cylinder strengths, f'_{cs} , varied from 8.8 to 24.8 MPa. For the sandwich plate specimens, columns were longitudinally reinforced with 4 No. 6 deformed bars and with No. 2 stirrups spaced 20 mm (8 in) apart. Slabs were reinforced at top and bottom with No. 4 deformed bars. Spacing of this reinforcement varied according to the type of connection being examined. Slab reinforcement ratios in the sandwich plate specimens varied approximately from 0.67 to 0.74 %. The steel yielding strength ranged from 295 MPa to 323 MPa. Sandwich columns were reinforced with 4 No. 6 deformed bars with No. 2 ties spaced at 200 mm. The yielding strength of the steel reinforcement ranged from 295 MPa to 323 MPa. This amount of reinforcement was also kept constant. Testing age of specimens was set at 28 days. Load was applied only to the columns. Duration of the tests ranged between 1.5 to 2 hours.

For the interior specimens, cracking started on the vertical face of the slab at mid-edge and progressed inwards to the column, directly over the slab reinforcement. Then, cracks formed around the slab-column contact surface. Finally, cracks formed in the columns above and below the slab. Interior specimens failed either on the top or the bottom column stubs.

For the edge and corner specimens, vertical cracks formed first in the visible face (or faces) of the joint. Then, cracks formed in the slab top and bottom levels around the column. Cracks then extended towards the slab edges, in line with the slab reinforcement. Failure occurred either in the visible face (or faces) of the joint or in the top or bottom column stubs.

For the sandwich columns, the first cracks were vertical splitting cracks in the sandwiched concrete joint. Failure occurred later at the joint region.

Bianchini et al. reported their test results by plotting the ratio of the maximum effective compressive strength to the floor concrete strength, f'_{ce}/f'_{cs} , against the ratio of the column concrete strength to the floor concrete strength, f'_{cc}/f'_{cs} . The term f'_{cc} represents the top or bottom column stub strength, whichever is lower.

Bianchini et al. calculated the joint effective compressive strength from the ACI code design equation for short tied columns.

$$P_o = 0.85 f'_c (A_g - A_{st}) + f_y A_{st} \quad [2.1]$$

Rearranging terms, and replacing the f'_c term by f'_{ce} yields

$$f'_{ce} = \frac{P_o - f_y A_{st}}{0.85 (A_g - A_{st})} \quad [2.2]$$

where $P_o = P_{col}$

Failure of the different test specimens was found to be dependent of the ratio of the column strength to the slab strength, f'_{cc}/f'_{cs} . They concluded that under certain ratios, the presence of the weaker-concrete slab may reduce the axial compressive strength of the column. For interior columns, this critical ratio was found to be equal to 1.5 . For edge and corner specimens, the ratio was found to be 1.4 .

When exceeding these ratios Bianchini et al. presented the following design recommendations to evaluate the column effective compressive strength. For interior connections they concluded that 75 percent of the column strength may be effective in sustaining the column load. For edge and corner columns, no significant benefits may be obtained by increasing the column strength beyond 1.4 times the floor strength.

2.2.2.2 CSA A23.3-M84 and ACI 318-89

Both the American and the previous edition of the Canadian code use the test results by Bianchini et al. as the background of their design provisions. Both codes present some guidelines for the design of columns intersected by floors built with weaker-strength concrete.

Design provisions establish that when the column concrete strength does not exceed by more than 40% the slab concrete strength, the design of the connection is based on the column concrete strength. When this differential is exceeded, three solutions are presented:

The first refers to the construction procedure of *puddling* in which column concrete is placed in the slab surrounding the joint. Since both concretes are cast at the same time, special care must be taken in order to avoid placement of the weaker concrete within the joint region. The top surface of the puddled column concrete must extend at least 600 mm (2 ft.) from the column face. Proper vibration of the column and slab concretes should be accomplished to guarantee an optimum integration between both materials.

The second provision states that the axial load capacity of interior, edge or corner columns may be calculated based on the lower intervening concrete strength (usually that of the slab) following the addition of vertical dowels or spirals to the connection. This provision is given as follows.

$$\frac{f'_{cc}}{f'_{cs}} > 1.4 ; f'_{ce} = f'_{cs} \quad [2.3]$$

The third design recommendation provides for the calculation of the column effective strength as a weighted average of both column and slab concrete strengths. Use of this equation is only applicable to interior slab or slab/beam column connections and is given as follows.

$$\frac{f'_{cc}}{f'_{cs}} > 1.4 ; f'_{ce} = 0.35 f'_{cs} + 0.75 f'_{cc} \quad [2.4]$$

2.2.2.3 Gamble and Klinar (1991)

Gamble and Klinar tested 6 edge and 6 interior sandwich plate specimens. Dimensions of test specimens are presented in table 2.1 . Recognizing the use of higher concrete and steel reinforcement strengths than those used by Bianchini et al., the differentials between the column and the slab concrete strength, f'_{cc}/f'_{cs} , were extended.

Major parameters involved in the experimental program were the type of specimen and the ratio of the column compressive strength to the slab compressive strength, f'_{cc}/f'_{cs} .

Column concrete strengths ranged between 72.4 and 104.8 MPa. Slab concrete varied from 15.9 to 45.5 MPa. 3/4" aggregate was used for manufacturing the slab concrete. Specimens were tested at ages between 61 to 157 days old. The amount of column

reinforcement was held constant. 4 No. 6 deformed bars were placed for this purpose. Transverse reinforcement for the columns was also kept constant with 1/4 in. stirrups at 250 mm spaces. No. 4 deformed bars were placed as the slab top reinforcement. Only one specimen (edge type) had No. 3 bars at the top running perpendicular to the slab edge. Spacing of the top slab rebar varied. Bottom reinforcement, if any, limited to 2 No. 4 bars passing through the joint in each direction. Slab flexural reinforcement ratio varied approximately from 1.11 to 1.23 % for the interior specimens and from 0.57 to 1.38 % for the edge specimens. Yielding strength of the column reinforcing bars was 486 MPa. Slab reinforcement yielding strength varied from 500 MPa (No. 4 bars) to 533 MPa (No. 3 bars).

Load was applied only to the column. Strain measurements were taken by means of electrical resistance foil type strain gauges. These were attached to the column and the slab rebar. Column gauges were attached at the joint mid-height and at levels above and below the concrete slab. Slab gauges were attached to the top reinforcing bars passing through the joint about 50 mm outside the column.

For the interior specimens, cracks formed in the slab near the column and radiated toward the slab boundaries. Because the slabs were reinforced with more top steel than bottom steel, the slab underside was pushed out more than the top, resulting in the slab curling upwards. At failure, cracks extended into the lower column stub and the specimen failed explosively.

For the edge specimens, vertical cracks formed first on the free face of the joint. Next, cracks appeared in the slab along the outline of the column. Vertical splitting cracks then formed in the columns. Finally, the specimen failed at the joint region, with the joint concrete at the free face spalling off and the column reinforcement buckling at that location. These specimens also failed explosively.

Test results are reported in a similar way to that used by Bianchini et al. An important conclusion of Gamble and Kliner is that the ratio f'_{cc}/f'_{cs} appears to be general across the range of strengths that were tested. This means that similar test results for a connection specimen with an f'_{cc}/f'_{cs} ratio of 3 are reached with either a 60 MPa column concrete and a 20 MPa slab concrete or with a 90 MPa column concrete and a 30 MPa slab concrete. Gamble and Kliner also suggest the column width-to-slab thickness ratio, c/h , affects the effective strength of the joint concrete. However, no tests were carried out to demonstrate this hypothesis.

For ratios of f'_{cc}/f'_{cs} less than 1.4, Gamble and Kliner conclude that the effective strength, f'_{ce} , is equal to the column strength, f'_{cc} . For higher ratios the column effective compressive strength is evaluated as follows:

For interior columns

$$f'_{ce} = 0.67 f'_{cs} + 0.47 f'_{cc} \geq 1.4 f'_{cs} \quad [2.5]$$

For edge columns

$$f'_{ce} = 0.85f'_{cs} + 0.32f'_{cc} \geq 1.4f'_{cs} \quad [2.6]$$

Gamble and Klinar found that design provisions in ACI 318-89 overestimate the strength of joints in which the ratio of column concrete strength to slab concrete strength is large.

2.2.2.4 Shu and Hawkins (1992)

Shu and Hawkins reported test results from 54 sandwich column specimens. This particular specimen shape was adopted to study the behaviour of joints restrained solely at the top and the bottom levels by the intersected column ends.

Major variables were the ratio of the slab thickness to the column width, h/c , and the ratio of the column concrete compressive strength to the slab concrete compressive strength, f'_{cc}/f'_{cs} .

Dimension of specimens are reported in table 2.1 . The h/c ratio ranged from 0.17 to 3.00 and the f'_{cc}/f'_{cs} ratio varied between 1.00 to 5.60. 3/4" size aggregate was used for the concrete. The amount of column longitudinal and transverse reinforcement was systematically varied to study the effect of this variable on the interaction of column and slab concrete. Axial compressive load was applied to the sandwich column specimens. Test duration was reported to be about 1 hour.

For specimens with small h/c ratios and a slab concrete strength close to that in the column stubs, vertical cracks appeared in the upper column. Such cracks widened enough so that column longitudinal reinforcing bars buckled and then the column core concrete crushed. For specimens with intermediate h/c ratios, cracks formed first in the sandwiched core and then extended into the upper column stub. For test specimens with high h/c ratios, failure was limited to the joint region. Specimens showed some ductility prior to failure.

Test results were not affected by the amount of column reinforcement. As in Bianchini et al., and Gamble and Klinar, the effective compressive strength was evaluated according to equations 2.1 and 2.2 . The main conclusion was that the h/c ratio is a significant variable affecting the effective strength of columns intersected by layers of weaker concrete. Test results were reported as a function of this ratio. As the h/c ratio increases, the column effective strength decreases.

Shu and Hawkins found the ACI provisions to be nonconservative for f'_{cc}/f'_{cs} ratios equal to or less than 1.4 . They also concluded that design provisions for f'_{cc}/f'_{cs} greater than 1.4 were unduly conservative for edge and corner columns. With regards to interior columns, they inferred that for certain h/c and f'_{cc}/f'_{cs} values, ACI design provisions may

be unsafe. They proposed the following design equation to evaluate the effective strength of edge and corner columns:

$$f'_{ce} = f'_{cs} + A(f'_{cc} - f'_{cs}) \quad [2.7]$$

where

$$A = \frac{1}{(0.4 + 2.66h/c)} \quad [2.8]$$

2.2.2.5 Kayani (1992)

Kayani tested 2 edge sandwich plates and 4 sandwich columns. Dimensions of these specimens are shown in table 2.1 . The column location and the ratio of the column compressive strength to the slab compressive strength, f'_{cc}/f'_{cs} , were the only parameters investigated. Column dimensions and slab thickness were kept constant, being equivalent to those of the specimens tested by Gamble and Klinar. Concrete strength for the columns ranged from 92.2 to 104.6 MPa. The slab concrete varied from 25.3 to 39.6 MPa.

The amount of column reinforcement varied according to the type of specimen. Two of the sandwich columns were provided with a steel hoop at the joint region. This consisted of a set of double No. 2 ties. For these columns 8 No. 6 longitudinal bars with single No. 2 ties spaced at 254 mm were provided. For the columns without hoop at the joint region, 4 No. 6 deformed bars were placed along with double No. 2 ties spaced at 254 mm.

For the edge specimens, columns had similar reinforcement than those with the double stirrup at mid-height. No. 3 and No. 4 bars spaced at 100 mm running in both directions were provided as the top slab reinforcement. Two reinforcing bars passing between the vertical column bars running parallel to the free edge of the specimen were placed at the bottom of the slab. The slab flexural reinforcement ratio varied approximately from 0.43 to 1.23 %. Grade 60 ksi bars were used for both the column and the slab reinforcement.

Specimens were instrumented with electrical resistance foil type strain gauges attached to the column vertical and lateral reinforcement. Gauges in the column vertical reinforcement were attached at the joint mid-height and outside the joint region. Specimens were tested at ages between 42 and 99 days old.

Only column load was applied to the specimens. Specimens were tested in a load-controlled way. Tests lasted between 40 and 60 minutes.

For the sandwich column specimens without ties at the joint region, splitting cracks formed at the joint at the very end of the test and specimens failed suddenly at or after the following load step. Neither buckling of the column longitudinal bars, spalling of concrete cover nor joint concrete crushing was observed prior to failure. Once the peak load was reached, the joint cross-section was destroyed.

For the sandwich columns with joint lateral reinforcement, spalling and crushing of concrete was observed. Buckling of the column longitudinal reinforcement was observed when the column load was increased after the maximum load was reached.

For the edge specimens, vertical splitting cracks formed at the visible face of the joint region after few load steps were applied. These splitting cracks continued forming throughout the test and later extended into the column stubs. First cracks on the slab top face were noticed at the end of the test. These formed extensively on all sides at the top surface. At failure, the column longitudinal bars buckled and the concrete in the joint region crushed.

Kayani reprocessed the test results from Bianchini et al. and from Gamble and Klinar. He suggested that sandwich column specimens adequately model corner slab-column connections. Similar to Shu and Hawkins, Kayani inferred that the amount of lateral or longitudinal steel in the columns does not affect the strength of the sandwiched layer of floor concrete.

With regard to existing code provisions, Kayani not only questioned the 1.4 ratio proposed in ACI 318-89 but also concluded that these provisions overestimate the effective strength of interior and edge columns intersected by floors made of weaker concrete, particularly when high f'_{cc}/f'_{cs} ratios were considered.

Kayani reports test results in a manner different to that previously adopted by Bianchini et al. and by Gamble and Klinar. The effective strength of the column was found to be proportional to the ratio of the product of the column and slab concrete strengths to the sum of the column and slab concrete strengths, as indicated in eq. 2.10 .

$$f'_{ce} = 2.0\lambda_G \frac{f'_{cc}f'_{cs}}{f'_{cc} + f'_{cs}} \quad [2.9]$$

Where λ_G is a constant which depends on the type of connection. The values of this constant are provided as follows.

i. Interior columns	1.25
ii. Edge columns	1.00
iii. Corner columns	0.90

2.2.2.6 CSA A23.3-94

Section 10.12 of the 1994 edition of the Canadian code refers to the transmissibility of column loads through concrete floors. The first design provision refers to concrete puddling. Rather than accounting for the 1.4 ratio as the limiting value for the f'_{cc}/f'_{cs}

ratio, the puddling solution is recommended when the column cylinder strength exceeds that of the slab concrete. The second provision suggests the calculation of the effective compressive strength of columns based upon its location.

For interior columns, a significant modification of the equation previously proposed by ACI 318-89 and the preceding CSA provisions is reported along with two new provisions for edge and corner connections. These design recommendations are as follows.

For interior columns,

$$f'_{ce} = 1.05 f'_{cs} + 0.25 f'_{cc} \leq f'_{cc} \quad [2.10]$$

For edge columns,

$$f'_{ce} = 1.4 f'_{cs} \leq f'_{cc} \quad [2.11]$$

For corner columns,

$$f'_{ce} = f'_{cs} \quad [2.12]$$

2.3 Discussion of test results and Code design provisions

2.3.1 Effect of Slab loading

For specimens without slab loads, the following behaviour may be predicted. Under the sole action of column loading, the joint concrete expands laterally due to Poisson's ratio. This expansion sets both top and bottom slab reinforcing bars near the column region under tension. Since no slab loads are applied, the only static requirement to be fulfilled is that the tensile stresses in the slab reinforcement be equilibrated by compression stresses from the surrounding concrete. The compressive character of these forces plus that of the applied column load allow us to assume the joint being subjected to a triaxial compressive state of stress. In light of this observation, the joint may be assumed to be confined across its full depth. Illustration of the system of forces acting on the joint region of a specimen without slab loads is provided in fig. 2.5 .

For specimens with slab loads, the slab-column connection is subjected to negative flexural moments. As a result, the top level of the slab near the column undergoes tension. Even in the absence of slab loading, significant tension of the top slab reinforcement crossing the column was reported by Gamble and Klinar for their specimens tested without slab loads. Under slab loading, it may be conjectured that the top slab bars be subjected to much higher tensile strains thereby imposing significant transverse tension to the upper part of the joint. For equilibrium of forces, the biaxial transverse tension applied at the top joint region is counteracted by compressive stresses acting at the bottom. The couple produced

by the top tension and the bottom compression forces equilibrates the negative flexural moment acting at the joint.

It follows then that an interior prototype sandwich plate joint may be viewed as a reinforced concrete prism subjected to two triaxial states of stress rather than one. At the top, the joint is subjected to vertical compression from the column load and to biaxial transverse tension from the slab bending. In this region, the joint concrete is pulled apart by the slab reinforcing bars traversing the joint rather than being confined. Conversely, the bottom joint region is subjected to a triaxial state of compressive stresses similar to that predicted for the full depth of joints under no slab loading. Taking this into account, full confinement of the joint only takes place at the joint bottom half. Figure 2.6 illustrates this behaviour.

Study of the effect of transverse tension on the compressive strength of reinforced concrete has been carried out by many authors. Since reporting of all these references lies beyond the scope of this thesis, this effect will be evaluated in light of the work reported by Chen and MacGregor (1993).

Chen and MacGregor (1993) found that transverse tension reduces the compressive strength of reinforced concrete panels subjected to axial compressive loads. This conclusion was based on test results on 40 reinforced concrete panels. Panels were 420 mm wide, 640 mm high and 70 mm thick. For specimens on which the axial compression and the transverse tension were applied simultaneously, the maximum reduction in the concrete compressive strength was 59%. This corresponds to a reinforced concrete panel on which a 3.4% ultimate transverse strain was applied.

This observation applies to the upper half of slab-column joints under column and slab loading. Since such portion of the joint region is subjected to transverse tension from the slab reinforcement due to the slab bending one would expect a significant reduction in the joint axial compressive strength.

Figures 2.7 to 2.9 illustrate the existing design provisions found in the literature for the calculation of the effective strength of interior, edge and corner slab-column connections. For completeness, figures also include the test results published in the past. Ratios of the column effective strength to the slab concrete strength, f'_{cc}/f'_{cs} , are plotted as the ordinates whereas ratios of the column concrete strength to the slab concrete strength, f'_{cc}/f'_{cs} , are plotted as the abscisses. The design equation proposed by Shu and Hawkins is not shown since it depends on the slab thickness to column width ratio, h/c . Discussion of this provision will be presented in chapter 5.

The design curves presented in the ACI 318-89 and the 1984 A23.3 Canadian standard are best fits for the tests of Bianchini et al. The design equations proposed by Gamble and Klinar are a lower bound for the tests reported by them and by Bianchini et al. Kayani's equations are a lower bound for tests reported by Bianchini et al., Gamble and Klinar and by Kayani himself. A significant variation between the existing design curves is observed.

It is worth mentioning that no slab loads were applied to the specimens tested by Bianchini et al. (1960), Gamble and Klinar (1991) and Kayani (1992). Any set of tests subjected only to column load tends to overestimate the strength of the joint concrete. It can hence be inferred that any design provision based solely on these tests is also likely to overestimate the joint strength.

2.3.2 Effect of the aspect ratio h/c

The effect of the h/c ratio on the joint strength may be anticipated based on a parallel between the test of a sandwich plate or column and the test of a concrete prism, cube or cylinder. In a sandwich plate or column, the joint concrete is subjected to a column load in a manner similar to the column load applied to a concrete specimen by a testing machine platens.

The confining effect provided to the joint concrete by the upper and lower column ends may be similar to that provided to a concrete prism, cube or cylinder by the platens of a testing machine. In a concrete cylinder test, the frictional forces at the interface between the concrete specimen ends and the testing machine plates restrain the transverse strain in the specimen. For high cylinder aspect ratios this restraint is reduced thereby resulting in a reduction in the specimen compressive strength.

Selection of realistic h/c ratios is desirable for testing of sandwich plate and sandwich column specimens. In multistorey buildings, higher concrete strengths are specified for the columns at lower levels. The slab thickness usually remains constant throughout the building. Under this conditions, the h/c ratio increases with the height of the building. Aspect ratios varying from 0.3 to 0.5 may be expected at lower levels of flat plate structures. Higher ratios may be found for waffle slabs or flat slab systems. For buildings whose first stories are utilized as parking levels, h/c ratios ranging from 0.6 to 1.0 may be observed. Taking into consideration the minimum column cross sectional dimensions recommended by current codes, h/c ratios greater than 1.0 are unlikely.

Thus far, the variable h/c has been unaccounted for in the testing of reinforced concrete sandwich plate specimens. Gamble and Klinar suggested the ratio of the column side to the slab thickness, c/h , as an important variable to evaluate the effective strength of columns intersected by normal-strength concrete floors. Nevertheless, no tests were carried out to further investigate the effect of this parameter.

Shu and Hawkins concluded that the effective compressive strength of unconfined joints increases as the h/c ratio increases. This reduction was more appreciable for large differentials between the column concrete strength, f'_{cc} , and the slab concrete strength, f'_{cs} . In their experimental program, Shu and Hawkins considered h/c ratios varying from 0.17 to 3.0. Test results of specimens with aspect ratios greater than the unity may be considered unrealistic since it is unlikely to find such h/c ratios in real life structures.

For lower h/c ratios, the effective strength of the unconfined joints was well predicted by the code design equation for confined interior slab-column joints (eq. 2.11) . This suggests that, so long as the h/c ratio is small enough, lateral confinement of the joint is not required.

However, Shu and Hawkins used 19 mm (3/4") size aggregate for the concrete in all their specimens. For the sandwich columns with h/c ratio equal to 0.17 the layer of the joint concrete was approximately 25 mm (1") thick. This means that the coarse aggregate was practically bridging the joint region from the bottom high-strength column to the top one. This would result in significant increase of the column compressive strength since the aggregates are stronger than the cement paste.

Considering the analogy to cylinder testing, the effect of using of 19 mm size aggregate may also be debatable according to the following observations.

Avram et al. (1981) remark that the effect of the aspect ratio cannot be separated from that of the maximum aggregate size. They suggest a maximum ratio of aggregate size to cube specimen side between 1/3 and 1/4 . Troxell et al. (1968) state that the diameter of a concrete cylinder should be not less than three or four times the maximum size of the aggregate in order to avoid undue influence of boundary conditions and other irregularities. Tests by Price (1951) show that for cylinders with an aspect ratio of two and maximum aggregate size greater than 1/4 the cylinder diameter, the strength of a 100-mm diameter cylinder exceeds by more than 4% the strength of a 150-mm diameter cylinder. It may be assumed that same enhancement will occur at the time of testing a sandwich column specimen whose joint concrete is made with aggregates larger than recommended.

Design provisions in ACI 318-89, CSA A23.3-M84 and CSA A23.3-94 do not account for the h/c ratio in evaluating the strength of sandwich connections. Adequacy of the American and the 1984 CSA provisions was already debated in the previous section. As far as to the h/c ratio is concerned, CAN A23.3-94 provisions may be unduly conservative when low h/c ratios intervene in the design of the connection.

Research found in the literature does not account either for the effect of the column rectangularity on the strength of columns intersected by concrete floors. Based on the recognition of the h/c ratio as a significant variable to assess the effective strength of columns intersected by weaker slabs, it is important to determine what column dimension should be used to determine the h/c ratio for the evaluation of the column strength.

2.3.3 Discussion of other provisions found in the Codes

In addition to providing design expressions to evaluate the effective strength of columns, both the Canadian and American standards provide some other guidelines for the design of high-strength concrete columns intersected by concrete floors of much less strength.

One of them is to puddle concrete of the strength specified for the column within the joint region. A detailed description of this process was already given in section 2.1 . Even though puddling has become a customary procedure in modern multi-storey building construction, it involves serious logistical problems. The fact that placement of slab concrete within the joint region must be avoided and that proper integration between the column and the slab concrete must be assured may generate some inconveniences. Moreover, coordination of the high-strength and normal-strength concrete mix deliveries may become difficult.

A second code provision included in ACI 318-89 and in the 1984 edition of the Canadian Standard refers to the calculation of the effective strength of interior, edge and corner columns based on the concrete cylinder strength of the intervening weaker concrete (usually the one cast in the floor) following the addition of dowels and spirals in the joint region. Several inconveniences may be found when putting this procedure on practice. Addition of the proposed reinforcement may be difficult since joint regions are usually congested zones. Moreover, a proper vibration of the joint concrete may not be guaranteed.

Addition of dowels, spirals or hoops is recommended by CSA A23.3-94 solely as a complementary solution to the design guidelines proposed in that standard. This provision is presented to enhance the strength of columns designed using the proposed design equations to evaluate the effective strength of columns intersected by floors of weaker concrete.

		Dimensions (mm)					Approximate reinf. ratios (%)	
Reference	Type	a	b	c	e	h	ρ col	ρ slab
Bianchini et al.	ISP	788	788	279	635	178	1.46	0.67
	ESP	533	788	279	635	178	1.46	0.67~0.74
	CSP	533	533	279	635	178	1.46	0.74
	SC	-	-	279	635	178	1.46	-
Gamble & Klinar	ISP	1067	1067	254	610	127 178	1.76	1.11~1.23
	ESP	762	1067	254	610	127	1.76	0.57~1.38
Shu and Hawkins	SC	-	-	152	305	25~458	1.23	-
Kayani	ESP	762	1067	254	610	178	1.76~3.52	0.43~1.23
	SC	-	-	254	610	178	1.82	-

Nomenclature: ISP : Interior sandwich plate.
 ESP : Edge sandwich plate.
 CSP : Corner sandwich plate.
 SC : Sandwich column.

Table 2.1 Description of test specimens found in the literature

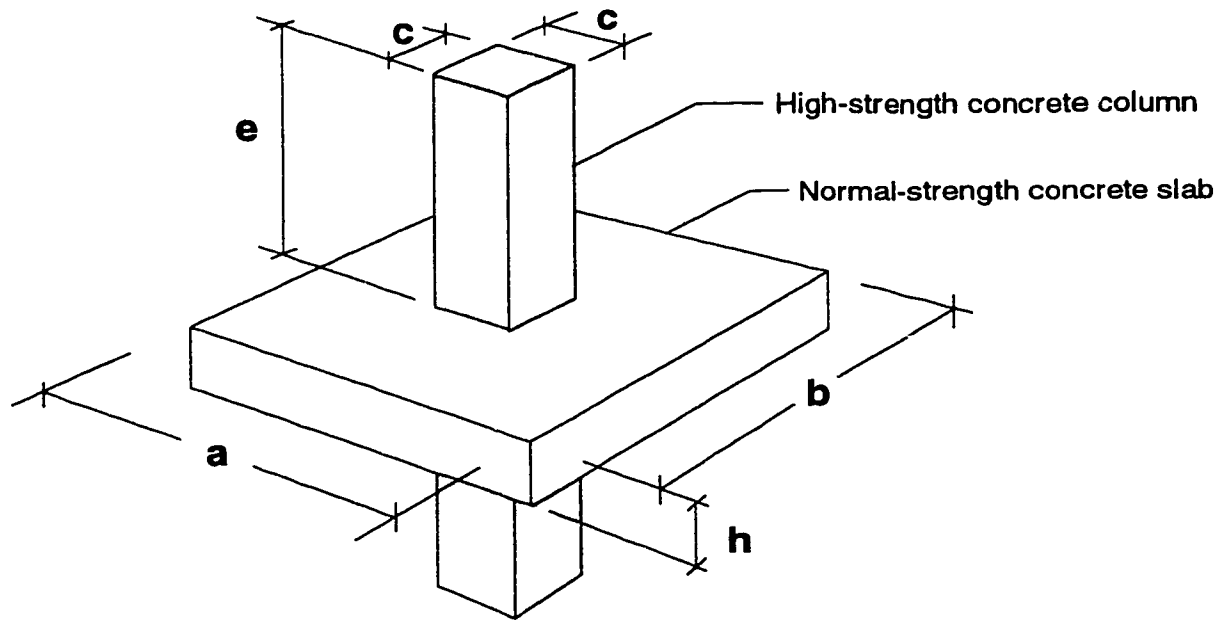


Figure 2.1 Interior sandwich plate specimen

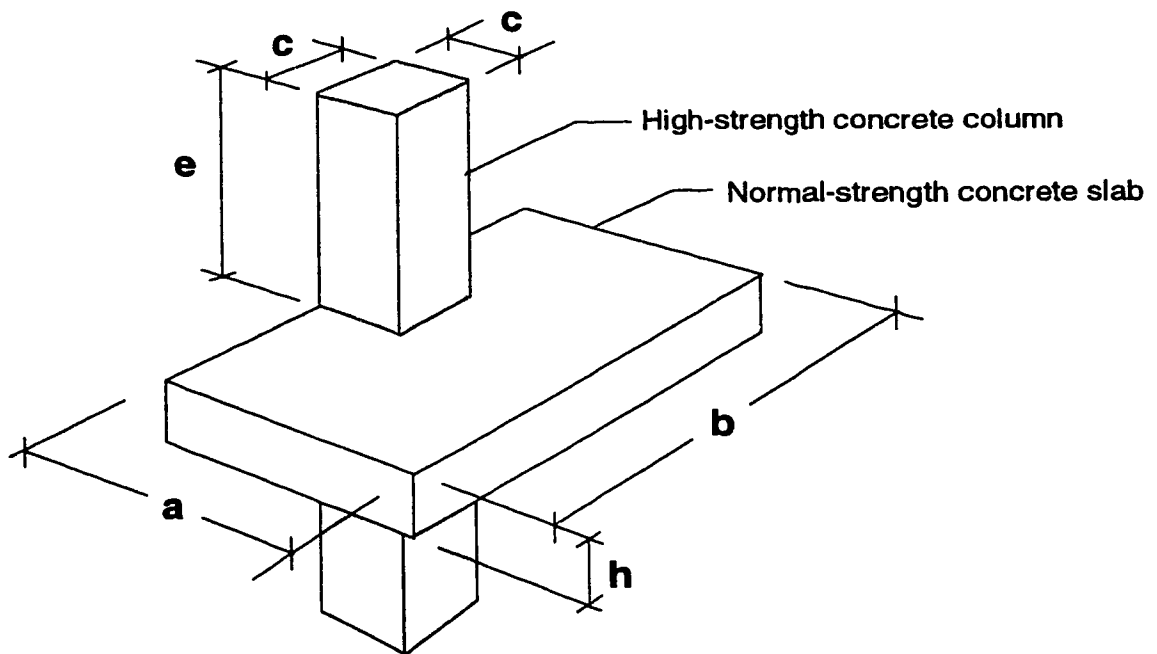


Figure 2.2 Edge sandwich plate specimen

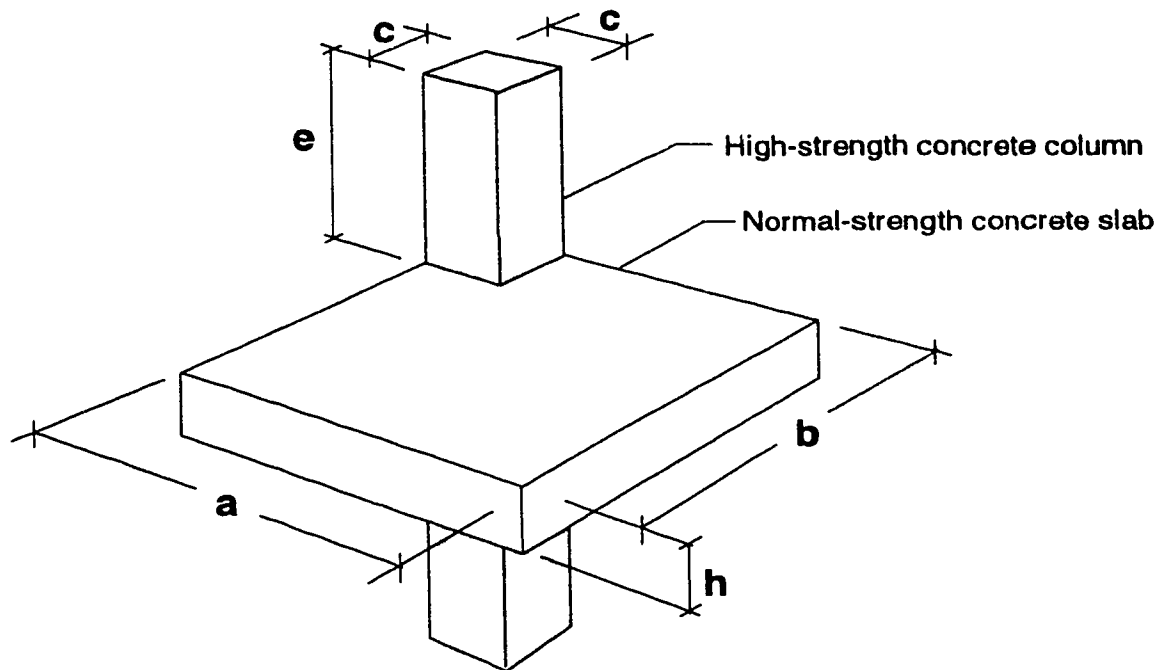


Figure 2.3 Corner sandwich plate specimen

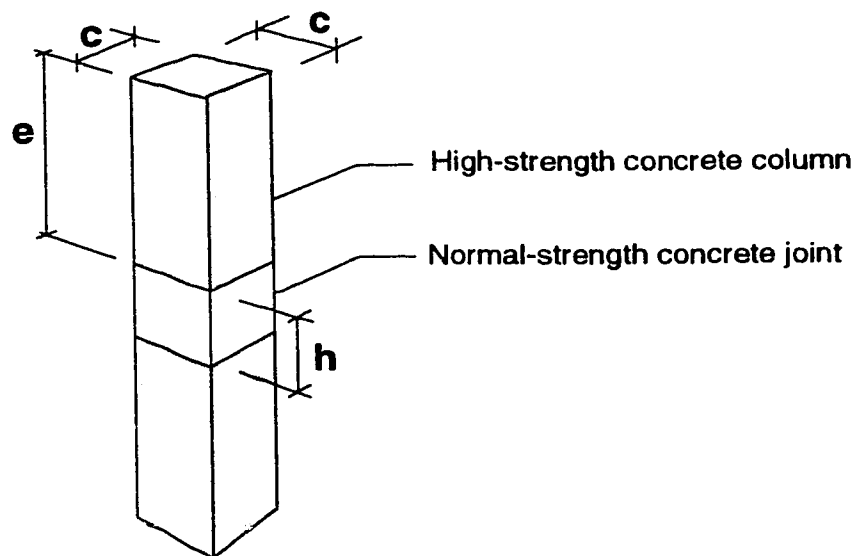


Figure 2.4 Sandwich column specimen

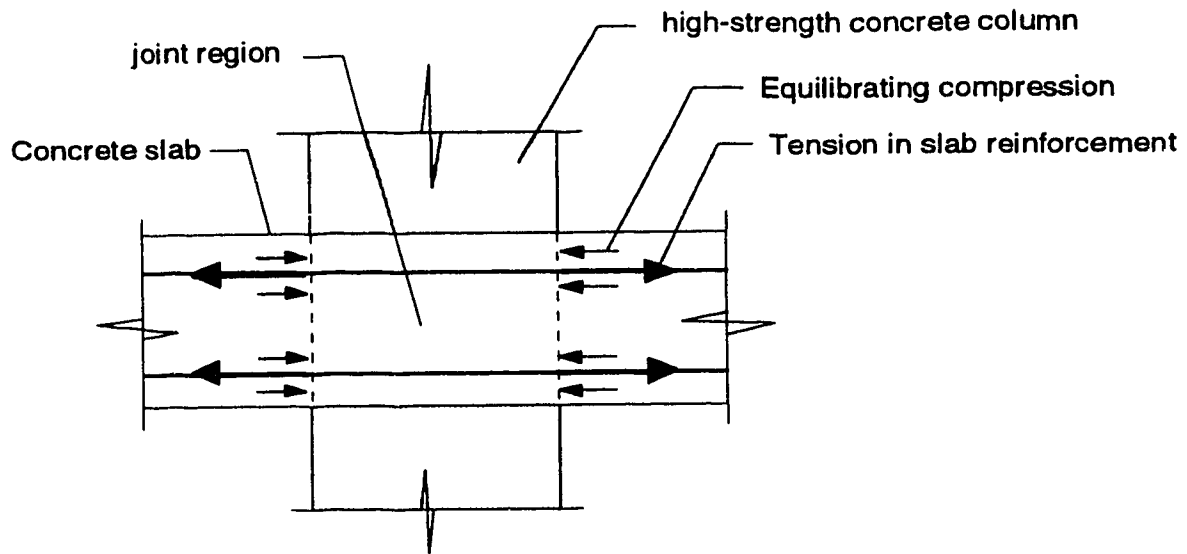


Figure 2.5 Stresses at joint region (specimens with unloaded slabs)

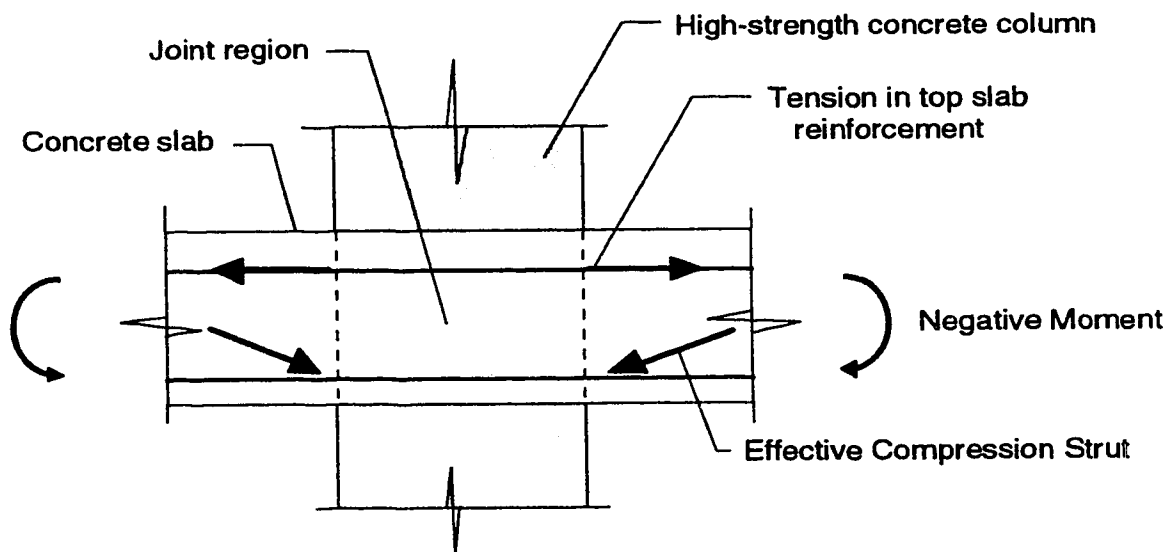


Figure 2.6 Stresses at joint region (specimens with loaded slabs)

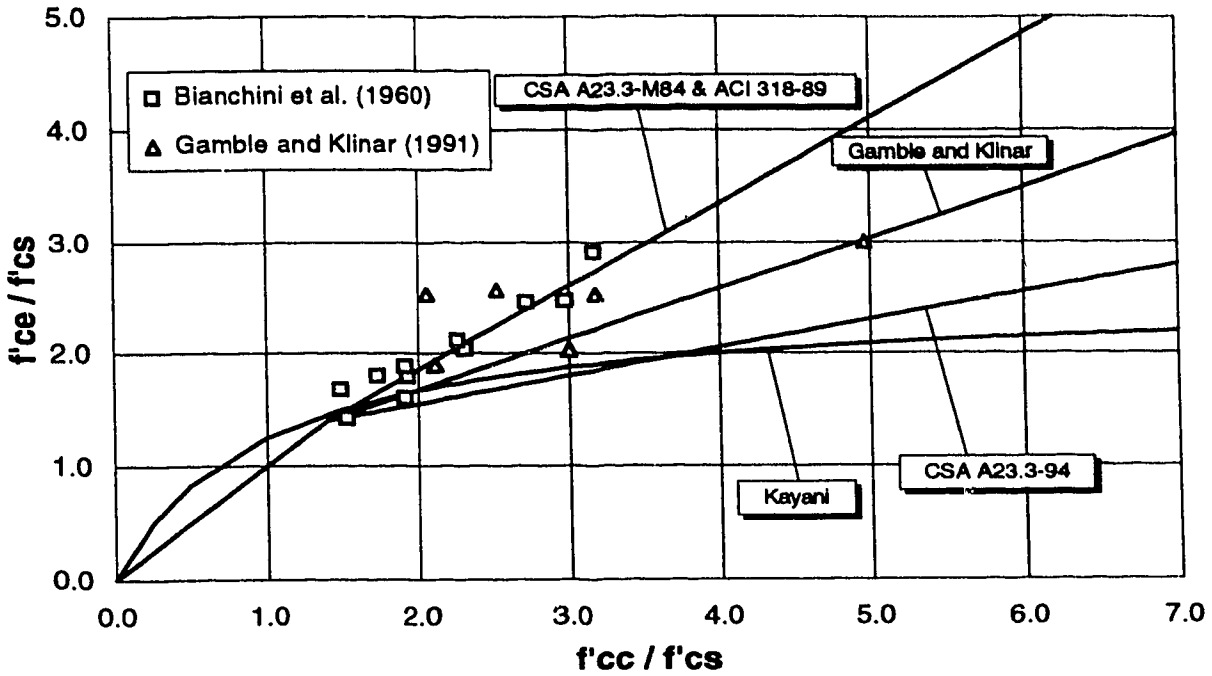


Figure 2.7 Existing design provisions for interior columns

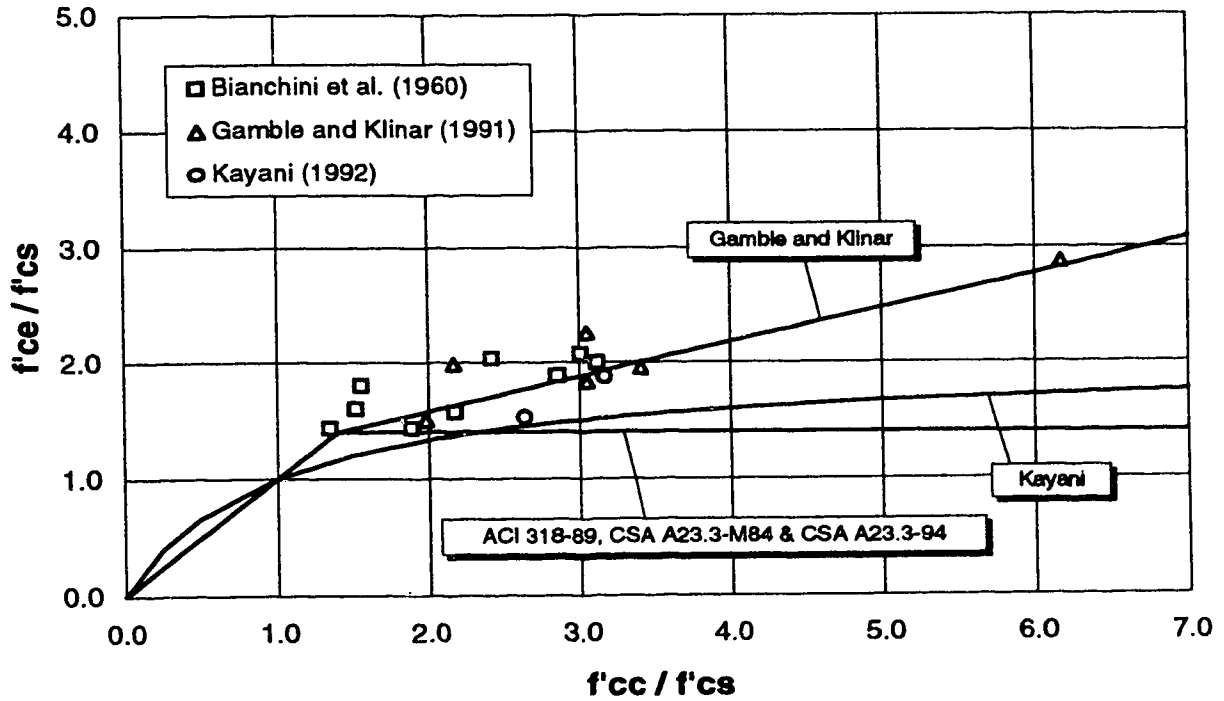


Figure 2.8 Existing design provisions for edge columns

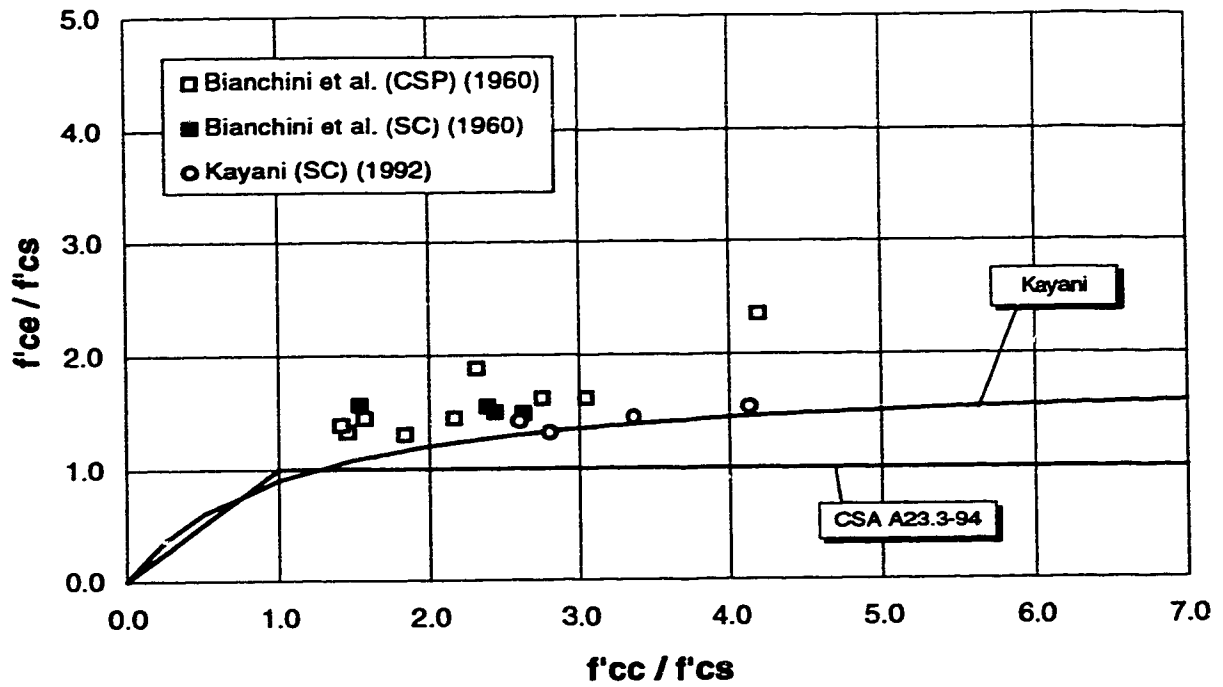


Figure 2.9 Existing design provision for corner columns

3. EXPERIMENTAL PROGRAM

3.1 Objectives of Testing

The primary objective of this project is the development of design provisions to evaluate the effective compressive strength of high-strength concrete columns intersected by floors made of lower-strength concrete. Two variables that have not been tested in the past are expected to have an effect on the strength of slab-column joints. These are the amount of slab loading and the ratio of the slab thickness to column width, h/c .

3.2 Experimental Program

A total of thirty specimens, in four separate phases, were built to model reinforced concrete slab-column connections in flat plate and flat slab multi-storey buildings. Of these, twenty were interior sandwich plates, six edge sandwich plates and four sandwich columns. Table 3.1 and figures 3.1 to 3.3 describe the geometry of these specimens.

Dimensions of the slab segments were generally selected in such a way that the magnitude and location of the applied slab loading resulted in moments and shears at the column face matching those in a prototype connection. However, the geometry of the connection specimens was also constrained by the capacity and the dimensions of the lab universal testing machine. Column dimensions were limited by the maximum capacity of the testing machine and the slab dimensions were determined according to the lateral clearance between the machine uprights.

3.3 Design of the experiments

3.3.1 Series A specimens (Interior sandwich plates)

The main purpose of this experimental series was to study the effect of slab loading on the joint compressive strength. Series A consisted of 12 interior sandwich plate specimens. Four sets of specimens were built and tested. Each set consisted of three specimens with equal f'_{cc}/f'_{cs} and h/c ratios. Three different slab load intensities were applied to each set. These correspond to high service, below service and zero load levels. Loads which produced a level of strain of 2000 microstrain on the slab top reinforcement near the column were considered to model high slab loads. Loads which produced a strain level of 1000 microstrain on the slab top steel near the columns simulated medium load levels. Each third specimen of each subset had no slab load applied on it. This was done not only to compare unloaded-slab specimens with the loaded ones but also to establish some parallels with tests by Bianchini et al. (1960) and by Gamble and Klinar (1991).

The level of slab load was set based on measured strain in the slab reinforcement. Readings were taken from strain gauges attached to the top slab reinforcing bars passing through the joint just 25 mm away from the column face. The slab load was increased until

the gauge readings averaged the target level of slab strain (1000 or 2000 $\mu\epsilon$). This established the target level of slab load to be maintained throughout the test.

The test region extended approximately 300 mm above and below the slab. The height of the high-strength concrete column stubs was selected in such a way that the axial compressive load could distribute uniformly throughout the test region. Height of the column ends was also determined accounting for the need of taking strain measurements along the columns. Overall height of series A interior sandwich plates varied according to the slab thickness.

Figure 3.1 illustrates the geometric dimensions of series A interior sandwich plates. Columns were square 200 mm wide. Slab thicknesses were either 100 or 150 mm. Specimens were reinforced according to reinforcement ratios likely to be provided in a prototype connection. Table 3.1 shows the concrete cylinder strengths of series A specimens. The cylinder compressive strength of the column was determined from the strength of the two column stubs, whichever was lower. Cylinder strengths correspond to those at the time of testing. High-strength concrete for the columns varied from 89 to 112 MPa. Slab cylinder compressive strengths ranged from 23 to 46 MPa. The ratio of column concrete strength to slab concrete strength, f'_{cc}/f'_{cs} , ranged from 2.43 to 4.61. The slab thickness-to-column width ratio, h/c , varied from 0.5 to 0.75. Table 3.3 shows the slab load intensities applied to the slab segments.

3.3.2 Series B specimens (Interior sandwich plates)

The main purpose of this series was to study the effect of the aspect ratio, h/c , on the strength of interior slab-column connections subjected to specified slab loads. One of the specimens (B-3) had a high-strength concrete core embedded in the joint region. This was done to study the behaviour of slab-column joints when strong concrete rather than weak concrete was placed at the joint region.

Connection specimens were intended to simulate slab-column connections in a prototype structure. A plan view of the prototype flat plate is shown in fig 3.4. Columns were spaced 4.45 m on centre. Column maximum side dimensions were set equal to 250 mm for the square column specimens, and 175 by 350 mm for the rectangular column specimens.

In this series, two different slab thickness were selected. Slabs 150 mm thick were intended to model a conventional flat plate structure whereas slabs 250 mm thick were selected to model either connections with intervening drop panels or waffle-slab connections. This results in values of the slab thickness-to-column width ratio, h/c , of 0.6 and 1.00 for the specimens with square columns. The effect of column rectangularity is also studied in this specimen series as a special case of the h/c effect. The main objective of these tests is to determine what column dimension should be used to evaluate the h/c ratio.

Specified dead and live load intensities were defined according to code provisions. Dead load included the structure self weight as well as the weight of partitions and finishing work. Reinforced concrete specific weight was assumed as 24 kN/m^3 . Live load was taken as 2.4 KPa whereas partitions and finishing work were set equal to 0.9 KPa.

3.3.2.1 Analysis of prototype connections and test specimens

Analyses were performed using a fully licensed educational version of the SAP90 program (Wilson and Habibullah (1992)). The purpose of these analyses was to ensure consistency between load and strain conditions in the joint specimen with those in a prototype joint. Analyses were carried out for the prototype structure and for the specimens with square columns.

The finite element mesh modeling of an interior prototype slab-column connection is shown in appendix A. The input data file and relevant information about the analysis procedure are also shown in appendix A. Level of applied slab load and moment values at the face of the prototype column are reported in table 3.2 .

Based on the results from the analysis of the prototype connections, analyses of the interior slab-column specimens were carried out. Appendix A includes the input data file used for these analyses. Table 3.2 reports the amount of slab loading applied to the specimens along with the resulting moments at the face of the column.

Comparison of the bending moment diagrams between the prototype connections and the specimen connection specimens is shown in figures 3.5 and 3.6, for h/c ratios equal to 0.6 and 1.0, respectively. Good agreement is observed between the moment at the specimen column face with that at the column face of both the prototype connection and the specimen.

Based on the analytical results, the expected level of strain at the slab top reinforcing bars crossing the column was calculated for each of the analyzed slab-column specimens. The strains were calculated at the face of the column. Evaluation of the strains was done to confirm the validity of the test results. Strain predictions proved to be more accurate for the specimens with thinner slabs (h/c ratio of 0.6) . For the specimens with thicker slab segments (h/c ratio of 1.0), the predicted strains exceeded in up to 40 % those measured experimentally by means of strain gauges.

Dimensions and cylinder compressive strengths of the series B sandwich plate specimens are reported in table 3.1 . Cylinder strengths correspond to those at the time of testing. Cylinder compressive strengths for the slab concretes varied from 15 to 44 MPa. The ratio of column concrete strength to slab concrete strength, f'_{cc}/f'_{cs} , ranged from 2.48 to 6.33. Levels of slab load applied to the specimen slab segments are reported in table 3.3 .

3.3.3 Series C specimens (Edge sandwich plates)

This series consists of 6 test specimens simulating edge connections in flat-plate structures. For this series, 2 sets of 3 edge specimens were built and tested. The main variable was the level of slab load applied to each slab segment. Each of the 3 specimens had similar f'_{cc}/f'_{cs} and h/c ratios but different slab load intensities. Slab loads which cause 0, 1000 or 2000 microstrain in the slab region surrounding the column outline were applied. The zero microstrain condition corresponds as expected to an specimen without slab loads. For the specimens with slab loads the loads were applied similar to the procedure followed in slab-loaded series A specimens. The slab loads were applied and increased until the readings from 8 top gauges located within the connection averaged 1000 or 2000 microstrain. This average included readings from 3 strain gauges located at the face of the column and from 5 gauges located outside the column periphery. It is expected for the gauge strain readings at the column face to be higher than the overall average strain.

The zero microstrain condition corresponds, as expected, to a specimen without slab loads. Specimens without slab loading were also intended to establish a comparison with the test results reported by Bianchini et al. (1960), by Gamble and Klinar (1991), and by Kayani (1992). Specimens undergoing 1000 and 2000 microstrain in an area around the column correspond to connections with slabs heavily loaded.

In general, specimens were subjected to slab loads similar to those calculated from the tributary area of an edge slab-column connection in the model slab shown in fig. 3.7 . Slab thickness was either 170 or 230 mm. For the edge specimens with 170 mm thick slabs, the prototype columns were assumed to be spaced 4 metres on centre. For the edge specimens with 230 mm thick slabs, the column spacing was increased up to 4.5 metres. Columns were square with 230 mm side dimensions. The h/c ratio was either 0.74 or 1.0 .

For the edge plates the column concrete strength was either 107 or 108 MPa. For the slab segments the concrete strength varied from 31 to 35 MPa. This led to column concrete-to-slab concrete ratios, f'_{cc}/f'_{cs} , varying from 3.06 to 3.48 .

Geometry of an edge sandwich plate specimen is illustrated in fig. 3.2 . Nomenclature and location of the point slab loads are also illustrated. Dimension of test specimens along with concrete cylinder strengths are reported in table 3.1 . Table 3.3 shows the slab load intensities applied to the edge specimens.

3.3.4 Series D specimens (Sandwich Columns)

Sandwich columns were tested to model unconfined slab-column joints in an attempt to reproduce test observations and conclusions reported by Kayani (1992) and Shu and Hawkins (1992). The main variable was the ratio of the slab concrete layer to the column side, h/c . Four specimens with equal f'_{cc}/f'_{cs} ratios were tested.

Columns were 250 mm square. Length-to-width ratios for the high-strength concrete column stubs were selected to provide a central test region of about 375 mm above and below the joint concrete. Thickness of the layer of floor concrete ranged from 75 mm to 250 mm. h/c ratios varied from 0.30 to 1.00. The overall height of the specimens was kept constant throughout the tests.

Column strength varied from 105 to 107 MPa. Floor concrete strength was 17 MPa. Cylinder strengths correspond to those at the time of specimen testing. f'_{cc}/f'_{cs} ratios varied from 6.18 to 6.29. Geometric description and concrete strengths of the sandwich column specimens are provided in table 3.1 and figure 3.3.

3.4 Materials

3.4.1 High-strength concrete

Bagged type 10 Portland cement was used in the high-strength concrete mixtures. Local coarse aggregates were used. They were washed and crushed gravel primarily composed of highquartzite sandstone, quartzite and hard sandstone with 14 mm maximum size chips. Locally available washed sand was utilized.

Use of silica fume has become almost mandatory if mixture strengths higher than 100 MPa are to be achieved. The product used for this purpose was condensed silica fume dissolved in a water slurry. The water content of this product is 51% by weight. Specific gravity of this product was taken as 1.36. The specific gravity of the solid silica fume was assumed as 2.2. Percentage by weight of Portland cement substituted by Silica fume was 10 percent. Superplasticizer was also used for the column concrete mixtures. The product used was a polynaphtalene sulfonate base mix. Dosage of superplasticizer ranged from 1.2 to 1.8% weight of solids by weight of cement and silica fume. Typical mix proportions for a high-strength concrete mixture are shown in table 3.4.

In order to evaluate the concrete compressive strengths, a minimum of 4 control cylinders were cast from each batch of concrete. Cylinders were 100 mm in diameter and 200 mm in height. Cylinders were cured during 7 days and tested at the time the specimen was tested. Cylinders were ground and tested dry in a 2600 kN capacity rock testing machine. Load was applied at a rate of 0.35 MPa/sec. Compressive strength values were obtained as the average of the cylinder test results. The overall column concrete compressive strength of a specific specimen was determined as the least of the two column stub compressive strengths. A typical stress-strain curve for a high-strength concrete control cylinder is shown in fig. 3.15.

3.4.2 Normal-strength concrete

The same cement and aggregates used in casting the high-strength concrete columns were used for manufacturing the slab concrete. No additives nor silica fume were added. Table 3.4 shows the mix proportions for a normal-strength concrete mixture.

For assessing the slab concrete strength a minimum of 4 control cylinders were cast from each batch of concrete. Plastic molds were used. These were 100 mm in diameter and 200 mm high for series A specimens and 150 mm by 300 mm for series B, C and D. Cylinders were cured in a water tank for at least 7 days. After drying, cylinders were capped with a sulfur-based compound. Cylinders were tested dry at the time of testing the connection specimen. Slab compressive strengths were obtained as an average of the cylinder test results linked to every specimen slab. A typical stress-strain curve for the slab concrete used in this experimental program is presented in fig. 3.16 .

3.4.3 Reinforcement

Columns were reinforced longitudinally with grade G30.12 M400 No. 15 M deformed bars. 6 mm diameter ties were used for series A and C specimens. No. 10 M ties were placed in series B and D. The amount of column longitudinal reinforcement as well as the tie spacing varied from phase to phase.

All of the intervening slabs have top and bottom layers of reinforcement running in both directions. 3/8" diameter deformed bars were used in series A and C specimens. Grade G30.12 M400 No. 10 M bars were used for series B specimens. Spacing of slab top reinforcement varied throughout the experimental program. Top reinforcing bars were hooked at the ends, accounting for development of reinforcement. 180 degree hooks were bent for this purpose. Tails of the hooks extended approximately 220 mm from the outer edges of the slab.

Integrity steel was only provided for series B specimens. These bars were placed at the bottom of the slab and crossed the joint between the column vertical reinforcement. Two No. 15 M deformed bars running in each direction were provided for this purpose.

Figure 3.8 through 3.11 show the column reinforcement layouts for the sandwich plate and sandwich column specimens. Slab reinforcement layouts are shown in figure 3.12 through 3.14 . Column and slab reinforcement ratios for all of the specimens are shown in table 3.1.

Characteristics of the slab and column steel reinforcement were taken from standard tension tests. Tests were carried out on 3 coupons taken from the same source. Typical stress-strain curves for No. 15M and No. 10M bars are shown in figures 3.17 and 3.18, respectively. Table 3.5 shows the properties of the steel reinforcing bars used in this investigation.

3.5 Fabrication of Specimens

3.5.1 Mixing, casting and curing procedures

3.5.1.1 Interior and Edge sandwich plates

Specimens were cast in 3 stages. Before casting the lower column, the column steel reinforcing cage was placed and aligned into wooden forms. Then, the high-strength concrete mixture for the lower column was mixed and poured into the forms. Control cylinders were filled and vibrated. The next step was to cast the slab concrete. To do this, the lower column forms were stripped and the slab forms installed so that the slab soffit coincided with the lower column top surface level. Slab forms were supported on the floor by a metal frame system. Next, the slab reinforcement was placed and the slab concrete was mixed and cast. The slab concrete was placed so that a single batch of concrete was located at the slab-column joint to guarantee uniformity of the joint concrete strength. Control cylinders were then cast and vibrated. Finally, the upper column forms were placed. Particular care was required to align the upper column with respect to the lower column. After the high-strength concrete was mixed the top column was cast. Control cylinders were cast and vibrated. Following the form stripping, specimens were cured for a period of 7 days.

3.5.1.2 Sandwich column specimens

With the sandwich column specimens, the column steel reinforcing cage was placed and aligned into the lower column forms. Stirrups were tied up along the lower column region. The high-strength concrete was mixed and then poured into the forms. The next day, the slab concrete was mixed and cast. The following day, forms were stripped and stirrups were tied up along the top column stub. Upper column stub forms were then lifted and mounted. High-strength concrete was mixed and cast into the upper column forms. Control cylinders were filled during the whole process. Proper vibration of column and slab concrete was also accomplished. Finally, the column top forms were stripped and the specimens were cured for a week.

3.6 Testing

3.6.1 Test Set-up

3.6.1.1 Sandwich plate specimens

Set-ups for interior and edge sandwich plates are given in figures 3.19 and 3.20, respectively. The primary load, P_{col} , was applied to the column by the stroke control system of a 6600 kN universal testing machine. The secondary load, P_{sl} , was applied to the slab segments by jacking against four 19 mm diameter steel load rods. The rods passed through the slab near the corners and were tied down to the lab strong floor. Locations at which the jacking loads were applied over each slab segment are shown in fig. 3.1 to 3.2 .

For series A and B specimens (interior sandwich plates) subjected to slab loading, jacks were placed symmetrically with respect to the concentric column stub. All of the jacks were connected to a common manifold. Level of loading was controlled by a single hand pump. Jacking loads were similar throughout the test. The slab edges were unrestrained.

For series C specimens (edge sandwich plates), symmetric load conditions did not take place. Jacks were placed asymmetrically with respect to the column axis parallel to the slab free edge and symmetrically with respect to the column axis perpendicular to the slab free edge. Two hand pumps were used since two different slab load intensities were applied. Jacks located near the slab free edge closer to the column applied less load than those located in the cantilever slab corners. For this reason, the slab loads in this series will be referred to as P_{11} and P_{12} , as illustrated in fig. 3.2 .

3.6.1.2 Sandwich column specimens

Since this type of specimen does not involve any slab concrete surrounding the sandwiched concrete layer, the primary load was a compressive-type load applied by the 6600 kN universal testing machine. Test set up of a sandwich column specimen is shown in fig. 3.21 .

3.6.2 Instrumentation

3.6.2.1 Linear variable-differential transformers (LVDT's)

LVDT's were used to measure the column axial longitudinal strain at the column region and at the slab-column joint. They were mounted on aluminum frames attached at 3 different locations along the column concrete. LVDTs attached outside the slab region provided information on the shortening of both top and bottom column stubs. Either single or coupled LVDTs were used for this purpose. LVDTs attached at the specimen mid-region supplied information on column shortening at that location, including a small fraction of the high-strength column shortening. Each of the 3 LVDT frames consisted of 2 extension arms. Aluminum arms were supported by 8 mm diameter threaded rods that traversed the column stubs. In all of the specimen series, each lower arm was fixed to the column. Fixed upper arms were used only in series B, C square column, and D specimens whereas pivoting arms were utilized in series A and C rectangular column specimens. Use of fixed upper arms implies that the measurement of the concrete shortening is done based on the average of two LVDTs mounted at the ends of the frame. When using pivoting upper arms the calculation of the column shortening reduces to the readings from only one LVDT mounted at one end of the rack. Sketches describing each of the LVDT set-ups throughout the experimental program are shown from fig. 3.22 to 3.26 .

3.6.2.2 Strain Gauges

120 ohm electrical resistance foil-type strain gauges were used in all of the specimens. At each gauge location, steel bar ribs were ground smooth. Grinding was minimized so that the impact of the strain gauge on the bond characteristics of the reinforcement was reduced. Each gauge was glued to the bar with an epoxy adhesive and waterproofed.

To corroborate the LVDT readings at low levels of strain, gauges were attached to the column longitudinal reinforcement for series B (interior sandwich plates) and D specimens (sandwich columns). Such gauges were attached at the middle of the joint and at levels 235 mm above and below the slab concrete. Column gauge layouts corresponding to these specimen series are illustrated in fig. 3.9 and 3.11 .

Gauges were attached to the slab top reinforcement for all of the specimen series. Strain gauges were attached at the bottom reinforcing bars for C series specimens. Slab gauges were placed in different patterns as it shown in figure 3.12 through 3.14 . For series A specimens (interior sandwich plates) gauges were attached to the slab top reinforcing bars crossing through the joint 20 mm outside the column face. For series B specimens (interior sandwich plates), gauges were attached both at the face of the column and at the centre of the joint. Strain readings of the slab top steel reinforcing bars passing through the joint provides significant information about confinement conditions at the joint above the neutral axis of bending. For series C specimens (edge sandwich plates), similar gauge layout as used for A series was adopted. Some additional slab gauges were attached outside the column region as well as at the slab bottom reinforcement.

3.6.2.3 Load Cells

The primary load was measured with the Universal testing machine load cell. Each of the slab jacking loads was measured with a 89 kN (20000 lb.) load cell placed in between a system of steel plates.

3.6.3 Calculation of the column strain through the slab thickness

The column strain through the slab thickness, ϵ_{sc} , was calculated using the results from LVDTs mounted at three different locations along the column. The column shortening through the joint region can also be calculated directly from strain gauges attached to the column reinforcement at the middle of the joint region. However, gauge readings are useful only up to the onset of the column reinforcement yielding. Beyond this level, strain readings are not reliable due to the short gauge length of the strain gauges. At this level, it is also expected that strain gauges get damaged by excessive abrasion of concrete.

In order to measure the column strain through the slab thickness, it is necessary to deduct the small portion of high-strength column strain included in the readings taken by the middle LVDT frame. The shortening of the high-strength column ends is calculated as an average of top and bottom LVDT readings.

Figures 3.27 and 3.28 along with the following equations illustrate the procedure to calculate the column strain through the slab thickness.

$$[3.4] \quad \epsilon_{col} = \frac{\epsilon_{topcol} + \epsilon_{botcol}}{2}$$

$$[3.5] \quad \epsilon_n = \frac{\epsilon_{mid}(2m + h) - \epsilon_{col}(2m)}{h}$$

where

ϵ_n : column strain through slab thickness

ϵ_{col} : average of strain at top and bottom high-strength stubs

ϵ_{mid} : strain at specimen midheight (includes small portion of high-strength column strain)

h : slab thickness

m : distance between the slab top and bottom levels and the location of the threaded rods on which the middle LVDT frame was mounted.

3.6.4 Test Procedure

3.6.4.1 Interior and edge sandwich plate specimens

Specimens were installed in the 6600 kN capacity universal testing machine. Column stubs were aligned with respect to the machine axes. The specimen top surface was ground in order to prevent the tips of the column reinforcing bars from projecting from the column. To prevent crushing of concrete at both top and bottom column ends, column ends were capped with steel confining shoes. A layer of plaster was placed between each column end and its protective metal box to ensure a smooth bearing surface. All electrical connections were made and checked.

For the specimens with unloaded slabs, the ramp function controlling the primary load, P_{col} , was started and the specimen was loaded to failure.

For the specimens with slab loads, the loading procedure was intended to mimic the loading sequence of a prototype structure. First, a small column preload was applied. This ranged from 200 to 400 kN for the A and B series specimens. This column seating load was increased to 500 kN for the edge plates with 170 mm thick slabs and to 700 kN for the edge sandwich plates with slabs 230 mm thick to prevent these specimens from overturning upon application of the slab loads. Then, the full load was applied to the slab by means of the four jacks traversing the overhanging slab segment. Jacking loads were controlled with one manual pump (interior specimens) or two manual pumps (edge

specimens). Throughout the tests, jacks were continually adjusted by using the hand pump(s) to maintain a relatively constant slab load throughout the test. Without this adjustment, the slab load decreased. Test duration ranged from 2 to 3.5 hours. Cracking patterns and structural behaviour of the specimens were recorded throughout the tests.

Selection of the loading procedure was adopted to allow comparisons with test results reported in the past. For all of the test results found in the literature, the columns were loaded monotonically to failure.

3.6.4.2 Sandwich column specimens

Sandwich column specimens were seated and aligned in the testing machine. Column ends were capped using re-usable metal shoes to prevent the ends from crushing. A layer of plaster was placed between the column ends and the steel shoes. Electrical connections were made and the specimen was carefully checked. Then, a compressive-type column preloading was applied over the specimen. This seating load varied between 100 and 200 kN. Then, the stroke control system of the universal testing machine was started and the specimen led to failure. Duration of the tests varied from 1 to 1.5 hours. Cracking patterns and observations were recorded.

Specimen	Dimensions (mm)					Concrete strength (MPa)		Reinforcement ratios (%)	
Mark	a	b	c	e	h	f _{cc}	f _{cs}	ρ col	ρ slab
A1-A,B,C	1380	1380	200	500	100	105 (27)	40 (28)	4.00	0.55
A2-A,B,C	1380	1380	200	500	100	112 (29)	46 (28)	4.00	0.41
A3-A,B,C	1380	1380	200	500	150	89 (27)	25 (28)	4.00	0.33
A4-A,B,C	1380	1380	200	500	150	106 (29)	23 (28)	4.00	0.33
B-1	1350	1350	250	625	250	104 (51)	42 (49)	1.28	0.26
B-2	1350	1350	250	675	150	104 (56)	42 (54)	1.28	0.47
B-3	1350	1350	250	625	250	113 (44)	44 (42)	1.28	0.26
B-4	1350	1350	250	675	150	113 (45)	44 (43)	1.28	0.47
B-5	1350	1350	250	625	250	95 (17)	15 (20)	1.28	0.26
B-6	1350	1350	250	675	150	95 (18)	15 (21)	1.28	0.47
B-7	1350	1350	175x350	625	250	120 (21)	19 (23)	1.28	0.26
B-8	1350	1350	175x350	675	150	120 (22)	19 (24)	1.28	0.47
C1-A	680	1220	230	465	170	107 (34)	32 (33)	3.02	0.27-0.32
C1-B	680	1220	230	465	170	107 (34)	35 (33)	3.02	0.27-0.32
C1-C	680	1220	230	465	170	107 (34)	34 (33)	3.02	0.27-0.32
C2-A	680	1220	230	435	230	108 (29)	31 (28)	3.02	0.20-0.22
C2-B	680	1220	230	435	230	108 (29)	34 (28)	3.02	0.20-0.22
C2-C	680	1220	230	435	230	108 (29)	33 (28)	3.02	0.20-0.22
D-SC1	-	-	250	712.5	75	105 (24)	17 (27)	1.28	-
D-SC2	-	-	250	687.5	125	105 (24)	17 (27)	1.28	-
D-SC3	-	-	250	675	150	107 (22)	17 (25)	1.28	-
D-SC4	-	-	250	625	250	105 (23)	17 (26)	1.28	-

Notes: 1. Concrete strengths correspond to those at the time of testing. Numbers in parentheses indicate column and slab concrete age in days.

2. Column strengths are those from upper or lower column stub, whichever is lower.

3. Slab reinforcement ratios were calculated based on a 25 mm cover for the interior sandwich plates and 20 mm for the edge sandwich plates.

Table 3.1 Description of Test Specimens

Case	h	c	dimensions	Load	M col face (KN.m)
Specimen slab	150	250	1.35m x 1.35m slab segment	4 point loads, 32.5 kN each	26.46
Prototype flat plate	150	250	4.45m x 4.45m flat plate	D.L.=3.6 kPa L.L.=3.3 kPa	26.22
Specimen slab	250	250	1.35m x 1.35m slab segment	4 point loads, 43.3 kN each	35.52
Prototype flat plate	250	250	4.45m x 4.45m flat plate	D.L.=6.0 kPa L.L.=3.3 kPa	35.34

Table 3.2 Dimensions and analysis results of specimen and prototype slabs

Series	Mark	Slab point loads (KN)		Total slab (KN)
		Ps ₁	Ps ₂	
A	A1-A	0	-	0
	A1-B	12	-	48
	A1-C	23.5	-	94
	A2-A	0	-	0
	A2-B	8.3	-	33.2
	A2-C	21.5	-	86
	A3-A	0	-	0
	A3-B	25	-	100
	A3-C	39.3	-	157.2
	A4-A	0	-	0
	A4-B	23.3	-	93.2
	A4-C	33.8	-	135.2
B	B-1	43.3	-	173.2
	B-2	32.5	-	130
	B-3	43.3	-	173.2
	B-4	0	-	0
	B-5	43.3	-	173.2
	B-6	32.5	-	130
	B-7	43.3	-	173.2
	B-8	32.5	-	130
C	C1-A	0	0	0
	C1-B	25.3	5.1	60.8
	C1-C	36.4	7.1	87
	C2-A	0	0	0
	C2-B	35.5	3.6	78.2
	C2-C	52.4	5.7	116.2

- Notes: 1. Location of slab loads is illustrated in fig. 3.1 and 3.2 .
2. For interior plates: Total slab load = $4Ps_1$.
3. For edge plates: Total slab load = $2Ps_1 + 2Ps_2$.

Table 3.3 Slab loads

Constituents	Mix Proportions	
	Column concrete Mix (120 MPa)	Slab concrete Mix (15 MPa)
Cement (Kg/m ³)	470	235
Water (Kg/m ³)	110	188
Coarse aggregate (Kg/m ³)	1040	1000
Sand (Kg/m ³)	650	878
Silica fume (solid) (Kg/m ³)	48	-
SPN * (l/m ³)	16	-
W/(C+SF)	0.23	0.80

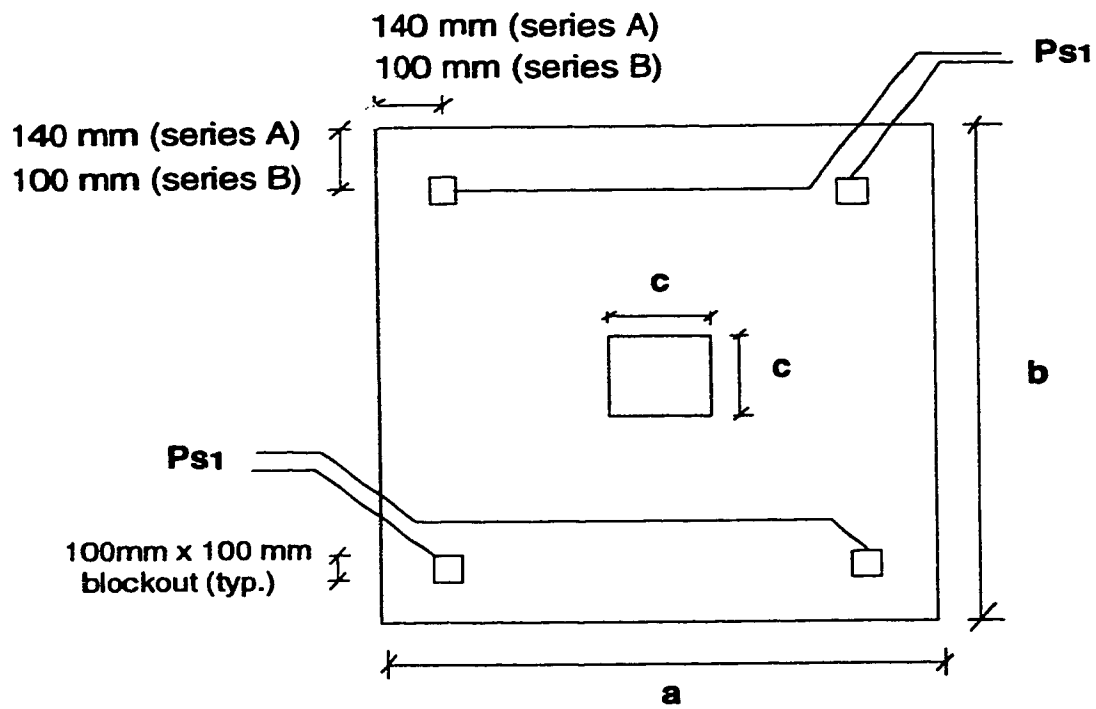
Mixes are based on 2% air content.

* SPN has 70% by weight water which was subtracted from the total amount of mixing water required.

Table 3.4 Concrete Mix Proportions

Bar size	Modulus of Elasticity (MPa)	Static yield strength (MPa)	Static ultimate strength (MPa)
No. 15M	190320	400	632
No. 10M	208530	424	638

Table 3.5 Properties of reinforcement steel



Note: Specimens B-7 and B-8 had a 175 by 350 mm rectangular column

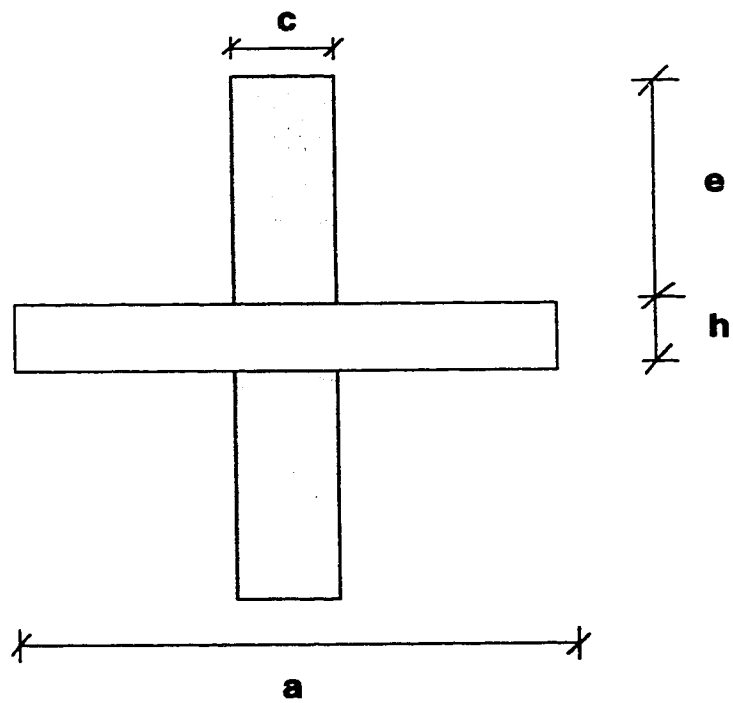


Figure 3.1 Geometry of interior sandwich plate specimens

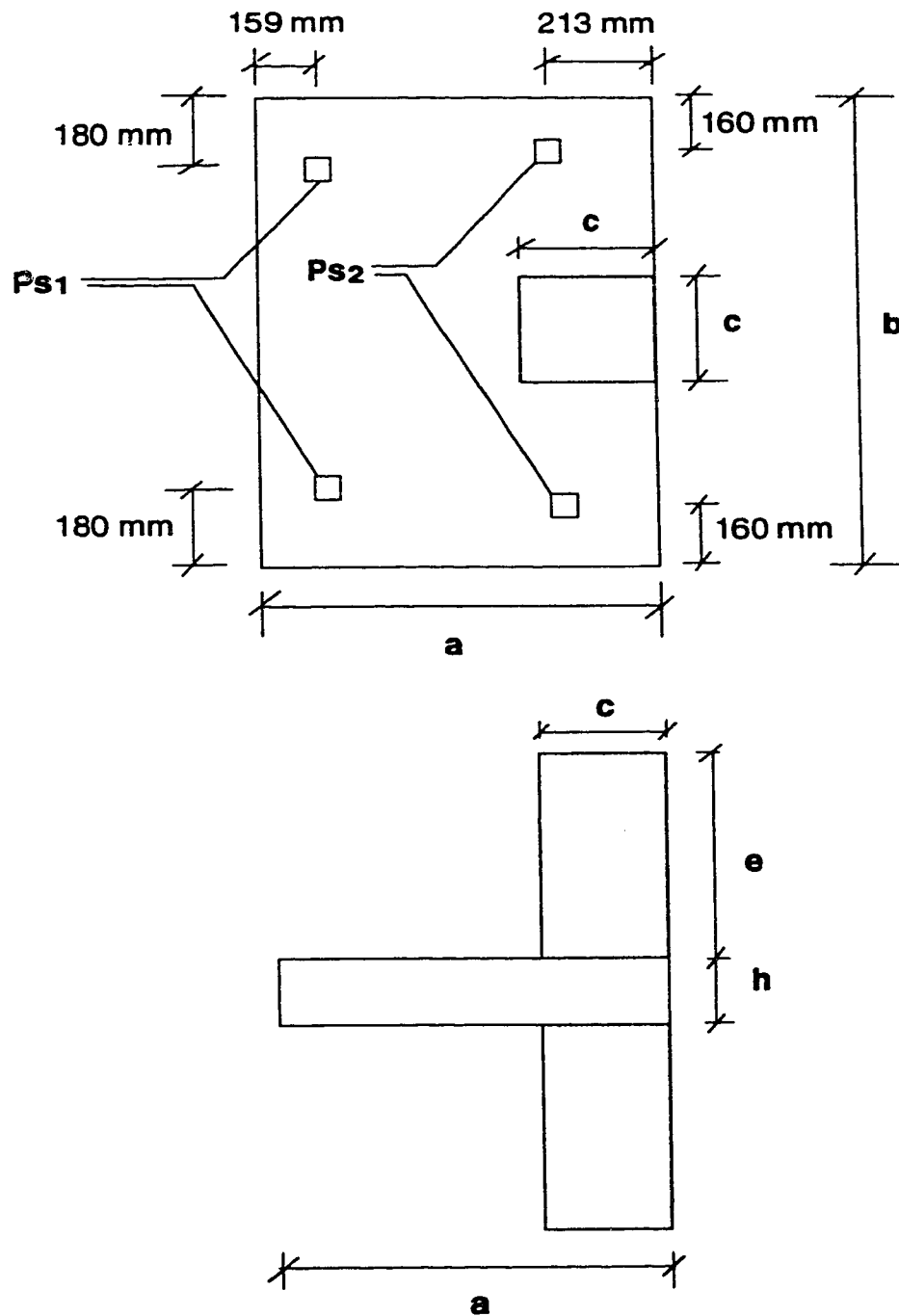


Figure 3.2 Geometry of edge sandwich plate specimens

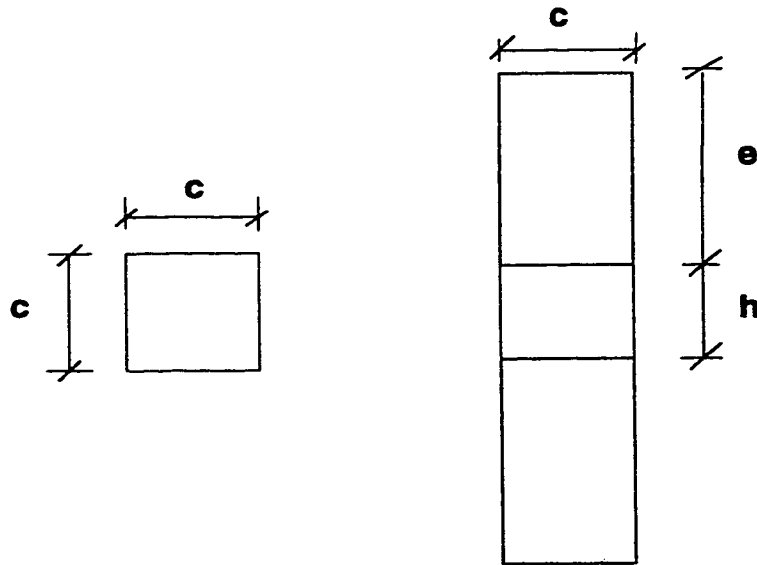
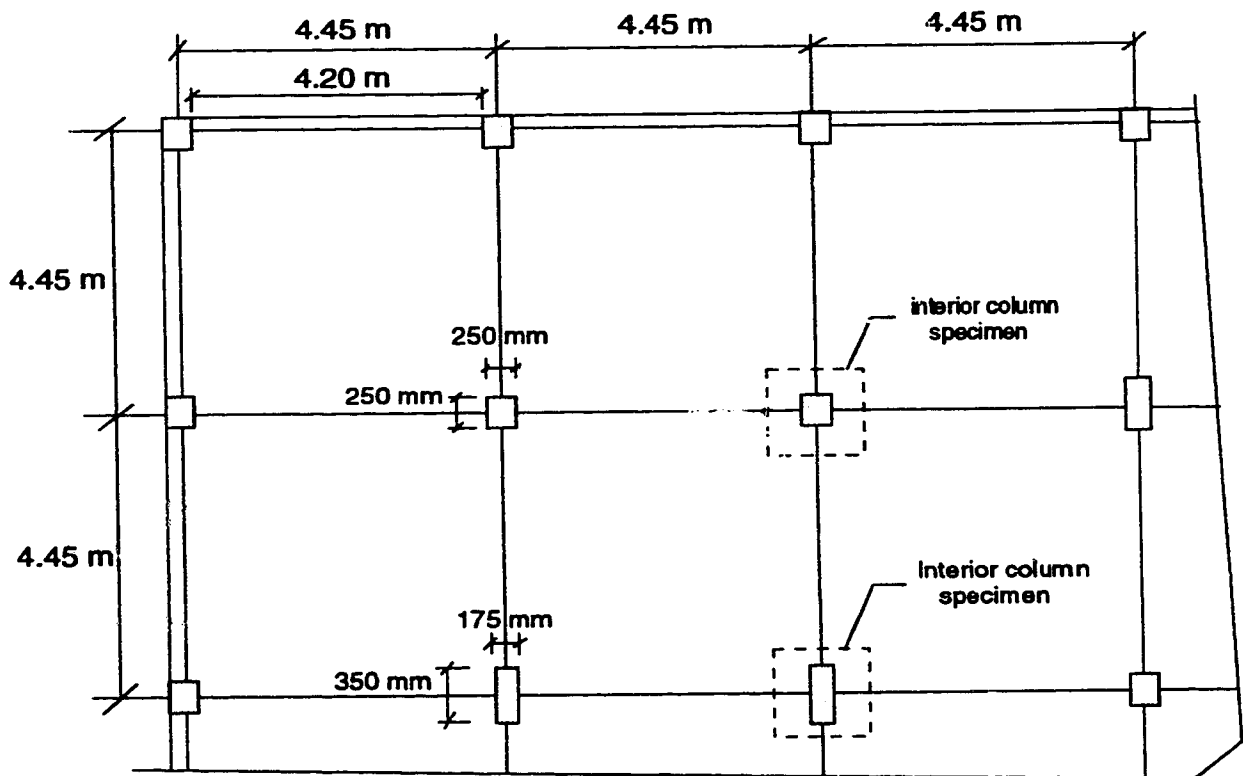
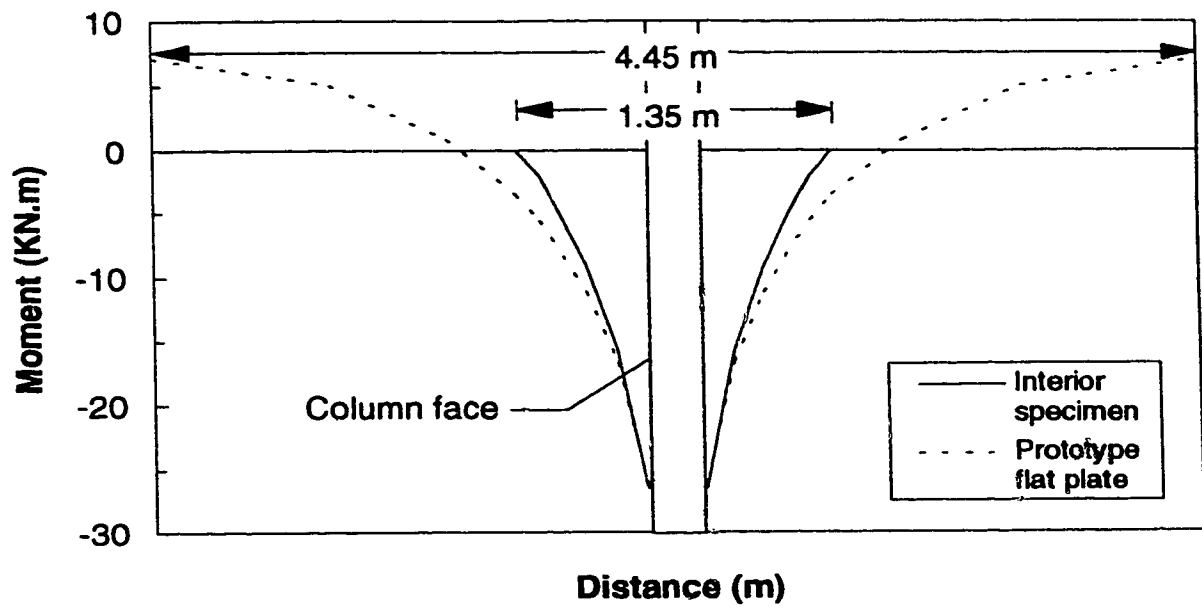


Figure 3.3 Geometry of sandwich column specimens

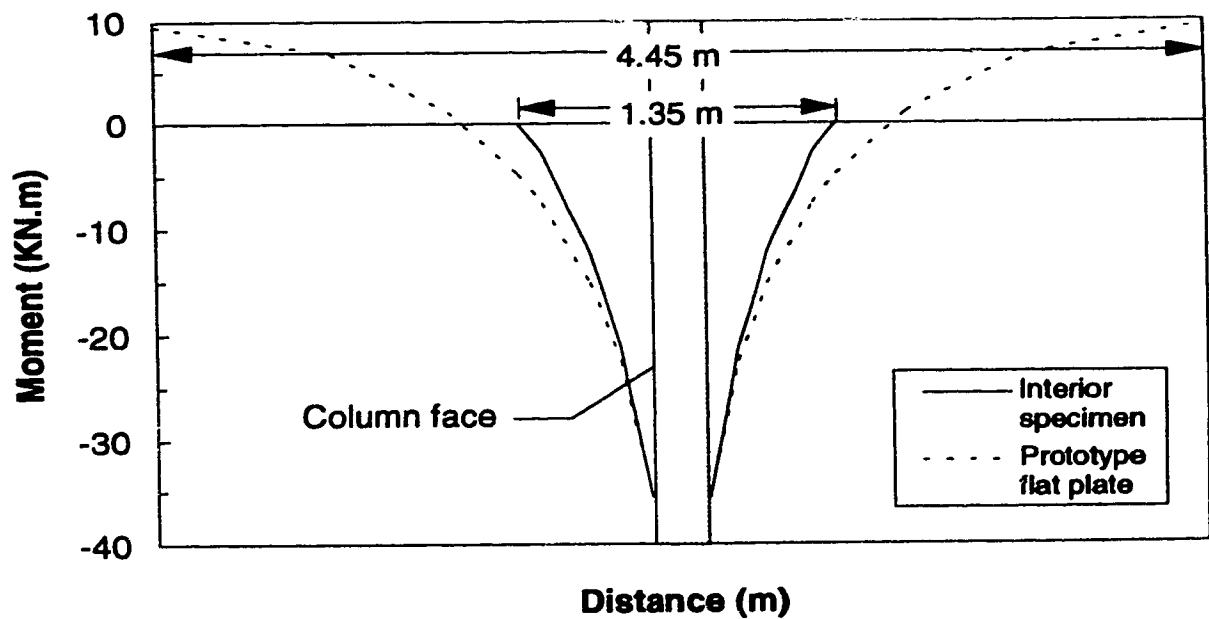


Note: Columns not drawn to scale

Figure 3.4 Prototype flat plate structure (series B specimens)



**Figure 3.5 Flexural Moments from SAP90 analyses
($h/c=0.60$)**



**Figure 3.6 Flexural Moments from SAP90 analyses
($h/c=1.00$)**

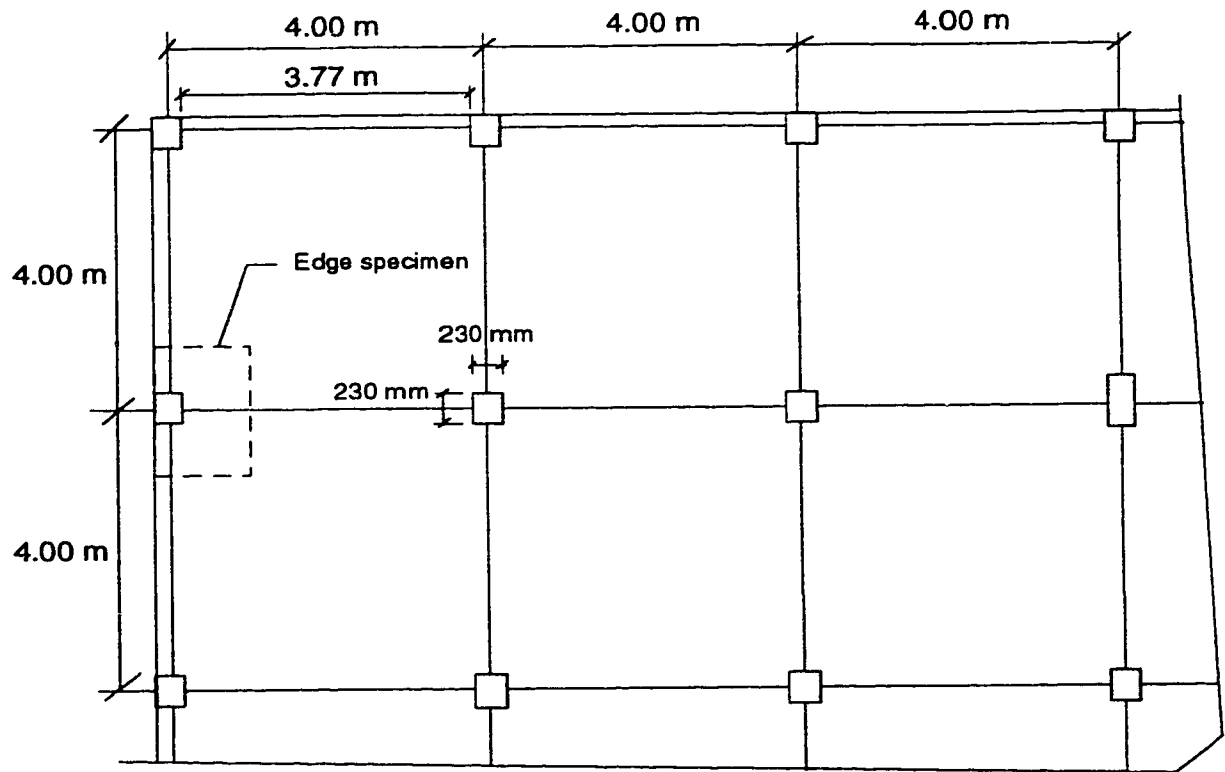


Figure 3.7 Prototype flat plate structure (series C specimens)

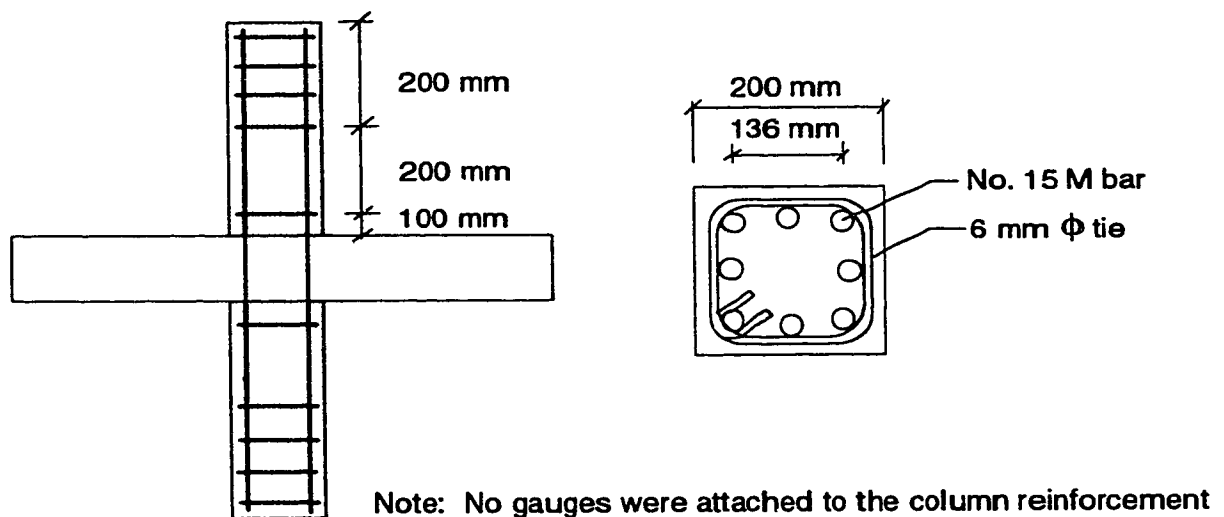


Figure 3.8 Column reinforcement layout (series A specimens)

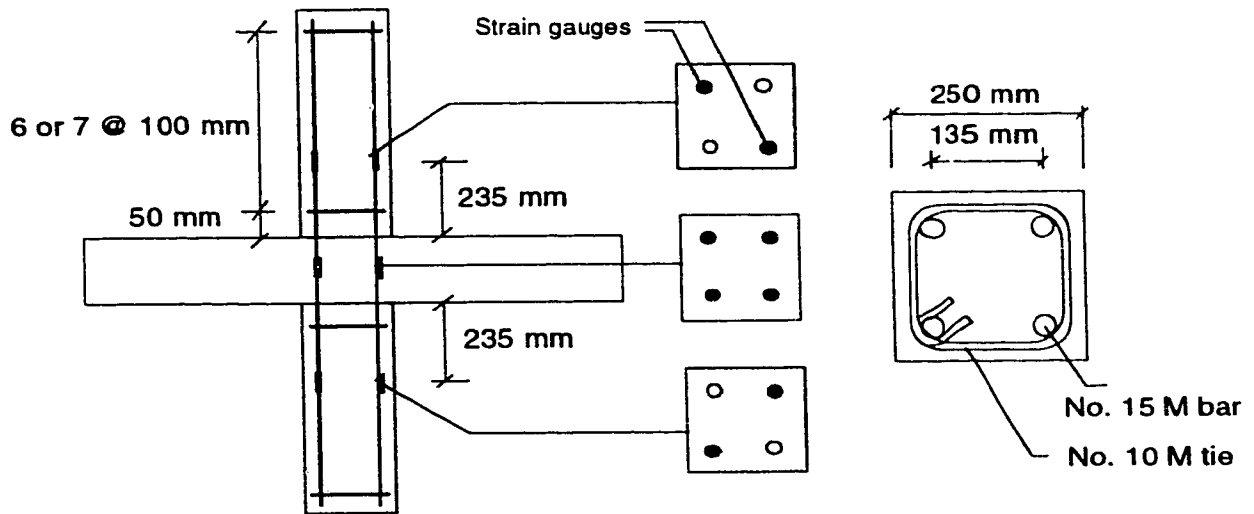


Figure 3.9 Column reinforcement and strain gauge layout (series B specimens)

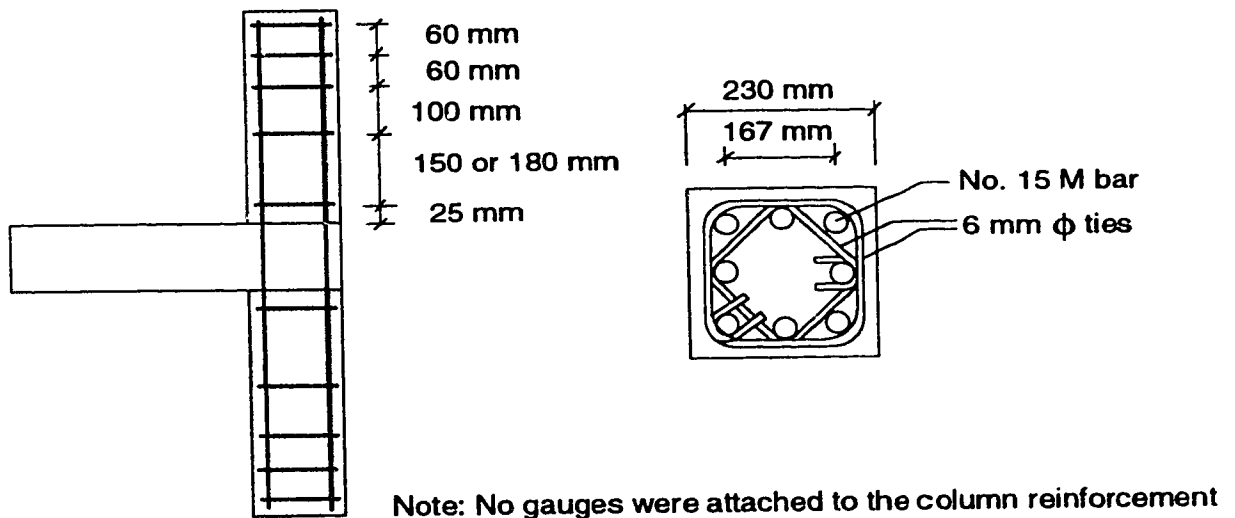


Figure 3.10 Column reinforcement layout (series C specimens)

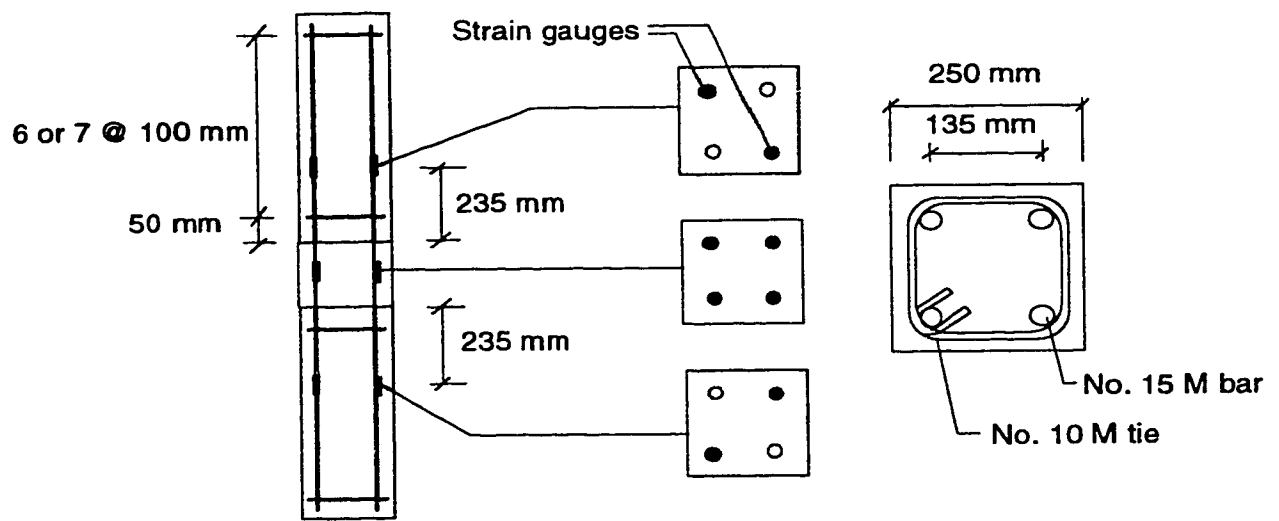
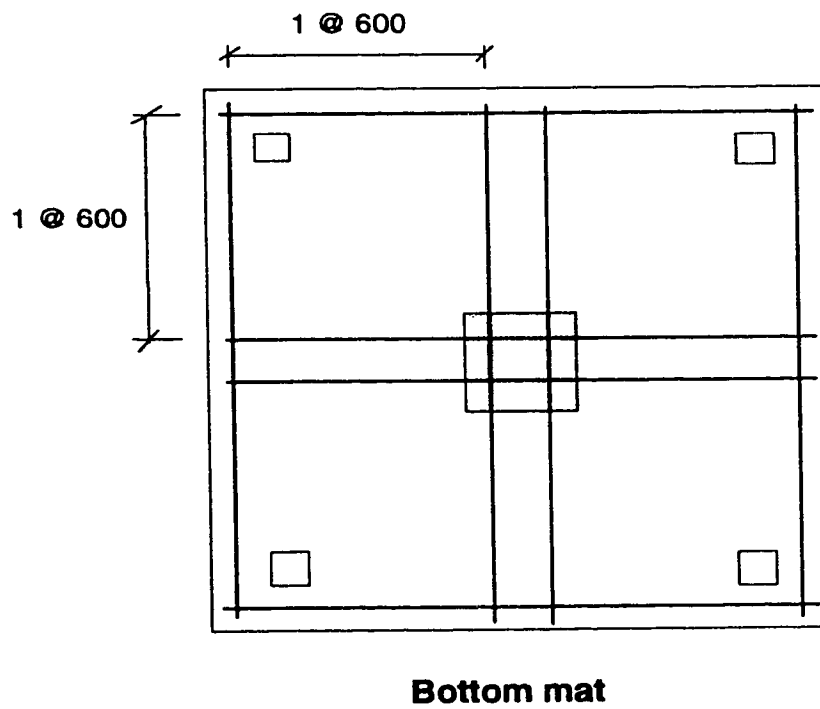
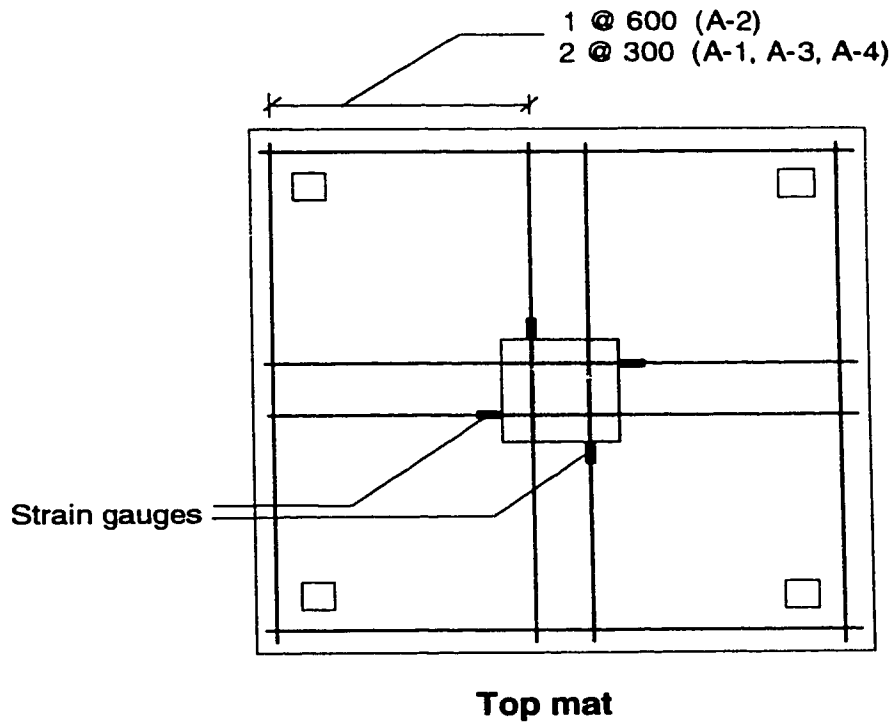
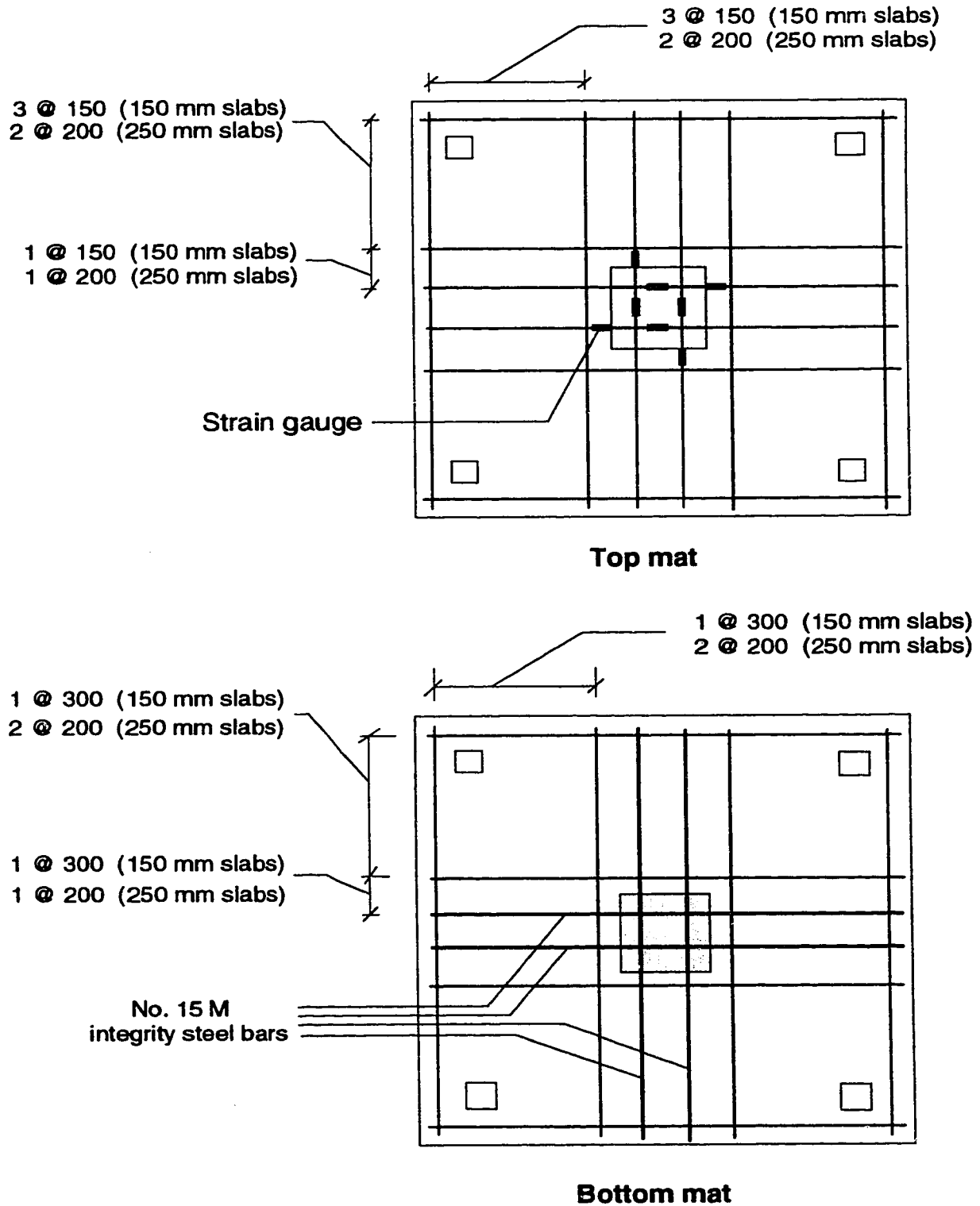


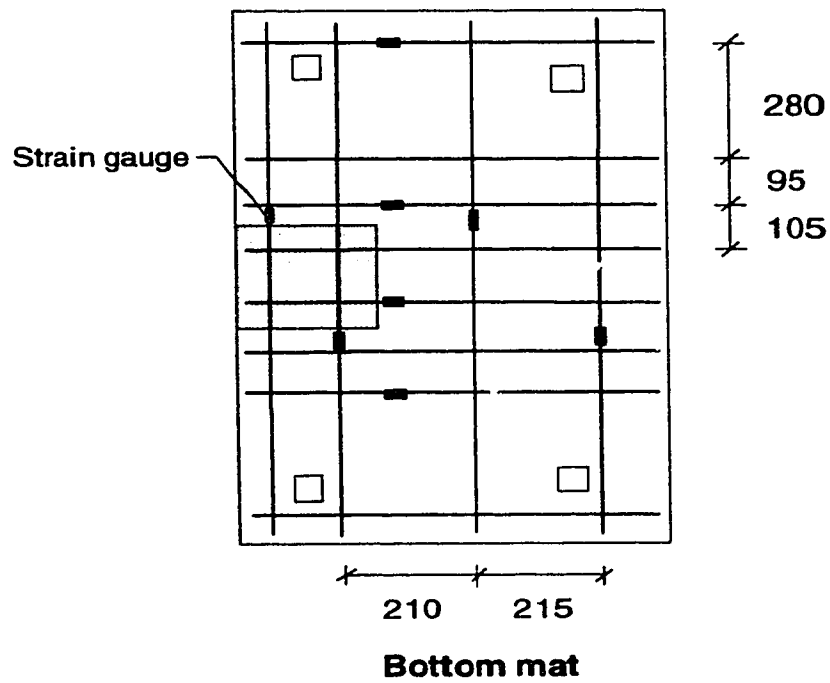
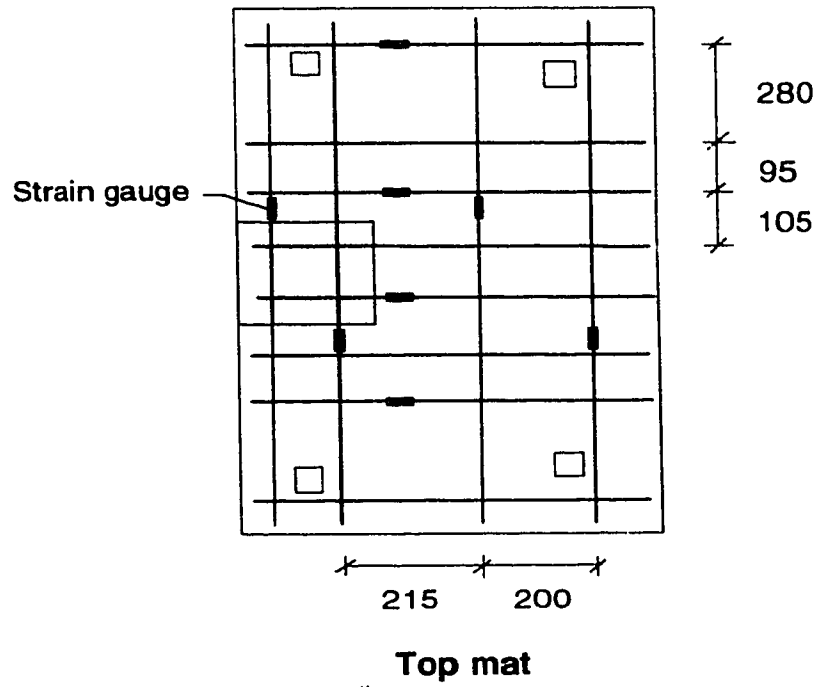
Figure 3.11 Column reinforcement and strain gauge layout (series D specimens)



**Figure 3.12 Slab reinforcement and strain gauge layouts
(Series A specimens)**



**Figure 3.13 Slab reinforcement and strain gauge layouts
(Series B specimens)**



**Figure 3.14 Slab reinforcement and strain gauge layouts
(Series C specimens)**

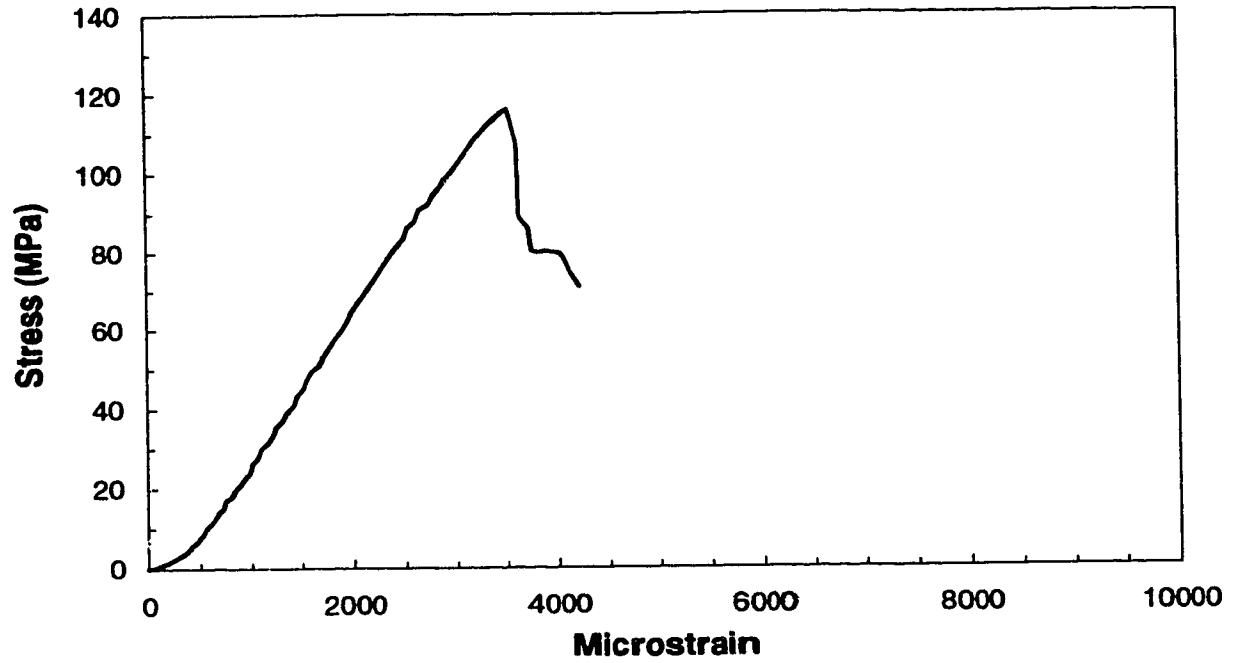


Figure 3.15 Stress-strain curve for HSC cylinder

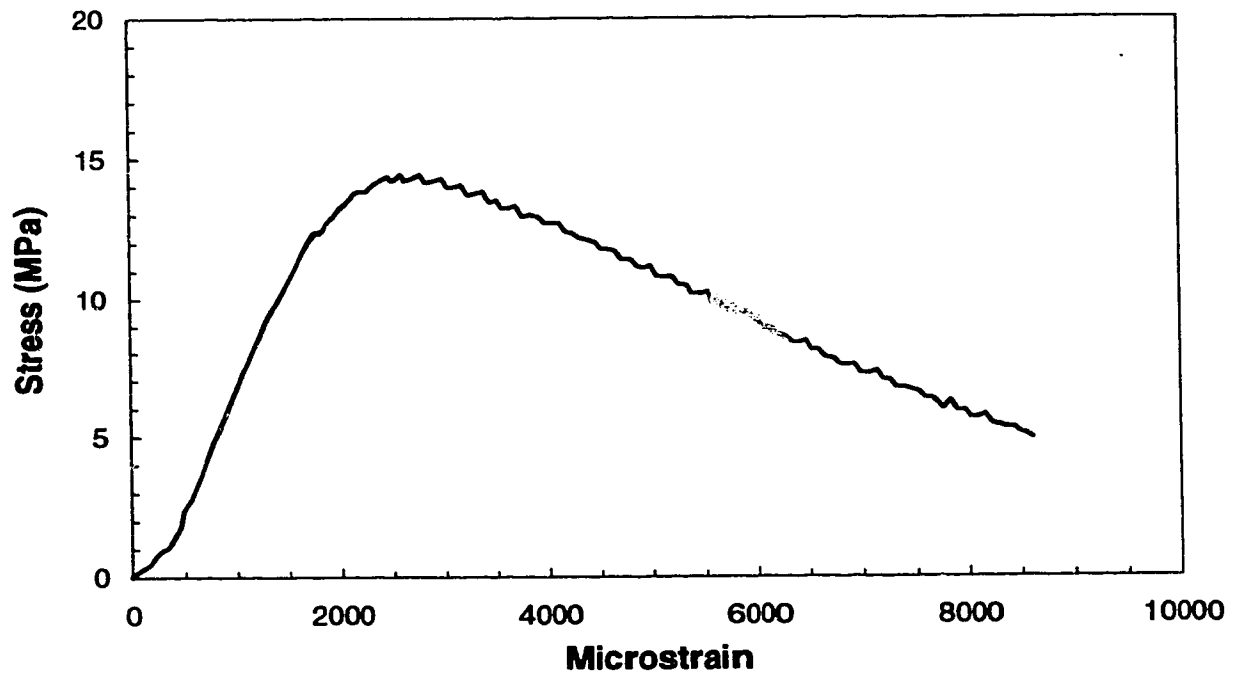


Figure 3.16 Stress-strain curve for slab concrete

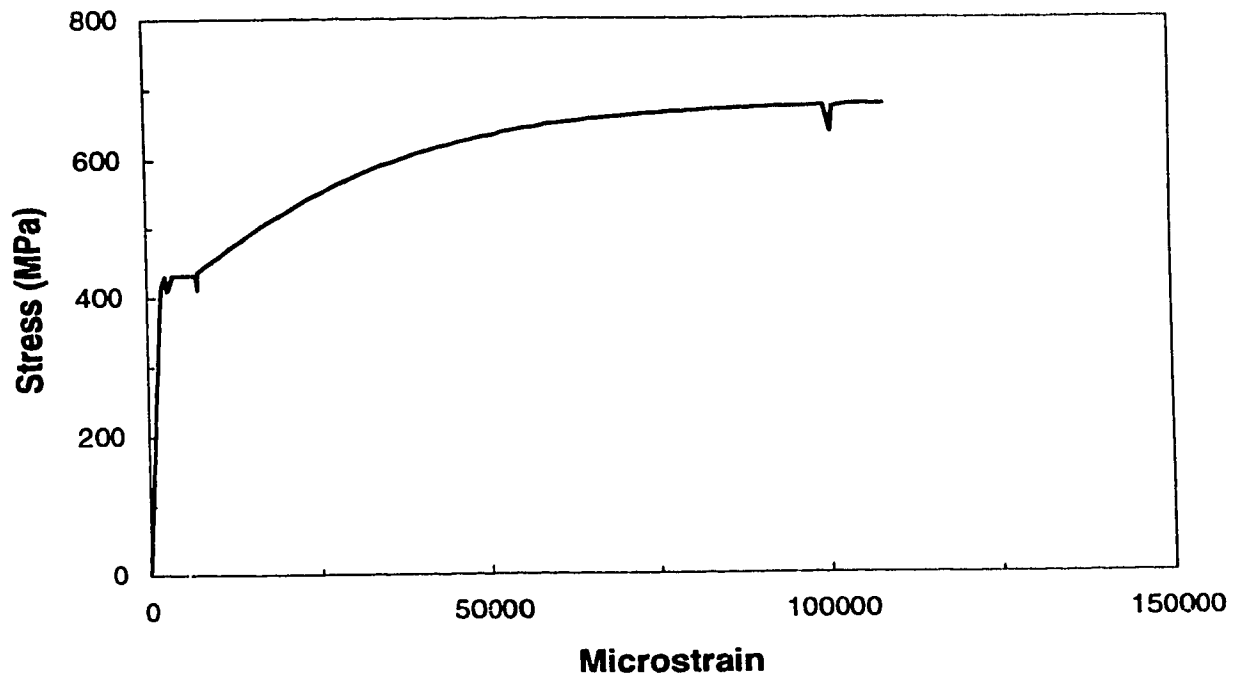


Figure 3.17 Stress-strain curve for No. 15 M bar

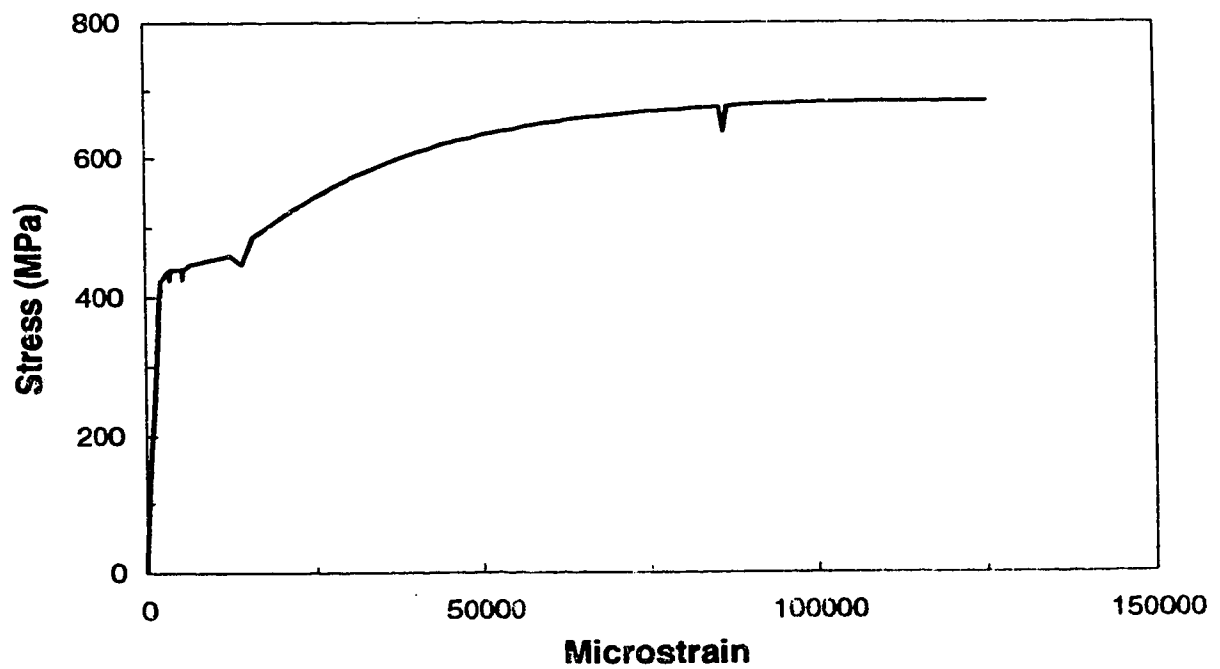


Figure 3.18 Stress-strain curve for No. 10 M bar

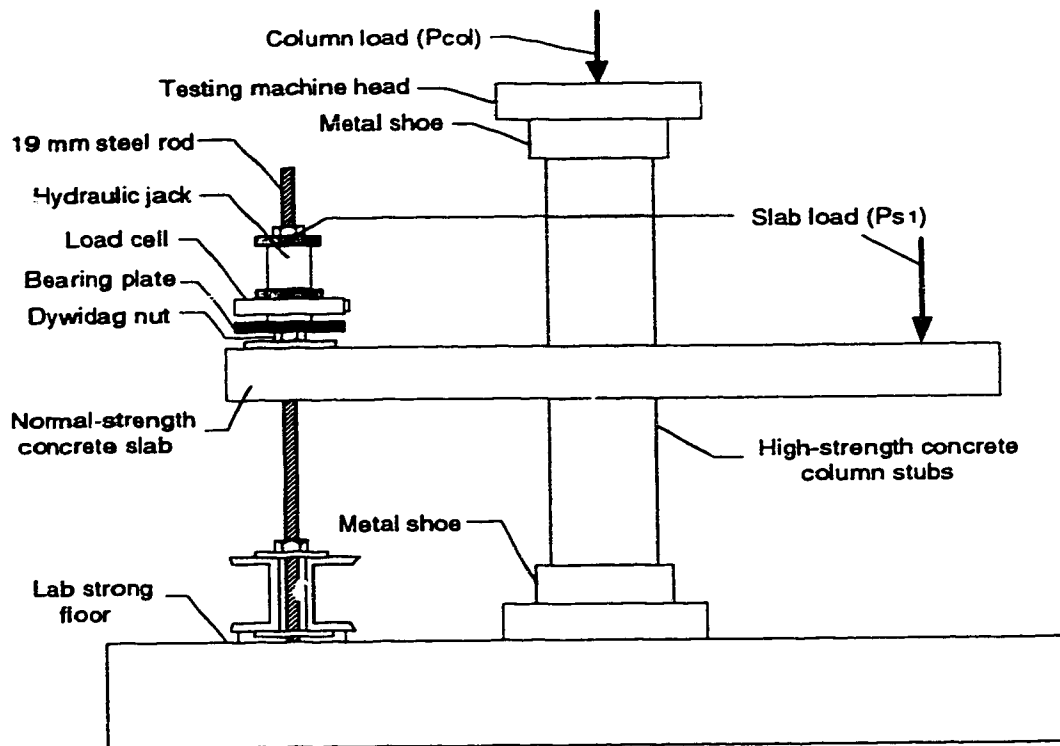


Figure 3.19 Test set-up for interior sandwich plate specimens

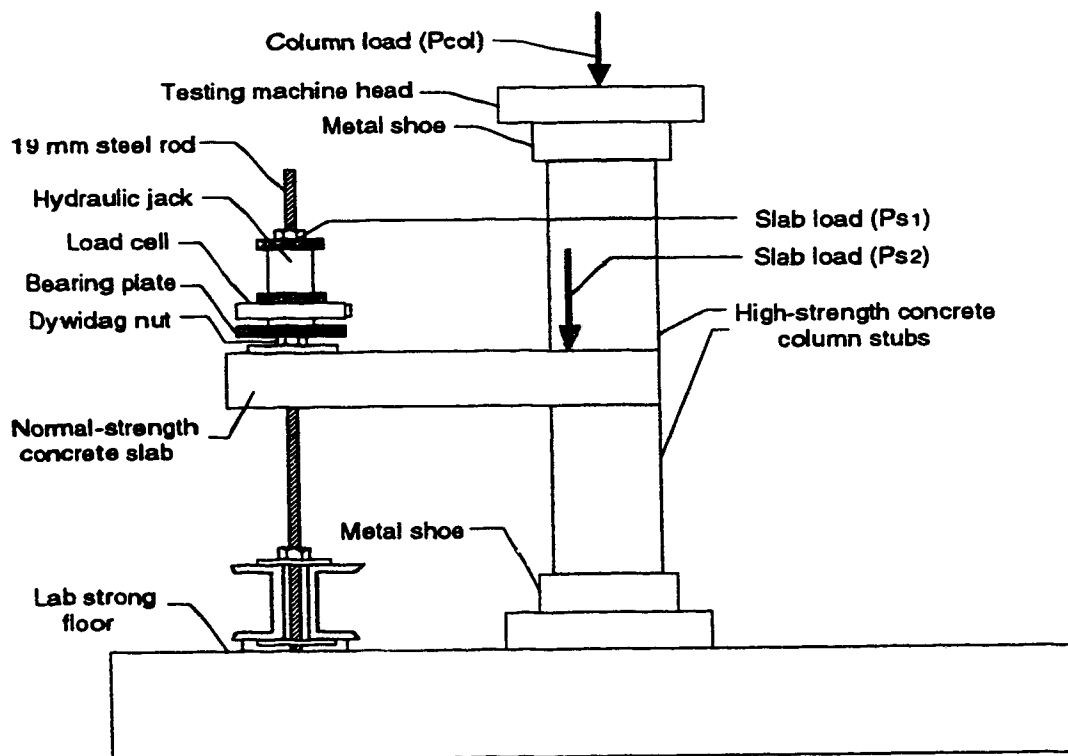


Figure 3.20 Test set-up for edge sandwich plate specimens

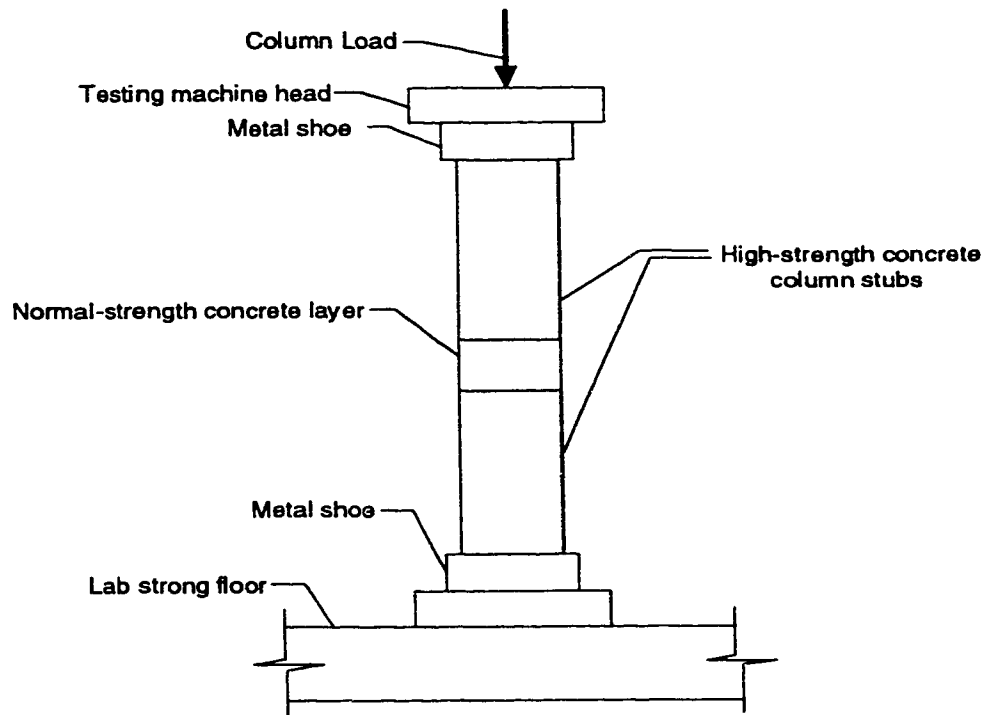


Figure 3.21 Test set-up for sandwich column specimens

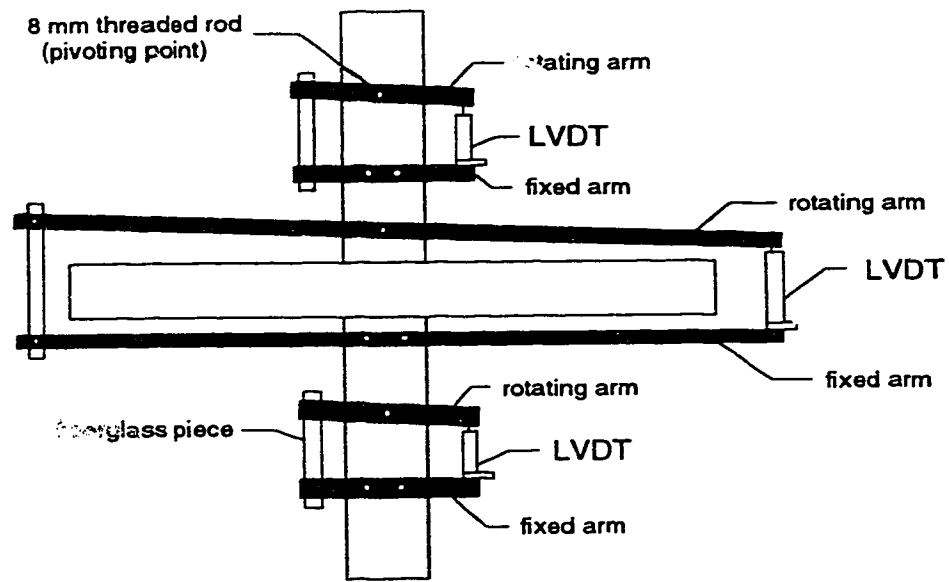


Figure 3.22 LVDT set-up for series A specimens

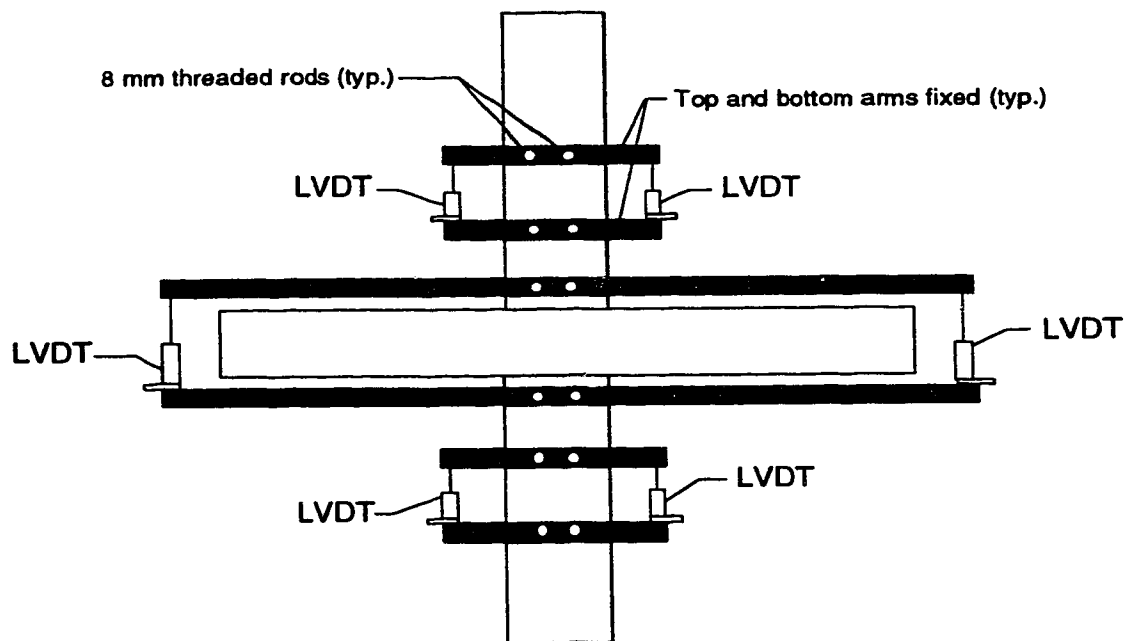


Figure 3.23 LVDT set-up for series B square column specimens

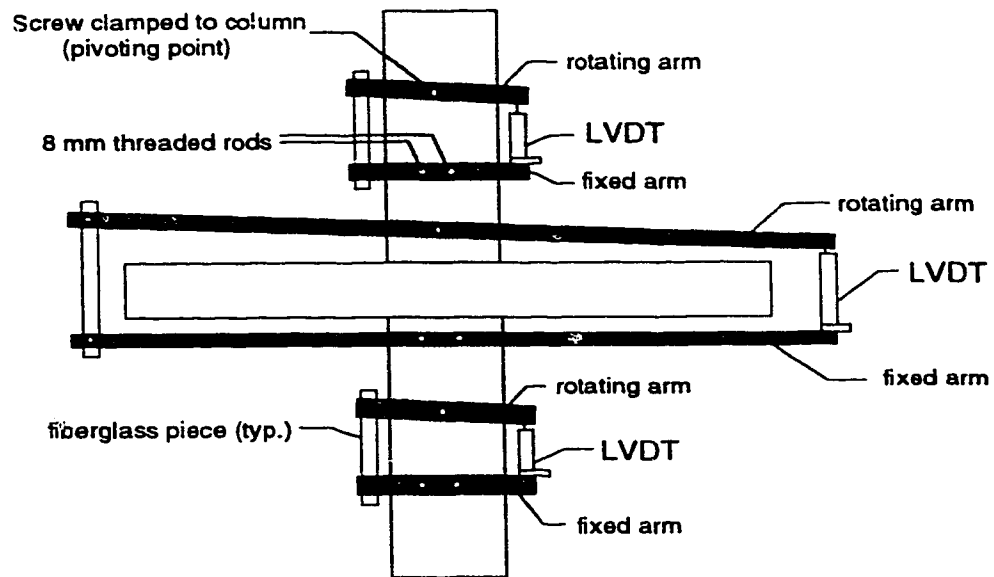


Figure 3.24 LVDT set-up for series B rectangular column specimens

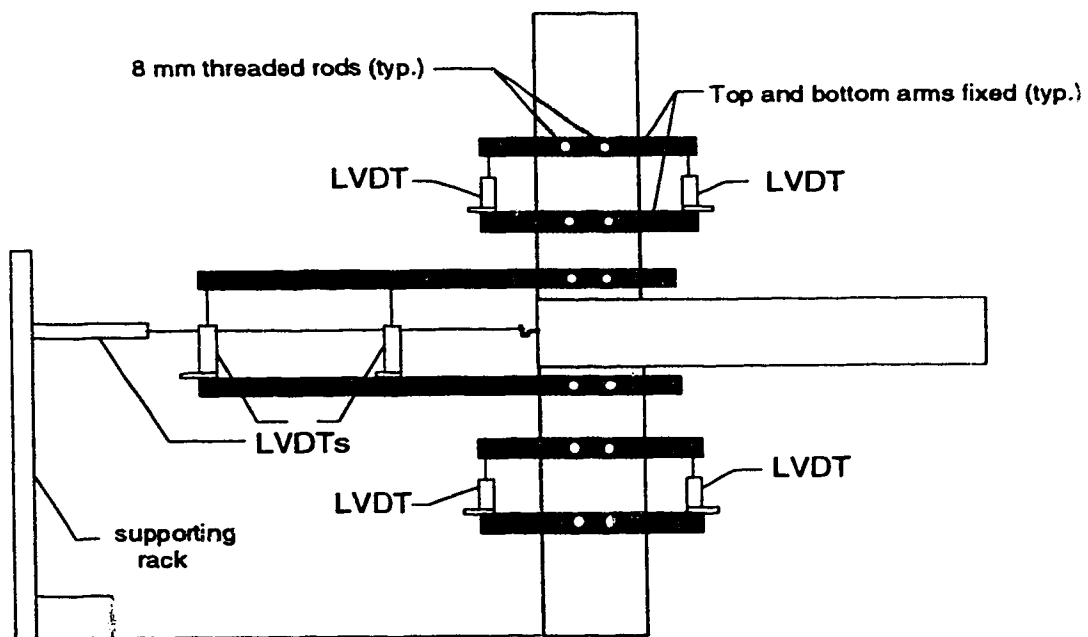


Figure 3.25 LVDT set-up for series C specimens

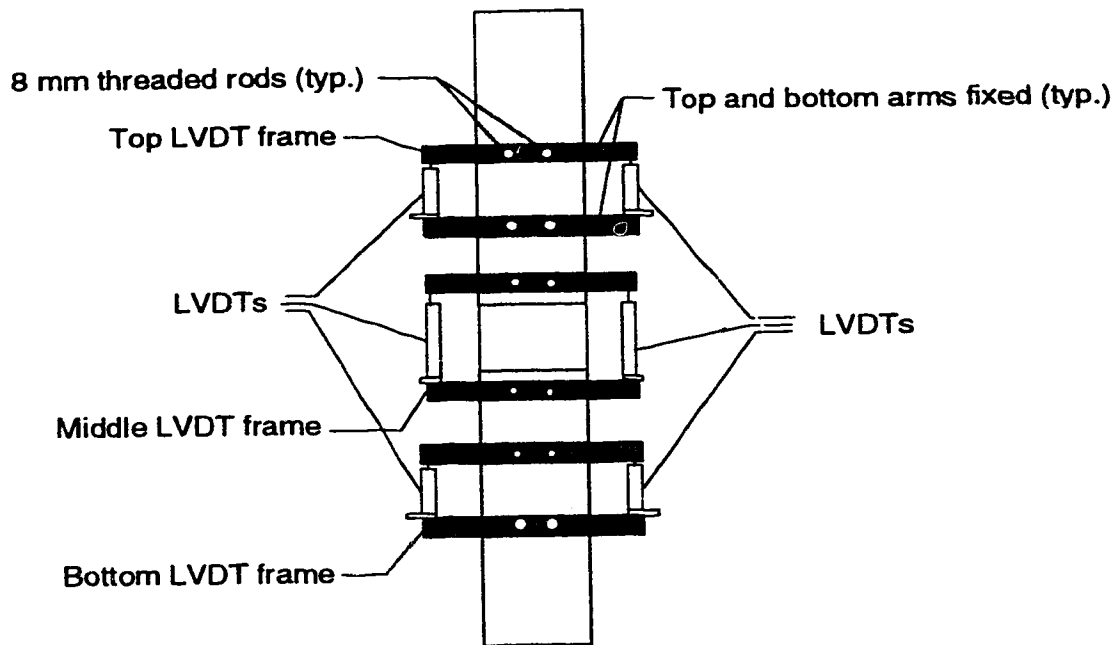


Figure 3.26 LVDT set-up for series D specimens

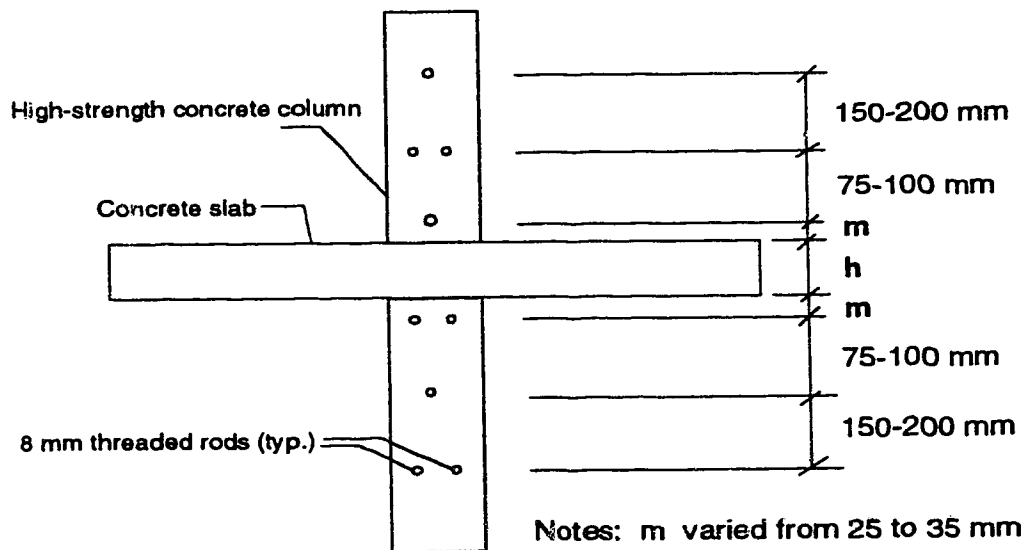


Figure 3.27 Parameters to calculate the column strain through the slab thickness

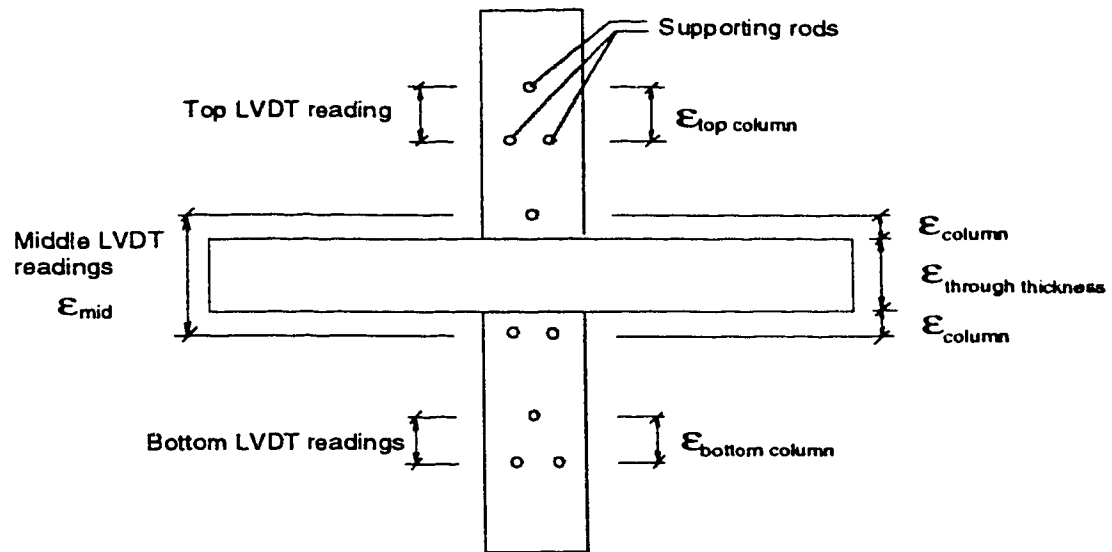


Figure 3.28 Relationship between the column strain through the slab thickness and the LVDT strain readings

4. TEST RESULTS AND OBSERVATIONS

4.1 General

Test results are summarized in table 4.1 . This table shows the ratios of slab thickness to column width, h/c , the ratios of column concrete cylinder strength to slab concrete cylinder strength, f'_{cc}/f'_{cs} , the maximum applied column loads, the maximum effective compressive strengths, f'_{ce} , and the ratios of column effective compressive strength to slab concrete cylinder strength, f'_{ce}/f'_{cs} , for all of the test specimens. Strain readings in the top slab reinforcement at the column face immediately after imposition of the slab loads are also included. Results are presented according to the type of specimen, namely interior sandwich plate, edge sandwich plate or sandwich column.

Stress-strain relationships for each of the test specimens are shown in appendix B. Stress-strain plots constitute a useful way to identify the different carrying load mechanisms within the specimens and to qualify the different cracking stages throughout the tests. Appendix B includes plots of the applied compressive stress in the column, f_{ce} , against the column longitudinal strain through the slab thickness and as a function of the strain readings from gauges attached to the column and/or the slab reinforcement.

This chapter also reports observed conditions through the tests along with sketches of crack patterns and pictures of the specimens during and after testing.

4.2 General behaviour of the test specimens

Figures 4.1 and 4.2 show schematic relationships between the column effective compressive strength, f'_{ce} , and the column strain through the slab thickness, for interior sandwich plate specimens with and without slab loads, respectively. Fig. 4.3 shows the idealized stress-strain curve for slab-loaded and slab-unloaded edge sandwich plates. The schematic stress-strain relationship for sandwich columns is provided in fig 4.4 .

For all of these figures, three distinct stages of behaviour are identified. Stage I illustrates the behaviour of the specimen at the commencement of the test. During this phase, the stress-strain curve exhibits a linear-elastic behaviour. The end of stage I and the beginning of stage II is indicated by a pronounced decrease in the slope of the stress-strain curve. This results from the crushing of the slab concrete at the joint region as the applied column effective stress reaches the cylinder strength of the slab concrete. This also coincides with yielding of the column vertical reinforcement at the joint region. Beyond this level, the stress-strain curve further increases. Across stage II, the specimen undergoes a continuous loss of stiffness. This is observed as a gradual decrease in the slope of the stress-strain curve. Length of stage II and magnitude of the slope of the stress-strain curve varied according to the type of specimen tested. The point at which the column maximum stress is reached marks the boundary between stage II and stage III. The strain corresponding to the peak stress is defined as the ultimate strain. Stage III covers the post-peak behaviour

of the specimen. Length and magnitude of stress-strain curve through stage III varied according to the type of specimen tested.

4.2.1 Interior sandwich plate specimens

4.2.1.1 Interior specimens with loaded slabs

The schematic stress-strain behaviour of an interior sandwich plate with loaded slab is shown in fig. 4.1 .

Cracks in the slab top level were first noticed after 50 to 60% the slab load was imposed. These cracks are believed to form from shrinkage cracks that just widened as a result of the slab loading. Cracks extended from the column to the slab boundaries directly on top of the slab reinforcement mat. This was accompanied by a downward deflection of the slab segment. No further slab cracking was noticed during stage I.

Crushing of the joint concrete and yielding of the column reinforcement at the slab portion occurred almost simultaneously. Direct observation of joint crushing was not possible since the joint was covered by the surrounding slab. Joint crushing coincided with the slab strains at the joint centreline overtaking those at the column face. Strain readings for the column longitudinal reinforcement are shown as well in appendix B. It can be seen that column strains in the joint are always higher than those outside the joint.

Yielding of the slab reinforcement at both column face and joint centre was observed at the beginning of stage II. Yielding of the slab steel was recorded at higher stresses for specimens with stronger slabs. Yielding of the column reinforcement outside the joint region was only observed for specimens B-2, B-3 and B-6.

When the applied column effective stress reached 70 to 85% the maximum column strength, the existing slab cracks began to widen and the slab deflected further downwards. At this level, additional cracks formed around the top column outline and within the slab corner around the jacks. Cracks along the column outline opened wide rather than closed. This suggests that the slab concrete provided little or no restraint to the upper portion of the joint. No cracks were observed on the slab underside at the end of stage II.

It is worth noting that throughout stage II it was necessary to pump the jacks at very short time intervals to keep the slab load constant. Failure to do so resulted in not only a decrease in the level of slab load but also in an increase of the column effective strength. This may be observed from the stress-strain curve of specimen B-5 shown in appendix B.

Immediately before reaching the maximum column strength splitting cracks extended from the joint into the top column stub. Spalling of column concrete was noticed in the corners of the column above the slab. This behaviour suggests that more restraint was provided to the lower half of the joint than to the upper portion. At this level, cracks formed on the

slab underside. These cracks formed along the diagonals of the slab segment, extending from the column corners towards the slab edges. Once the maximum column load was reached, additional spalling of concrete at the corners of the top column stub was observed. Column cracks widened and penetrated further into the column. Stage II covered approximately 70 to 80% of the ultimate strain.

Through stage III, specimens with loaded slabs displayed a ductile behaviour. Cracking of concrete at the top column progressed rapidly with concrete chunks frequently falling off. Spalling of column concrete below the slab was rarely observed. Tests were suspended when significant reduction of the axial load capacity was attained. However, it is worth mentioning that the specimens continued carrying load when the tests were terminated. Buckling of the column reinforcement at the slab region was not observed for these specimens. At final stages of the tests, deflections of at least 30 mm were measured at the slab corners.

Pictures of interior sandwich plates under testing are presented in fig. 4.5 and 4.6. These correspond to interior sandwich plates with h/c ratios of 1.0 and 0.6, respectively. Figure 4.7 shows the typical crack pattern of an interior sandwich plate with a slab thickness-to-column width ratio, h/c , of 1.0. A crack pattern of an interior specimen with an h/c ratio of 0.6 is illustrated in fig. 4.8.

4.2.1.2 Interior specimens with unloaded slabs

Fig. 4.2 illustrates a typical stress-strain relationship for interior sandwich plates tested in the absence of slab loads.

As with the specimens subjected to slab loading, specimens with no slab loads displayed linear elastic behaviour through stage I. No cracks were observed during this phase. Crushing of the joint concrete coincided with yielding of the column longitudinal bars at the joint region. First cracks in the slab top level were noticed when the applied column stress was approximately 60% the maximum column strength. These cracks formed along the slab diagonals, starting at the column corners and extending towards the slab corners. These cracks result from the lateral expansion of the joint concrete because of the Poisson's ratio effect. Cracks formed approximately at 45° to the slab reinforcement since this is the direction of minimum stiffness for a reinforcement mesh with equally spaced bars running at each direction. The observed cracking pattern suggests the formation of diagonal compression struts along the slab diagonals interacting with tension rings acting along the slab segment periphery. These tension ties resemble the behaviour of a square hoop, as shown in fig. 4.9.

As the column load further increased, existing cracks widened and extended towards the slab corners. At this level, yielding of the column longitudinal reinforcement outside the joint region was observed. Later, cracks formed at the slab mid-edges right in between the cracks along the slab diagonals and progressed towards the column. These cracks formed through the full slab thickness. For this reason, top and bottom cracking patterns were

similar. As illustrated in fig. 4.10, this cracking behaviour resembles that of a deep beam lying in the plane of the slab. Tension in the top and bottom slab reinforcing steel resulting from the joint lateral expansion is equilibrated by tensile stresses in the slab reinforcing steel.

Just before the maximum column load was attained, the lateral expansion of the joint concrete caused splitting cracks to penetrate into the upper column stub. Because the slabs were more reinforced at the bottom portion of the joint, more restraint is applied to the joint lower region than at the top. Stage II spanned approximately 80 to 90% the ultimate column strain through the slab thickness. Ultimate strains ranged from 0.006 to 0.02.

Following the formation of splitting cracks in the upper column, failure of the specimen was imminent. The observed failure was explosive and brittle. Large portions of column concrete spalled off violently above the slab and the column longitudinal reinforcement buckled at the same location. The sole specimen with unloaded slab in exhibiting a ductile behaviour across stage III was specimen A4-A. This is attributed to the presence of lower strength concrete in the slab segment, and a relatively thick slab.

A picture of specimen B-4 under testing is shown in fig. 4.11 . Figure 4.12 illustrates the failure at the specimen top column stub. A sketch of the typical crack pattern of an interior sandwich plate with unloaded slab is shown in fig. 4.13.

4.2.2 Edge sandwich plate specimens

4.2.2.1 Edge specimens with loaded slabs

The stress-strain behaviour of edge specimens under slab loading follows the schematic path shown in fig. 4.3 .

After imposing the slab loads, cracks formed on top of the slab in the direction perpendicular to the slab free edge. These cracks may have resulted from existing shrinkage cracks that became visible due to the imposition of the jacking loads. As a result of the slab loads, the slab segment deflected downwards. Average strain readings at the face of the column are included in appendix B.

At the beginning of stage II, vertical splitting cracks formed at the visible face of the joint. Cracks in the slab widened and progressed from the column towards the slab edge, parallel to the free edge, forming directly over the slab top reinforcement. It became difficult to keep the jack loads at the desired level. As was the case for the interior sandwich plates, a decrease in the jacking loads resulted in an increase in the column strength.

As the column load increased, torsional cracks formed at the free face of the joint starting at the corners of the slab-top column interface. This was followed by the formation of

diagonal cracks on the slab top level close to the column. These cracks propagated from the interior corners of the upper column outline and spread apart until reaching the slab free edge. Based on these observations and also on the strain readings from gauges attached at both top and slab bottom reinforcing bars crossing the joint, the system of forces acting on the edge joints is illustrated in fig. 4.14.

Following the formation of the torsional cracks, splitting cracks in the joint extended into the top column. Significant loss of stiffness during stage II was observed compared to that for the interior plates. Stage II covered 90% of the ultimate strain. After stage III started, spalling of concrete was observed in the top column above the slab. This was followed by buckling of the column longitudinal reinforcement at the same location. Spalling of column concrete limited to upper column stub. Cracks in the slab underside were not observed. When tests were stopped, the column still was carrying a significant amount of load.

A picture of an edge specimen under testing is shown in fig. 4.15 .Figure 4.16 illustrates the typical crack pattern for an edge sandwich plate with slab heavily loaded.

4.2.2.2 Edge specimens with unloaded slabs

The stress-strain behaviour of an edge plate not subjected to slab loading is also similar to that displayed in fig. 4.3 . Specimens remained intact until stage II began. At this level, vertical splitting cracks formed at the joint free face. These cracks are attributed to the lateral expansion of the joint because of the Poisson's ratio effect. Cracks then formed on the slab top level. These cracks radiated from the column region towards the slab boundaries in a similar way than that exhibited by the interior plates with unloaded slabs.

As the column load increased, splitting cracks extended from the joint into the upper and lower column stubs. At the joint region, the concrete spalled resulting in the loss of readings of the joint lateral expansion. Later, column cracks widened and lengthened. This was followed by spalling of concrete in the corners of the upper column right above the slab. Splitting cracks were observed in much less degree at the bottom column stub. This is attributed to the fact that specimens were provided with more reinforcement at the joint bottom region than at the top.

Through stage II, Edge specimens with unloaded slabs displayed additional loss of stiffness compared to the edge plates with loaded slabs. Ultimate strains for the edge plates tested in absence of slab loads exceeded those recorded for the specimens with loaded slab segments. Stage II covered approximately 90% of the ultimate strain.

Shortly after reaching the maximum column strength buckling of the column vertical bars was observed at the joint region. This was accompanied by the opening of joint concrete along the path of these bars. Unlike the majority of interior plates without slab loads, the slab-unloaded edge specimens exhibited a ductile behaviour. Tests were suspended with the column concrete still carrying load.

Picture of an edge plate specimen without slab loads after conclusion of test is shown in fig. 4.17 . A representative crack pattern of this specimen is shown in fig. 4.18 .

4.2.3 Sandwich column specimens

The schematic shape of the stress-strain curve for the sandwich column specimens is similar to that recorded for the interior sandwich plates. However, significant reduction in strength and ultimate strain are observed for the sandwich columns. The schematic stress-strain relationship is shown in fig. 4.4 .

As is the case of most axial compression tests, no visible column cracking was noticed until the applied effective stress in the column was close to the maximum column compressive strength. Specimens remained intact along stage I. First cracks to be observed corresponded to vertical splitting cracks forming at the joint region at 90% the failure load. This was followed by concrete spalling off at the joint region and splitting cracks extending into both top and bottom column ends. Spalling of concrete was then observed in both top and bottom high-strength concrete column ends.

The maximum column strength was reached shortly after the cylinder strength of the joint concrete was reached. At the end of stage III, buckling of the column longitudinal reinforcement was observed along with significant widening of cracks within the columns. Specimens displayed some ductility and when tested were suspended the columns were still carrying the applied compressive load.

Figure 4.19 shows a sandwich column under testing. A picture of the four sandwich columns after failure is given in fig. 4.20 . A typical cracking of a sandwich column is illustrated in fig. 4.21 .

4.3 Effect of slab loading

Figures 4.22 and 4.23 show the effect of slab loading on the strength of interior sandwich plate specimens. Fig. 4.24 illustrates the same effect for edge sandwich plates.

The observed behaviour confirms that the behaviour of the specimens with loaded slabs is significantly different from the specimens with no slab loads. Figure 4.22 shows a comparison of the stress-strain curves exhibited by specimens A4-A, A4-B and A4-C. With all other factors being equal, slab loads of zero, medium and high intensity were applied.

Figure 4.23 shows a comparison of the stress-strain behaviour displayed by specimens B-2 and B-4. Specimen B-2 was tested with service level slab loads whereas specimen B-4 had no slab loads. Figure 4.24 shows the stress-strain behaviour of three edge plates tested under three different levels of slab loading, ranging from zero to heavy load levels.

Figure 4.25 compares the joint transverse strain at column face and at column centreline for two interior sandwich plate specimens, specimen B-2 (slab-loaded) and specimen B-4 (slab-unloaded). At early stages of the test, strains at both column face and column centreline indicate that the slab top level is subjected to tension.

For specimen B-2 (loaded slab) the tensile strains at the face of the joint through stage I are higher than those at the joint centre. This difference became larger for specimens with thinner slabs. Following the imposition of slab loads the strains at the joint centreline increased at a faster rate than at the joint face. Strains at the joint face remained almost constant throughout stage I. Strains at the joint centreline overtake those at the column face when the joint concrete crushes and the column vertical bars yield. Beyond this level, both strain readings increase in tandem.

For specimen B-4 (unloaded-slab) the tensile strains at the face of the joint are less than the strains at the column centreline. This observation applies for the entire duration of the test.

It can be seen from fig. 4.25 that the stress-strain curves at the joint centreline and at the column face for specimen B-2 (loaded slab) virtually parallel the corresponding stress-strain curves for the specimen B-4 (unloaded slab). At the joint centreline the difference in strain between both curves is 1000 microstrain. At the column face this difference increases up to 1500 microstrain.

The fact that strains at the column face are higher than those at the column centreline implies that under column and slab loading the upper half of the joint not only loses the benefits from confinement but also that the top joint region is pulled apart by the slab bending action. At the top, the joint may be viewed as a concrete prism subjected to a triaxial state of stress consisting of longitudinal compression from the column load and biaxial transverse tension from the slab bending. This effect leads to a reduction in the column axial load capacity because concrete under transverse tension softens (Chen and MacGregor (1993)). Since it is required for equilibrium of forces and moments that the transverse tension at the top be equilibrated at the bottom by transverse compression, only the bottom portion of the joint is subjected to confinement from the surrounding slab concrete. At the bottom portion, a triaxial state of stresses consisting of the longitudinal compressive column load plus biaxial transverse compression may be identified. Fig. 4.26 illustrates this behaviour.

For the specimens with no slab loads, the tension of the top and bottom slab reinforcing bars crossing the column is equilibrated by compression from the surrounding slab concrete since no flexural moment is applied. In this case, the compressive triaxial state of stress acts over the full depth of the joint, in other words, the joint is fully confined by the surrounding slab concrete. This is illustrated in fig. 4.27. Since confinement acts over the full depth of the joint an enhancement of column effective compressive strength is expected in joints with unloaded slabs compared to that in joints with loaded slabs.

4.4 Effect of the h/c ratio

The effect of the slab thickness to column width ratio, h/c , on the stress-strain behaviour of interior sandwich plates and sandwich columns is shown in fig. 4.28 and 4.29, respectively. These figures show graphs of the stress-strain behaviour of specimens built with similar column and slab concrete strengths and different h/c ratios. The ratio of column concrete to slab concrete strength, f'_{cc}/f'_{cs} , was 6.33 for the interior sandwich plates and 6.18 for the sandwich columns.

For both the interior plate and the sandwich column specimens the slope of the stress-strain curve across stage II decreases as the h/c ratio increases. Higher peak strengths and strains were reached for the interior plate specimens as it is expected for joints surrounded by floor concrete on all of their four sides. The post-peak behaviour appears to be similar for both cases.

For the sandwich column specimens the joint concrete may be considered as a concrete prism compressed by two stronger column ends. These column ends act as the platens of a testing machine. These ends are responsible to provide transverse restraint at the top and bottom levels of the sandwiched layer of concrete. For joints with lower h/c ratios the whole layer of sandwiched concrete benefits from the end condition effect. For joints with higher h/c ratios the confinement effect reduces to the top and bottom levels of the concrete layer thereby reducing the strength of the sandwiched prism.

4.5 Effect of column rectangularity

The effect of column rectangularity is presented in fig. 4.30. This chart shows the stress-strain relationship of two interior sandwich plates built with similar column and slab concrete strengths and with columns of equal cross-section but different in shape. Specimen B-5 had a square column 250 mm wide whereas specimen B-7 had a rectangular column, 175 mm wide and 350 mm deep.

It can be observed that the stress-strain curves are virtually identical. This is attributable to the fact that the column area was almost equal for both specimens. However, it is worth mentioning that the column and slab concrete strengths used in specimen B-7 were slightly higher than those used in specimen B-5. This means that a higher strength was expected for specimen B-7, which in fact, did not occur.

4.6 Effect of high-strength concrete core at the joint region

Figure 4.31 shows the stress-strain behaviour of two interior sandwich plate specimens built with similar dimensions and concrete strengths. The only difference between these two specimens is that specimen B-3 was provided with a high-strength concrete prism at the joint region. This comparison was intended to evaluate the eventual benefits or disadvantages of this constructive feature.

During stage I, both specimens displayed similar behaviour. It can be seen that crushing of the joint concrete occurred at identical levels for both specimens. Through stage II however, the stress-strain curve of the specimen with the built-in core was steeper. A higher column strength was recorded for the specimen with the built-in core whereas a higher ultimate strain was reached for the conventionally-built specimen. This behaviour is similar to that exhibited by high-strength and normal-strength concrete. Likewise, the specimen with the high-strength concrete core displayed a brittle post-peak behaviour compared to the ductile behaviour observed for the coreless specimen.

Phase	Specimen	h/c	P col (KN) *	f'_{ce} (MPa)**	Slab strain ($\mu\epsilon$) †	f'_{cc}/f'_{cs}	f'_{ce}/f'_{cs}
A	A1-A	0.5	3914	100.31	0	2.63	2.51
	A1-B	0.5	3678	93.08	1000	2.63	2.33
	A1-C	0.5	3498	87.56	2000	2.63	2.19
	A2-A	0.5	3820	97.43	0	2.43	2.12
	A2-B	0.5	3807	97.03	1000	2.43	2.11
	A2-C	0.5	3591	90.41	2000	2.43	1.97
	A3-A	0.75	3437	85.69	0	3.56	3.43
	A3-B	0.75	3174	77.63	1000	3.56	3.11
	A3-C	0.75	2275	50.09	2000	3.56	2.00
	A4-A	0.75	3272	80.64	0	4.61	3.51
	A4-B	0.75	2927	70.07	1000	4.61	3.05
	A4-C	0.75	2376	53.19	2000	4.61	2.31
B	B-1	1.0	4072	71.54	750	2.48	1.70
	B-2	0.6	5359	96.08	1600	2.48	2.29
	B-3	1.0	5078	90.72	600	2.57	2.06
	B-4	0.6	6298	113.99	0	2.57	2.59
	B-5	1.0	2703	45.44	1500	6.33	3.03
	B-6	0.6	3720	64.83	2000	6.33	4.32
	B-7 ‡	0.7	2758	47.45	1200	6.32	2.50
	B-8 ‡	1.17	4032	72.25	1800	6.32	3.80
C	C1-A	0.74	3246	59.76	0	3.34	1.87
	C1-B	0.74	3049	55.25	2800	3.06	1.58
	C1-C	0.74	2959	53.18	3200	3.15	1.56
	C2-A	1.0	2936	52.65	0	3.48	1.70
	C2-B	1.0	2736	48.69	1500	3.18	1.43
	C2-C	1.0	2564	44.12	3300	3.27	1.34
D	D-SC1	1.0	1421	21.00	-	6.18	1.24
	D-SC2	0.6	1716	26.61	-	6.18	1.57
	D-SC3	0.5	1991	31.87	-	6.29	1.87
	D-SC4	0.3	2279	37.35	-	6.18	2.20

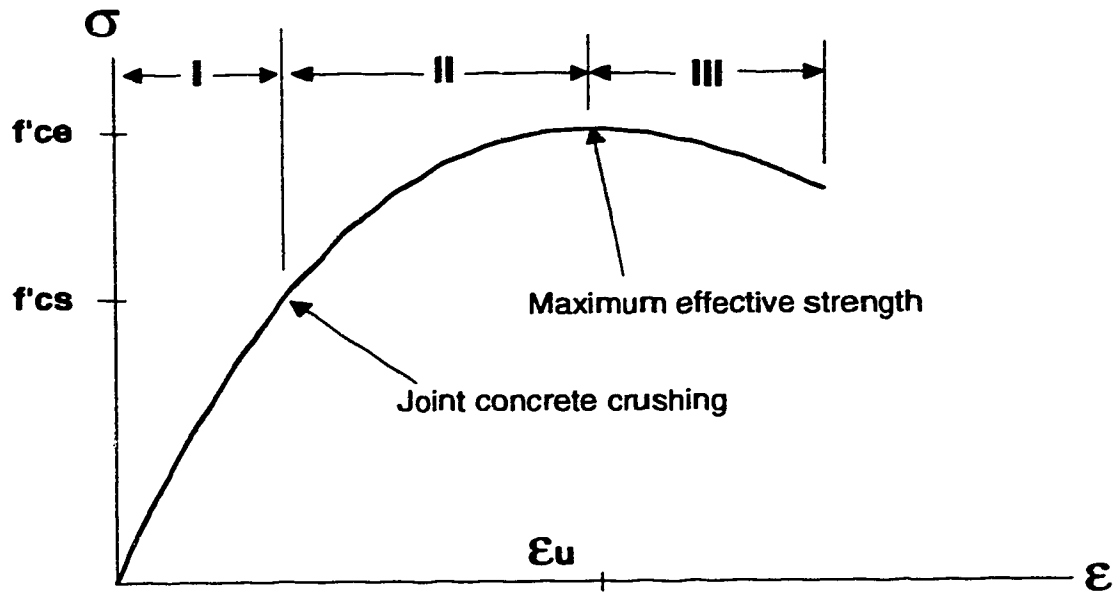
* Maximum column load applied in the test.

** Calculated according to equation 2.2 .

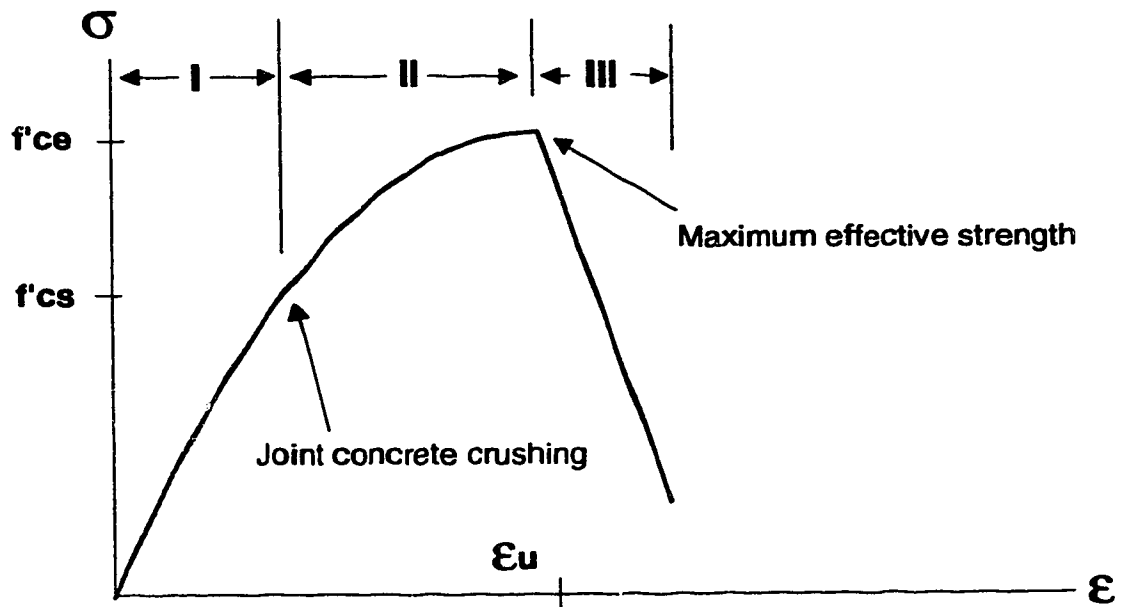
† Average slab strain measured at the face of the column shortly after slab loads were applied.

‡ The h/c ratio was calculated based on the shorter column dimension.

Table 4.1 Test results



**Figure 4.1 Schematic stress-strain curve
(interior plates with loaded slabs)**



**Figure 4.2 Schematic stress-strain curve
(interior plates with unloaded slabs)**

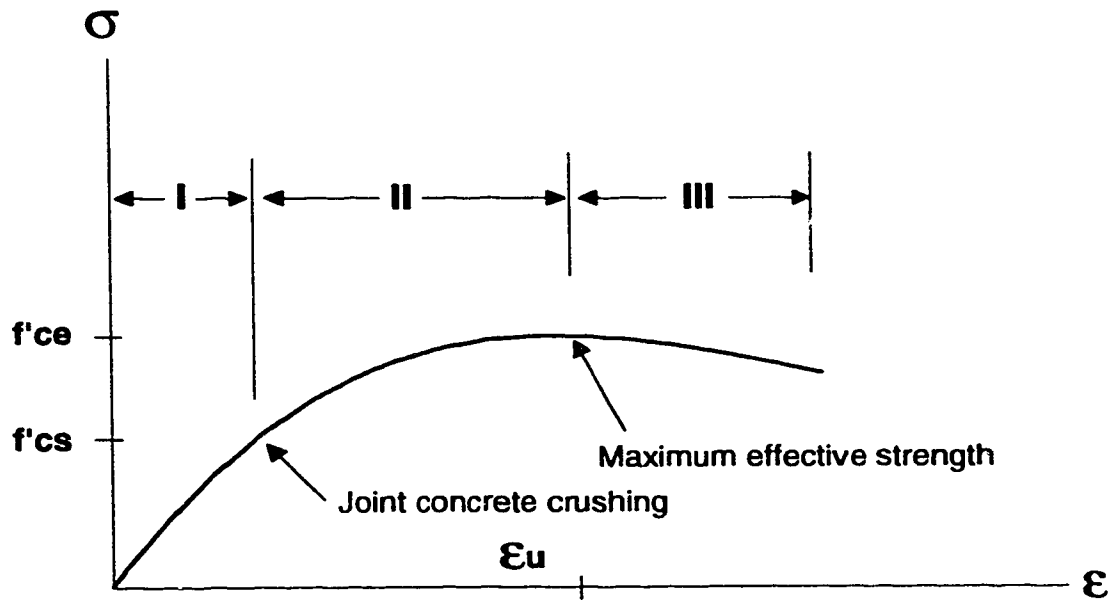


Figure 4.3 Schematic stress-strain curve (edge plates)

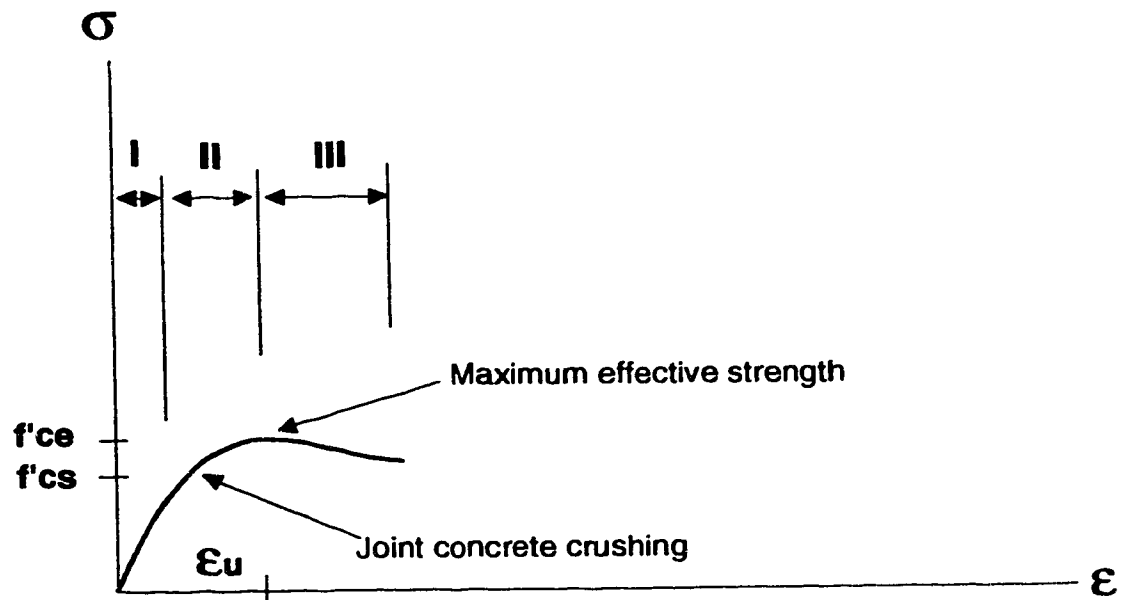


Figure 4.4 Schematic stress-strain curve (sandwich columns)



Figure 4.5 Testing of interior sandwich plate
with slab loads ($h/c=1.0$)

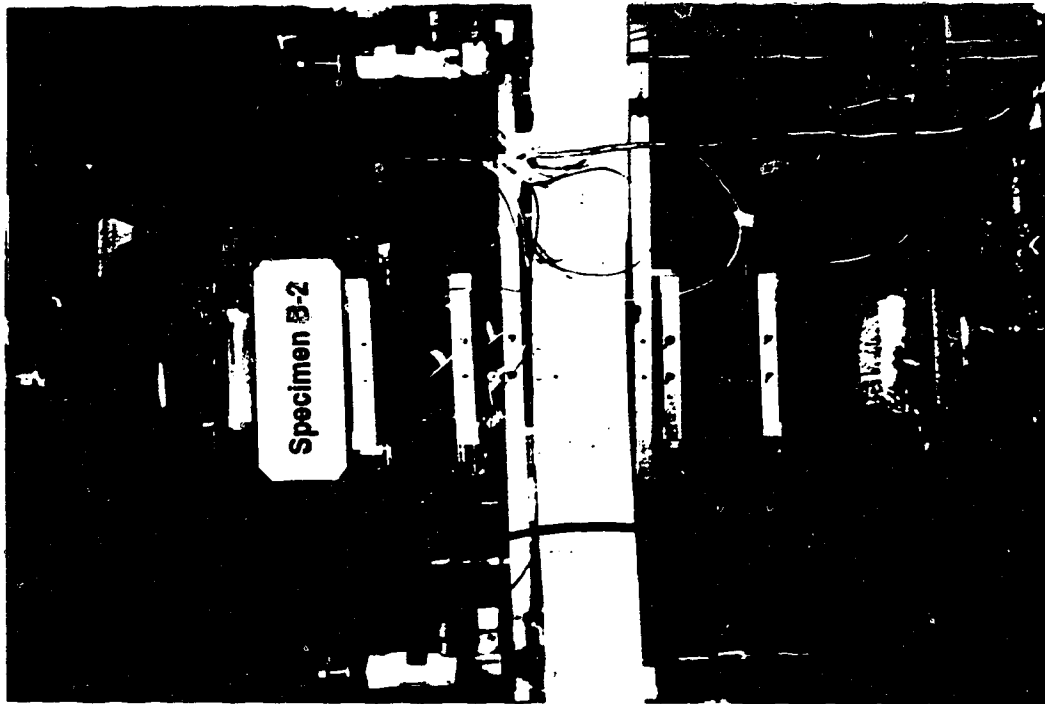
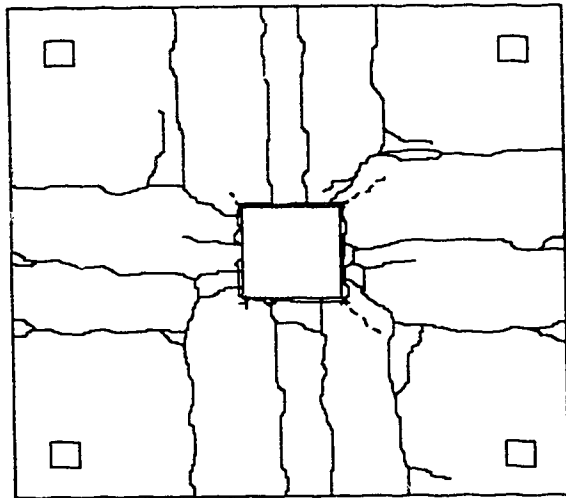
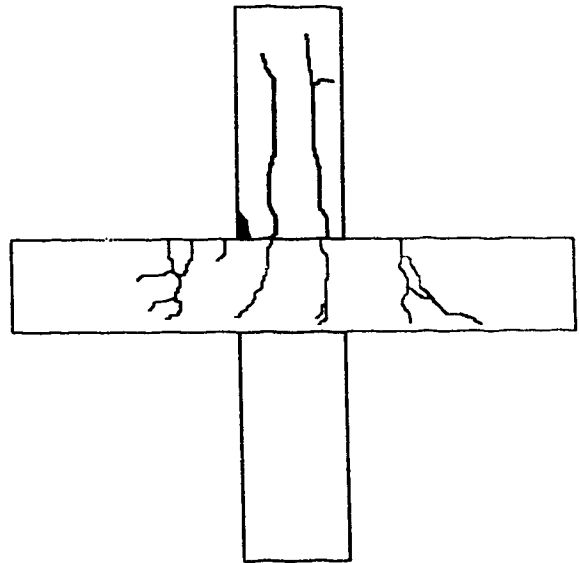


Figure 4.6 Testing of interior sandwich plate
with slab loads ($h/c=0.6$)

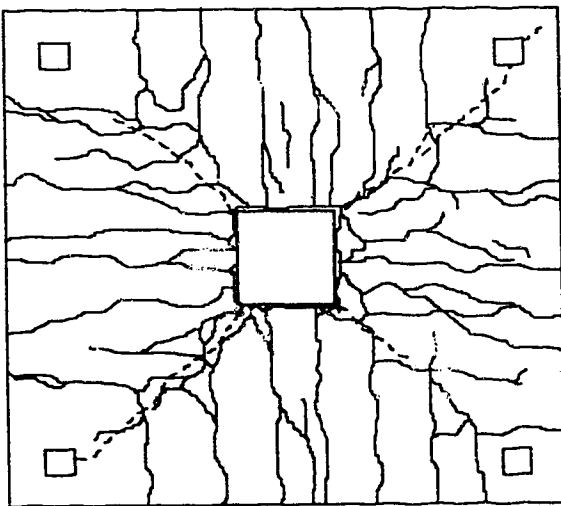


— Top slab cracks
 - - - Bottom slab cracks

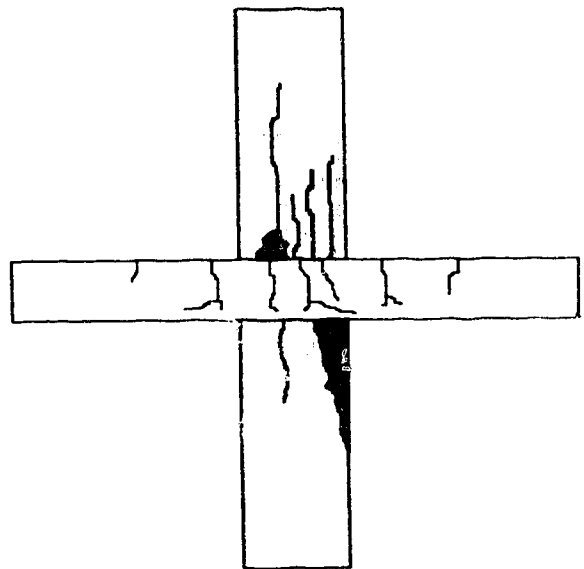


 Spalling of column concrete

Figure 4.7 Cracking pattern (Specimen B-1)



— Top slab cracks
 - - - Bottom slab cracks



 Spalling of column concrete

Figure 4.8 Cracking pattern (Specimen B-2)

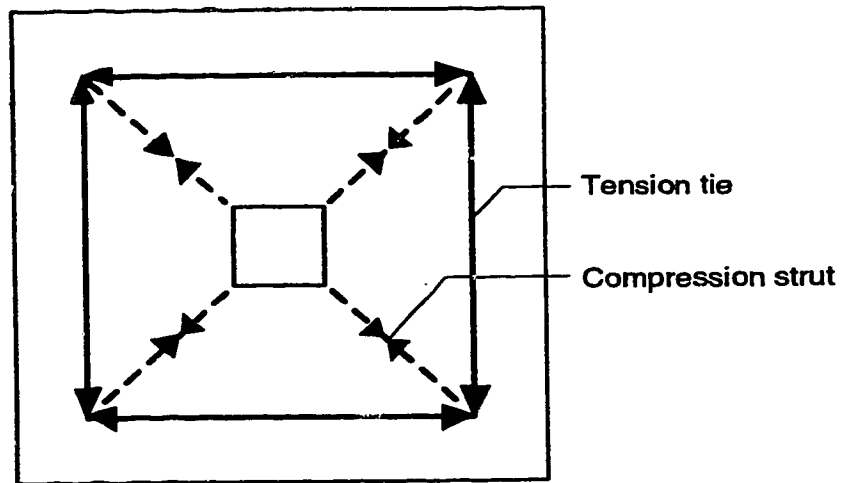


Figure 4.9 Square hoop behaviour of interior sandwich plate with unloaded slab

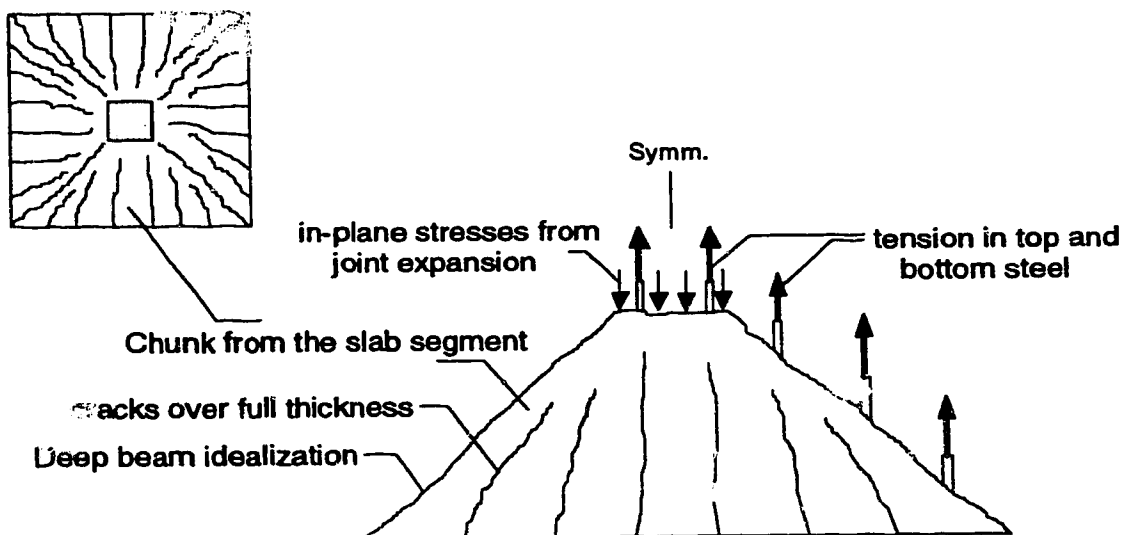
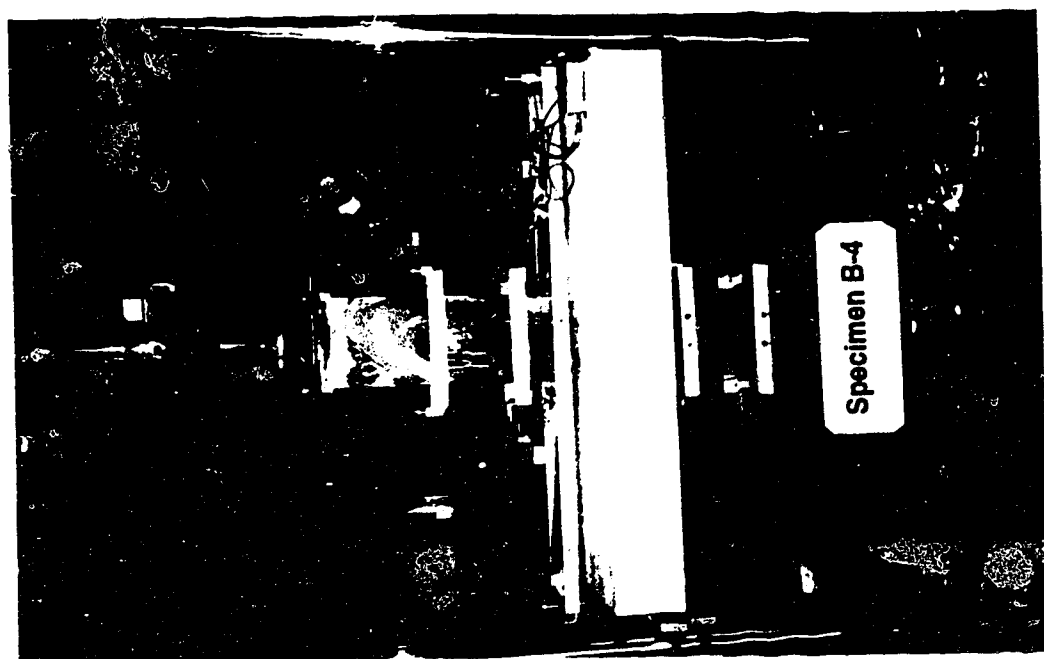
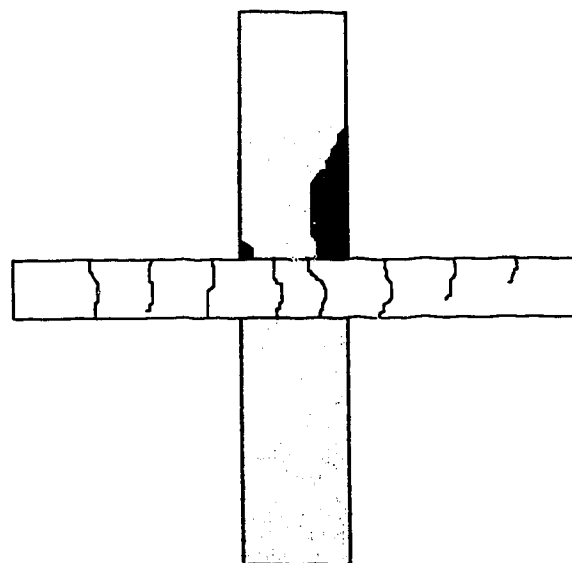
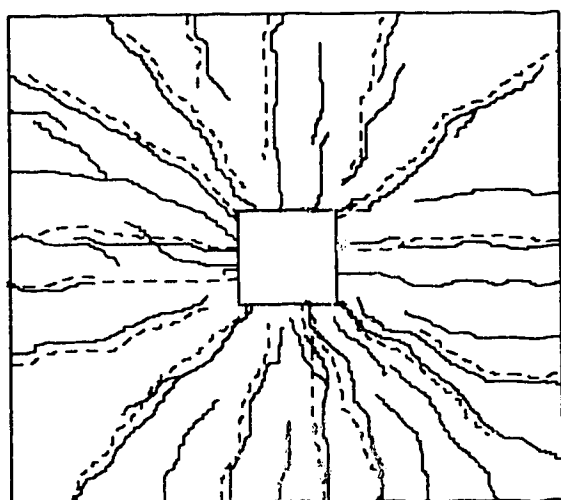



Figure 4.10 Deep beam behaviour of interior sandwich plate specimen with unloaded slab





 Top slab cracks
 Bottom slab cracks

 Spalling of column concrete

Figure 4.13 Cracking pattern (Specimen B-4)

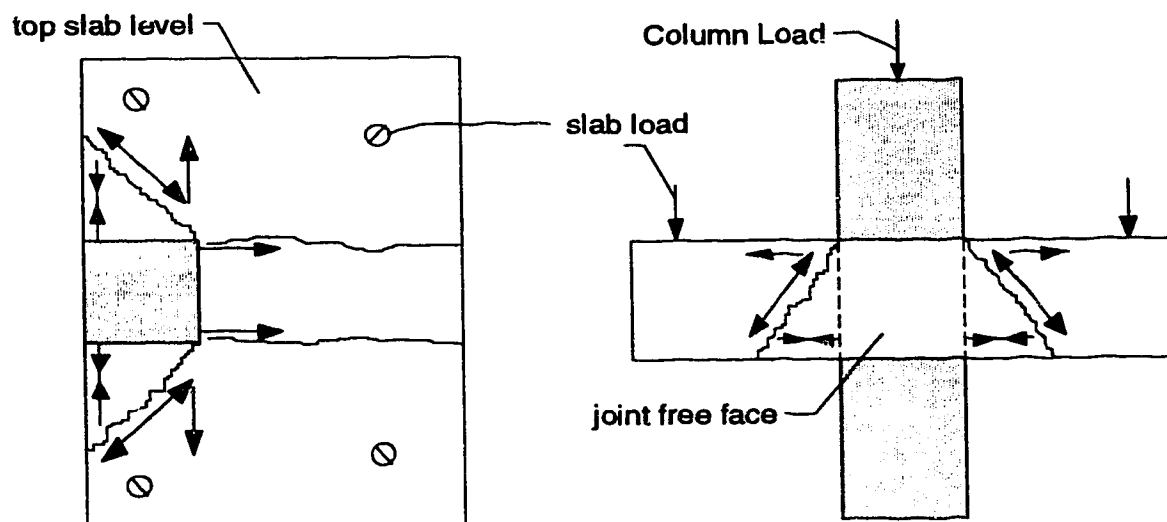


Figure 4.14 System of forces acting over an edge slab-column joint with slab loads

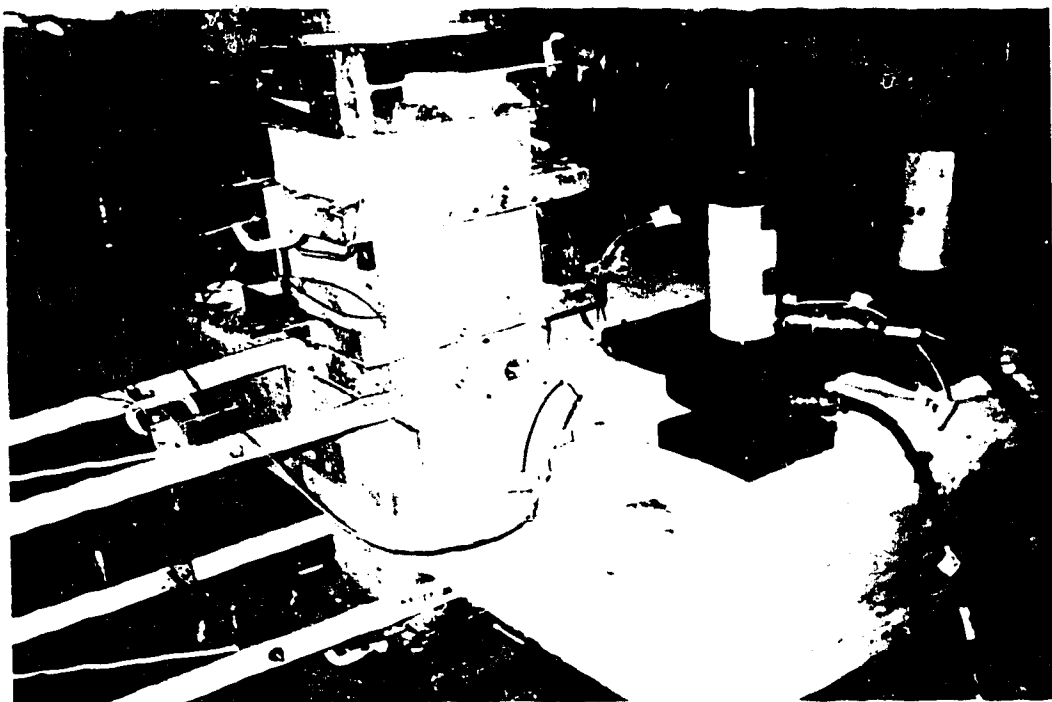
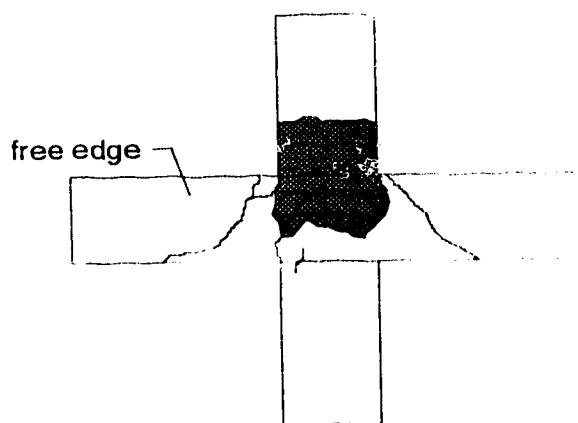
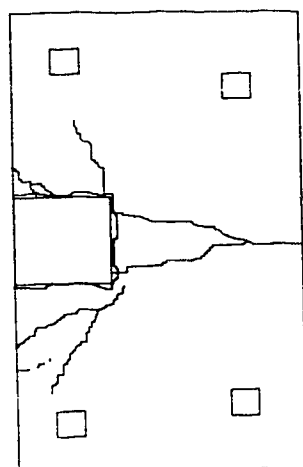

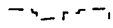


Figure 4.15 Testing of Edge Sandwich Plate with Slab Loads



 Top slab cracks
 Bottom slab cracks

 Spalling of concrete

Figure 4.16 Cracking pattern (Specimen C2-C)

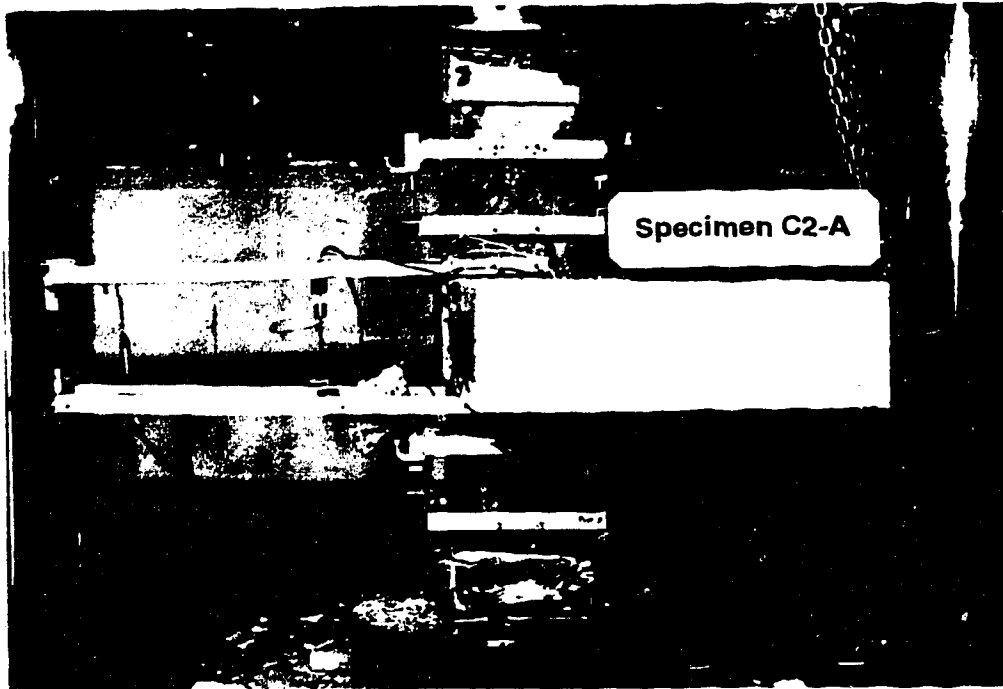


Figure 4.17 Testing of Edge Sandwich Plate without Slab Loads

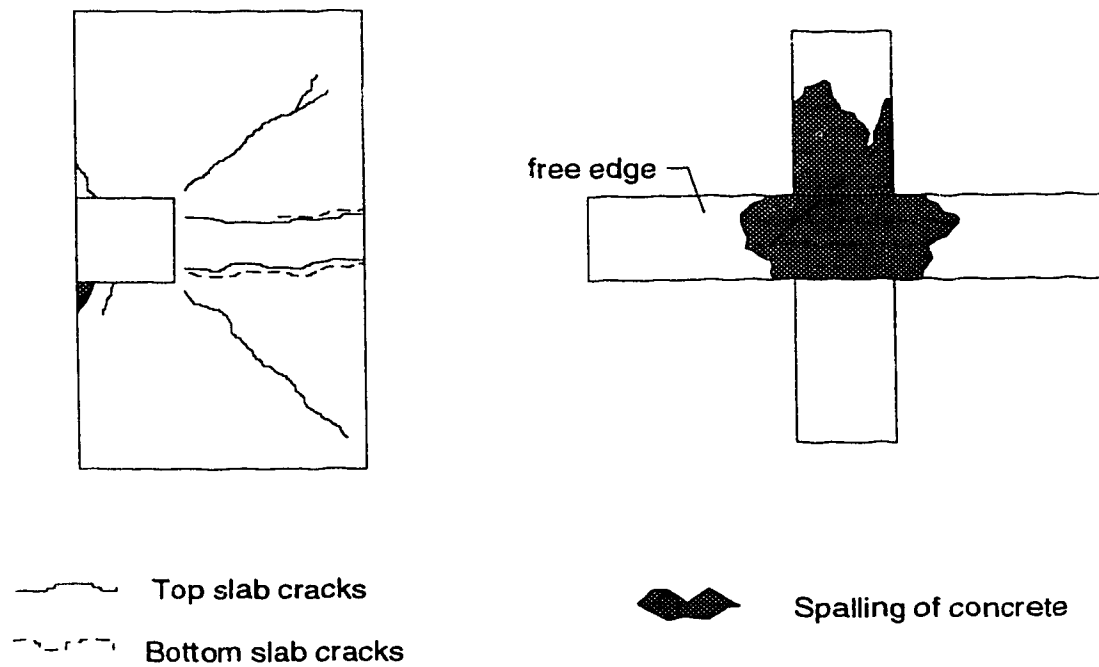


Figure 4.18 Cracking pattern (Specimen C2-A)



Figure 4.19 Testing of Sandwich Column Specimen

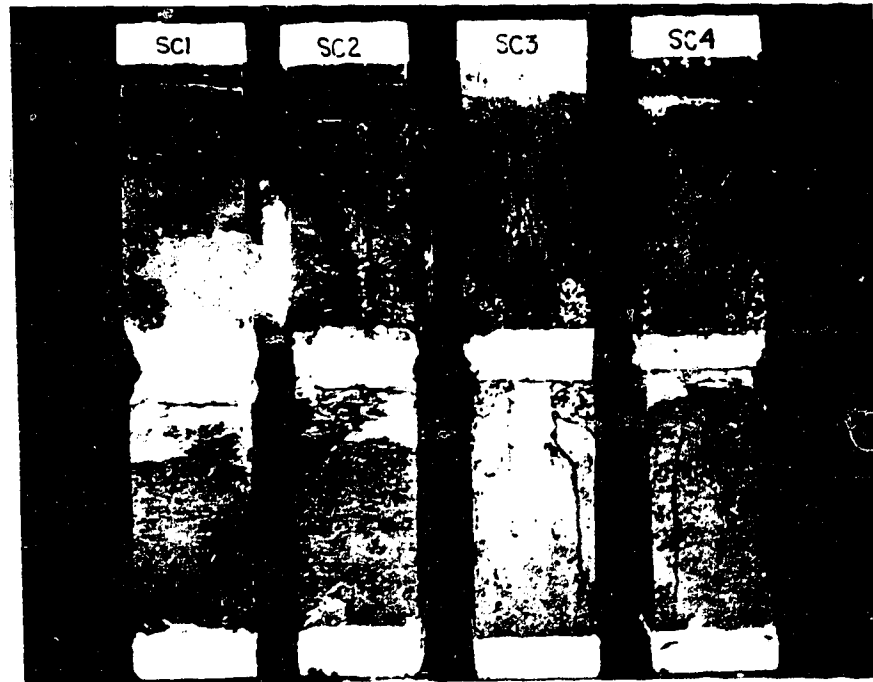


Figure 4.20 Sandwich Column Specimens after testing



Spalling of column concrete

Figure 4.21 Cracking pattern (Specimen D-SC1)

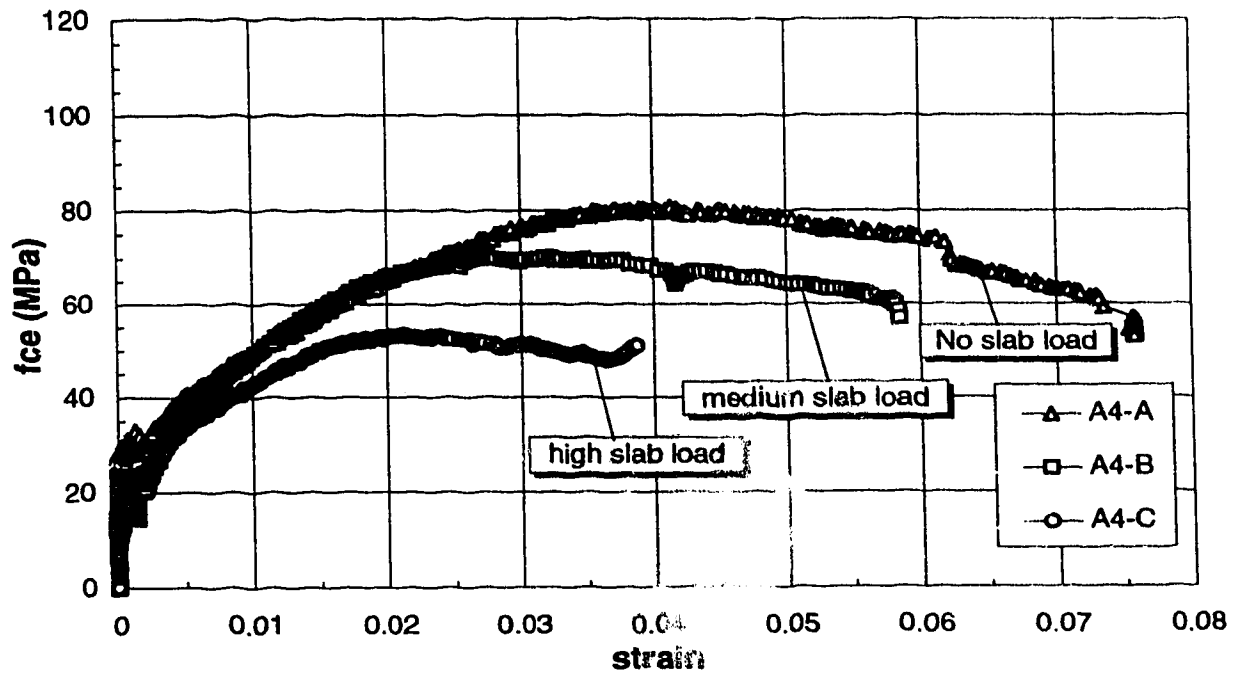


Figure 4.22 Effect of slab loading (ISP)

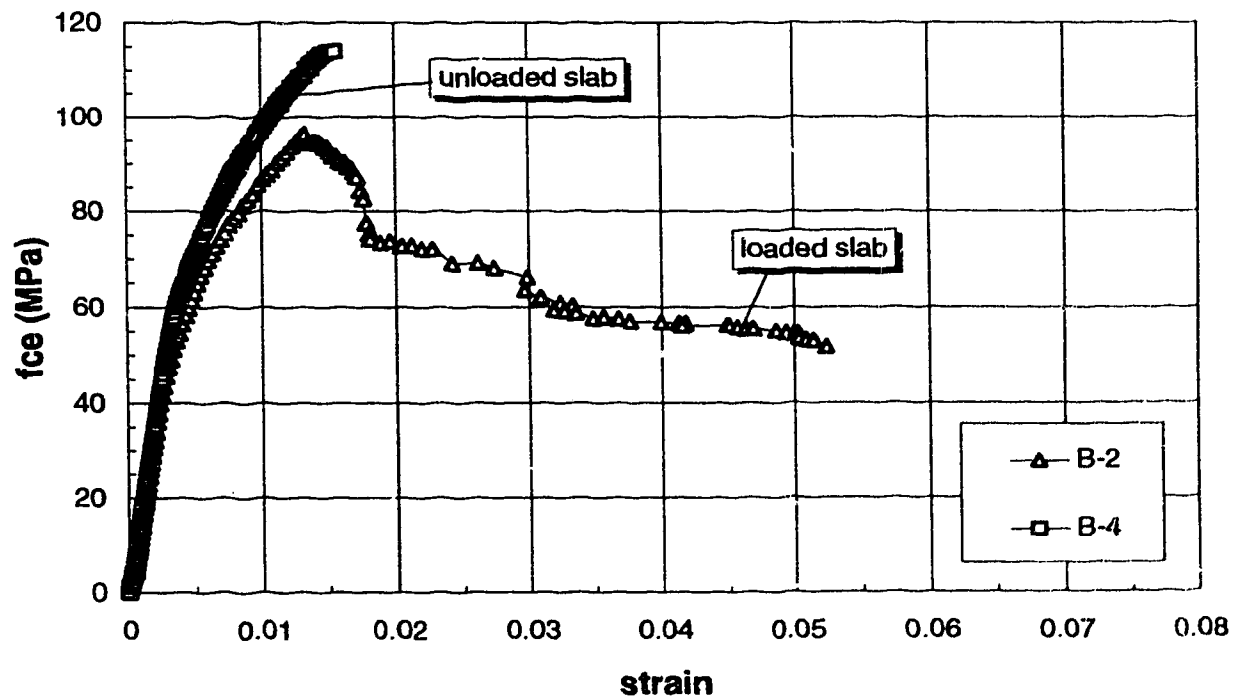


Figure 4.23 Effect of slab loading (ISP)

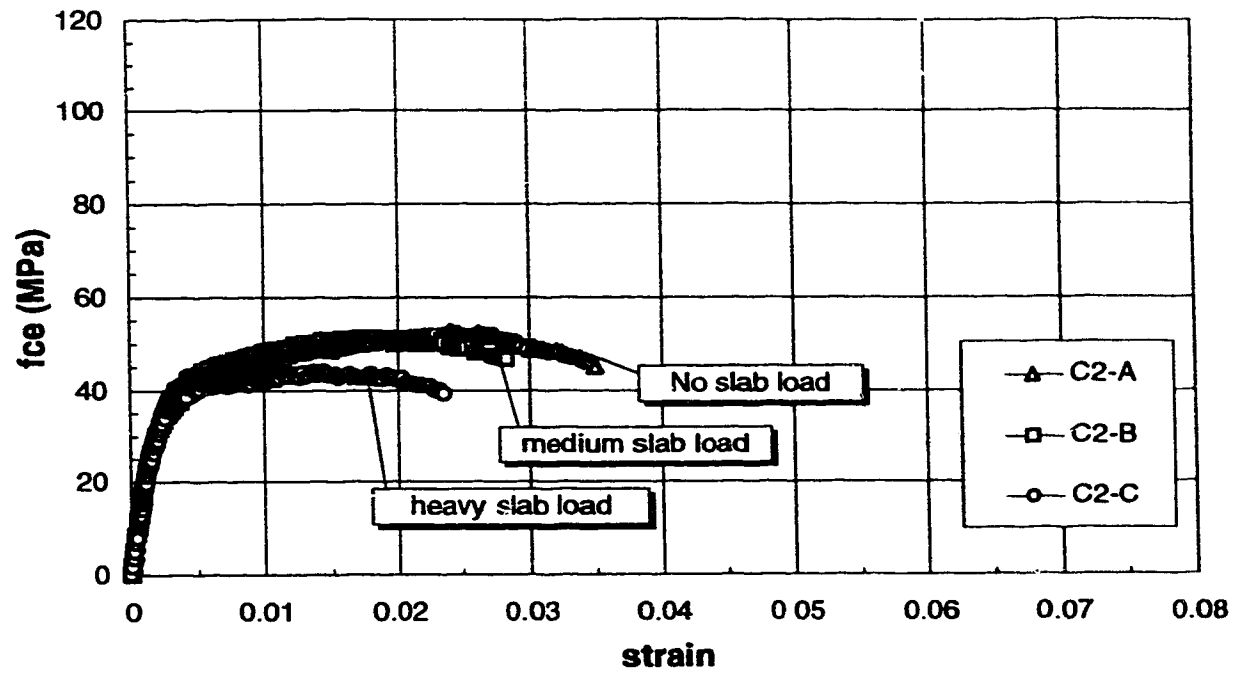


Figure 4.24 Effect of slab loading (ESP)

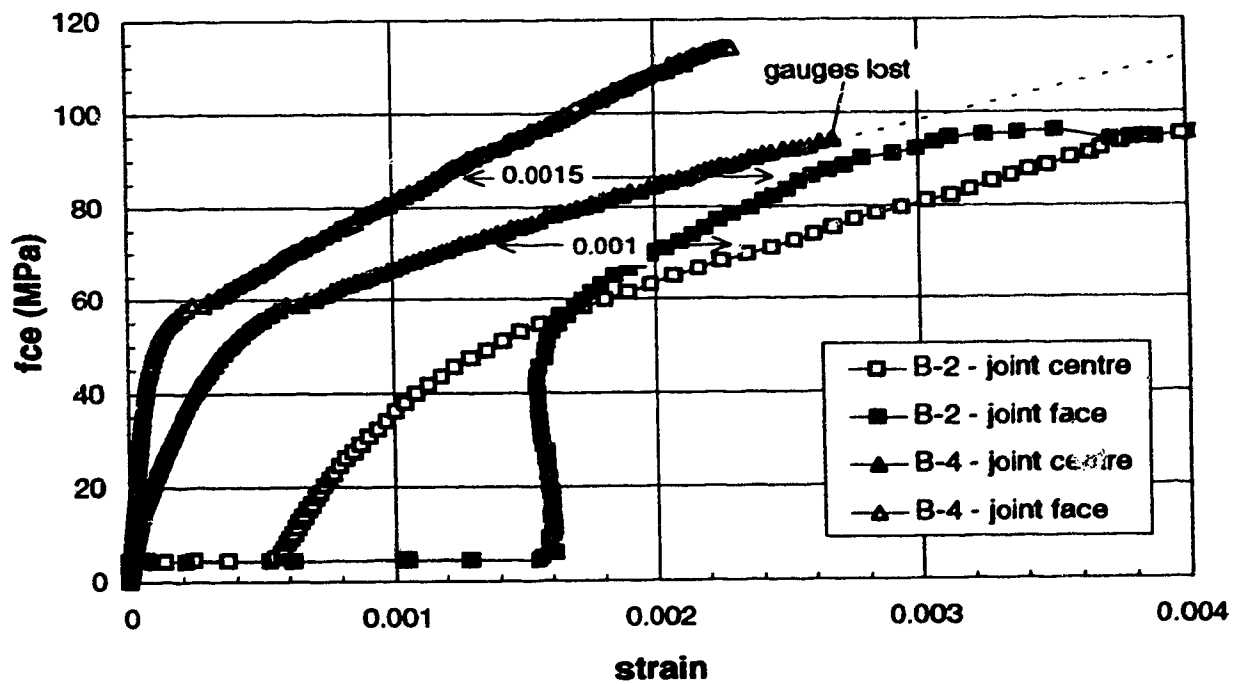
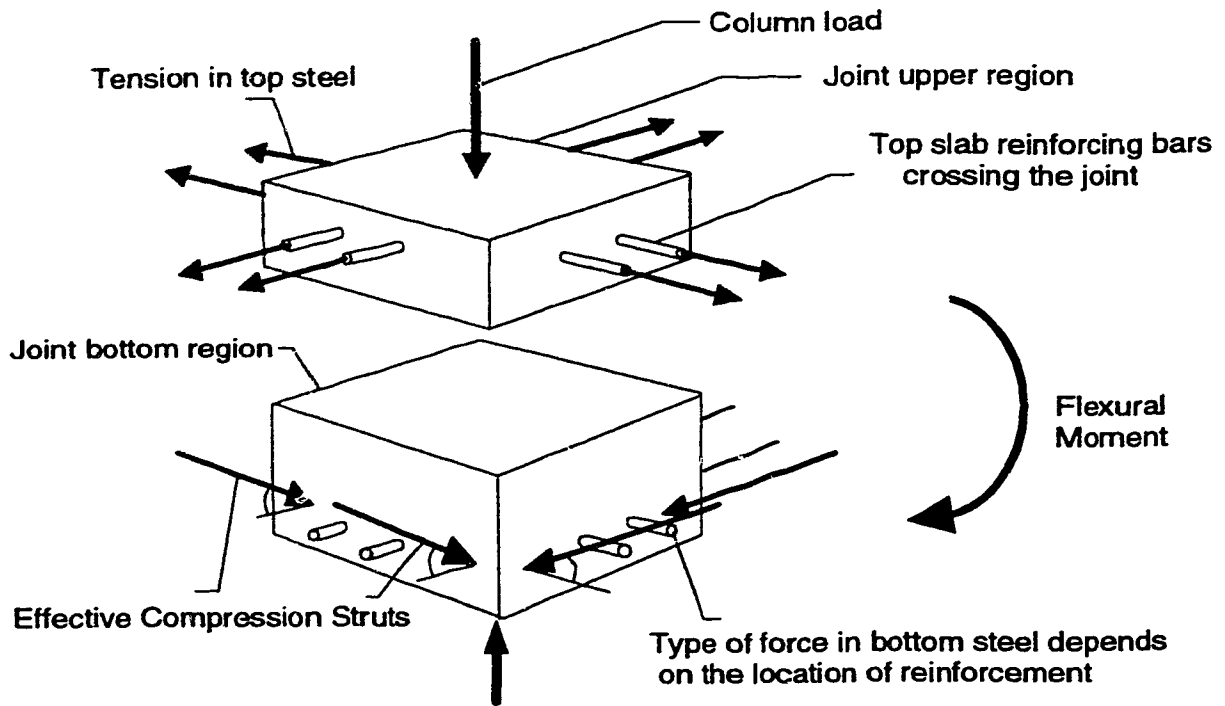
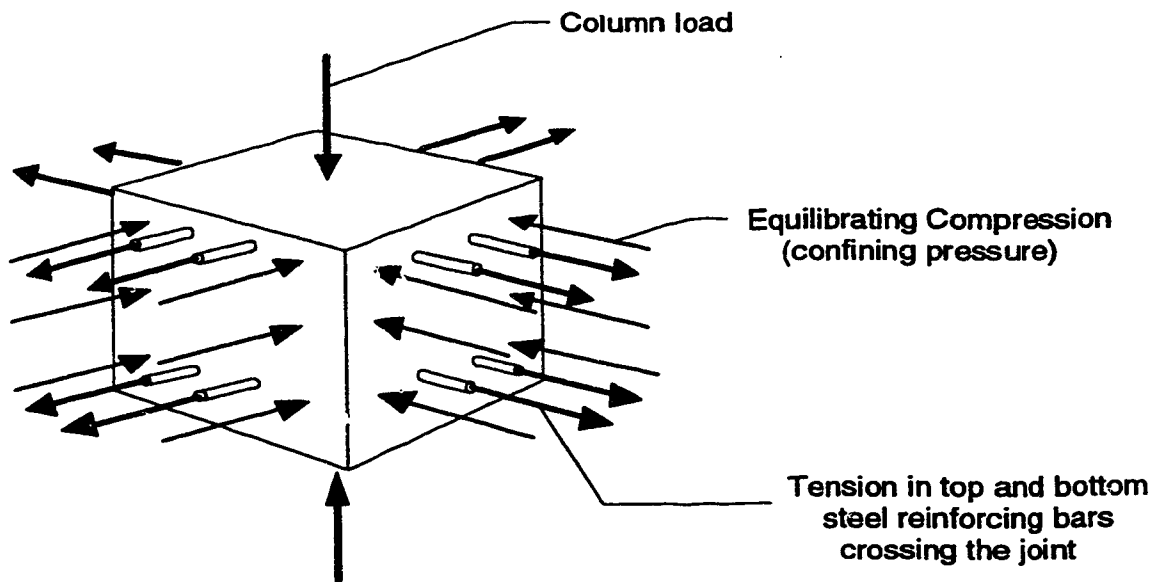


Figure 4.25 Slab loading effect on joint transverse strain



**Figure 4.26 Triaxial state of stresses at joint region
(Interior plates with loaded slabs)**



**Figure 4.27 Triaxial state of stresses at joint region
(Interior plates with unloaded slabs)**

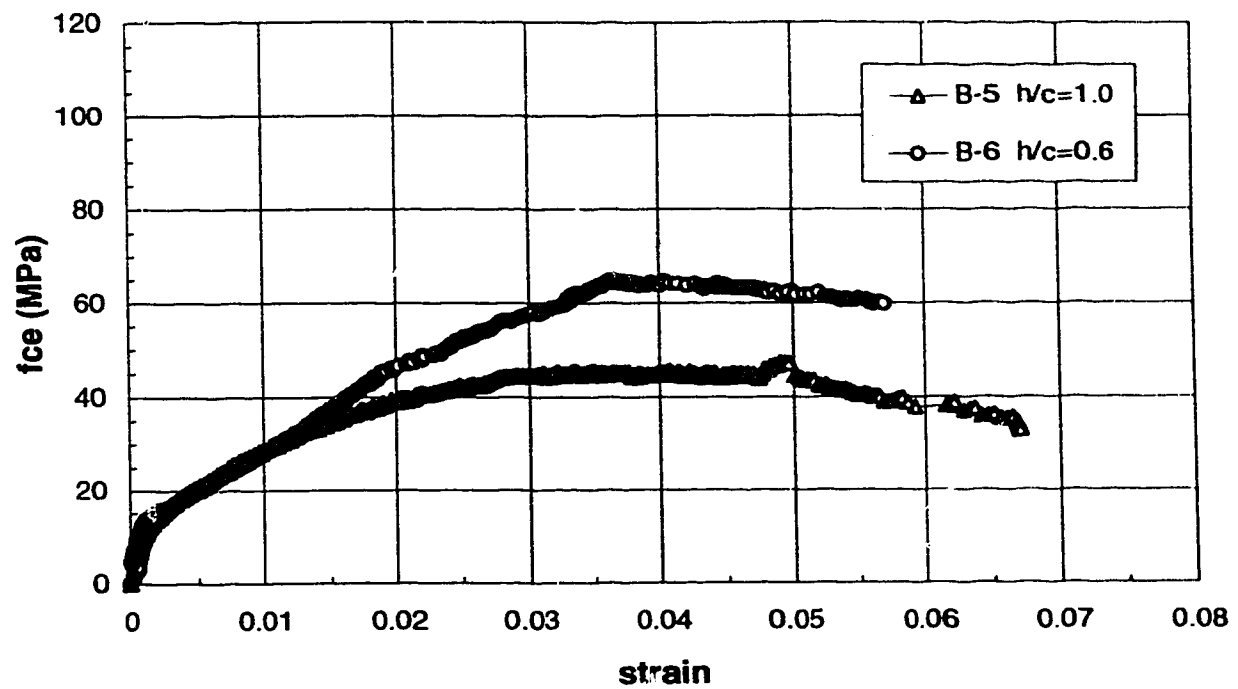


Figure 4.28 Effect of the h/c ratio (ISP)

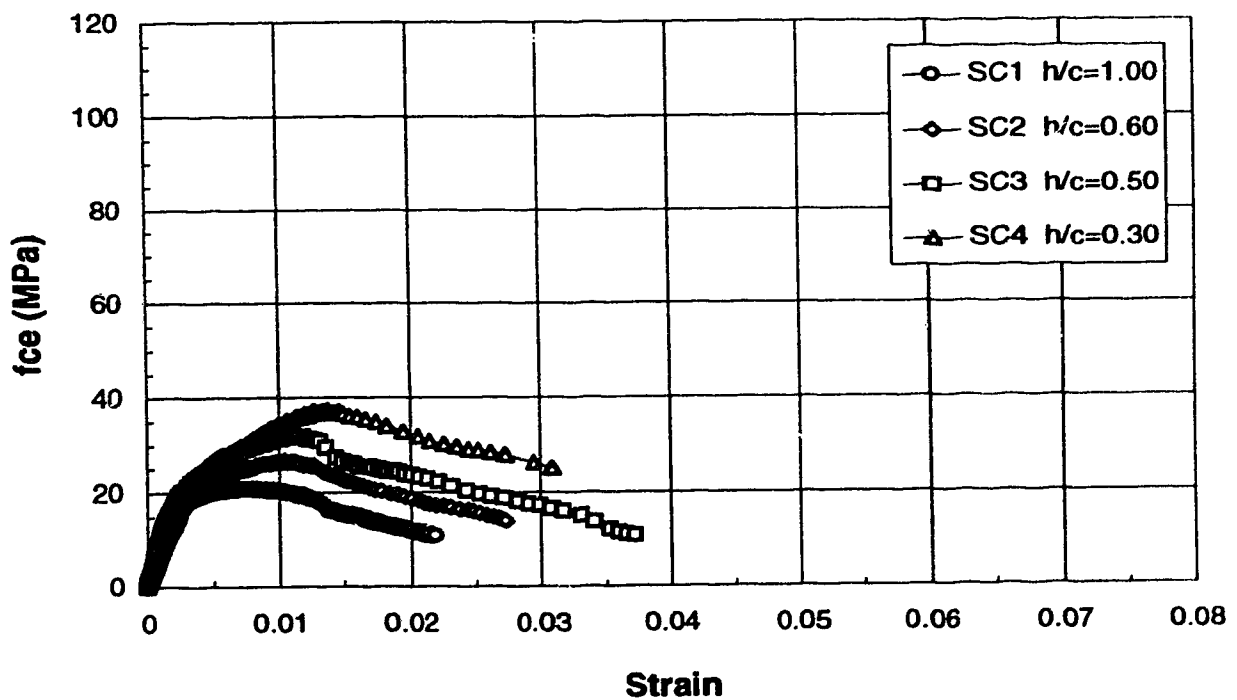


Figure 4.29 Effect of the h/c ratio (SC)

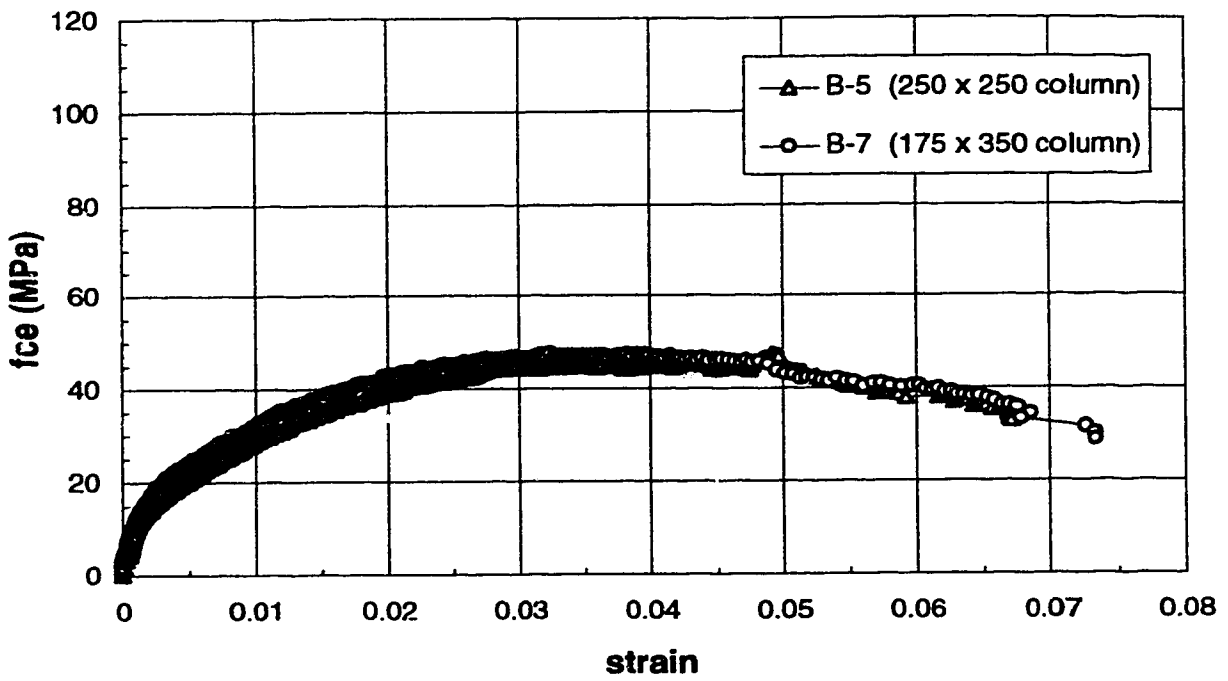


Figure 4.30 Effect of column rectangularity (ISP)

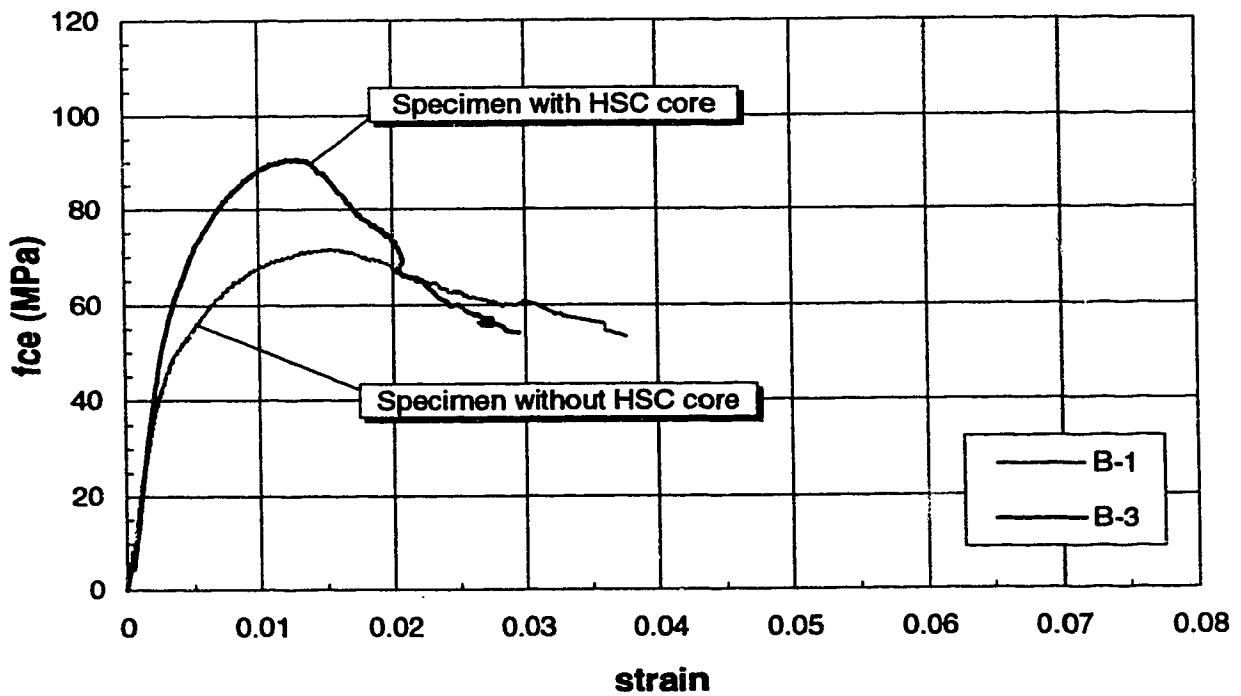


Figure 4.31 Effect of HSC core within joint region

5. EFFECT OF TEST VARIABLES

5.1 General

This chapter presents the evaluation of the variables that affect the strength of concrete columns intersected by concrete slabs. Comparison of test results from this experimental program with those reported in the past is included. Evaluation of existing design provisions is also reported.

Results of tests conducted in this experimental program on interior sandwich plate specimens are summarized in fig. 5.1 . Test results on edge sandwich plates are presented in fig. 5.2 and results on sandwich columns are shown in fig. 5.3 .

This chapter also includes a reevaluation of the column effective compressive strength accounting for the new flexural design provisions contained in CSA A23.3-94.

5.2 Effect of Slab loading

Test results on interior and edge sandwich plates without slab loads are reported in fig. 5.4 and 5.5, respectively. These include results from this experimental program along with those presented by researchers in the past. To establish some useful comparisons, the design curves to evaluate the effective strength of columns intersected by concrete floors recommended by ACI 318-89, CSA A23.3 M-84 and CSA A23.3-94 and by Gamble and Klinar are reported.

For the case of interior columns, it can be seen that the both ACI 318-89 and CSA A23.3-M84 design curve tends to overestimate the strength of columns with high f'_{cc}/f'_{cs} ratios. In contrast, the 1994 Canadian provisions appear to be conservative. The design equation proposed by Gamble and Klinar falls in between the ACI 318-89 and the 1994 Canadian Standard curves. It can be noticed that two of the results reported by Gamble and Klinar lie on their design line. However, their equation constitutes a reasonable lower bound for the test results shown.

With respect to edge columns without slab loads, ACI 318-89 and both the 84 and 94 Canadian Standard provisions establish a constant design value of f'_{ce}/f'_{cs} equal to 1.4 for column concrete 1.4 times stronger than the slab concrete. A 45 degree line for f'_{cc}/f'_{cs} ratios less than 1.4 is assumed since the design provision establishes that the effective strength of the column, f'_{ce} , shall never be greater than the column strength, f'_{cc} . Both ACI and CSA provisions are a suitable lower bound for the shown tests on edge columns.

For edge columns, Gamble and Klinar propose a more liberal equation than do the design codes. As was the case for interior columns, their design provision is an adequate lower limit for the results reported by them and by Bianchini et al. However, test results reported by Kayani and by the author fall below the design curve proposed by Gamble and Klinar.

The effect of slab loading on interior and edge sandwich plates is presented in fig. 5.6 and 5.7 . These figures show plots of f'_{ce}/f'_{cs} versus f'_{cc}/f'_{cs} for interior and edge type specimens subjected to three different slab load intensities. It can be concluded from these figures that as the slab load intensity increases the column strength decreases. The reduction in column strength varies according to the type of specimen and the f'_{cc}/f'_{cs} and h/c ratios. The reduction in column strength between specimens without slab loads and specimens with heavily loaded slabs was higher for the interior plates. The column strength reduction varied from 13 to 34% for the interior columns, and from 17 to 21% for the edge columns. The higher reduction took place for the set of specimens with higher f'_{cc}/f'_{cs} and h/c ratios.

Based on this conclusion, any realistic amount of slab loading would reduce the strength of the specimens tested by Bianchini et al., Gamble and Klinar, and Kayani. Consequently, any design provisions based solely on these test results may be unsafe. In effect, ACI 318-89 and CSA A23.3-M84 provisions appear to be not conservative particularly for slab-column connections with high f'_{cc}/f'_{cs} ratios. For the interior column case the calculated effective strength for specimen A-4C (with heavy slab loads) is 65% lower than the evaluation according to ACI 318-89 and 1984 CSA standard. For f'_{cc}/f'_{cs} ratios varying from two to three, typical in medium rise buildings, the difference between test results and the ACI 318-89 and CSA A23.3 design equations is not as dramatic as in the previous case. However, the results for these specimens lie below the design curves. In contrast, the design equation for interior columns given in the 1994 CSA standard appears to be conservative for the vast majority of tests herein reported. This design provision overestimates the strength of only one specimen (B-7), as observed in fig. 5.1 .

As far as to the edge specimens is concerned, the ACI 318-89 and 1984 CSA provisions appear to be a reasonable lower bound for the majority of specimens tested with slab loads. Only one specimen (C2-C) falls below the design curve. The design equation for edge columns contained in CSA A23.3-94 lies below the ACI 318-89 and 1984 Canadian code design equation. The 1994 CSA design curve is in all cases a lower limit for the edge specimens tested with slab loads.

The only tests on corner sandwich plates known to the author are the tests on corner sandwich plates without slab loads carried out by Bianchini et al. Taking into account that a higher column strength reduction due to the slab loading effect takes place for interior columns compared to edge columns, it may be then extrapolated that the column strength reduction in corner columns would be less than that in edge columns. As a result, any imposition of slab load on the corner plates tested by Bianchini et al. would have led to only a minimum decrease in column strength. This observation suggests that testing of sandwich columns does not reduce to simulate the behaviour of a corner sandwich plate without slab loads, but also to model the behaviour of corner column specimens with loaded slabs.

5.3 Effect of the h/c ratio

The effect of varying the ratio of the slab thickness to column dimension, h/c , is shown in fig. 5.8 . This figure presents the test results of specimens B-1 and B-2 along with those of specimens B-5 and B-6. It can be concluded that the effective compressive strength of the column decreases as the aspect ratio, h/c , increases. Moreover, this reduction increases as the f'_{cc}/f'_{cs} ratio increases. In effect, the column strength dropped 25 to 30% for a variation in the h/c ratio from 0.6 to 1.0 , for f'_{cc}/f'_{cs} ratios varying from 2.48 to 6.33, respectively.

The effect of the h/c ratio depends on the confinement provided to the joint concrete by the column ends framing into the connection. It is therefore presumed that the effect of this parameter also applies to edge and corner columns.

Tests evaluating the effect of this parameter on the strength of edge columns were not carried out in this investigation. The effect of the h/c ratio on the strength of corner and sandwich columns is shown in fig. 5.9 . This figure shows the test results of corner sandwich plates and sandwich columns reported by Bianchini et al. along with test results of sandwich columns reported by Kayani and by the author.

As was the case for interior and the edge columns, the effective compressive strength of the sandwich column reduces as the h/c ratio increases. It can be seen that test results on sandwich columns reported in this investigation are consistent with the tests on corner and sandwich columns reported in the past. A reduction of 27% in the sandwich column strength was noticed for an increase in the h/c ratio from 0.6 to 1.0 . This reduction is similar to that observed for interior sandwich plates with similar f'_{cc}/f'_{cs} ratio and h/c ratio varying from 0.6 and 1.0 . This confirms the hypothesis that the h/c parameter affects the strength of joints with different degree of confinement. It also suggests that the reduction in interior column strength due to the aspect ratio effect may be simulated with testing of sandwich columns, which are easier and cheaper to test.

From fig. 5.9 it can also be seen that for the sandwich columns with a similar value of h/c f'_{ce}/f'_{cs} appears to be independent of f'_{cc}/f'_{cs} .

In accordance with all of these observations, it is concluded that the effect of the parameter h/c on the strength of sandwich plates and sandwich columns is similar to that in the test of concrete cylinders or prisms. Correction factors for the strength of concrete cylinders varying with the cylinder's aspect ratio have been reported in the past. A correction factor can be interpreted as an equivalent f'_{ce}/f'_{cs} ratio for a given h/c ratio. Correction factors independent of the cylinder strength are provided by ASTM C42-84a. Avram et al. (1981) present correction factors with respect to the cube strength for concrete prisms. These factors are independent of the concrete strength. Correction factors dependent of the cylinder strength are reported by Murdock and Kesler (1957).

These correction factors are presented in fig. 5.10 . Test results of sandwich columns reported by Bianchini et al., Kayani and the author are included for comparison. Test results by Shu and Hawkins for sandwich columns with a f'_{cc}/f'_{cs} ratio slightly less than that of the sandwich columns tested in this experimental program are also provided for comparison. Good agreement between the correction factors and the test results by Bianchini et al., Kayani and the author supports the analogy between the test of concrete cylinders or prisms and the test of sandwich column joints. It also confirms the validity of the variable h/c as an important parameter to evaluate the strength of columns intersected by floors. Test results by Shu and Hawkins show a similar trend for the h/c effect but the magnitude of the f'_{ce}/f'_{cs} values appears to be excessively high.

Figure 5.11 highlights the difference between the test results of sandwich columns tested by Shu and Hawkins (1991) with those reported by the author. Even though the same trend is observed for Shu and Hawkins' results significant disagreement is observed between the results. Shu and Hawkins reported the use of 3/4" aggregate for the column and slab concrete. According to the column dimensions, the slab portion of the specimen with an h/c ratio of 0.17 is barely longer than the aggregates. This suggests that the coarse aggregate was practically bridging the joint region from the lower to the upper column end. This leads to an unduly increase in the joint strength since the aggregates are stronger than the cement paste.

None of the existing proposed design equations treated in this thesis consider the h/c ratio to evaluate the strength of columns intersected by concrete floors. According to the observations herein stated ACI 318-89 and CSA A23.3-M84 are found unconservative when high h/c ratios intervene in the connection. Conversely, the 1994 Canadian provisions are found unduly conservative for low h/c ratios. Figure 5.8 further illustrates these conclusions.

For the case of edge columns, ACI 318-89 and both the 1984 and 1994 editions of the Canadian code appear to be adequate. Additional test results of edge specimens are required to assess the effect of the h/c ratio in a more complete way. For corner columns, ACI 318-89 and CSA A23.3-M84 design equation appears to be slightly above of the existing test results. The 1994 CSA provisions however, look to be a suitable lower bound for the available tests.

5.4 Effect of column rectangularity

The evaluation of this parameter is presented based only on four test results. Additional tests are required to further confirm the validity of the conclusions.

To avoid the addition of unnecessary parameters, the column rectangularity effect can be accounted for by means of the aspect ratio, h/c . When dealing with rectangular columns, there is no guidance to determine whether the shorter dimension, the longest dimension or some value in between is the appropriate value of c to be used in the calculation of the h/c ratio.

The effect of column rectangularity is examined based on the comparison of two sets of interior sandwich plates, each built with identical slab thicknesses and f'_{cc}/f'_{cs} ratios but with different column shapes. Figure 5.12 compares values of f'_{ce}/f'_{cs} against values of f'_{cc}/f'_{cs} for these four tests. As expected, lower f'_{ce}/f'_{cs} ratios were reached for the specimens with thicker slabs compared to those with thinner slab segments. Moreover, the specimens with square columns outperformed the rectangular column sandwich plate specimens by 14 to 21%.

According to these comparisons, it is presumed that the shorter column dimension is appropriate in evaluating the h/c ratio of a rectangular column. Selection of the shortest column side results in a higher value of h/c and therefore, leads to a decrease in the predicted column strength.

Thus far the effect of column rectangularity has not been accounted for in the development of design provisions. It is important to notice that the test result of one of the specimens with rectangular columns (B-7) falls below the design equation proposed by the 1994 Canadian Standard. Both ACI 318-89 and CSA A23.3-M84 are not conservative for the two tests on rectangular column sandwich plate specimens reported in this investigation.

5.5 Effect of high-strength concrete core at the joint region

Figure 5.13 shows the effect of the inclusion of a high-strength concrete core in the joint region of a slab-column connection. According to this figure the specimen with high-strength core (specimen B-3) outperformed the conventionally built specimen by 21%. Taking into consideration that the high-strength concrete core occupied only 9% of the column cross-section the enhancement in strength is considerable. By transforming the joint region into a weighted average of concrete area it also becomes noticeable that the high-strength core is responsible for sustaining at least 2/3 of the column load.

Use of high-strength cores in slab-column joints may be useful particularly in larger scale columns where larger core areas may be available. Its use not only may lead to higher strengths but also it would avoid puddling and the addition of dowels as a possible solution to the problem. This procedure may constitute a very feasible way of achieving higher column strengths. However, additional testing of sandwich plates with embedded high-strength cores is required to establish a more reliable conclusion. Extensive use of this proposed procedure is also subjected to an exhaustive evaluation of any eventual constructive-type inconvenience.

5.6 Evaluation of the effective strength, f'_{ce} , in light of CSA A23.3-94

Evaluation of the stress block factors in the 1994 edition of the Canadian code differs from CSA A23.3-M84 and ACI 318-89. In CSA A23.3-M84 the α_1 factor is assumed constant and equal to 0.85. ACI 318-89 also defines the same value for this stress block factor. In

the 1994 version of the Canadian code the α_1 factor ceases to be constant and it is defined as dependent of the compressive strength of concrete, as indicated in eq. 5.1 .

$$\alpha_1 = 0.85 - 0.0015 f'_c \geq 0.67 \quad [5.1]$$

In CSA A23.3-94 the axial load resistance of a tied column is defined as

$$P_{ro} = \alpha_1 \phi_c f'_c (A_g - A_{st}) + \phi_s f_y A_{st} \quad [5.2]$$

Following the same procedure as in chapter 2, and treating the f'_c parameter as f'_{ce} , the column effective strength can be calculated as

$$f'_{ce} = \frac{P_{ro} - \phi_s f_y A_{st}}{\alpha_1 (A_g - A_{st})} \quad [5.3]$$

Since eq. 5.1 and 5.3 are not independent, it is necessary to equate terms and solve for α_1 . The solution of the resulting quadratic equation gives an expression for the α_1 factor. This expression is given as follows.

$$\alpha_1 = \frac{0.85 + \sqrt{0.85^2 - 0.006k}}{2} \geq 0.67 \quad [5.4]$$

$$\text{where } k = \frac{P_{ro} - \phi_s f_y A_{st}}{\phi_c (A_g - A_{st})}$$

Table 5.1 shows the values of the α_1 factor and the corresponding effective compressive strength, f'_{ce} , of the specimens tested in this investigation. In all cases, the calculated values are less than 0.85. Consequently, the values of the effective compressive strength, f'_{ce} , always exceed those calculated based on a constant α_1 factor equal to 0.85 .

According to table 5.1 the greatest variation in the evaluation of the column effective strength when applying the 1994 CSA α_1 factor occurs for the specimens with higher column effective strength and lower f'_{cc}/f'_{cs} ratio. The minimum variation occurs for the specimens with lower column axial load capacity and higher f'_{cc}/f'_{cs} ratio.

Figures 5.14 to 5.15 show the test results for the interior and edge sandwich plates tested in this investigation accounting for a variation in the α_1 factor. Test results for the sandwich columns in accordance to CSA A23.3-94 are shown in fig. 5.16 . For comparison, the ACI 318-89 and the 1984 and 1994 CSA design equations are shown.

For interior columns, the ACI 318-89 and CSA A23.3-M84 appear not to be a conservative provision. Even though the variation in the α_1 factors led to higher values of \bar{f}'_{ce}/f'_{cs} , the majority of the interior plate specimens with slab loads lie below these design curves. Conversely, the 1994 CSA Standard curve provides for a suitable lower bound for all of the specimens. For the edge columns, all the code provisions look appropriate to evaluate the effective strength of this type of connection. For the sandwich columns, the CSA A23.3-94 design curve constitutes a conservative lower limit for the four sandwich plate specimens tested in this research work.

Phase	Specimen	h/c	f'_{cc}/f'_{cs}	α_1	f'_{ce} (MPa)	f'_{ce}/f'_{cs}
A	A1-A	0.5	2.63	0.67	127.25	3.18
	A1-B	0.5	2.63	0.67	117.4	2.93
	A1-C	0.5	2.63	0.69	108.23	2.71
	A2-A	0.5	2.43	0.67	123.6	2.69
	A2-B	0.5	2.43	0.67	123.1	2.68
	A2-C	0.5	2.43	0.68	112.91	2.45
	A3-A	0.75	3.56	0.69	105.24	4.21
	A3-B	0.75	3.56	0.71	92.85	3.71
	A3-C	0.75	3.56	0.77	55.53	2.22
	A4-A	0.75	4.61	0.70	97.37	4.23
	A4-B	0.75	4.61	0.73	81.91	3.56
	A4-C	0.75	4.61	0.76	59.42	2.58
B	B-1	1.0	2.48	0.72	83.99	2.0
	B-2	0.6	2.48	0.67	121.89	2.9
	B-3	1.0	2.57	0.68	113.43	2.58
	B-4	0.6	2.57	0.67	144.61	3.29
	B-5	1.0	6.33	0.78	49.82	3.32
	B-6	0.6	6.33	0.74	74.67	4.98
	B-7	0.7	6.32	0.77	52.27	2.75
	B-8	1.17	6.32	0.72	84.99	4.47
C	C1-A	0.74	3.34	0.75	67.9	2.12
	C1-B	0.74	3.06	0.76	62.04	1.77
	C1-C	0.74	3.15	0.76	59.41	1.75
	C2-A	1.0	3.48	0.76	58.74	1.89
	C2-B	1.0	3.18	0.77	53.79	1.58
	C2-C	1.0	3.27	0.78	48.23	1.46
D	D-SC1	1.0	6.18	0.82	21.83	1.28
	D-SC2	0.6	6.18	0.81	28.0	1.65
	D-SC3	0.5	6.29	0.80	33.89	1.99
	D-SC4	0.3	6.18	0.79	40.21	2.37

**Table 5.1 Evaluation of the effective compressive strength
in accordance to CSA A23.3-94**

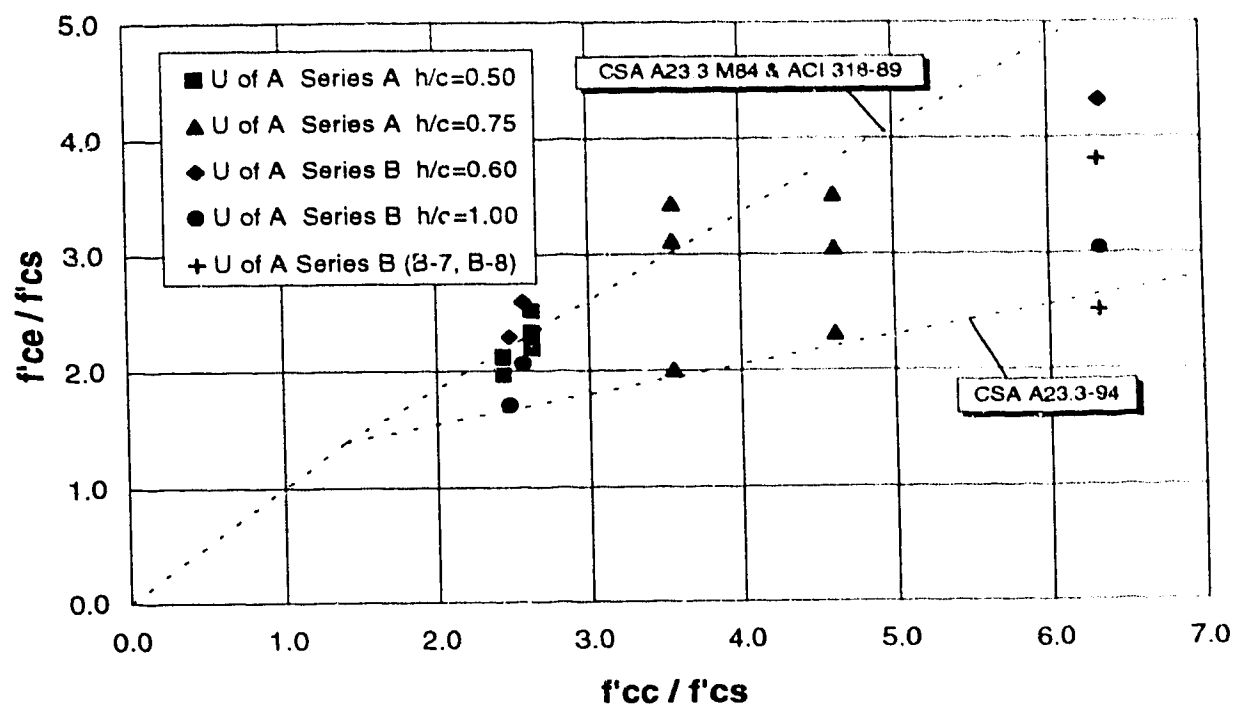


Figure 5.1 Test results of interior sandwich plates

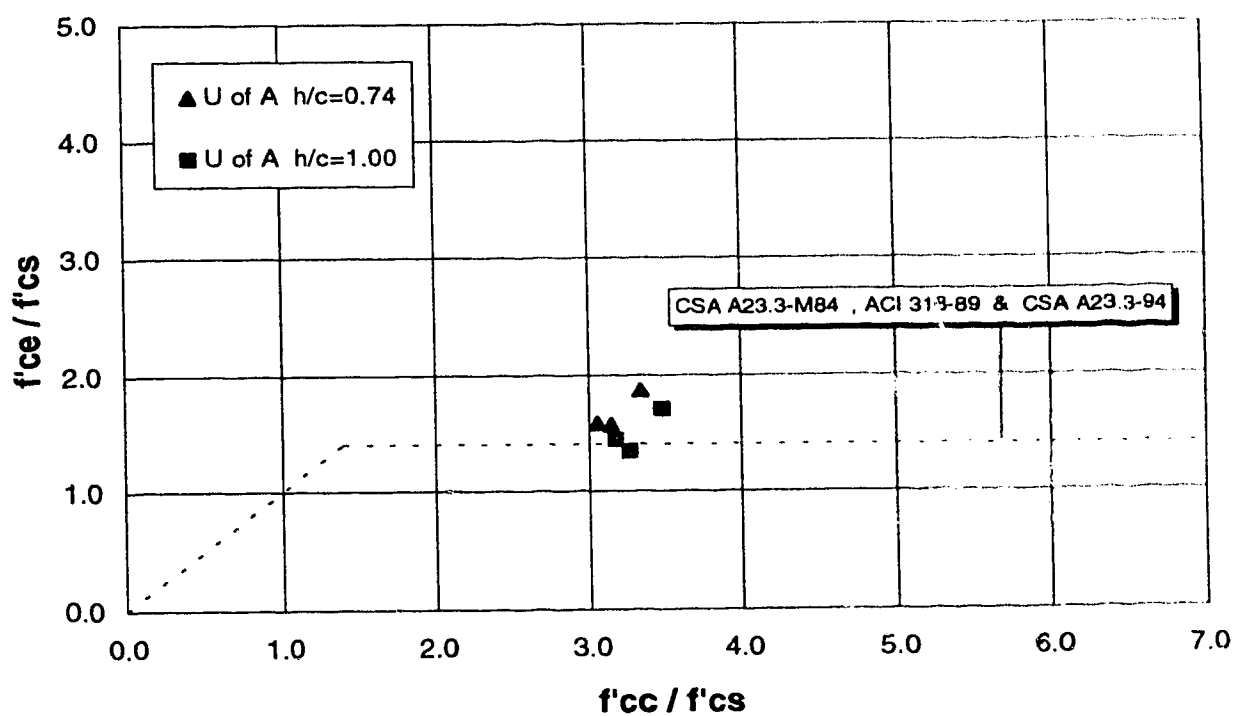


Figure 5.2 Test results of edge sandwich plates

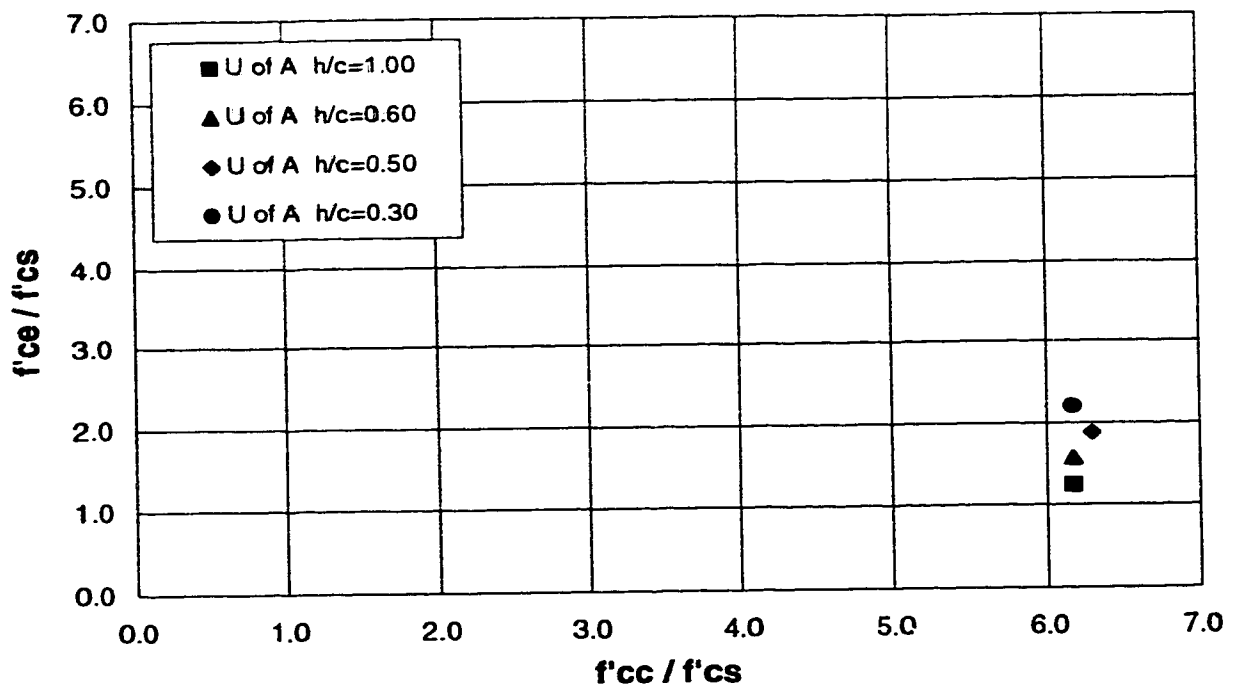


Figure 5.3 Test results on sandwich columns

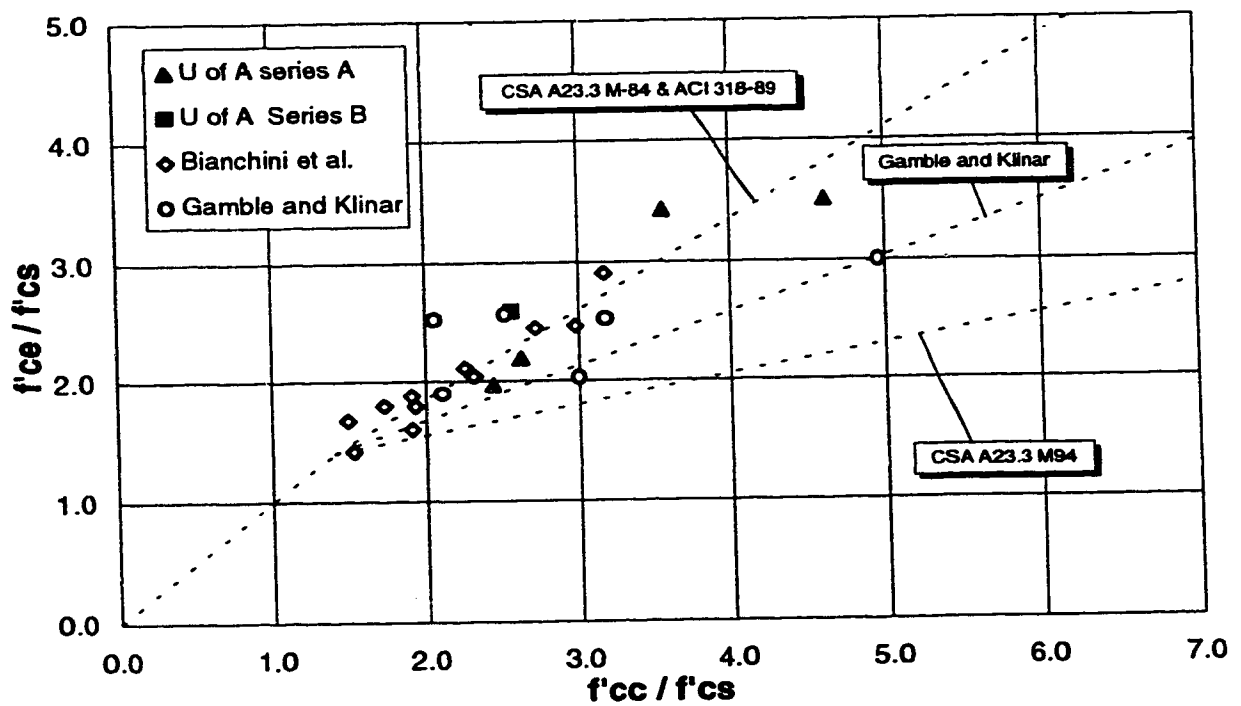


Figure 5.4 Tests of slab-unloaded interior plates

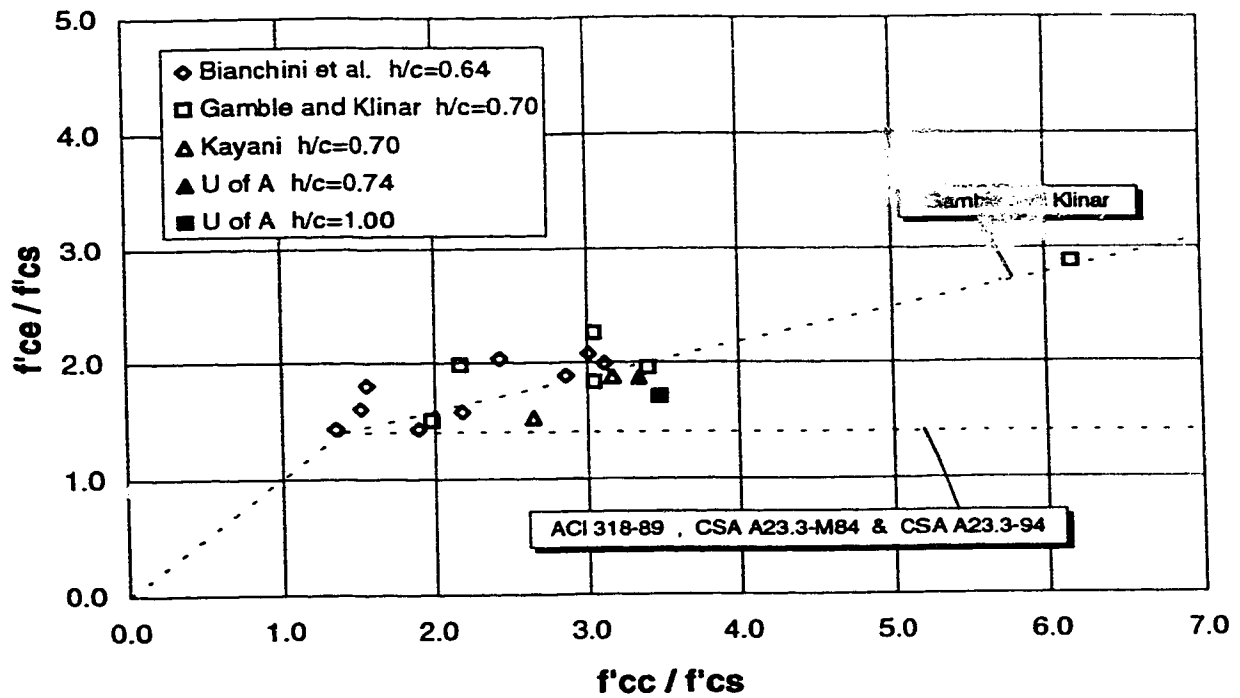


Figure 5.5 Tests of slab-unloaded edge sandwich plates

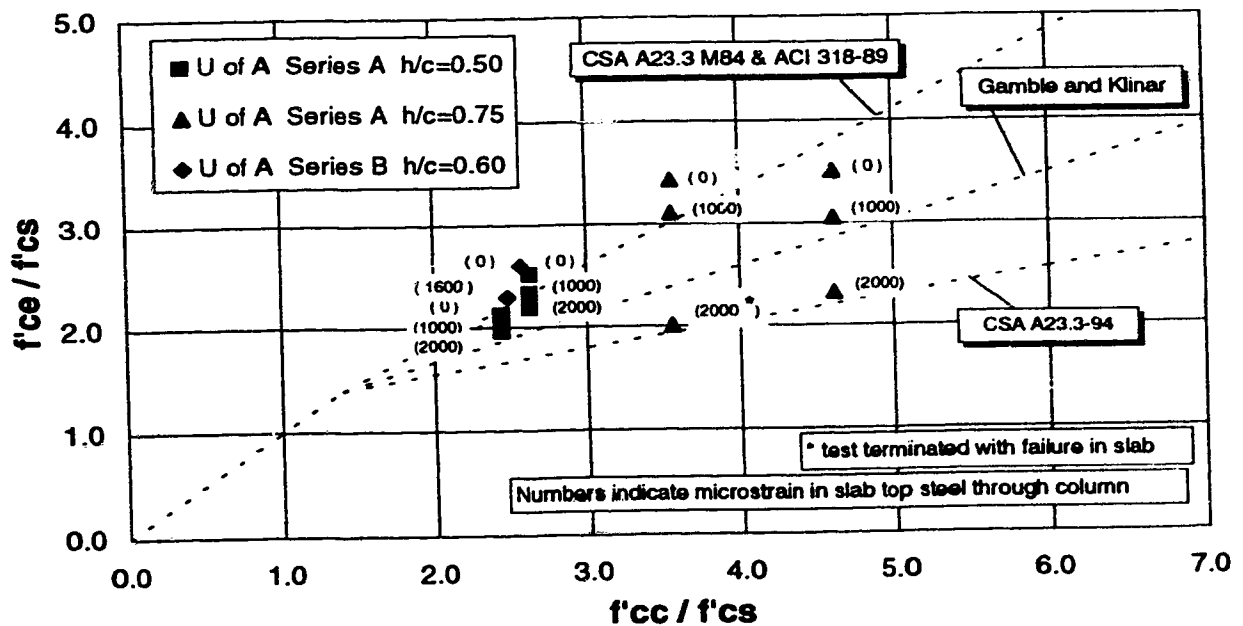


Figure 5.6 Slab load effect on interior joint strength

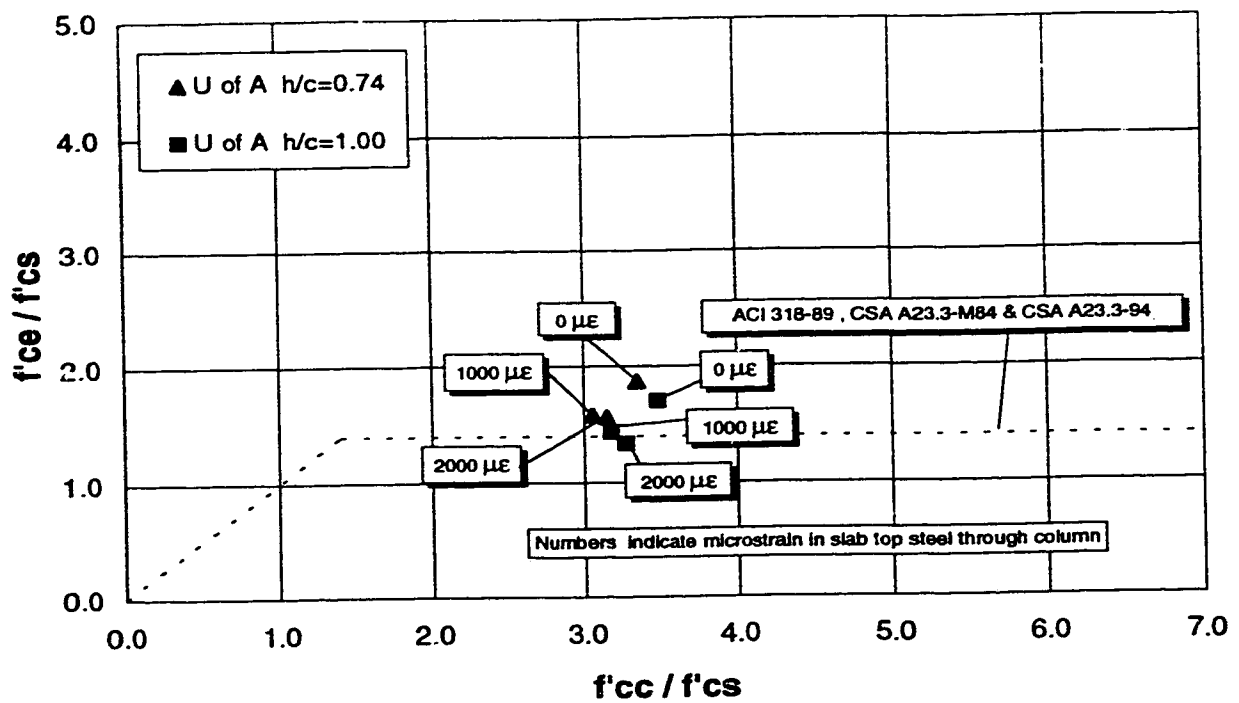


Figure 5.7 Slab load effect on edge joint strength

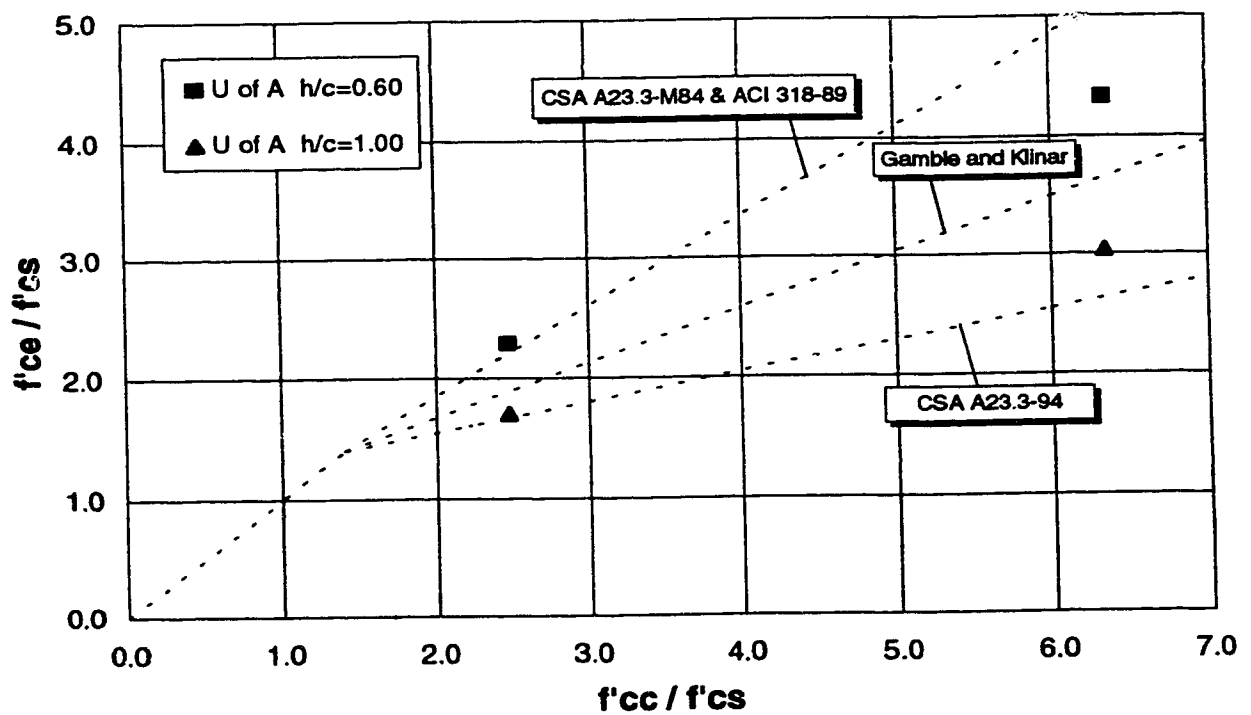


Figure 5.8 Effect of h/c on interior joint strength

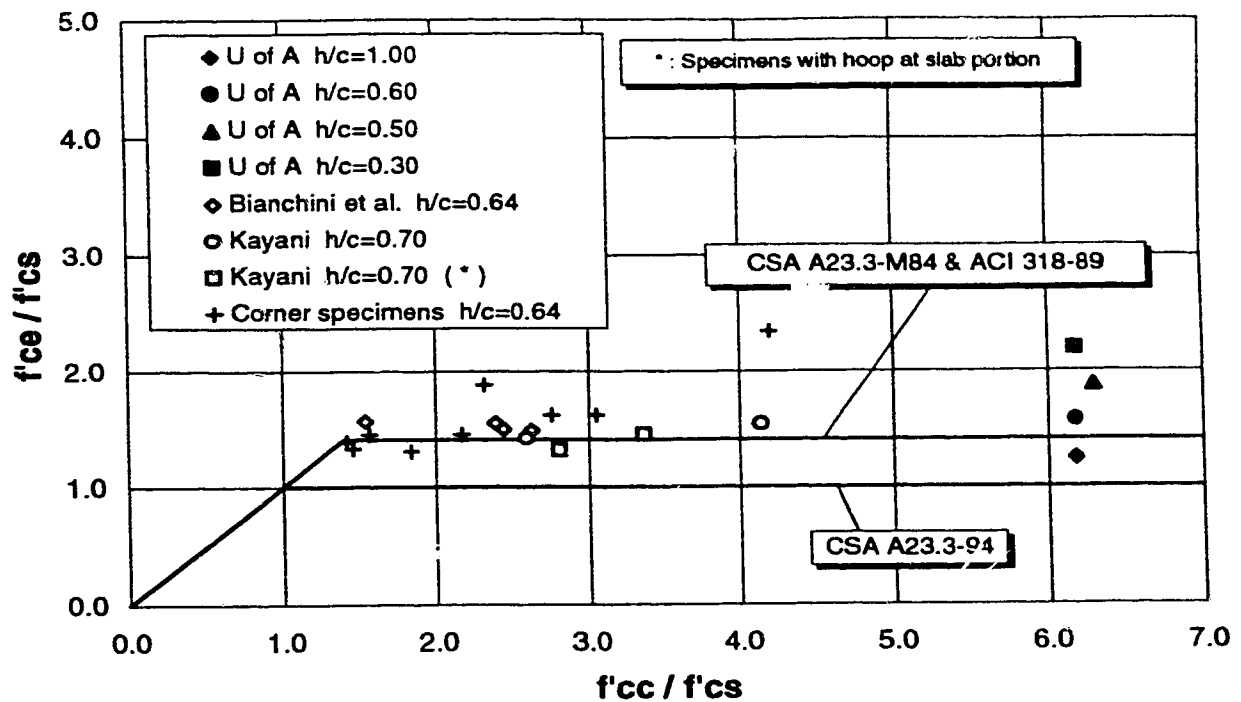


Figure 5.9 Test results of corner and sandwich columns

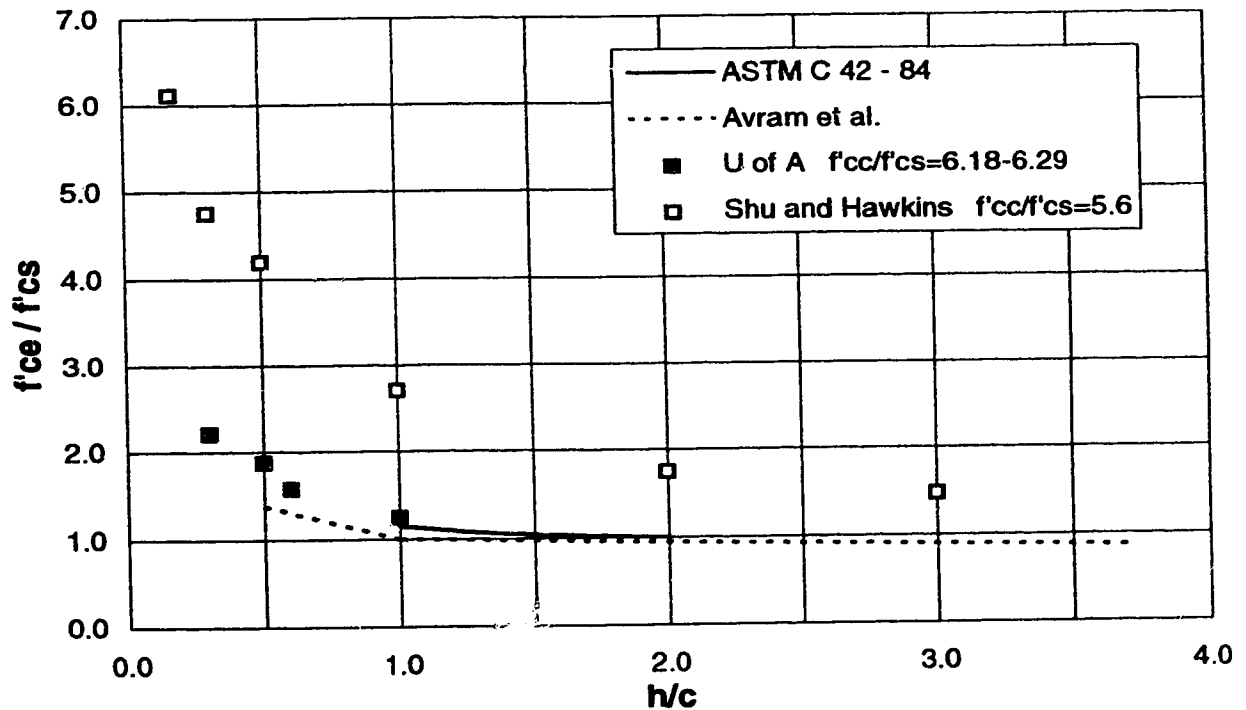


Figure 5.10 Correction factors for cylinder and cube tests

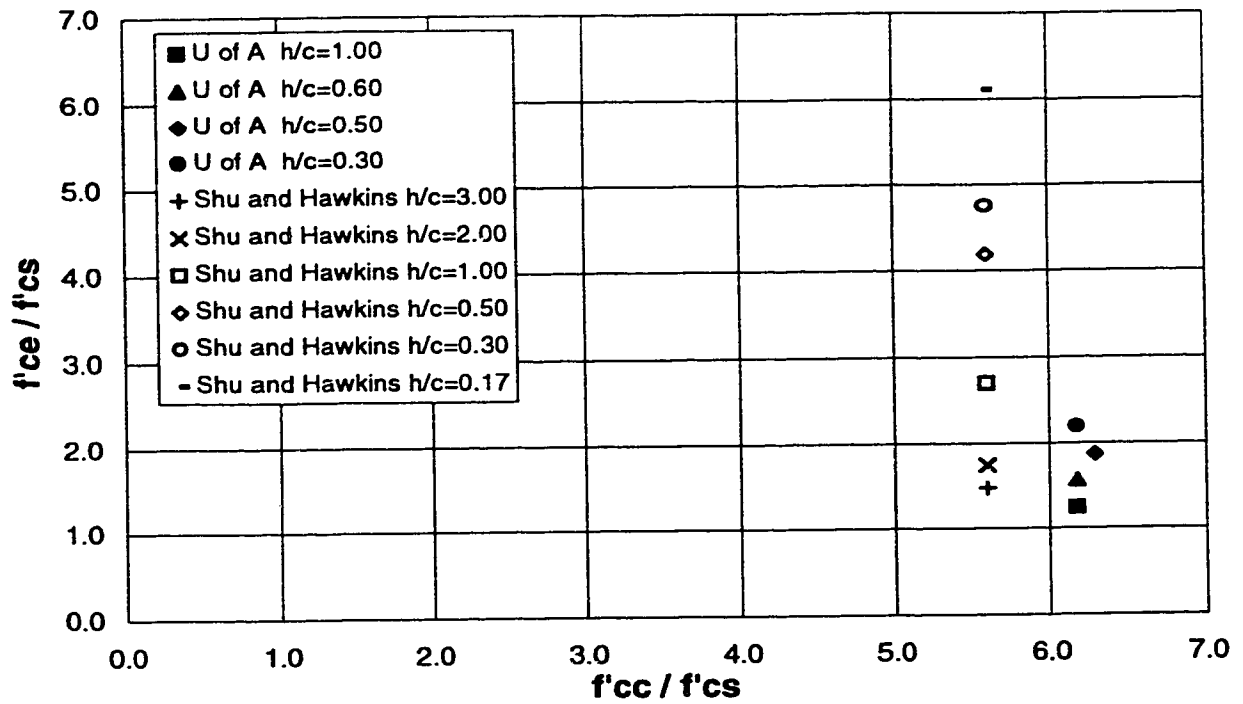


Figure 5.11 Comparison of tests on sandwich columns

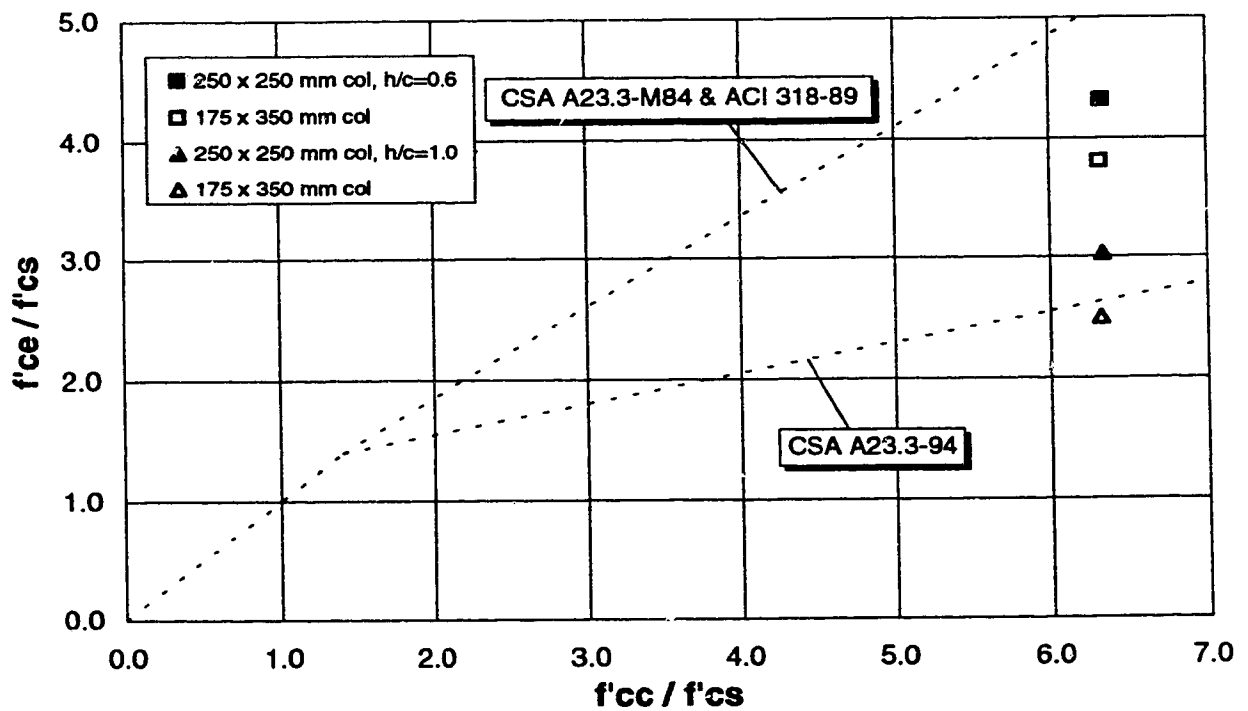


Figure 5.12 Effect of column rectangularity (ISP)

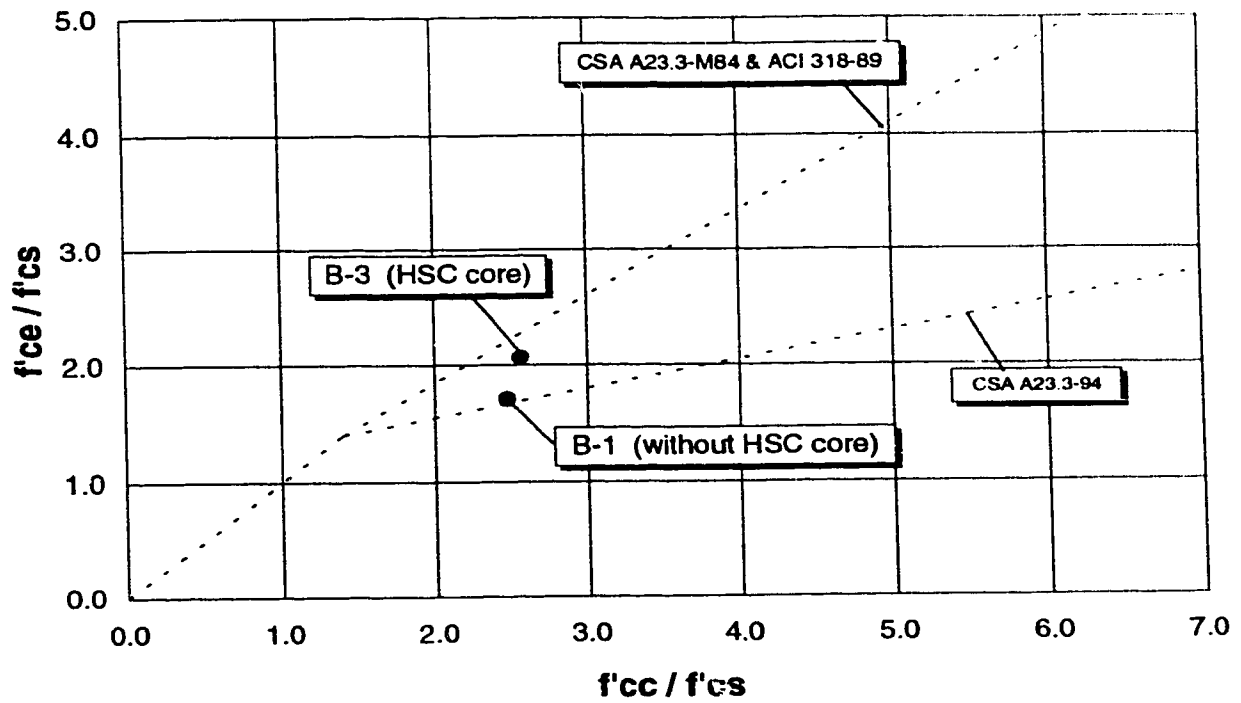


Figure 5.13 Effect of HSC core on interior joint strength

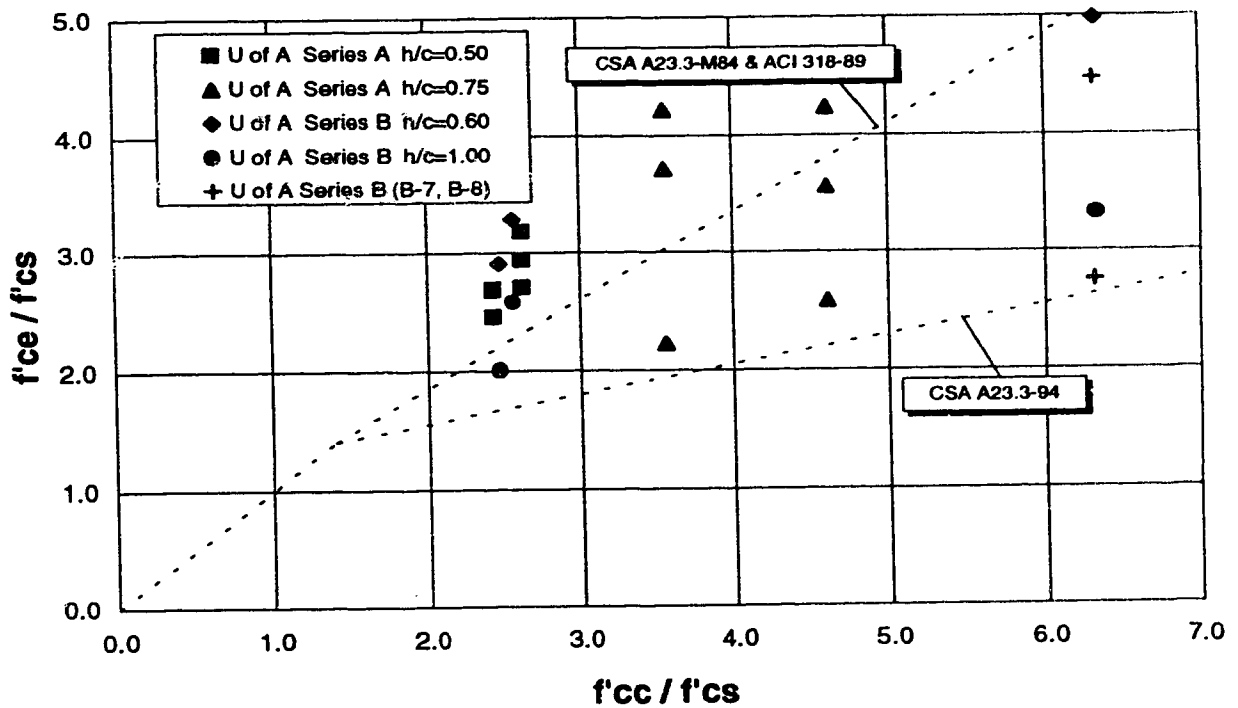


Figure 5.14 Test results of ISP according to A23.3-94

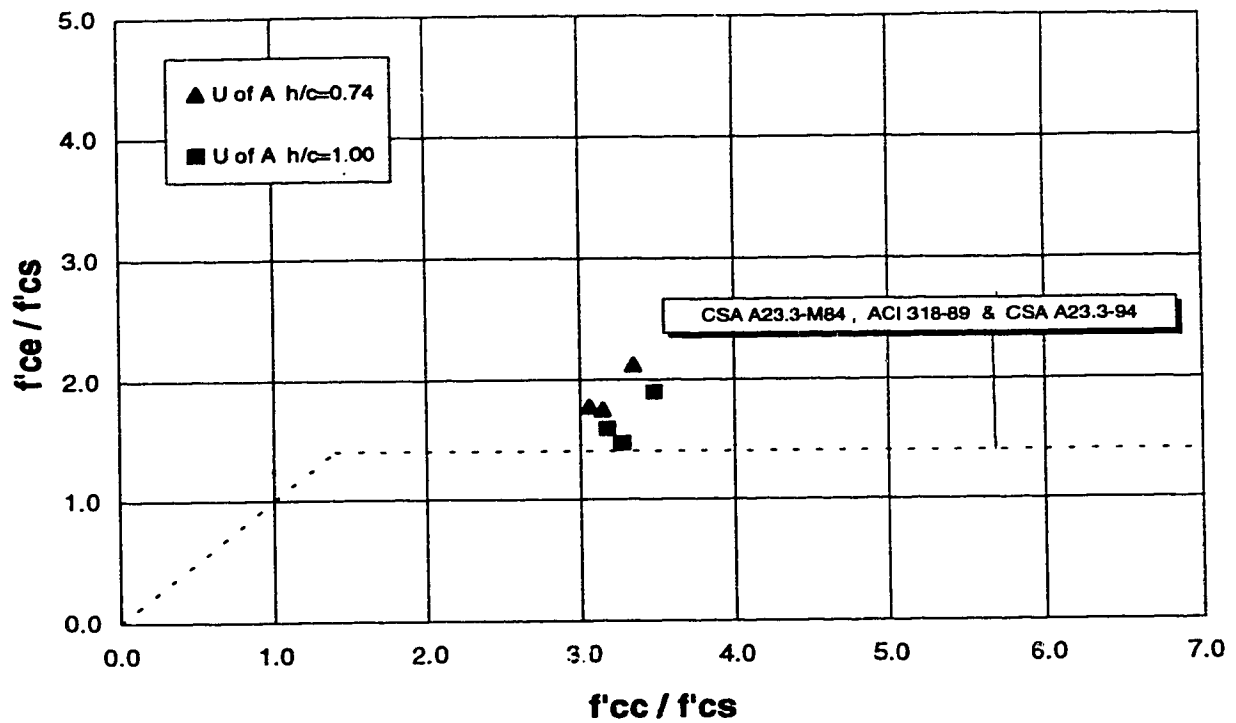


Figure 5.15 Test results of ESP according to A23.3-94

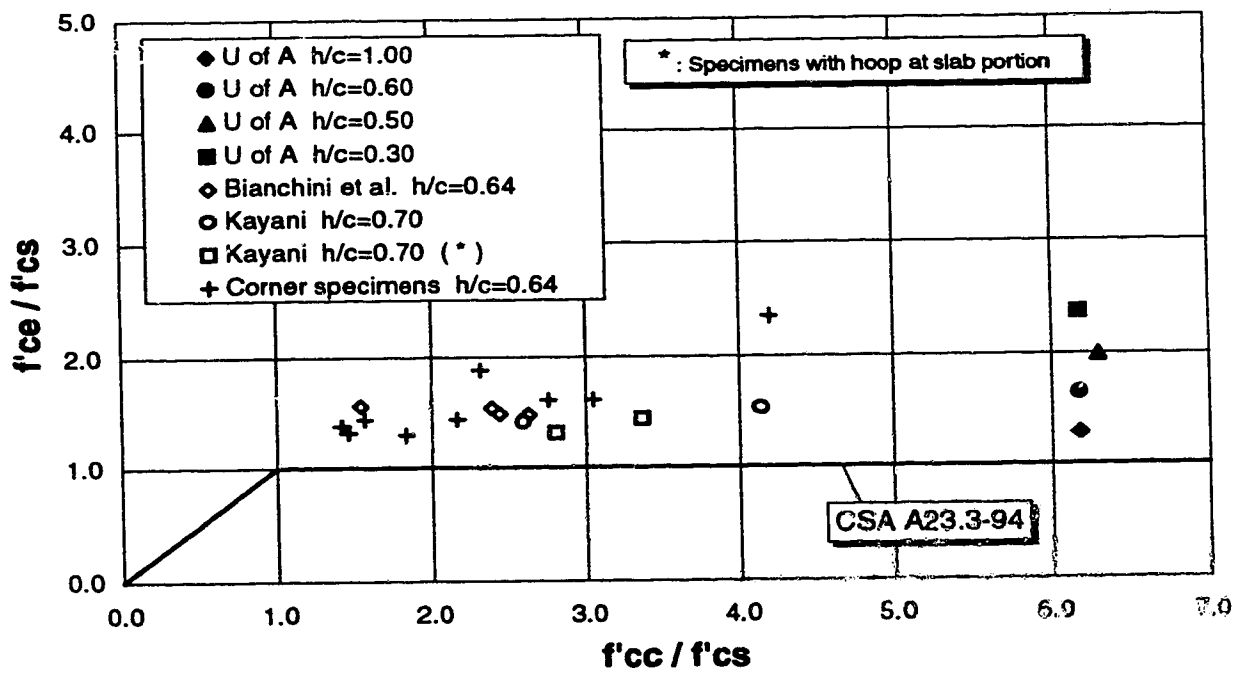


Figure 5.16 Test results of sandwich and corner columns according to A23.3-94

6. PROPOSED DESIGN PROVISIONS

6.1 General

Different design provisions have been proposed in the past to evaluate the effective strength of columns intersected by concrete floors. Earlier in chapter 5, the effect of slab loading and the aspect ratio, h/c , were identified as playing a significant role when evaluating the effective strength of interior, edge and corner columns. Among all of the existing design recommendations only the 1994 CSA provisions account for the effect of slab loading. The effect of the h/c ratio has not been accounted for in any of the existing building design codes.

The same format proposed by Bianchini et al. and by Gamble and Klinar is adopted. The effect of both slab loading and the aspect ratio, h/c , on the column strength can be identified in plots of the ratio of column effective strength to slab concrete strength, f'_{ce}/f'_{cs} , against the ratio of column concrete strength to slab concrete strength, f'_{cc}/f'_{cs} .

6.2 Design provisions

6.2.1 Interior columns

Taking into consideration that lack of experimental data makes it impossible to propose an accurate design recommendation, this investigation would support initially the 1.4 ratio as the limit at which the strength of an interior column is reduced by the intervening slab concrete. For higher differentials of column to slab concrete, f'_{cc}/f'_{cs} , this experimental program would support an equation of the form

$$f'_{ce} = \left(1.4 - \frac{0.35}{h/c} \right) f'_{cs} + \frac{0.25}{h/c} f'_{cc} \leq f'_{cc} , \quad 1/3 \leq h/c \quad [6.1]$$

This design equation is recommended for interior slab-column connections whose slab thickness is greater than 1/3 times the column dimension. For h/c ratios equal to 1/3 the proposed design curve matches the ACI 318-89 design curve for interior columns. According to this, use of the ACI 318-89 equation may be adequate for values of h/c less than 1/3. For h/c ratios equal to one, equation 6.1 aligns with the 1994 CSA design curve.

Figure 6.1 shows plots of f'_{ce}/f'_{cs} versus f'_{cc}/f'_{cs} for h/c ratios varying from one-third to one. Design equations proposed by ACI 318-89 and by CSA A23.3-M84 and CSA A23.3-94 are also shown for comparison.

Figure 6.2 shows the design curves for h/c ratios of 0.6 and 1.0 and the corresponding test results.

Table 6.1 shows the ratios of test to predicted effective strength for the series B interior sandwich plate specimens subjected to slab loads. Comparison is made in light of ACI 318-89, CSA A23.3-94 and the design provision proposed by the author.

In general, ratios of test to predicted column strengths less than 1.0 were obtained with the ACI 318-89 design equation. Differences up to 51 % were calculated with such provision. With regards to the CSA A23.3-94 provisions, ratios of test to predicted strengths greater than unity were obtained for the majority of specimens. The only specimen in which such ratio was less than 1.0 was specimen B-7 which had a rectangular column. Differences up to 64% were calculated for specimen B-6 which had a f'_{cc}/f'_{cs} ratio of 6.33 and an h/c ratio of 0.6 .

Test-to-predicted column strength ratios calculated with the design equation proposed by the author led always to conservative values. Such ratios were always greater than 1.0 with the maximum variation between test and predicted strengths being 34% for the case of specimen B-8, a rectangular column specimen with an h/c ratio of 0.86 .

6.2.2 Edge Columns

This investigation supports the design guideline contained in the 1994 CSA Standard. This design provision appears to be a reasonable lower bound for the available test results. Even though one test result falls below the proposed design curve there is not enough data to modify the design equation. Moreover, that test result corresponds to an edge plate specimen with heavy slab loads. Slab load intensities close to the load level applied in that specific test may be unlikely to be applied in residential/office buildings. The design provision for edge columns is stated as follows.

$$f'_{ce} = 1.4 f'_{cs} \leq f'_{cc} \quad [6.2]$$

This equation is shown in fig. 6.3 . For comparison, test results on edge sandwich plates with slabs heavily loaded are also included.

6.2.3 Corner columns and unconfined joints

All available results from corner column and unconfined sandwich column tests are presented in fig. 6.4 .

The design equation proposed in CSA A23.3-94 for the design of corner columns intersected by concrete floors appears to be a conservative guideline for the design of this type of connection. However, based on these test results a f'_{cc}/f'_{cs} ratio of 1.2 appears to be also a safe lower bound. Beyond this value, the value of f'_{ce}/f'_{cs} appears to be independent of f'_{cc}/f'_{cs} . According to this, the proposed design provision for the design of corner columns is shown as follows.

$$f'_{ce} = 1.2 f'_{cs} \leq f'_{cc} \quad [6.3]$$

Specimen		ACI 318-89		CSA A23.3-94		Author	
Mark	$f'_{ce\ test}$	$f'_{ce\ calc}$	$\frac{f'_{ce\ test}}{f'_{ce\ calc}}$	$f'_{ce\ calc}$	$\frac{f'_{ce\ test}}{f'_{ce\ calc}}$	$f'_{ce\ calc}$	$\frac{f'_{ce\ test}}{f'_{ce\ calc}}$
B-1	71.54	92.70	0.77	70.10	1.02	72.10	1.02
B-2	96.08	92.70	1.04	70.10	1.37	77.63	1.24
B-3	90.72	100.15	0.91	74.45	1.22	74.45	1.22
B-5	45.44	76.50	0.59	39.50	1.15	39.50	1.15
B-6	64.83	76.50	0.85	39.50	1.64	51.83	1.25
B-7	47.45	96.65	0.49	49.95	0.95	42.93	1.11
B-8	72.25	96.65	0.75	49.95	1.45	53.75	1.34
Average			0.77		1.26		1.19
Standard Deviation			0.1848		0.2448		0.1065

Notes: 1. $f'_{ce\ test}$ values were calculated based on an α_1 factor equal to 0.85.
2. Specimen B-4 was not subjected to slab loading.

Table 6.1 Ratios of test to predicted column effective strength

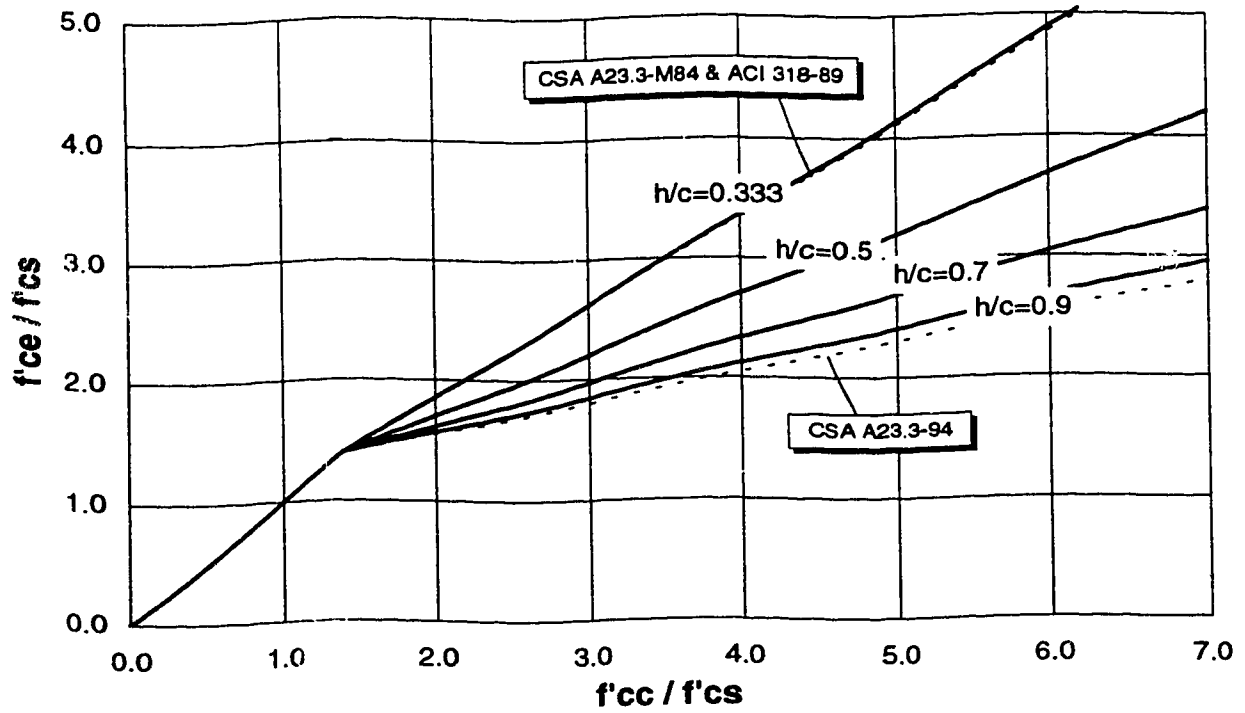


Figure 6.1 Proposed design curves for interior columns

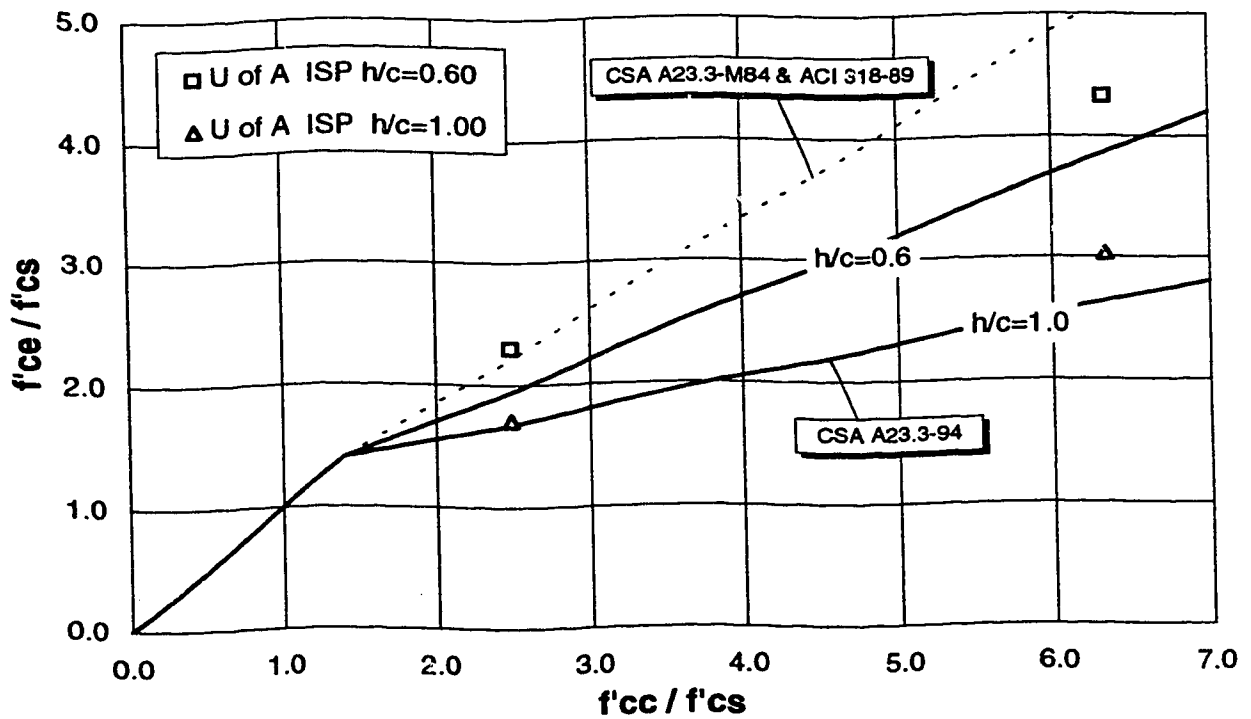


Figure 6.2 Design curves and test results

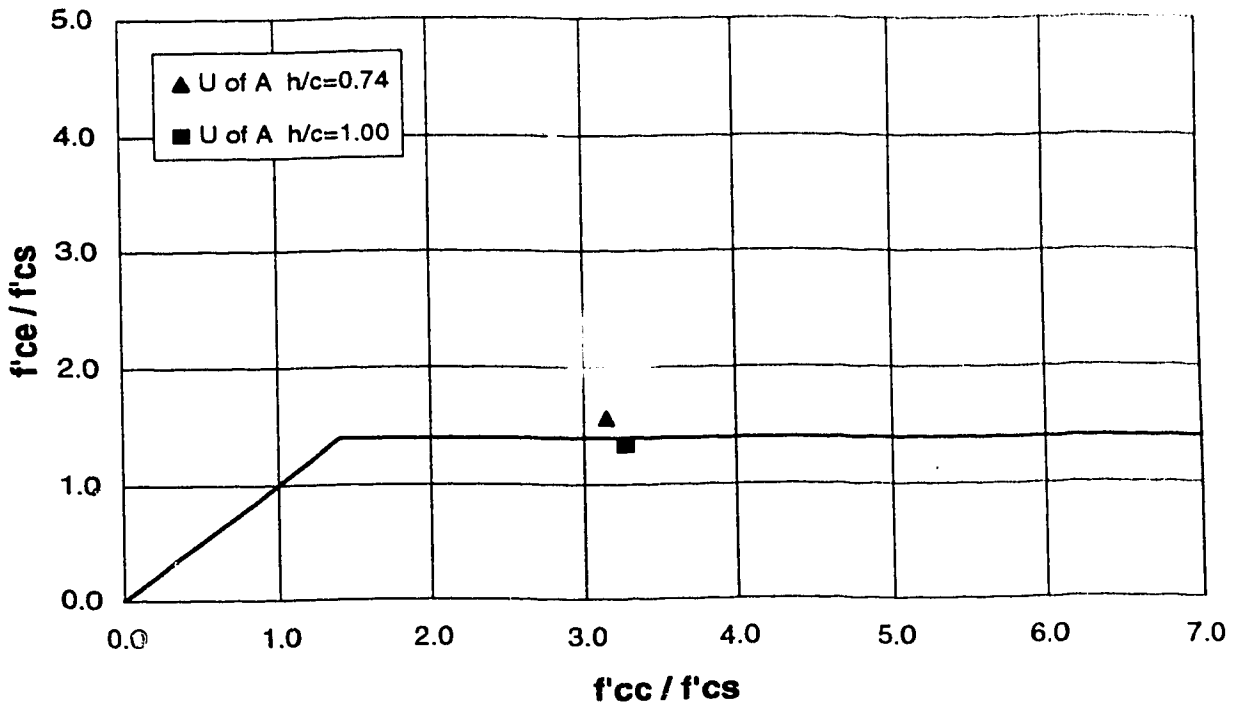


Figure 6.3 Proposed design curve for edge columns

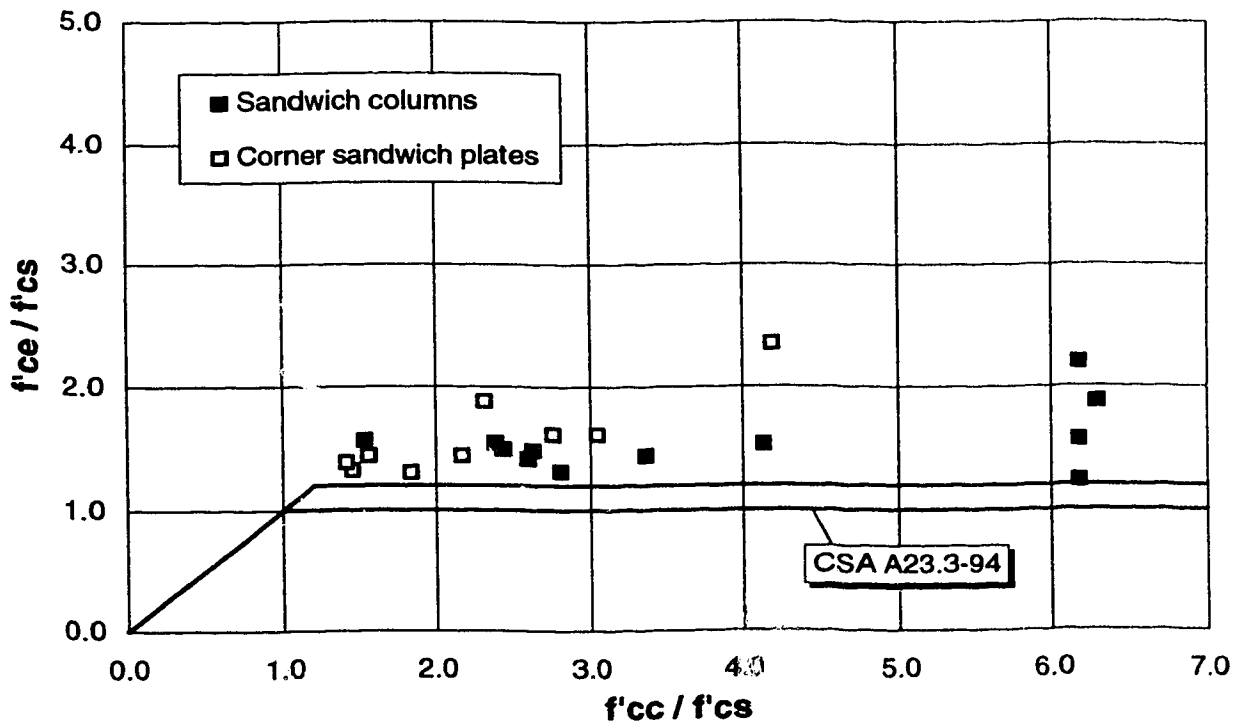


Figure 6.4 Proposed design curve for corner columns

7. SUMMARY, CONCLUSIONS AND RECOMMENDATIONS

7.1 Summary

Taking into consideration that columns in modern buildings may be usually cast with concrete much stronger than that used in the intervening floor, it is important to evaluate the effect that the intersecting layer of weaker concrete has on the strength of the column. The main factor which determines how strong the slab portion of a column may be is the amount of confinement supplied to the joint region by the surrounding floor concrete. Two main variables that may substantially modify the confinement regime at the joint region are the level of gravity load applied on the slab and the ratio of the slab thickness to column dimension, h/c .

A literature survey showed that the effects of these variables have thus far not been accounted for when ascertaining the strength of high-strength concrete columns intersected by concrete floors. This observation led to the experimental program developed in this research work.

Results from 30 specimens simulating slab-column joints are presented. Of these, 26 were sandwich plate specimens and 4 were sandwich columns. Sandwich plate specimens consist of two high-strength concrete column stubs intersected by a slab segment. Sandwich column specimens consist of two high-strength concrete column ends intersected by a layer of slab concrete at the specimen mid-height.

The experimental program was separated up into four series. Series A examined the effect of slab loading on interior slab-column connections. Twelve sandwich plate specimens were built and tested for this purpose. Series B examined the effect of aspect ratio, h/c , column rectangularity and the placement of high-strength core within the joint region, as well as the effect of slab loading on the column strength. Eight sandwich plates were built and tested. Series C consisted of six edge sandwich plate specimens that were tested to evaluate the effect of slab loading on edge slab-column connections. Series D consisted of four sandwich column specimens. The main objective of this series was to evaluate the effect of the h/c ratio on the strength of unconfined joints.

Sandwich plate specimens were subjected to either column load or to column load plus slab loads. Sandwich column specimens were subjected to column load only.

Column concrete strengths varied from 89 to 120 MPa. Slabs and unconfined joint concrete strengths varied from 15 to 46 MPa.

The column longitudinal shortening and the transverse strain applied to the joint by the top slab reinforcement were measured.

According to test results design provisions were developed to evaluate the strength of interior, edge and corner concrete columns intersected by concrete slabs.

7.2 Conclusions

7.2.1 Conclusions from testing

1. As the level of load applied on the slab increases the effective compressive strength of the column decreases. This decrease in strength is higher for specimens with columns built with concrete much stronger than that used in the floor.
2. Dimension of both slab and column play an important role in modifying the confinement conditions at the joint region. As the ratio of slab thickness to column width, h/c , increases, the effective compressive strength of the column decreases. This reduction is greater for higher ratios of column concrete cylinder strength to slab concrete cylinder strength, f'_{cc}/f'_{cs} .
3. For rectangular columns, it is the shortest column dimension that should be used in calculating the h/c ratio of the joint.
4. Placement of a high-strength concrete core within the joint region increases the strength of the column.

7.2.2 Conclusions regarding code provisions

1. Code provisions should be based on results of specimens tested with slab loads. Omission of the slab load effect leads to unconservative designs. For this reason, the design equations contained in ACI 318-89 and CSA A23.3-M84 used to evaluate the effective strength of concrete columns intersected by concrete floors are not adequate. CSA A23.3-94 provides a lower bound for existing test results of specimens with slab loads.
2. No code procedure accounts for the effect of the h/c ratio when evaluating the strength of columns intersected by floors. According to test results, ACI 318-89 and CSA A23.3-M84 design provisions may become unconservative for slab-column connections with high h/c ratios. Conversely, CSA A23.3-94 provisions may become overly conservative for connections with low h/c ratios.
3. No special provision for the design of rectangular columns intersected by floors of weaker concrete strength is given in any code design provision.
4. A modification to the CSA A23.3-94 provision for interior columns to account for h/c is proposed in chapter 6.
5. A design provision for edge connections is also proposed. This investigation supports the design equation for edge columns presented by CSA A23.3-94.

6. For the design of corner columns, a modification to the CSA A23.3-94 design curve is proposed as well.

7.3 Recommendations

Design provisions for the design of interior, edge and corner columns intersected by weaker concrete slabs are presented in chapter 6. Accuracy of these proposed design equations clearly depends on availability of experimental data. In view of the scarcity of such experimental results the following recommendations are made.

1. Further testing of interior, edge and corner slab-column connections under realistic slab loading is required to enhance the available data base. Selection of f'_{cc}/f'_{cs} ratios varying from 1.0 to 2.0 would be desirable to reexamine the point at which the column concrete strength is affected by the intervening slab concrete.
2. Tests need also to be extended to slab/beam-column connections. Previous research on this type of specimen was carried out by Bianchini et al. (1960) and Siao (1994). There is a need for this type of test with properly controlled boundary conditions.
3. Further evaluation of the effect the aspect ratio, h/c , is required to improve the design provisions herein proposed. Tests of specimens with low h/c ratios may be preferred since these ratios are more likely to be found in modern buildings.
4. Test results reported in this thesis constitute the only source of information of tests on sandwich slab-column connection specimens subjected to both column and slab loads. These tests are also the sole source of information of tests on slab-column connections accounting for the slab and column dimensions. There is a need to reproduce and confirm these results in order to enhance the scope of the proposed design provisions.
5. Tests further evaluating the effect of column rectangularity and column circularity are also recommended.
6. Exhaustive assessment of the effect of the placement of a high-strength concrete core within the joint region is also suggested. This constructive technique may constitute an alternative solution to the problem of transmission of loads from high-strength concrete columns through normal-strength concrete floors.

LIST OF REFERENCES

- ACI Committee 318, 1989, "Building Code Requirements for Reinforced Concrete (ACI 318-89) (Revised 1992) and Commentary-ACI 318R-89 (Revised 1992)", American Concrete Institute, Detroit, 353 pp.
- ASTM Committee C-9, 1984, "ASTM C42-84a: Standard Method of Obtaining and Testing Drilled Cores and Sawed Beams of Concrete", American Society for Testing and Materials, Philadelphia.
- Avram, C., Facaoaru, I., Filimon, O. and Terteu, I., 1981, Concrete Strength and Strains, Elsevier Scientific Publishing Company, Amsterdam, 558 pp.
- Bianchini, A. C., Woods, R. E. and Kesler, C. E., 1960, "Effect of Floor Concrete Strength on Column Strength", ACI journal, Proceedings Vol. 31, No. 11, pp. 1149-1169.
- Canadian Standards Association, 1984, "Design of Concrete Structures for Buildings (CSA CAN3-A23.3-M84)", Canadian Standards Association, Rexdale, Ontario, 280 pp.
- Canadian Standards Association, 1994, "Design of Concrete Structures for Buildings (CSA A23.3-94)", Canadian Standards Association, Rexdale, Ontario, 199 pp.
- CEB/FIP, 1994, "Application of High Performance Concrete", CEB Bulletin d'Information No. 222, Comité Euro-International du Béton (CEB)/Fédération Internationale de la Précontrainte (FIP), Lausanne, 65 pp.
- Chen, S. A. and MacGregor, J. G., 1993, "A Shear-Friction Truss Model for Reinforced Concrete Beams subjected to Shear", Structural Engineering Report No. 188, Department of Civil Engineering, University of Alberta, 359 pp.
- Gamble, W. L. and Klinar, J. D., 1991, "Tests of High-Strength Concrete Columns with Intervening Floor Slabs", Journal of Structural Engineering, ASCE, Vol. 117, No. 5, pp. 1462-1476.
- Howard, N. L. and Leatham, D. M., 1992, "The Production and Delivery of High-Strength Concrete", ACI compilation 17, American Concrete Institute, Detroit, pp. 20-24.
- Kayani, M. K., 1992, "Load Transfer from High-Strength Concrete Columns through Lower Strength Concrete Slabs", PhD thesis, Department of Civil Engineering, University of Illinois, Urbana-Champaign, 111 pp.
- Moreno, J., 1990, "225 W. Wacker Drive", Concrete International, Vol. 12, No. 1, American Concrete Institute, Detroit, pp. 35-39.

Murdock, J. W. and Kesler, C. E., 1957, "Effect of Length to Diameter Ratio of Specimen on the Apparent Compressive Strength of Concrete", ASTM bulletin, pp. 68-73.

Neville, A. M., 1981, Properties of Concrete, 3d edition, Pitman Publishing Ltd., London, 779 pp.

Price, W. H., 1951, "Factors Influencing Concrete Strength", ACI Journal, Vol. 22, No. 6, American Concrete Institute, Detroit, pp. 417-432.

Randall, V. and Foot, K., 1992, "High-Strength Concrete for Pacific First Center", ACI compilation 17, American Concrete Institute, Detroit, pp. 54-56.

Shu, Ch-Ch. and Hawkins, N. M., 1992, "Behavior of Columns Continuous through Concrete Floors", ACI Structural Journal, Vol. 89, No. 4, American Concrete Institute, Detroit, pp. 405-414 .

Siao, W. B., 1994, "Reinforced Concrete Column Strength at Beam/Slab and Column Intersection", ACI Structural Journal, Vol. 91, No. 1, American Concrete Institute, Detroit, pp. 3-9 .

Troxell, G. E., Davis, H. E. and Kelly, J. W., 1968, Composition and Properties of Concrete, McGraw-Hill Book Company, New York, 529 pp.

Wilson, E. L. and Habibullah, A., 1992, SAP90, A Series of Computer Programs for the Finite Element Analysis of Structures, Computers and Structures, Inc., Berkeley.

APPENDIX A

Finite element modelling of prototype slab-column connections and connection specimens

**FEM of prototype R/C interior connection (h=250mm, c=250mm)
SYSTEM**

L=1 : Accounts for both Dead and Live Load

JOINTS

C

1 X=0.00 Y=0.00 Z=0.00

2 X=0.75

3 X=1.25

4 X=1.55

5 X=1.65

6 X=1.85

7 X=1.975

8 X=2.10

9 X=2.35

10 X=2.475

11 X=2.60

12 X=2.80

13 X=2.90

14 X=3.20

15 X=3.70

16 X=4.45

C

17 X=0.00 Y=0.75

18 X=0.75

19 X=1.25

20 X=1.55

21 X=1.65

22 X=1.85

23 X=1.975

24 X=2.10

25 X=2.35

26 X=2.475

27 X=2.60

28 X=2.80

29 X=2.90

30 X=3.20

31 X=3.70

32 X=4.45

C

33 X=0.00 Y=1.25

34 X=0.75

35 X=1.25

36 X=1.55

37 X=1.65

38 X=1.85

39 X=1.975

40 X=2.10

41 X=2.35

42 X=2.475

43 X=2.60

44 X=2.80

45 X=2.90

46 X=3.20

47 X=3.70

48 X=4.45

C

49 X=0.00 Y=1.55

50 X=0.75

51 X=1.25

52 X=1.55

53 X=1.65

54 X=1.85

55 X=1.975

56 X=2.10

57 X=2.35

58 X=2.475

59 X=2.60

60 X=2.80

61 X=2.90

62 X=3.20

63 X=3.70

64 X=4.45

C

65 X=0.00 Y=1.65

66 X=0.75

67 X=1.25

68 X=1.55

69 X=1.65

70 X=1.85

71 X=1.975

72 X=2.10

73 X=2.35

74 X=2.475

75 X=2.60

76 X=2.80

77 X=2.90

78 X=3.20

79 X=3.70

80 X=4.45

C

81 X=0.00 Y=1.85

82 X=0.75

83 X=1.25

84 X=1.55

85 X=1.65

86 X=1.85

87 X=1.975

88 X=2.10

89 X=2.35

90 X=2.475

91 X=2.60

92 X=2.80

93 X=2.90

94 X=3.20

95 X=3.70

96 X=4.45

C

97 X=0.00 Y=1.975

98 X=0.75

99 X=1.25

100 X=1.55

101 X=1.65

102 X=1.85

103 X=1.975

104 X=2.10

105 X=2.35

106 X=2.475

107 X=2.60

108 X=2.80

109 X=2.90

110 X=3.20

111 X=3.70

112 X=4.45

C

113 X=0.00 Y=2.10

114 X=0.75

115 X=1.25

116 X=1.55

117 X=1.65

118 X=1.85

119 X=1.975

120 X=2.10

121 X=2.35

122 X=2.475

123 X=2.60

124 X=2.80

125 X=2.90

126 X=3.20

127 X=3.70

128 X=4.45

C

129 X=0.00 Y=2.35

130 X=0.75

131 X=1.25

132 X=1.55

133 X=1.65

134 X=1.85

135 X=1.975

136 X=2.10

137 X=2.35

138 X=2.475

139 X=2.60

140 X=2.80

141 X=2.90

142 X=3.20

143 X=3.70

144 X=4.45

C

145 X=0.00 Y=2.475

146 X=0.75

147 X=1.25

148 X=1.55

149 X=1.65

150 X=1.85

151 X=1.975

152 X=2.10

153 X=2.35

154 X=2.475

155 X=2.60

156 X=2.80

157 X=2.90

158 X=3.20

159 X=3.70

160 X=4.45

C

161 X=0.00 Y=2.60

162 X=0.75

163 X=1.25

164 X=1.55

165 X=1.65

166 X=1.85

167 X=1.975

168 X=2.10

169 X=2.35

170 X=2.475

171 X=2.60

172 X=2.80

173 X=2.90

174 X=3.20

175 X=3.70

176 X=4.45

C

177 X=0.00 Y=2.80

178 X=0.75

179 X=1.25

180 X=1.55

181 X=1.65

182 X=1.85

183 X=1.975

184 X=2.10

185 X=2.35

186 X=2.475

187 X=2.60

188 X=2.80

189 X=2.90

190 X=3.20

191 X=3.70

192 X=4.45

C

193 X=0.00 Y=2.90

194 X=0.75

195 X=1.25
 196 X=1.55
 197 X=1.65
 198 X=1.85
 199 X=1.975
 200 X=2.10
 201 X=2.35
 202 X=2.475
 203 X=2.60
 204 X=2.80
 205 X=2.90
 206 X=3.20
 207 X=3.70
 208 X=4.45
 C
 209 X=0.00 Y=3.20
 210 X=0.75
 211 X=1.25
 212 X=1.55
 213 X=1.65
 214 X=1.85
 215 X=1.975
 216 X=2.10
 217 X=2.35
 218 X=2.475
 219 X=2.60
 220 X=2.80
 221 X=2.90
 222 X=3.20
 223 X=3.70
 224 X=4.45
 C
 225 X=0.00 Y=3.70
 226 X=0.75
 227 X=1.25
 228 X=1.55
 229 X=1.65
 230 X=1.85
 231 X=1.975
 232 X=2.10
 233 X=2.35
 234 X=2.475
 235 X=2.60
 236 X=2.80
 237 X=2.90
 238 X=3.20
 239 X=3.70
 240 X=4.45
 C
 241 X=0.00 Y=4.45
 242 X=0.75
 243 X=1.25
 244 X=1.55
 245 X=1.65

246 X=1.85
 247 X=1.975
 248 X=2.10
 249 X=2.35
 250 X=2.475
 251 X=2.60
 252 X=2.80
 253 X=2.90
 254 X=3.20
 255 X=3.70
 256 X=4.45
 C

RESTRAINTS

18 31 1 R=0,0,0,0,0
 34 47 1 R=0,0,0,0,0
 50 63 1 R=0,0,0,0,0
 66 79 1 R=0,0,0,0,0
 82 95 1 R=0,0,0,0,0
 98 111 1 R=0,0,0,0,0
 114 119 1 R=0,0,0,0,0
 122 127 1 R=0,0,0,0,0
 130 135 1 R=0,0,0,0,0
 138 143 1 R=0,0,0,0,0
 146 159 1 R=0,0,0,0,0
 162 175 1 R=0,0,0,0,0
 178 191 1 R=0,0,0,0,0
 194 207 1 R=0,0,0,0,0
 210 223 1 R=0,0,0,0,0
 226 239 1 R=0,0,0,0,0
 C
 120 121 1 R=1,1,1,0,0,0 :Joints at
 Column-Slab location
 136 137 1 R=1,1,1,0,0,0 :Joints at
 Column-Slab location
 C
 1 16 15 R=0,0,0,1,1,1 :Corner joints
 241 256 15 R=0,0,0,1,1,1 :Corner joints
 C
 2 15 1 R=0,0,0,1,0,1 :Edge joints along
 X direction
 242 255 1 R=0,0,0,1,0,1 :Edge joints
 along X direction
 C
 17 225 16 R=0,0,0,0,1,1 :Edge joints
 along Y direction
 32 240 16 R=0,0,0,0,1,1 :Edge joints
 along Y direction
 C
SHELL
 NM=1 Z=-1
 C
 1 E=22500000 U=0.20 W=37.2

C :W represents Dead load + Live Load
 C :E=4500sqr(f'c)
 C :Units:E(KN/m2), W(KN/m3)
 C
 1 JQ=1,2,17,18 TH=0.25 M=1 G=15,15 LP=0 ETYPE=0

COMBO

1 C=1.0 : 1.0

FEM of prototype R/C interior connection (h=150mm, c=250mm) SYSTEM

L=1 : Accounts for both dead and live Load

JOINTS

C	37 X=1.65
1 X=0.00 Y=0.00 Z=0.00	38 X=1.85
2 X=0.75	39 X=1.975
3 X=1.25	40 X=2.10
4 X=1.55	41 X=2.35
5 X=1.65	42 X=2.475
6 X=1.85	43 X=2.60
7 X=1.975	44 X=2.80
8 X=2.10	45 X=2.90
9 X=2.35	46 X=3.20
10 X=2.475	47 X=3.70
11 X=2.60	48 X=4.45
12 X=2.80	C
13 X=2.90	49 X=0.00 Y=1.55
14 X=3.20	50 X=0.75
15 X=3.70	51 X=1.25
16 X=4.45	52 X=1.55
C	53 X=1.65
17 X=0.00 Y=0.75	54 X=1.85
18 X=0.75	55 X=1.975
19 X=1.25	56 X=2.10
20 X=1.55	57 X=2.35
21 X=1.65	58 X=2.475
22 X=1.85	59 X=2.60
23 X=1.975	60 X=2.80
24 X=2.10	61 X=2.90
25 X=2.35	62 X=3.20
26 X=2.475	63 X=3.70
27 X=2.60	64 X=4.45
28 X=2.80	C
29 X=2.90	65 X=0.00 Y=1.65
30 X=3.20	66 X=0.75
31 X=3.70	67 X=1.25
32 X=4.45	68 X=1.55
C	69 X=1.65
33 X=0.00 Y=1.25	70 X=1.85
34 X=0.75	71 X=1.975
35 X=1.25	72 X=2.10
36 X=1.55	73 X=2.35
	74 X=2.475

75	X=2.60	126	X=3.20
76	X=2.80	127	X=3.70
77	X=2.90	128	X=4.45
78	X=3.20	C	
79	X=3.70	129	X=0.00 Y=2.35
80	X=4.45	130	X=0.75
C		131	X=1.25
81	X=0.00 Y=1.85	132	X=1.55
82	X=0.75	133	X=1.65
83	X=1.25	134	X=1.85
84	X=1.55	135	X=1.975
85	X=1.65	136	X=2.10
86	X=1.85	137	X=2.35
87	X=1.975	138	X=2.475
88	X=2.10	139	X=2.60
89	X=2.35	140	X=2.80
90	X=2.475	141	X=2.90
91	X=2.60	142	X=3.20
92	X=2.80	143	X=3.70
93	X=2.90	144	X=4.45
94	X=3.20	C	
95	X=3.70	145	X=0.00 Y=2.475
96	X=4.45	146	X=0.75
C		147	X=1.25
97	X=0.00 Y=1.975	148	X=1.55
98	X=0.75	149	X=1.65
99	X=1.25	150	X=1.85
100	X=1.55	151	X=1.975
101	X=1.65	152	X=2.10
102	X=1.85	153	X=2.35
103	X=1.975	154	X=2.475
104	X=2.10	155	X=2.60
105	X=2.35	156	X=2.80
106	X=2.475	157	X=2.90
107	X=2.60	158	X=3.20
108	X=2.80	159	X=3.70
109	X=2.90	160	X=4.45
110	X=3.20	C	
111	X=3.70	161	X=0.00 Y=2.60
112	X=4.45	162	X=0.75
C		163	X=1.25
113	X=0.00 Y=2.10	164	X=1.55
114	X=0.75	165	X=1.65
115	X=1.25	166	X=1.85
116	X=1.55	167	X=1.975
117	X=1.65	168	X=2.10
118	X=1.85	169	X=2.35
119	X=1.975	170	X=2.475
120	X=2.10	171	X=2.60
121	X=2.35	172	X=2.80
122	X=2.475	173	X=2.90
123	X=2.60	174	X=3.20
124	X=2.80	175	X=3.70
125	X=2.90	176	X=4.45

C
 177 X=0.00 Y=2.80
 178 X=0.75
 179 X=1.25
 180 X=1.55
 181 X=1.65
 182 X=1.85
 183 X=1.975
 184 X=2.10
 185 X=2.35
 186 X=2.475
 187 X=2.60
 188 X=2.80
 189 X=2.90
 190 X=3.20
 191 X=3.70
 192 X=4.45

C
 193 X=0.00 Y=2.90
 194 X=0.75
 195 X=1.25
 196 X=1.55
 197 X=1.65
 198 X=1.85
 199 X=1.975
 200 X=2.10
 201 X=2.35
 202 X=2.475
 203 X=2.60
 204 X=2.80
 205 X=2.90
 206 X=3.20
 207 X=3.70
 208 X=4.45

C
 209 X=0.00 Y=3.20
 210 X=0.75
 211 X=1.25
 212 X=1.55
 213 X=1.65
 214 X=1.85
 215 X=1.975
 216 X=2.10
 217 X=2.35
 218 X=2.475
 219 X=2.60
 220 X=2.80
 221 X=2.90
 222 X=3.20
 223 X=3.70
 224 X=4.45

C
 225 X=0.00 Y=3.70

226 X=0.75
 227 X=1.25
 228 X=1.55
 229 X=1.65
 230 X=1.85
 231 X=1.975
 232 X=2.10
 233 X=2.35
 234 X=2.475
 235 X=2.60
 236 X=2.80
 237 X=2.90
 238 X=3.20
 239 X=3.70
 240 X=4.45

C
 241 X=0.00 Y=4.45
 242 X=0.75
 243 X=1.25
 244 X=1.55
 245 X=1.65
 246 X=1.85
 247 X=1.975
 248 X=2.10
 249 X=2.35
 250 X=2.475
 251 X=2.60
 252 X=2.80
 253 X=2.90
 254 X=3.20
 255 X=3.70
 256 X=4.45

C

RESTRAINTS

18 31 1 R=0,0,0,0,0
 34 47 1 R=0,0,0,0,0
 50 63 1 R=0,0,0,0,0
 66 79 1 R=0,0,0,0,0
 82 95 1 R=0,0,0,0,0
 98 111 1 R=0,0,0,0,0
 114 119 1 R=0,0,0,0,0
 122 127 1 R=0,0,0,0,0
 130 135 1 R=0,0,0,0,0
 138 143 1 R=0,0,0,0,0
 146 159 1 R=0,0,0,0,0
 162 175 1 R=0,0,0,0,0
 178 191 1 R=0,0,0,0,0
 194 207 1 R=0,0,0,0,0
 210 223 1 R=0,0,0,0,0
 226 239 1 R=0,0,0,0,0

C

62

120 121 1 R=1,1,1,0,0,0 :Joints at Column-Slab location

136 137 1 R=1,1,1,0,0,0 :Joints at Column-Slab location

C

1 16 15 R=0,0,0,1,1,1 :Corner joints

241 256 15 R=0,0,0,1,1,1 :Corner joints

C

2 15 1 R=0,0,0,1,0,1 :Edge joints along X direction

242 255 1 R=0,0,0,1,0,1 :Edge joints along X direction

C

17 225 16 R=0,0,0,0,1,1 :Edge joints along Y direction

32 240 16 R=0,0,0,0,1,1 :Edge joints along Y direction

C

SHELL

NM=1 Z=-1

C

1 E=22500000 U=0.20 W=46

C :W represents Dead load + Live Load

C :E=4500sqr(f'c)

C :Units: E(KN/m2), W(KN/m3)

C

1 JQ=1,2,17,18 TH=0.15 M=1 G=15,15 LP=0 ETYPE=0

COMBO

1 C=1.0 : 1.0

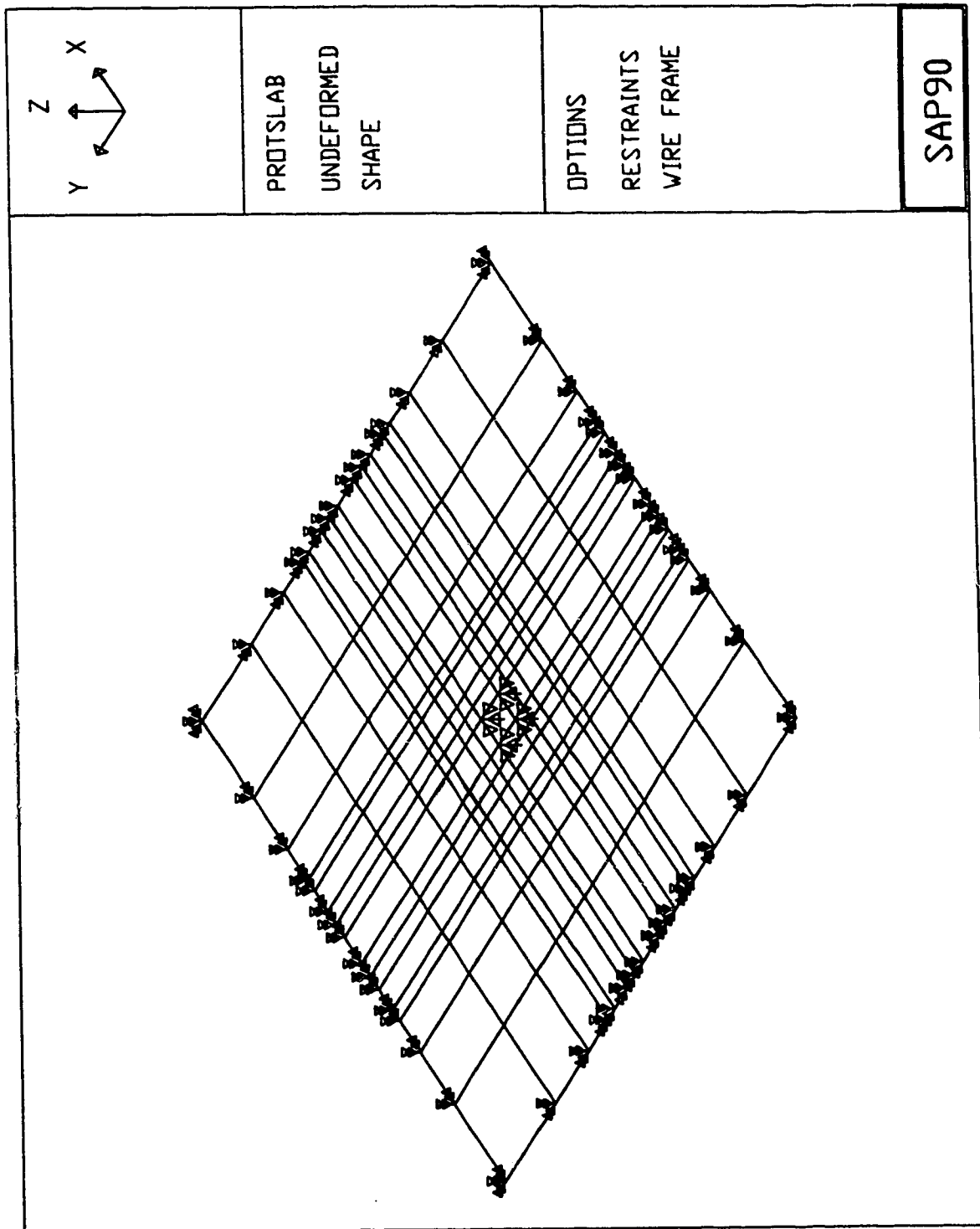


Figure A.1 3-D View of Finite Element Mesh (Prototype Connection)

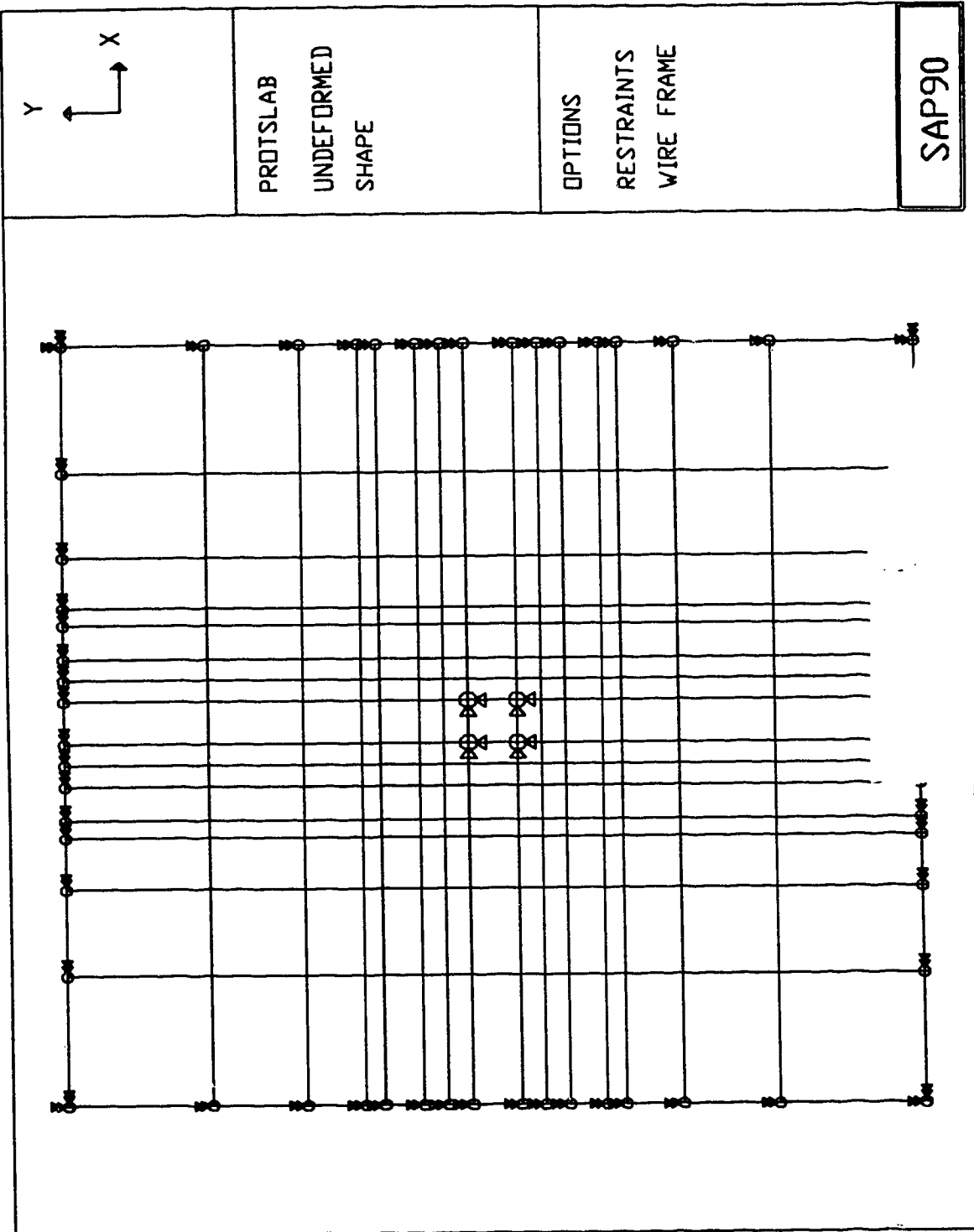


Figure A.2 Plan View of Finite Element Mesh (Prototype Connection)

FEM of R/C specimen (h=250mm, c=250mm)**SYSTEM**

L=1 : Accounts only for the slab point loads applied with the jacks.

JOINTS

C
1 X=0.00 Y=0.00 Z=0.00
C
2 X=0.10
3 X=0.30
4 X=0.425
5 X=0.55
6 X=0.80
7 X=0.925
8 X=1.05
9 X=1.25
10 X=1.35
C
11 X=0.00 Y=0.10
12 X=0.10
13 X=0.30
14 X=0.425
15 X=0.55
16 X=0.80
17 X=0.925
18 X=1.05
19 X=1.25
20 X=1.35
C
21 X=0.00 Y=0.30
22 X=0.10
23 X=0.30
24 X=0.425
25 X=0.55
26 X=0.80
27 X=0.925
28 X=1.05
29 X=1.25
30 X=1.35
C
31 X=0.00 Y=0.425
32 X=0.10
33 X=0.30
34 X=0.425
35 X=0.55
36 X=0.80
37 X=0.925
38 X=1.05
39 X=1.25
40 X=1.35
C
41 X=0.00 Y=0.55
42 X=0.10
43 X=0.30

44 X=0.425
45 X=0.55
46 X=0.80
47 X=0.925
48 X=1.05
49 X=1.25
50 X=1.35
C
51 X=0.00 Y=0.80
52 X=0.10
53 X=0.30
54 X=0.425
55 X=0.55
56 X=0.80
57 X=0.925
58 X=1.05
59 X=1.25
60 X=1.35
C
61 X=0.00 Y=0.925
62 X=0.10
63 X=0.30
64 X=0.425
65 X=0.55
66 X=0.80
67 X=0.925
68 X=1.05
69 X=1.25
70 X=1.35
C
71 X=0.00 Y=1.05
72 X=0.10
73 X=0.30
74 X=0.425
75 X=0.55
76 X=0.80
77 X=0.925
78 X=1.05
79 X=1.25
80 X=1.35
C
81 X=0.00 Y=1.25
82 X=0.10
83 X=0.30
84 X=0.425
85 X=0.55
86 X=0.80
87 X=0.925
88 X=1.05
89 X=1.25

90 X=1.35

C

91 X=0.00 Y=1.35

92 X=0.10

93 X=0.30

94 X=0.425

95 X=0.55

96 X=0.80

97 X=0.925

98 X=1.05

99 X=1.25

100 X=1.35

C

RESTRAINTS

1 44 1 R=0,0,0,0,0,0

45 46 1 R=1,1,1,0,0,0 :Restrain at Column-Slab location

47 54 1 R=0,0,0,0,0,0

55 56 1 R=1,1,1,0,0,0 :Restrain at Column-Slab location

57 100 1 R=0,0,0,0,0,0

SHELL

NM=1 Z=-1

C

1 E=22500000 U=0.20 W=24

C :W represents only the slab self-weight

C :Units: E (KN/m²), W (KN/m³)

C

1 JQ=1,2,11,12 TH=0.25 M=1 G=9,9 LP=0 ETYPE=0

LOADS

C

12 19 7 L=1 F=0,0,-43.3 :2 point loads, (43.3 KN each)

82 89 7 L=1 F=0,0,-43.3 :2 point loads, (43.3 KN each)

COMBO

1 C=1.0

FEM of R/C specimen (h=150mm, c= 250mm)

SYSTEM

L=1 :Accounts only for the point loads applied with the jacks

JOINTS

C

1 X=0.00 Y=0.00 Z=0.00

C

2 X=0.10

3 X=0.30

4 X=0.425

5 X=0.55

6 X=0.80

7 X=0.925

8 X=1.05

9 X=1.25

10 X=1.35

C

11 X=0.00 Y=0.10

12 X=0.10

13 X=0.30

14 X=0.425

15 X=0.55

16 X=0.80

17 X=0.925

18 X=1.05

19 X=1.25

20 X=1.35

C

21 X=0.00 Y=0.30

22 X=0.10

23 X=0.30

24 X=0.425

25 X=0.55

26 X=0.80

27 X=0.925

28 X=1.05

29 X=1.25

30 X=1.35

C

31 X=0.00 Y=0.425

32 X=0.10

33 X=0.30

34 X=0.425

35 X=0.55

36 X=0.80

37 X=0.925

38 X=1.05

39 X=1.25

40 X=1.35

C

41 X=0.00 Y=0.55

42 X=0.10

43 X=0.30

44 X=0.425

45 X=0.55

46 X=0.80

47 X=0.925

48 X=1.05

49 X=1.25

50 X=1.35

C

51 X=0.00 Y=0.80

52 X=0.10

53 X=0.30

54 X=0.425

55 X=0.55

56 X=0.80

57 X=0.925

58 X=1.05

59 X=1.25

60 X=1.35

C

61 X=0.00 Y=0.925

62 X=0.10

63 X=0.30

64 X=0.425

65 X=0.55

66 X=0.80

67 X=0.925

68 X=1.05

69 X=1.25

70 X=1.35

C

71 X=0.00 Y=1.05

72 X=0.10

73 X=0.30

74 X=0.425

75 X=0.55

76 X=0.80

77 X=0.925

78 X=1.05

79 X=1.25

80 X=1.35

C

81 X=0.00 Y=1.25

82 X=0.10

83 X=0.30

84 X=0.425

85 X=0.55

86 X=0.80

87 X=0.925

88 X=1.05

89 X=1.25

90 X=1.35

C

91 X=0.00 Y=1.35

92 X=0.10

93 X=0.30

94 X=0.425

95 X=0.55

96 X=0.80

97 X=0.925

98 X=1.05

99 X=1.25

100 X=1.35

C

RESTRAINTS

1 44 1 R=0,0,0,0,0,0
45 46 1 R=1,1,1,0,0,0 :Restrain at Column-Slab location
47 54 1 R=0,0,0,0,0,0
55 56 1 R=1,1,1,0,0,0 :Restrain at Column-Slab location
57 100 1 R=0,0,0,0,0,0

SHELL

NM=1 Z=-1

C

1 E=22500000 U=0.20 W=24

C :W represents only the slab self-weight

C :Units: E (KN/m²), W (KN/m³)

C

1 JQ=1,2,11,12 TH=0.15 M=1 G=9,9 LP=0 ETYPE=0

LOADS

C

12 19 7 L=1 F=0,0,-32.5 :2 point loads, (32.5 KN each)

82 89 7 L=1 F=0,0,-32.5 :2 point loads, (32.5 KN each)

COMBO

1 C=1.0

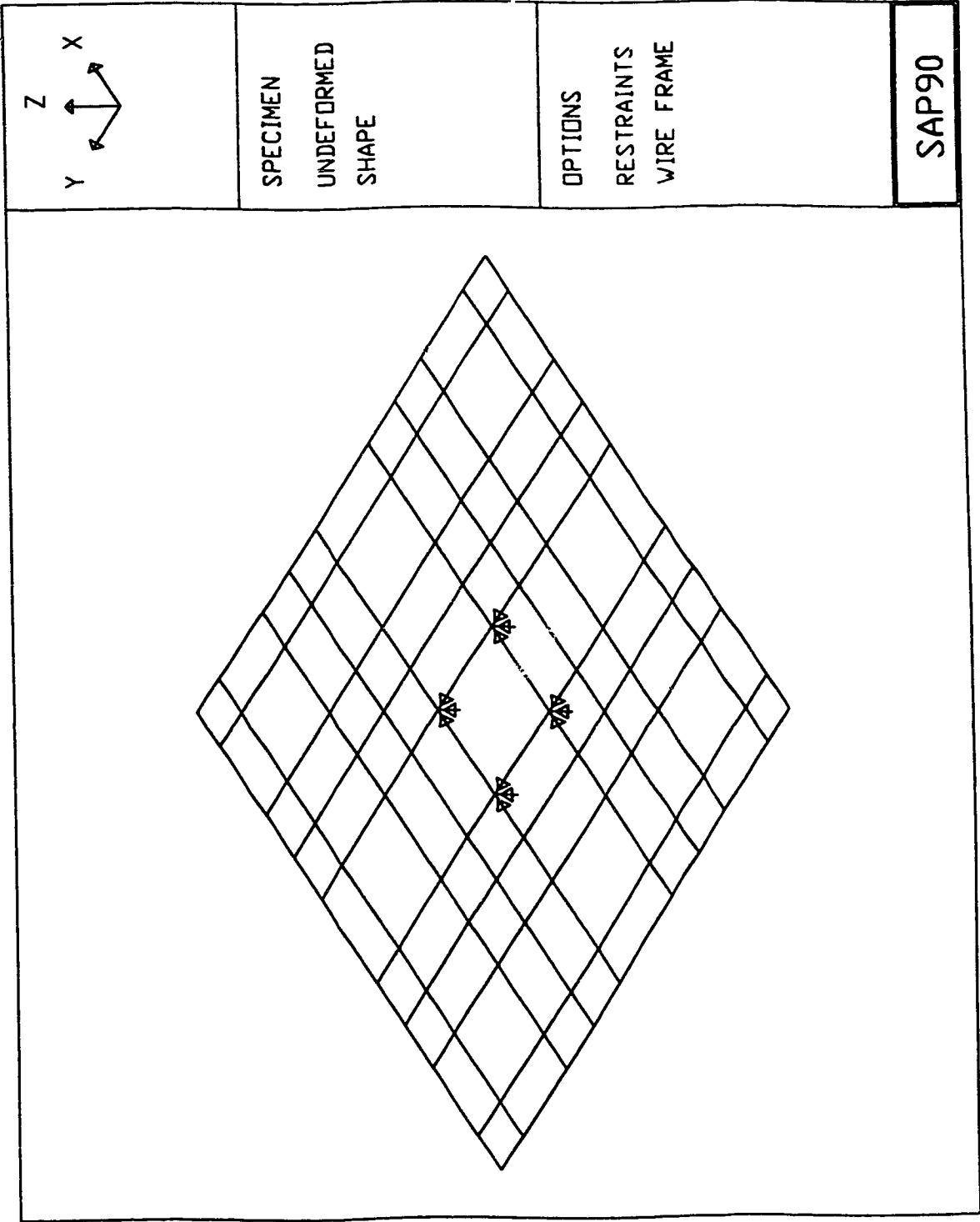


Figure A.3 3-D View of Finite Element Mesh (Connection Specimen)

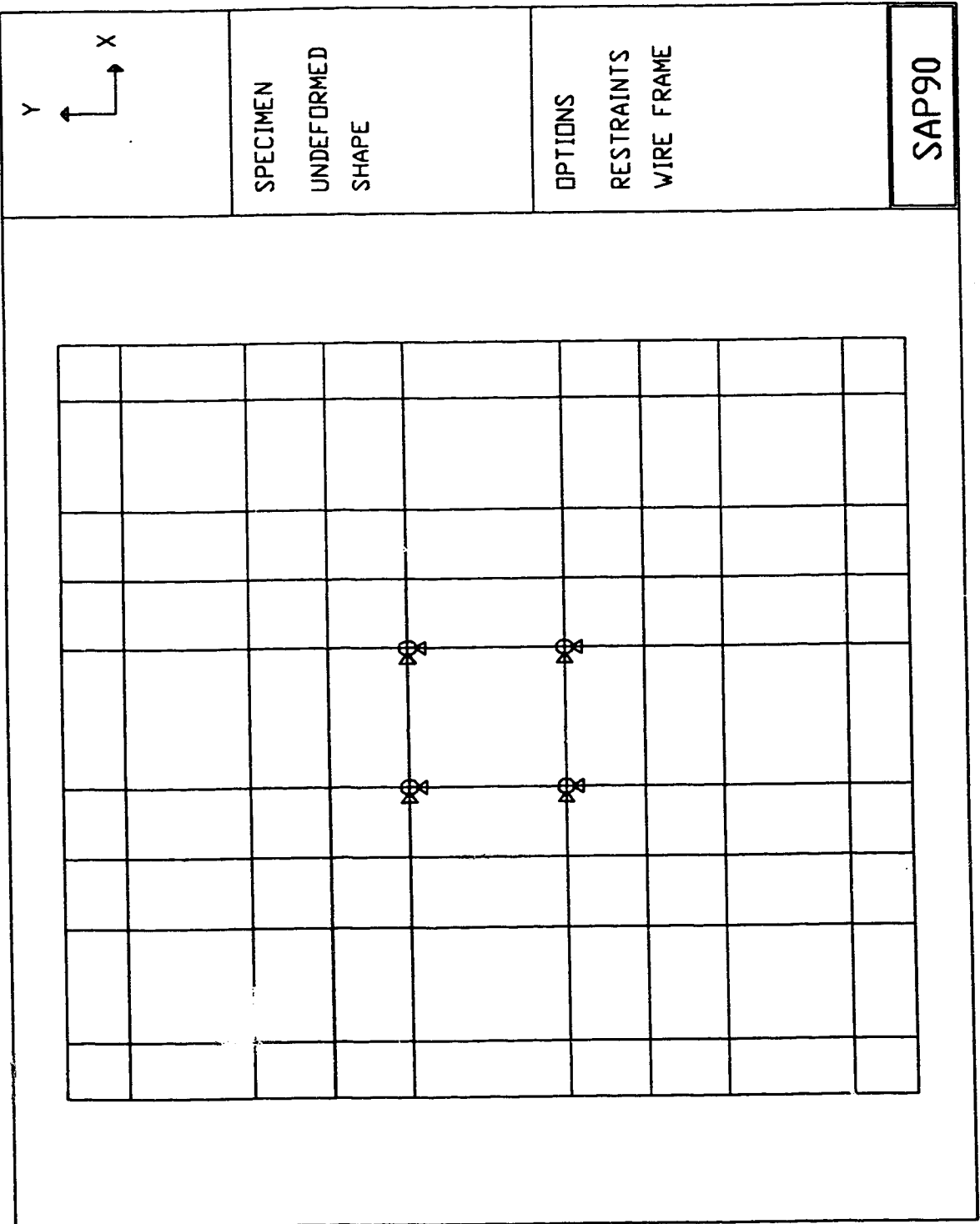


Figure A.4 Plan View of Finite Element Mesh (Connection Specimen)

APPENDIX B

Test results

Series A specimens
-Interior Sandwich Plates-

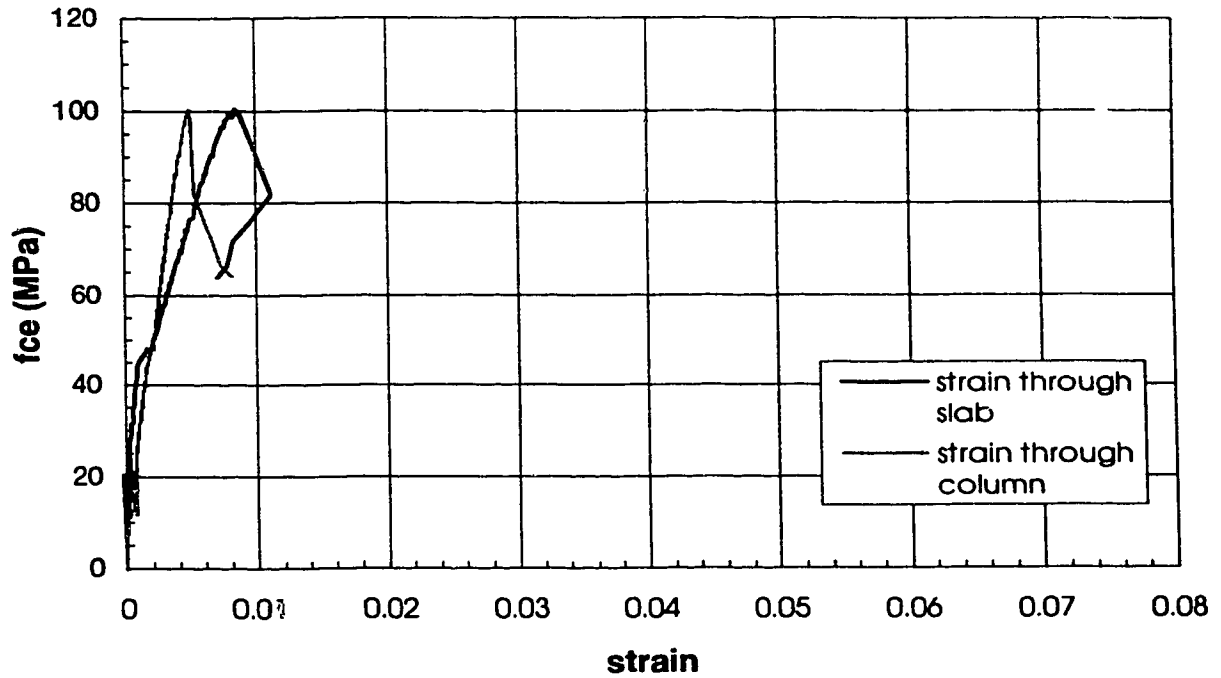


Figure B.1 Stress-strain behaviour (Specimen A1-A)

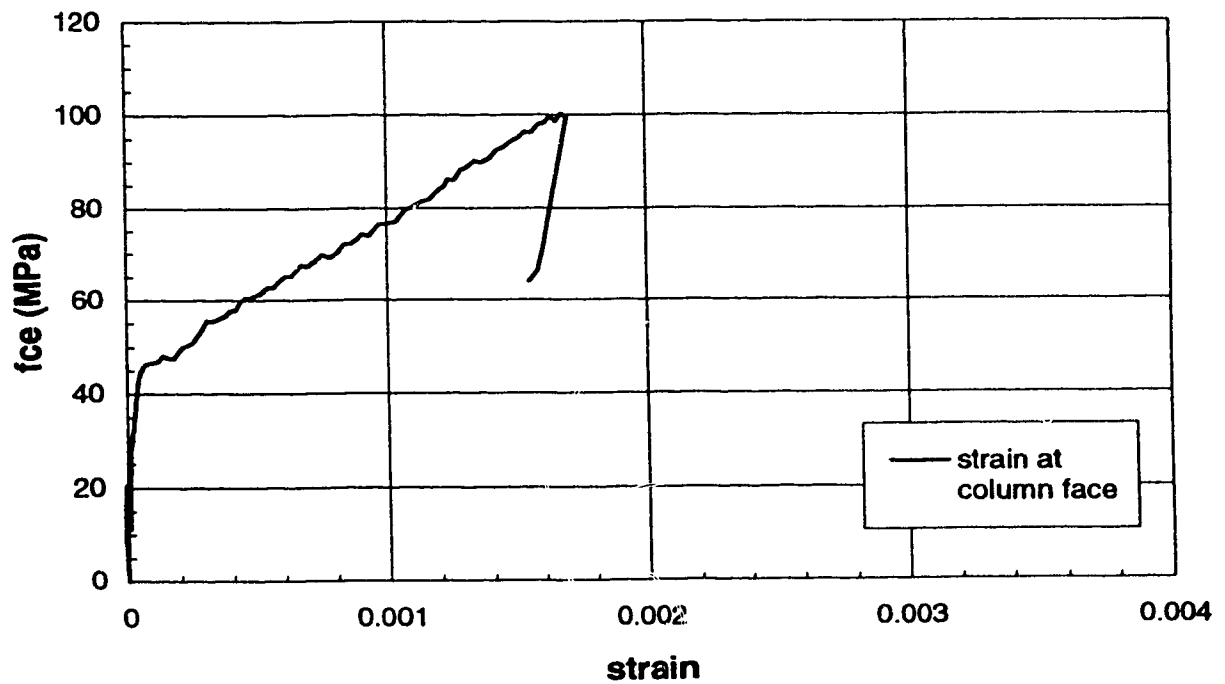


Figure B.2 Slab transverse strain (Specimen A1-A)

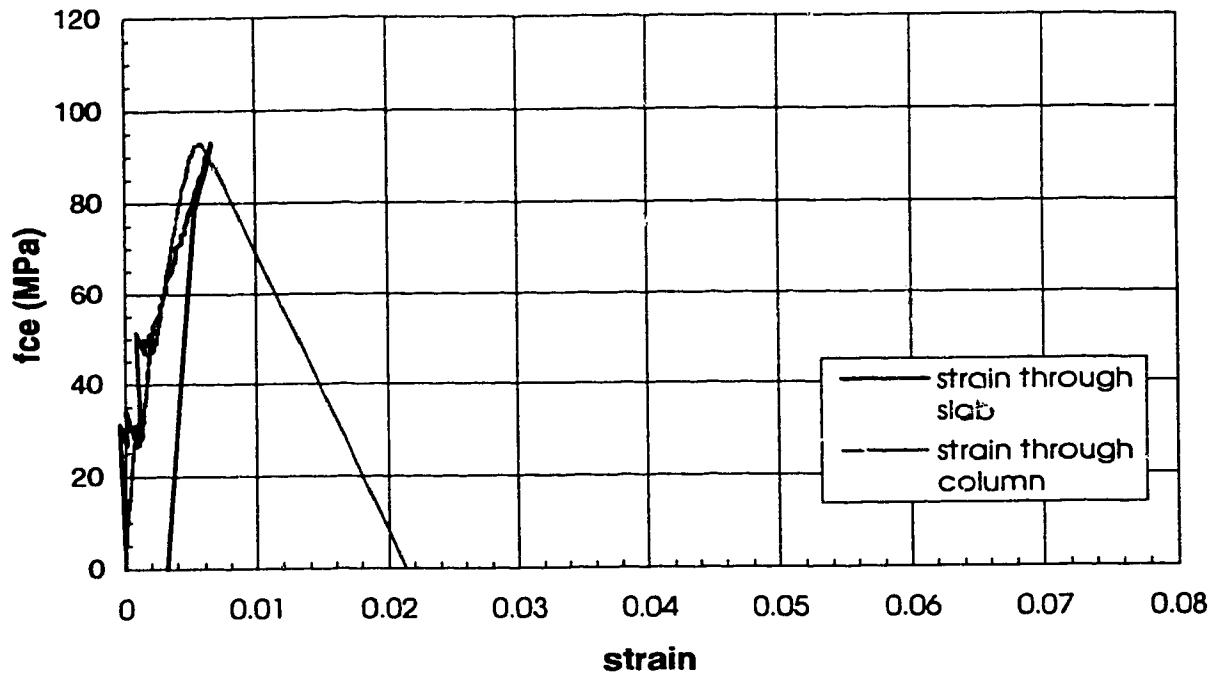


Figure B.3 Stress-strain behaviour (Specimen A1-B)

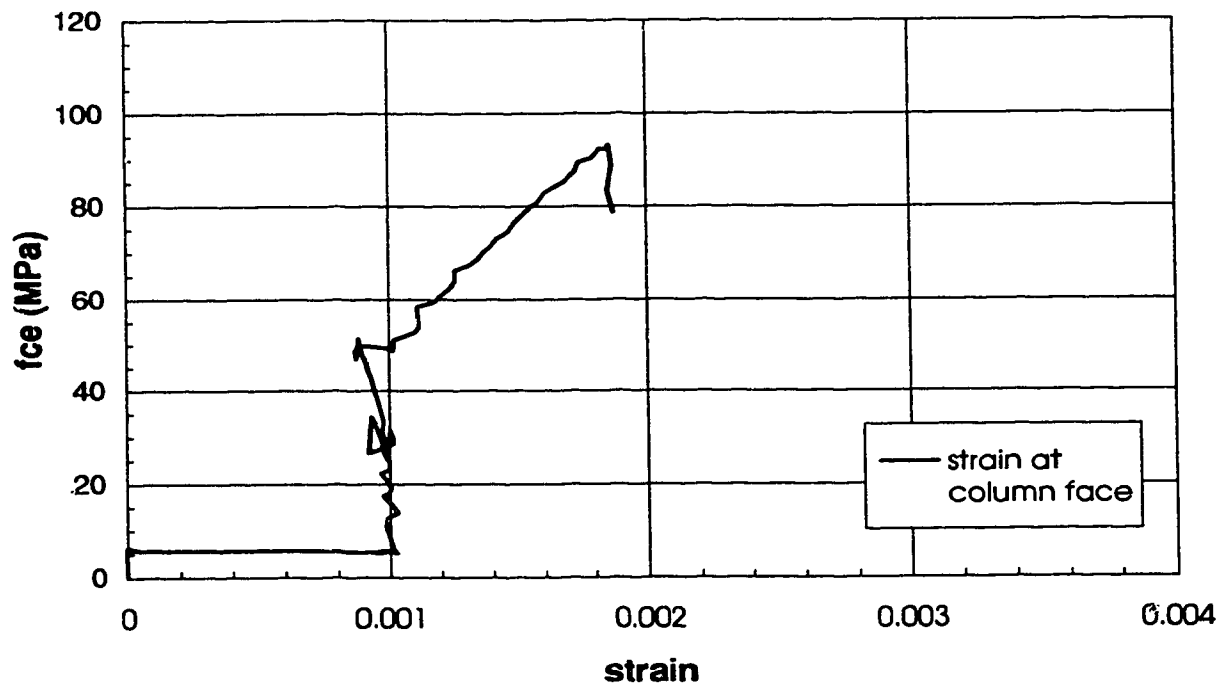


Figure B.4 Slab transverse strain (Specimen A1-B)

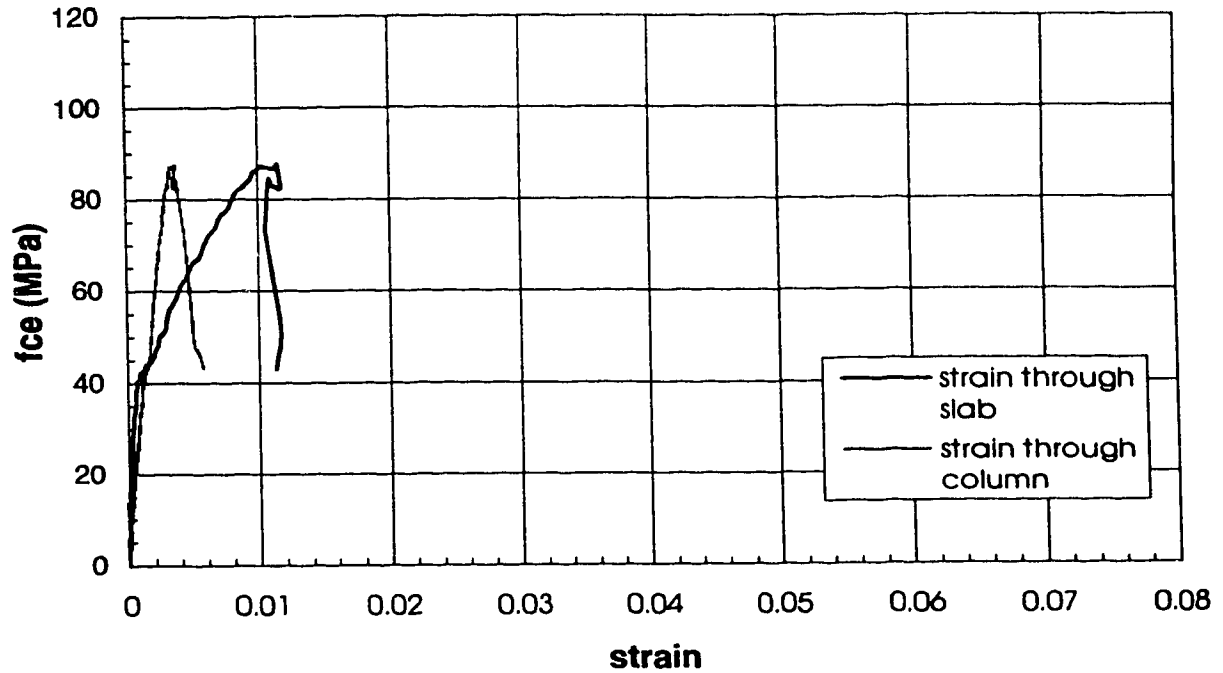


Figure B.5 Stress-strain behaviour (Specimen A1-C)

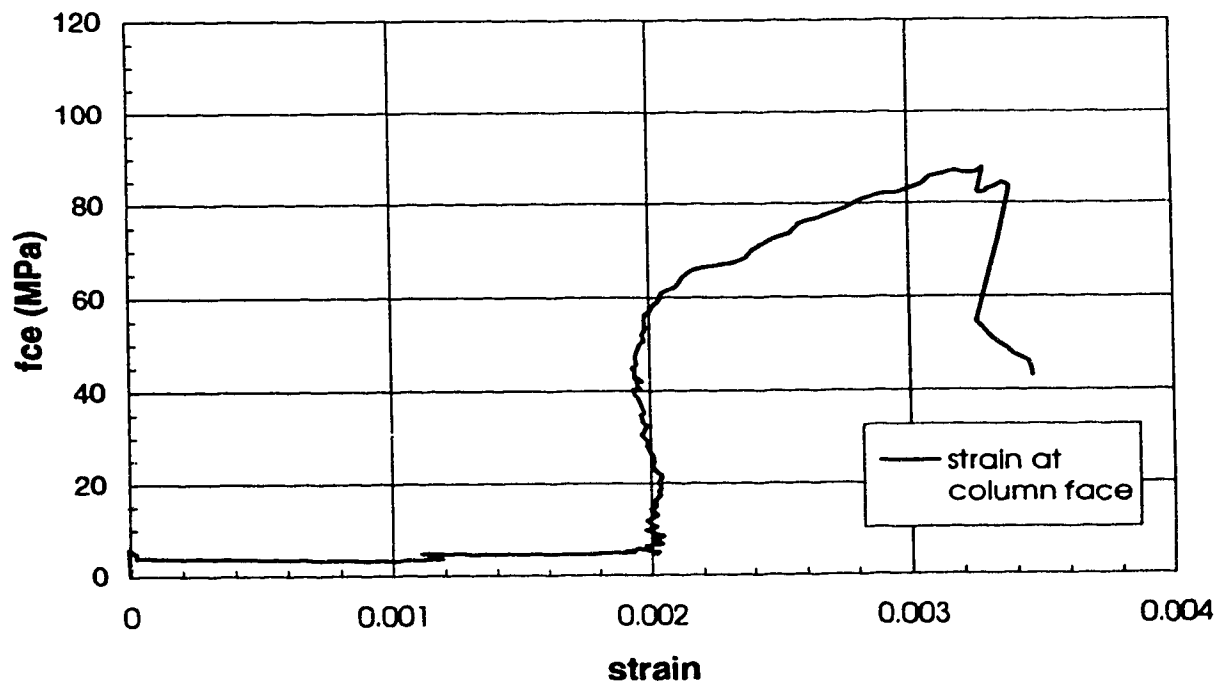


Figure B.6 Slab transverse strain (Specimen A1-C)

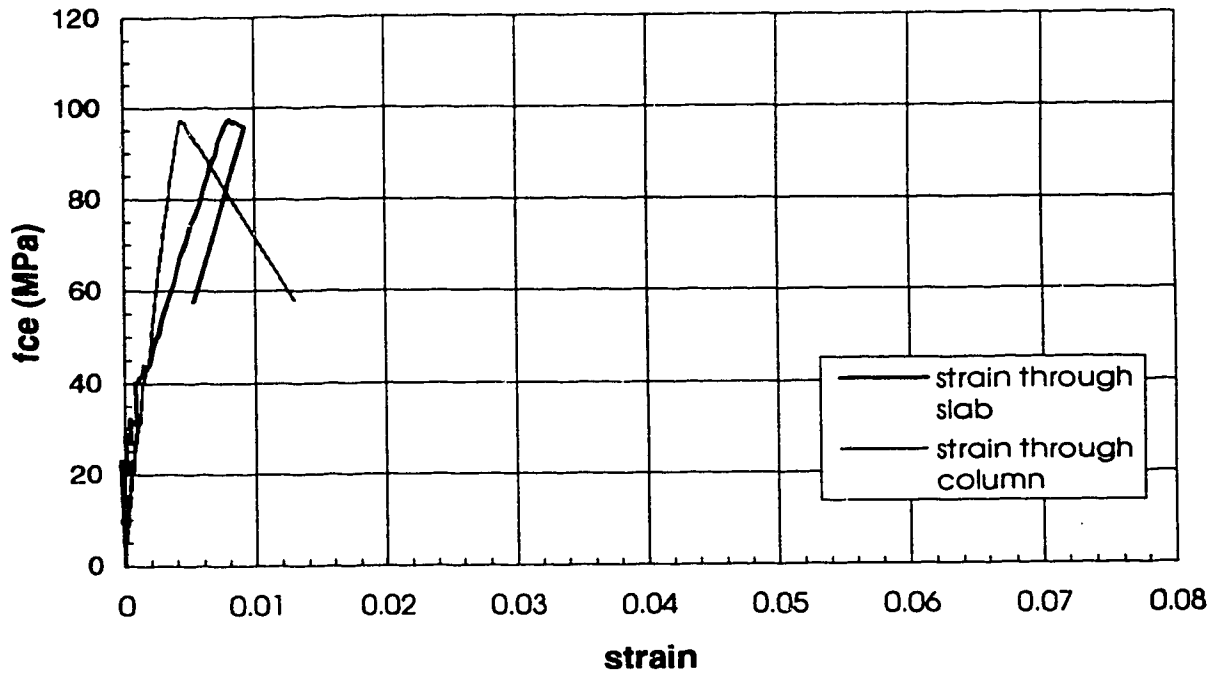


Figure B.7 Stress-strain behaviour (Specimen A2-A)

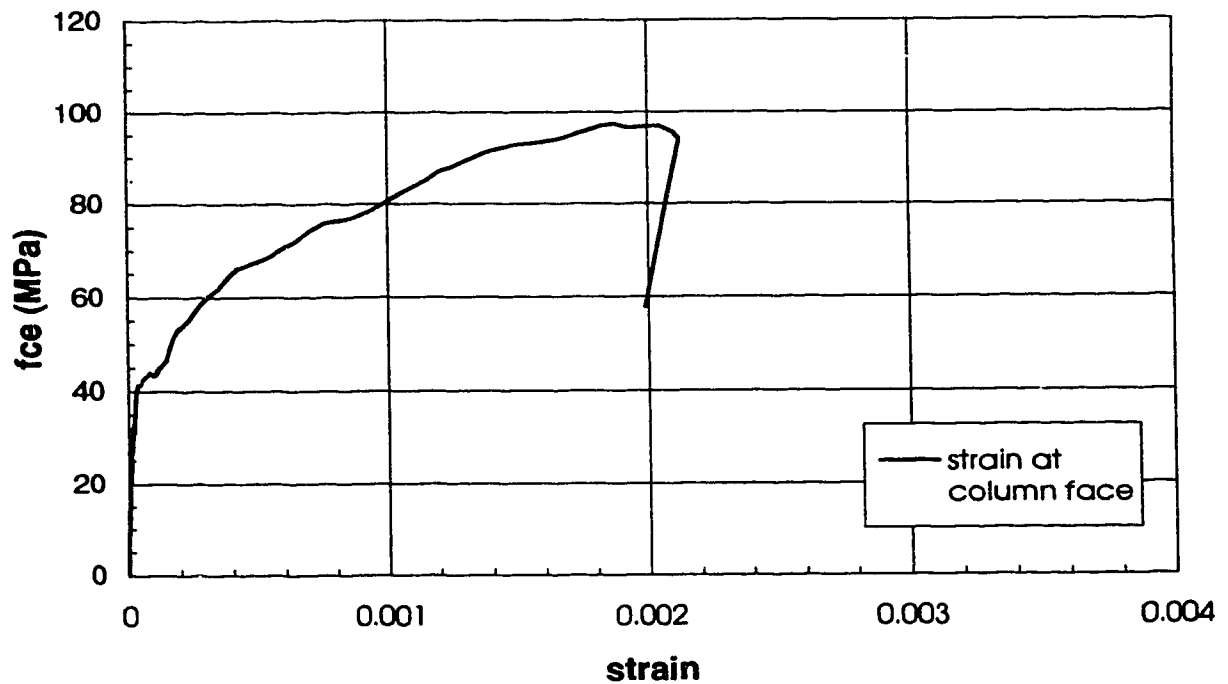


Figure B.8 Slab transverse strain (Specimen A2-A)

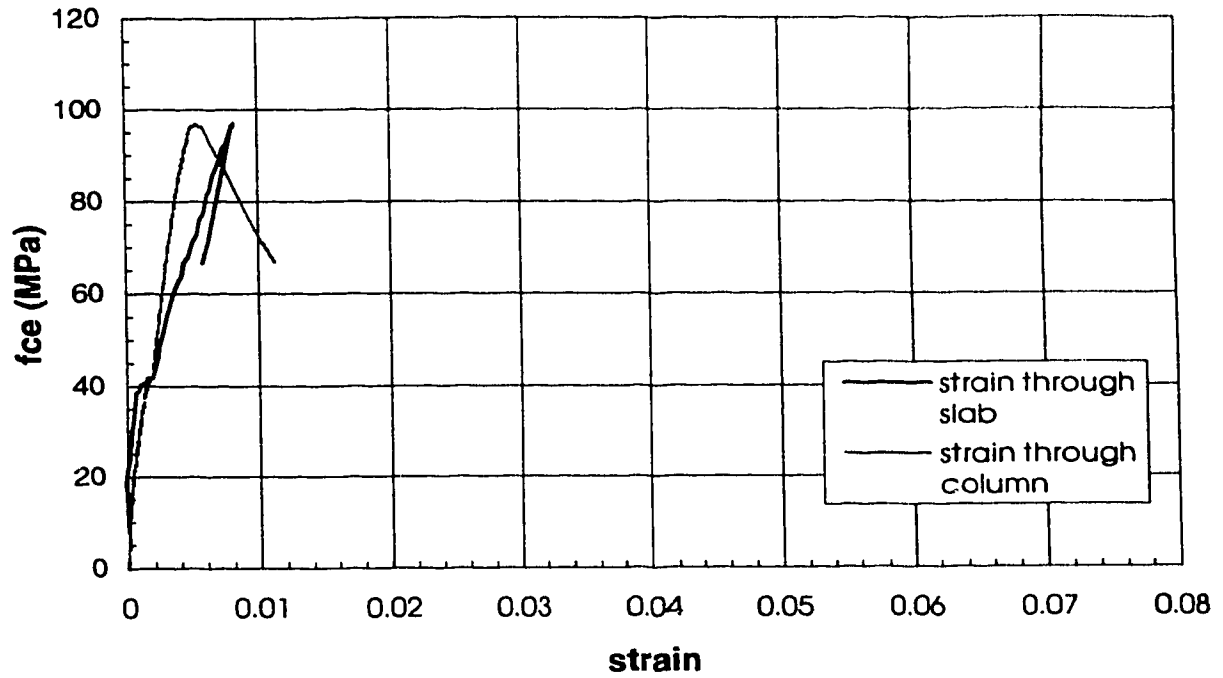


Figure B.9 Stress-strain behaviour (Specimen A2-B)

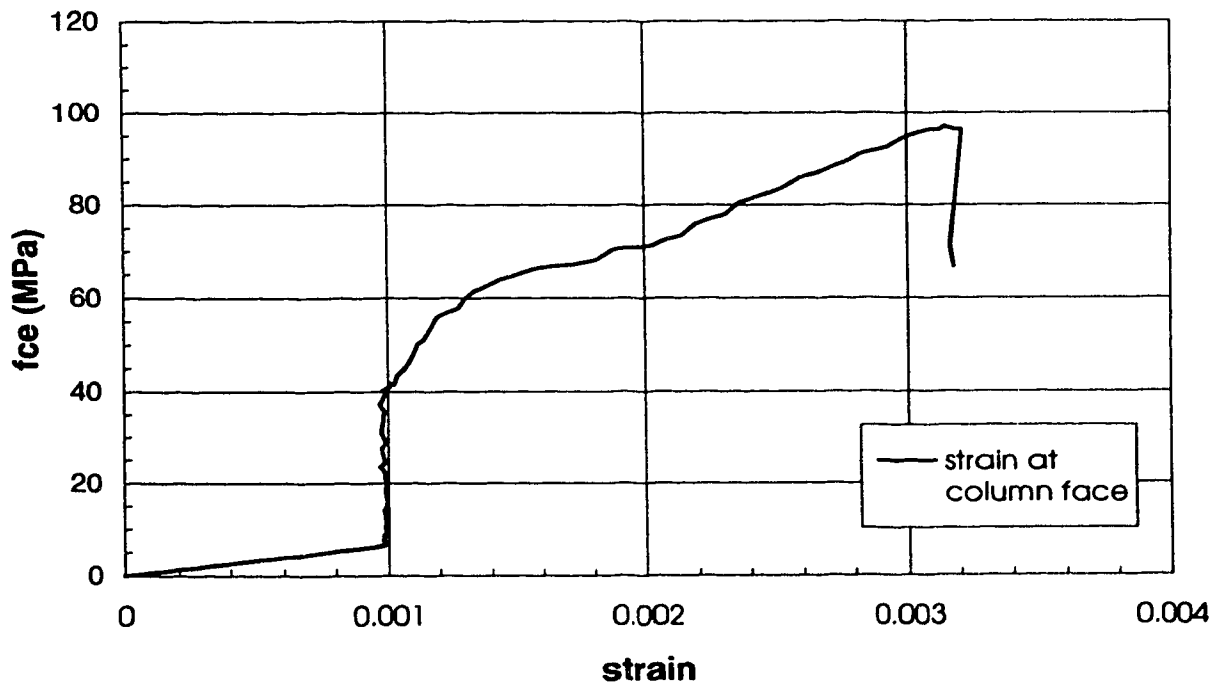


Figure B.10 Slab transverse strain (Specimen A2-B)

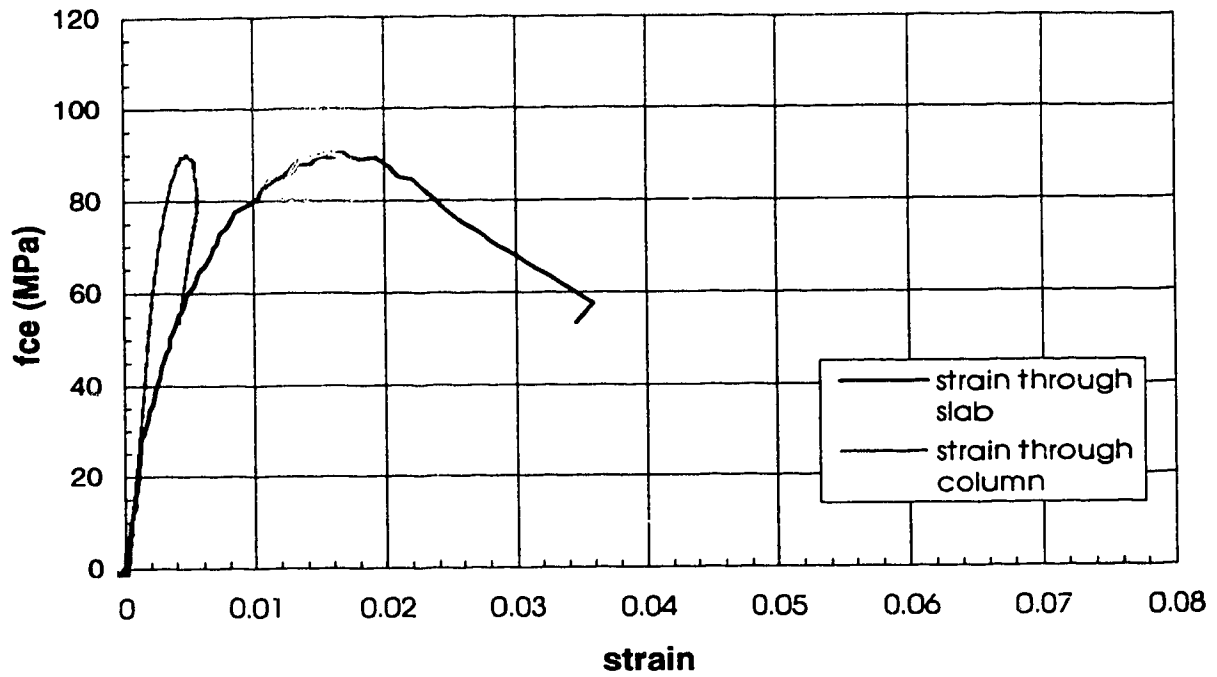


Figure B.11 Stress-strain behaviour (Specimen A2-C)

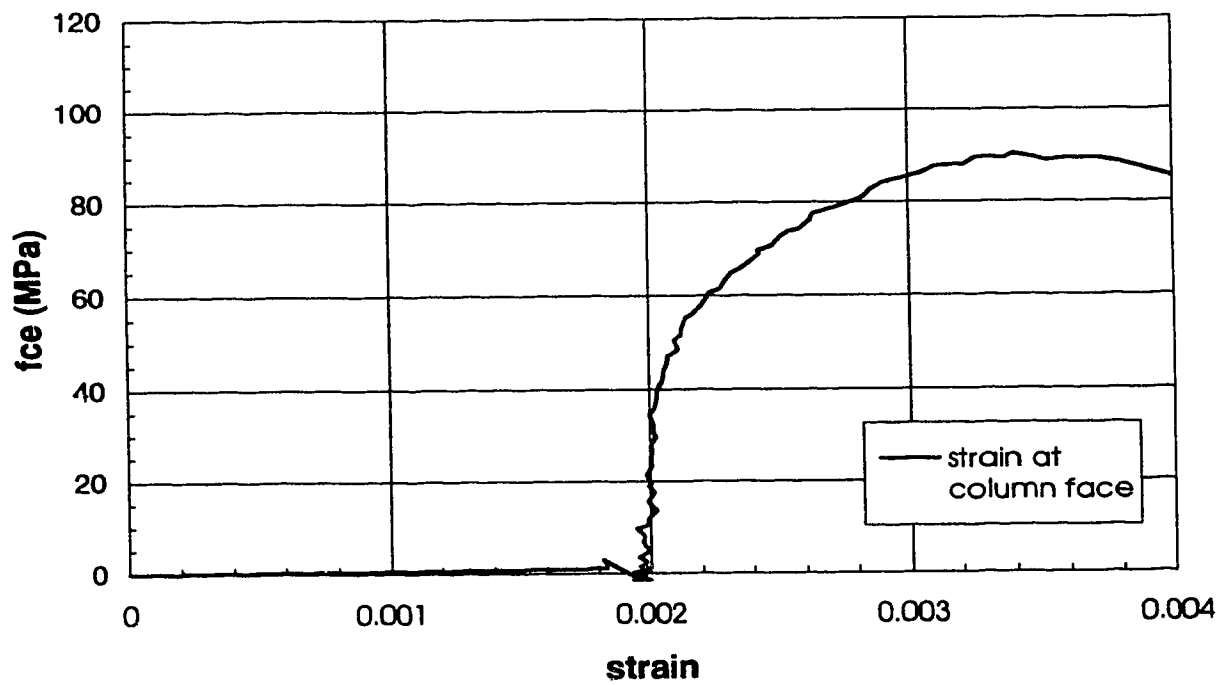


Figure B.12 Slab transverse strain (Specimen A2-C)

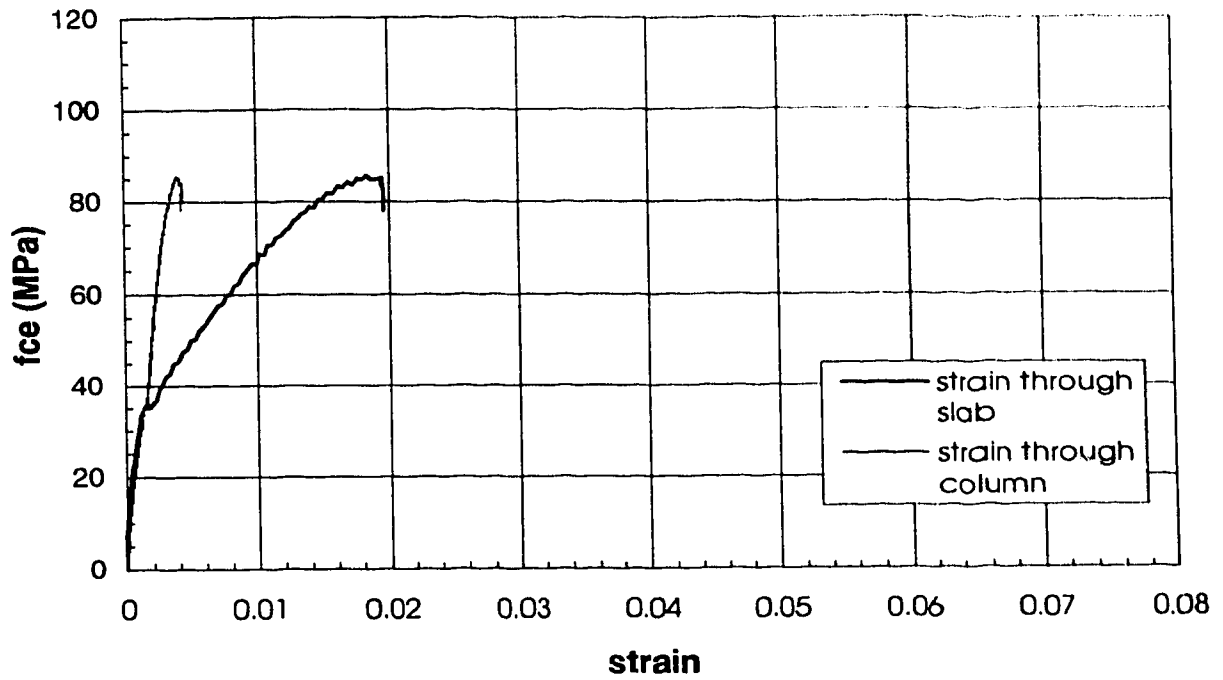


Figure B.13 Stress-strain behaviour (Specimen A3-A)

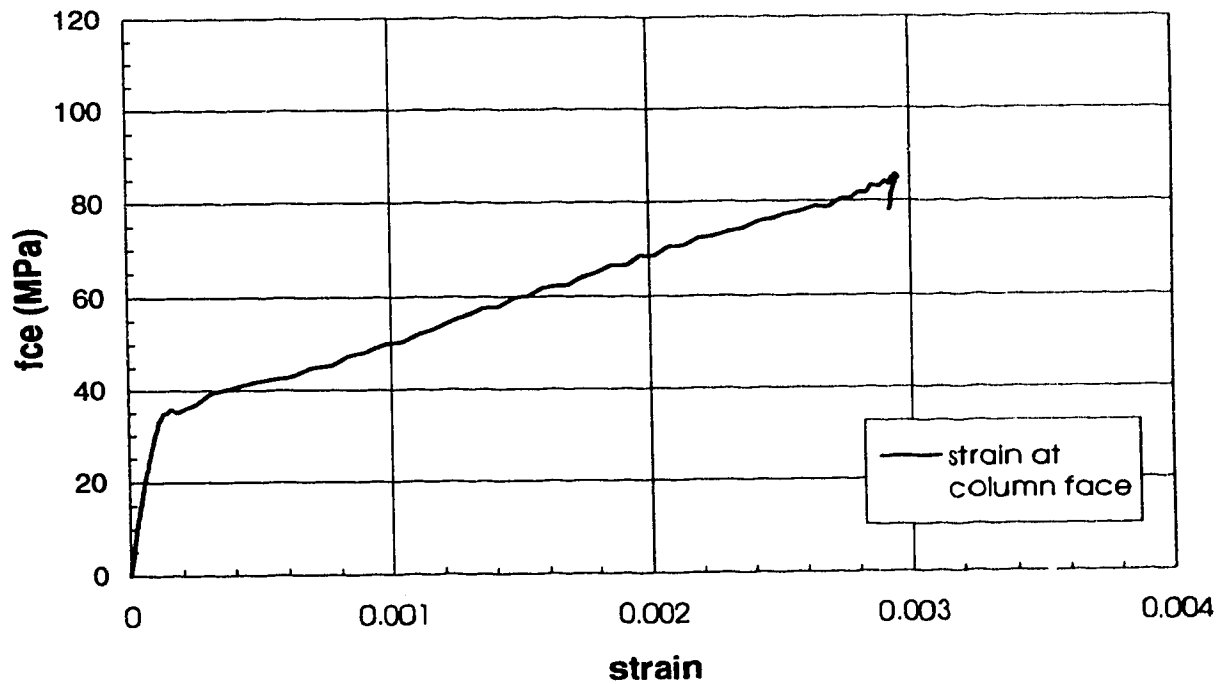


Figure B.14 Slab transverse strain (Specimen A3-A)

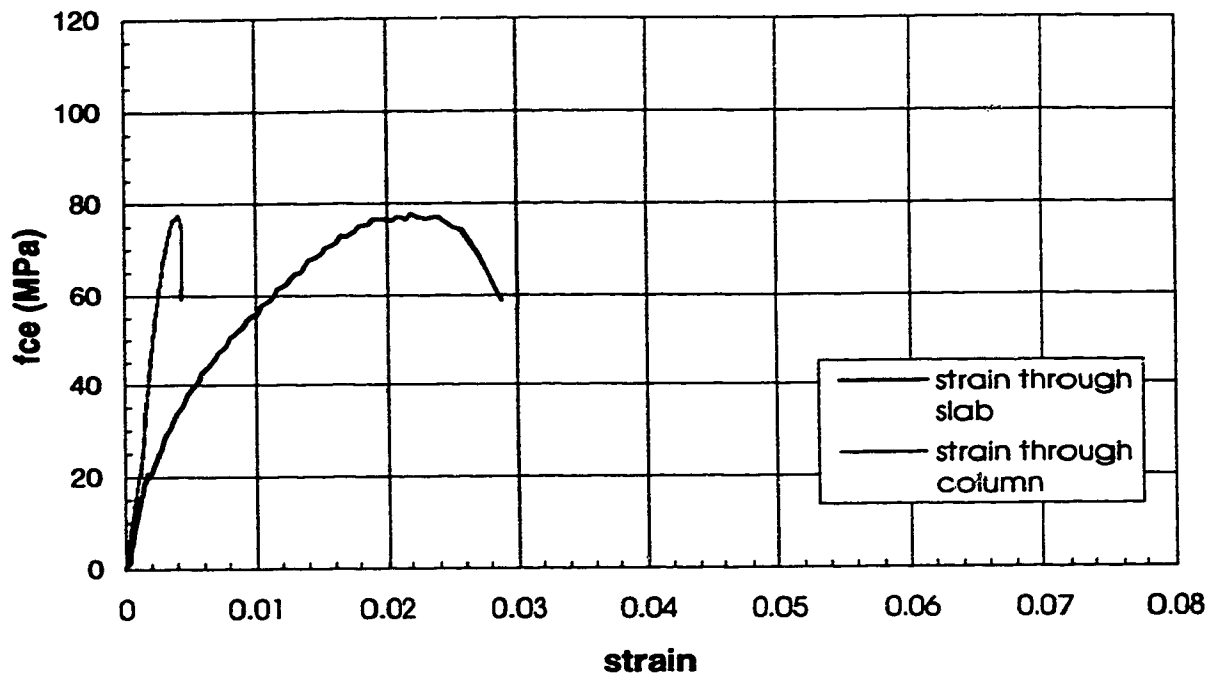


Figure B.15 Stress-strain behaviour (Specimen A3-B)

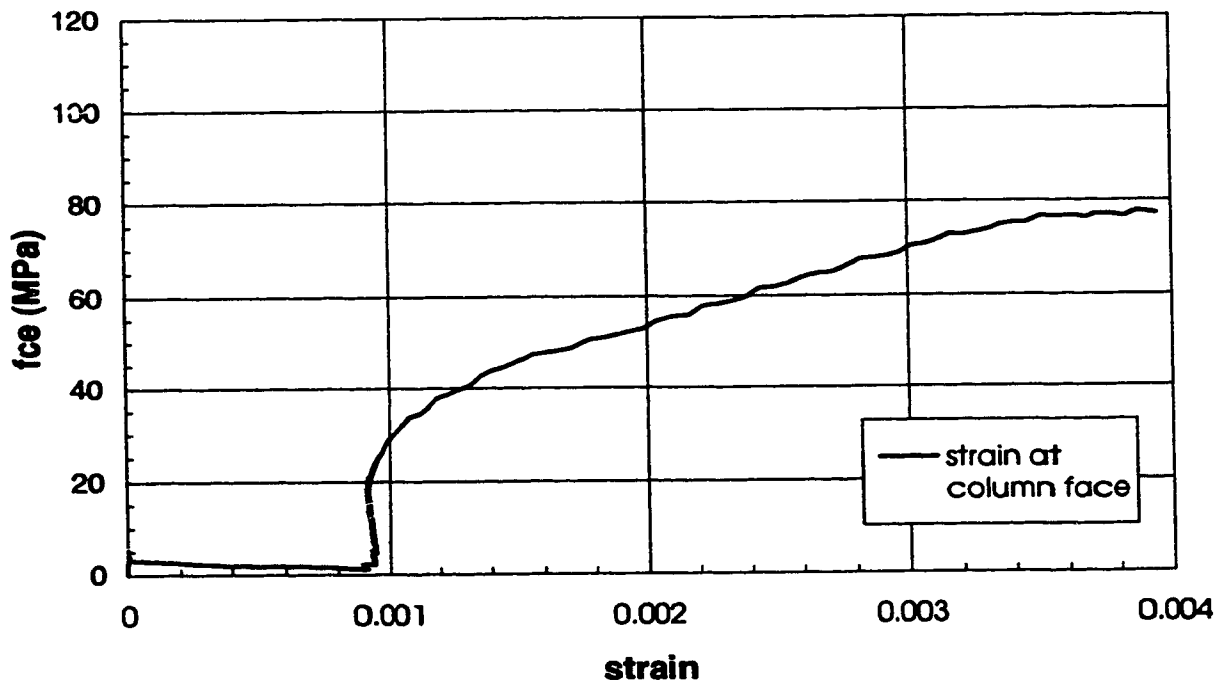


Figure B.16 Slab transverse strain (Specimen A3-B)

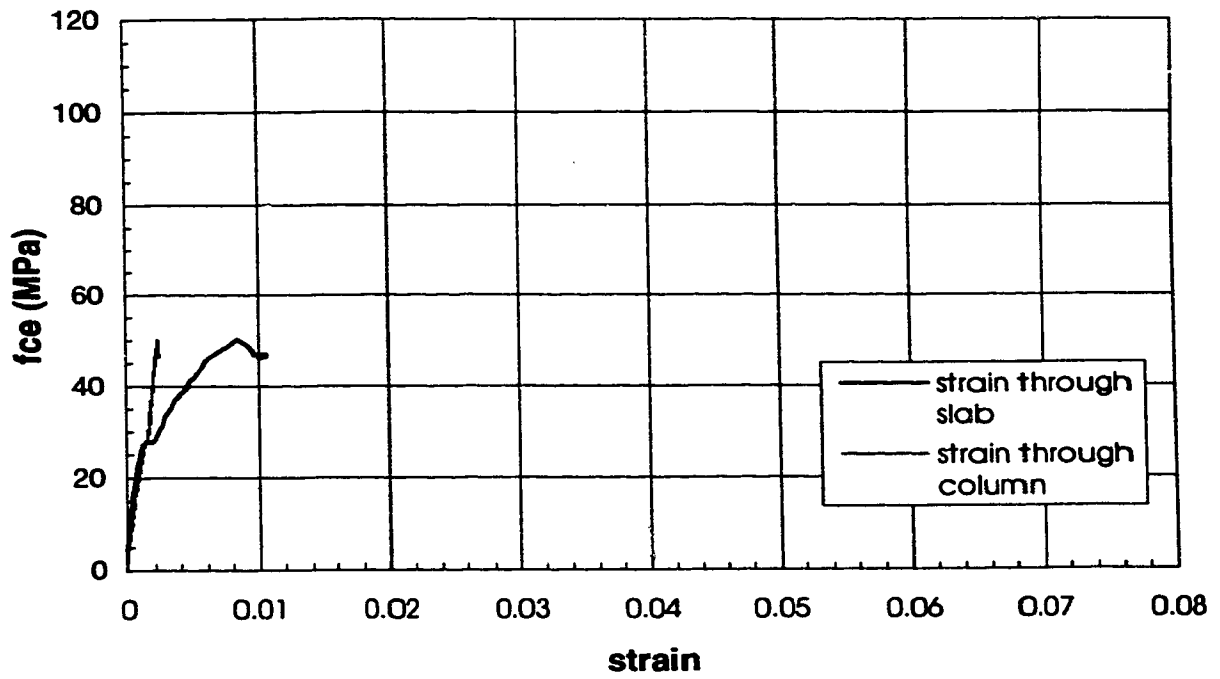


Figure B.17 Stress-strain behaviour (Specimen A3-C)

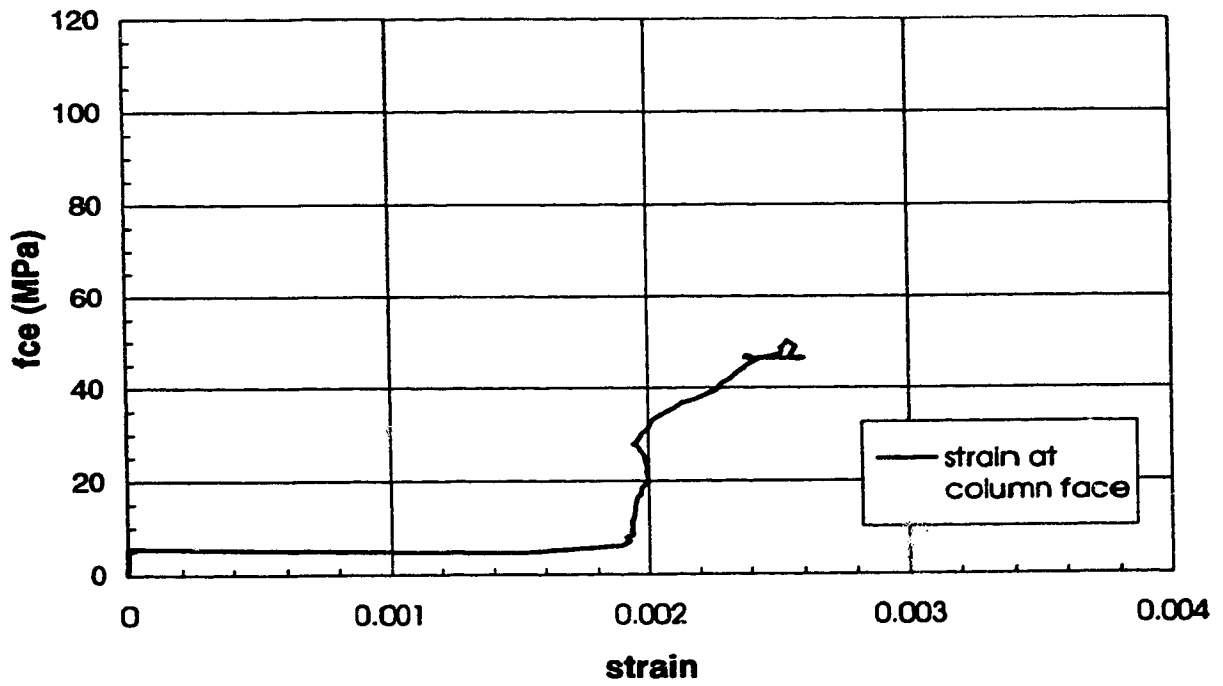


Figure B.18 Slab transverse strain (Specimen A3-C)

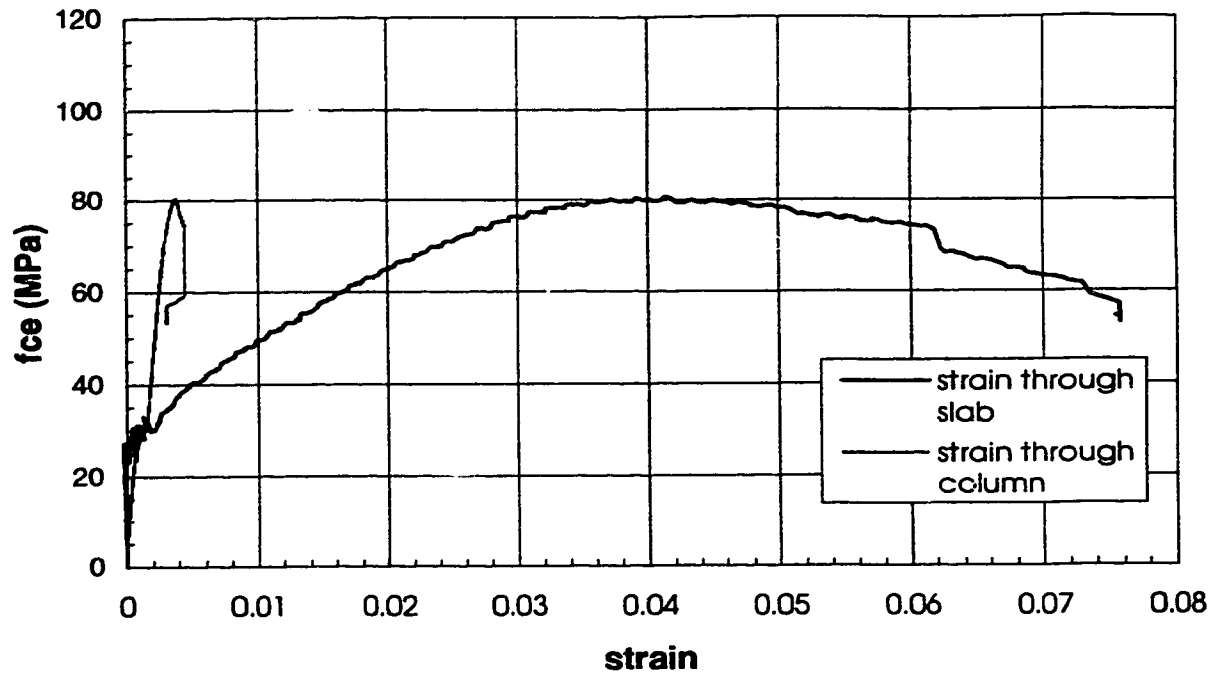


Figure B.19 Stress-strain behaviour (Specimen A4-A)

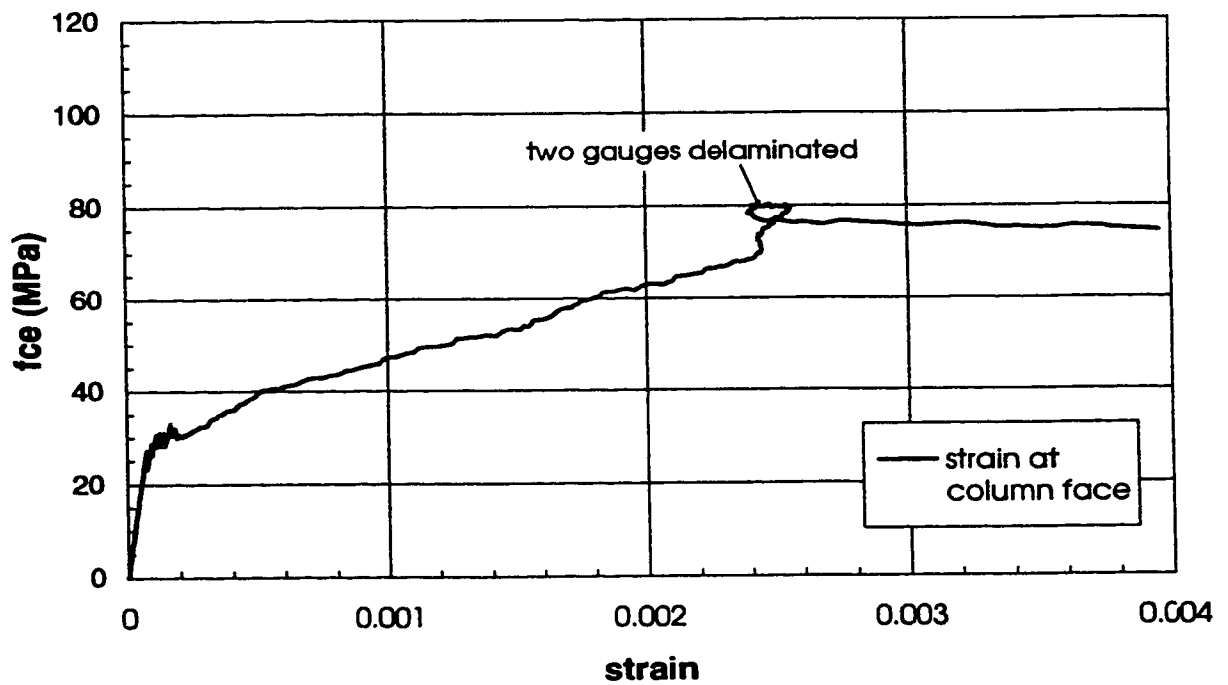


Figure B.20 Slab transverse strain (Specimen A4-A)

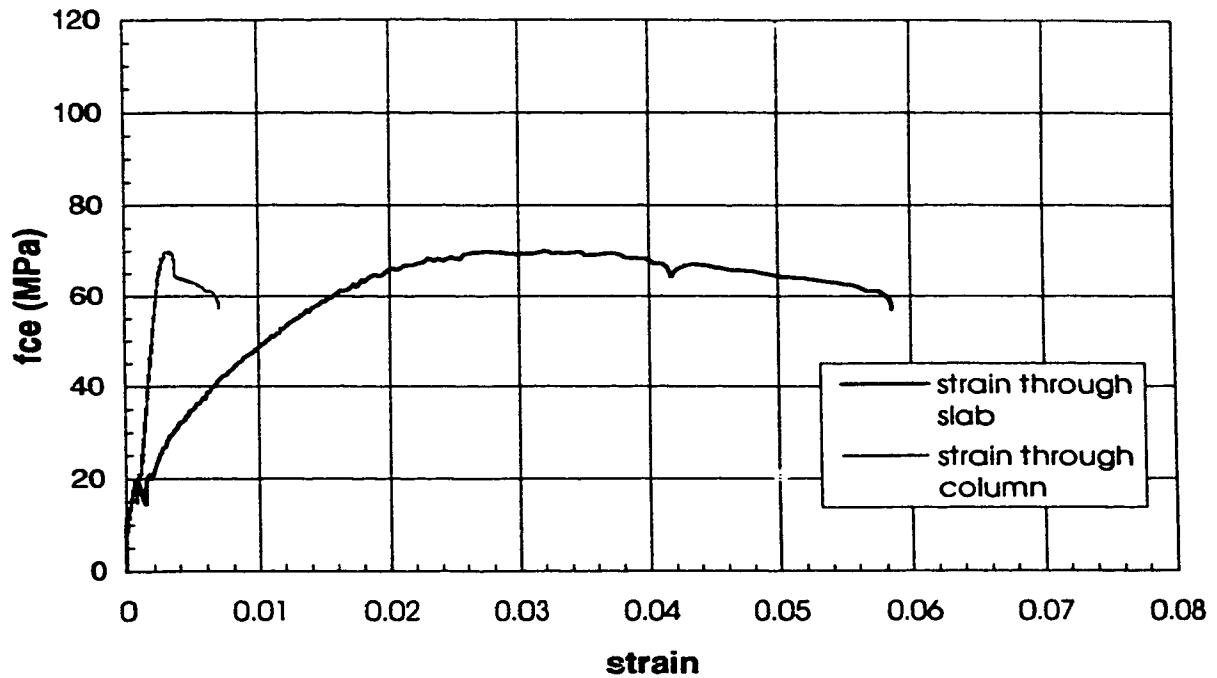


Figure B.21 Stress-strain behaviour (Specimen A4-B)

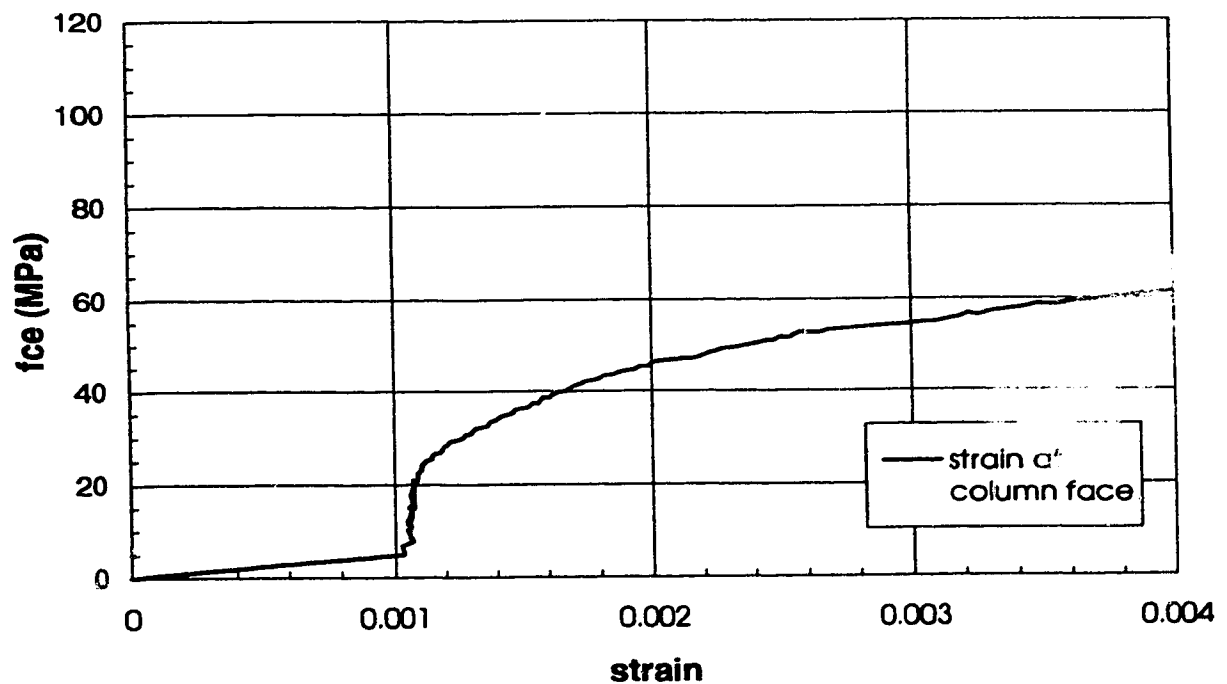


Figure B.22 Slab transverse strain (Specimen A4-B)

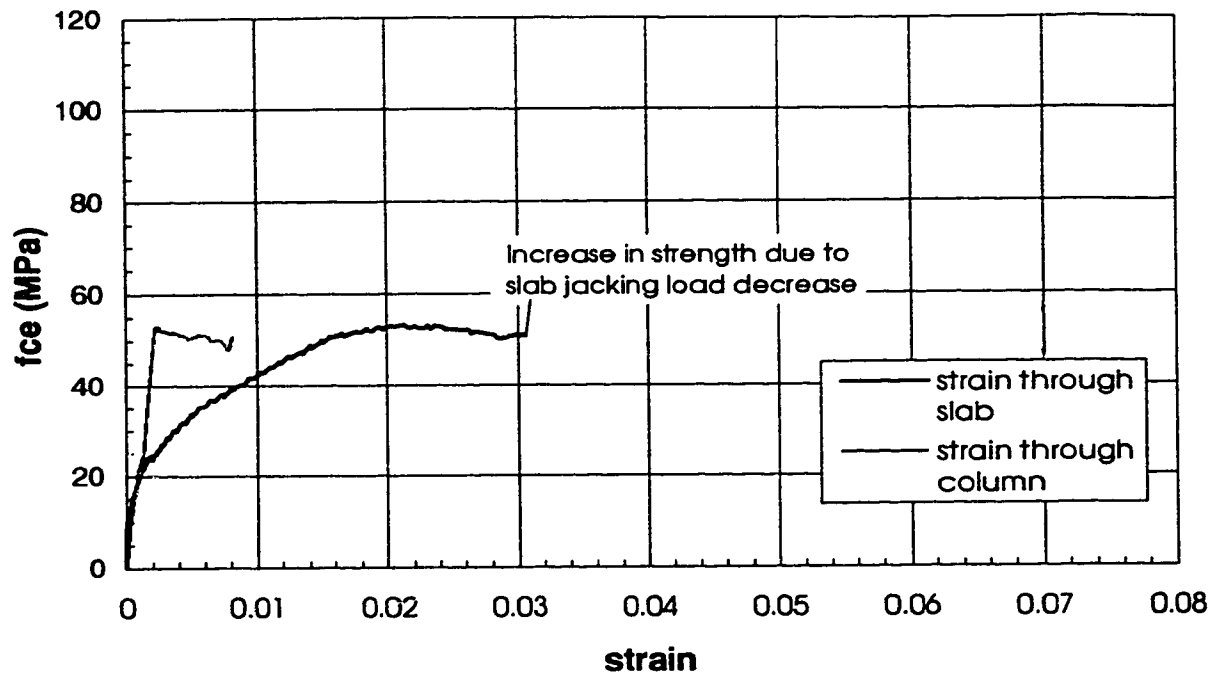


Figure B.23 Stress-strain behaviour (Specimen A4-C)

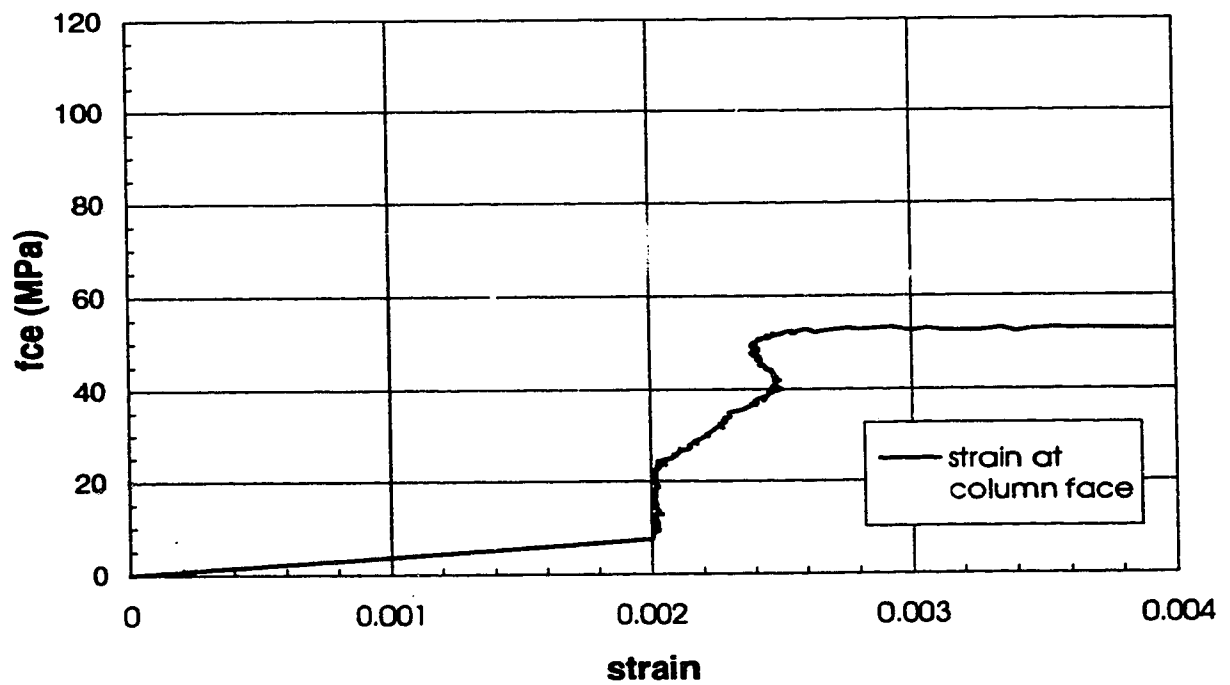


Figure B.24 Slab transverse strain (Specimen A4-C)

Series B specimens

-Interior Sandwich Plates-

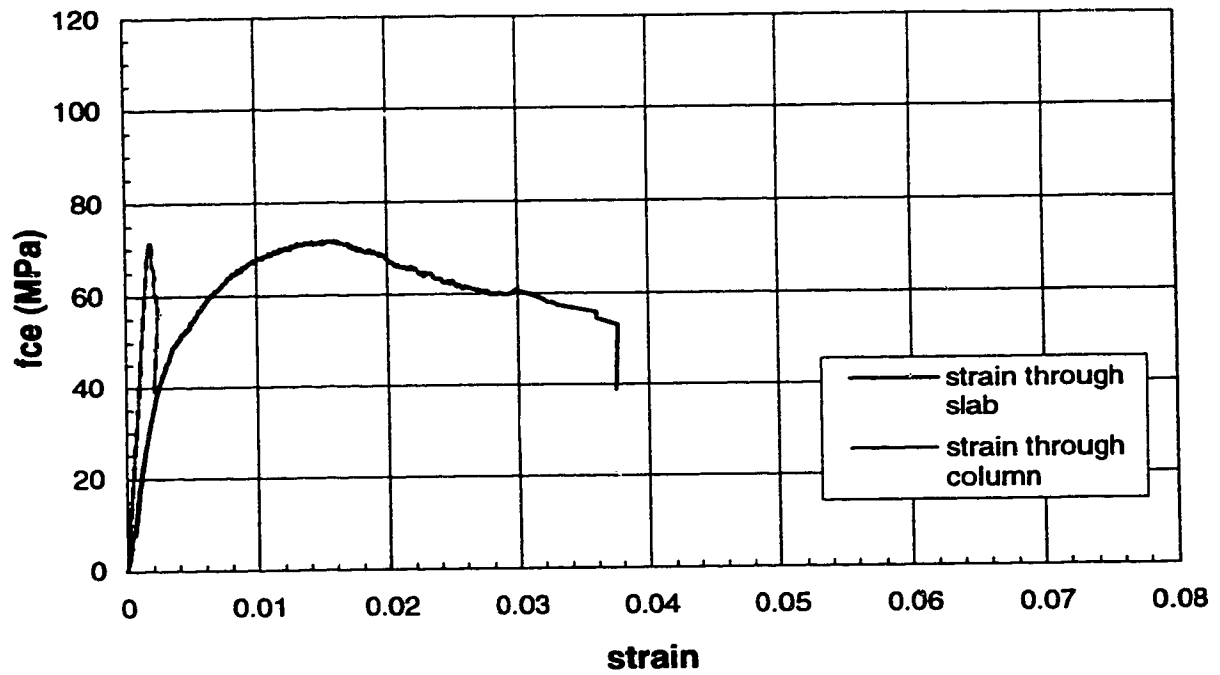


Figure B.25 Stress-strain behaviour (Specimen B-1)

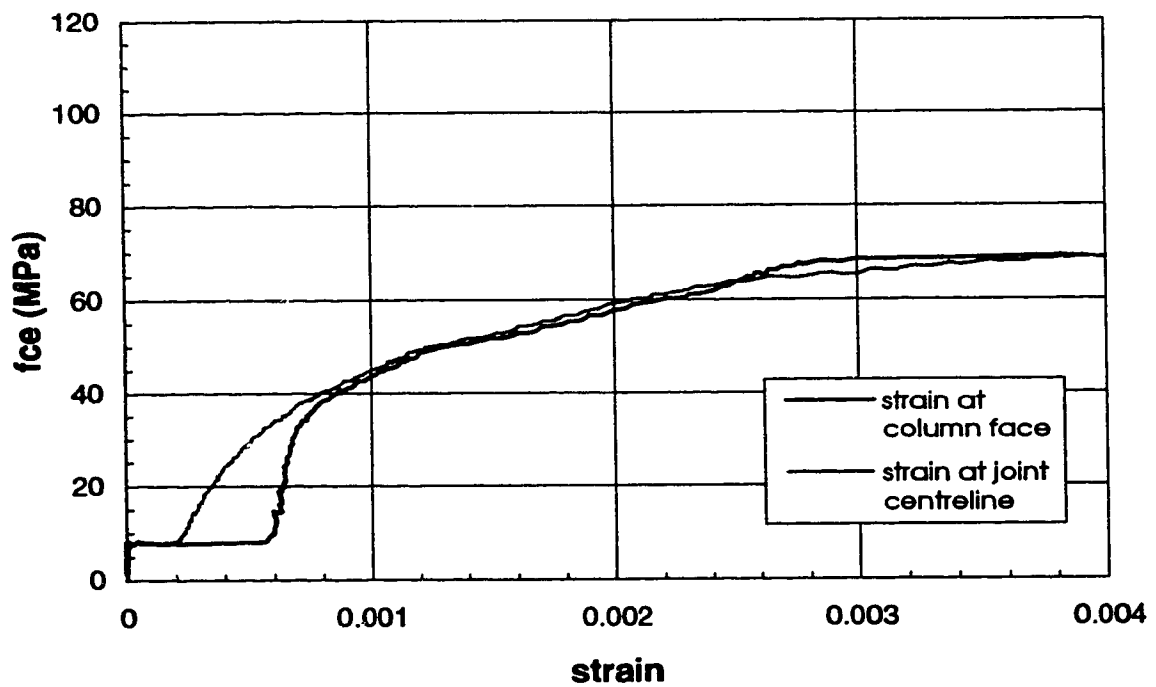


Figure B.26 Slab transverse strain (Specimen B-1)

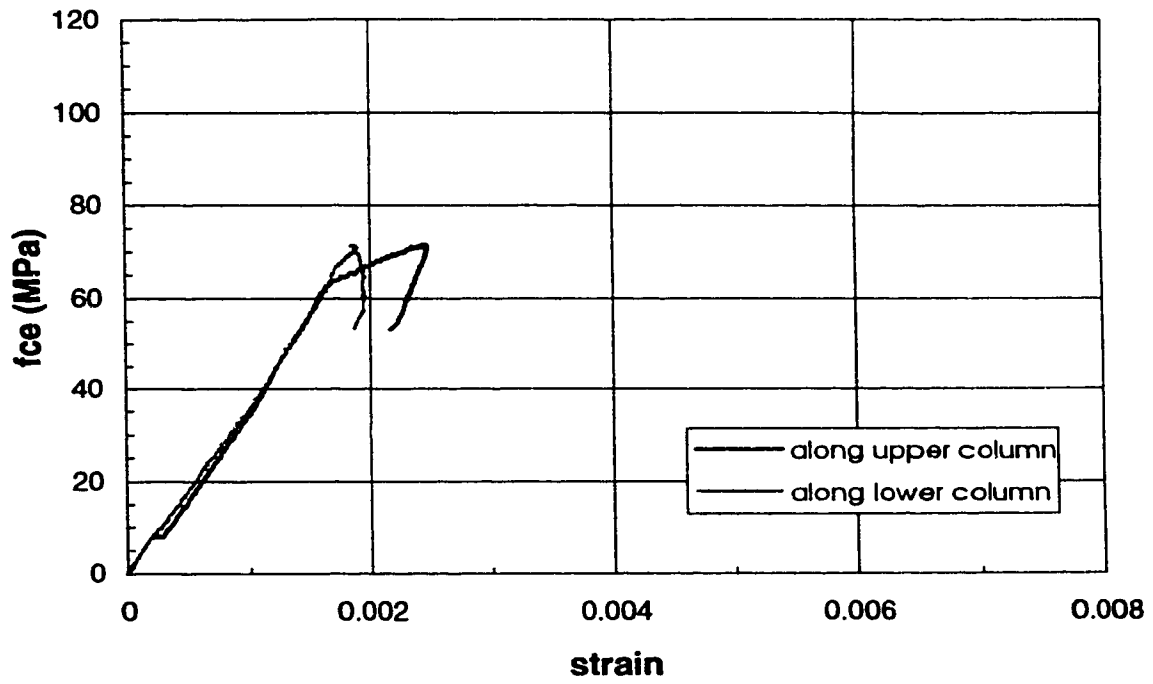


Figure B.27 Column longitudinal strain (Specimen B-1)

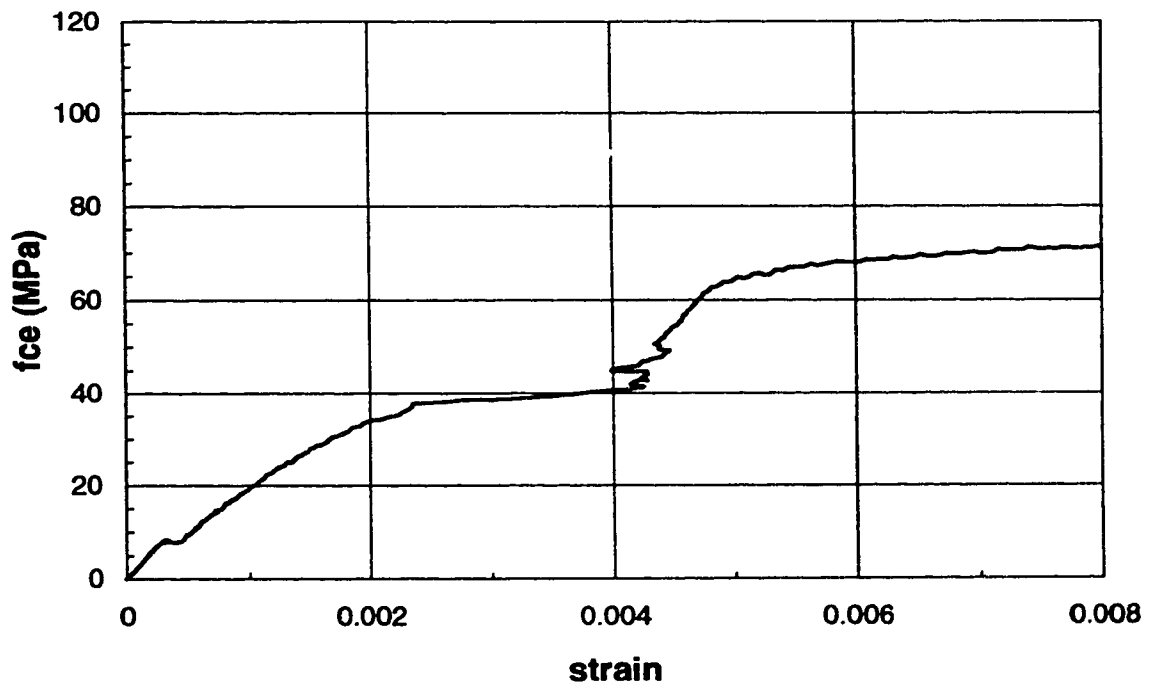


Figure B.28 Column strain through slab (Specimen B-1)

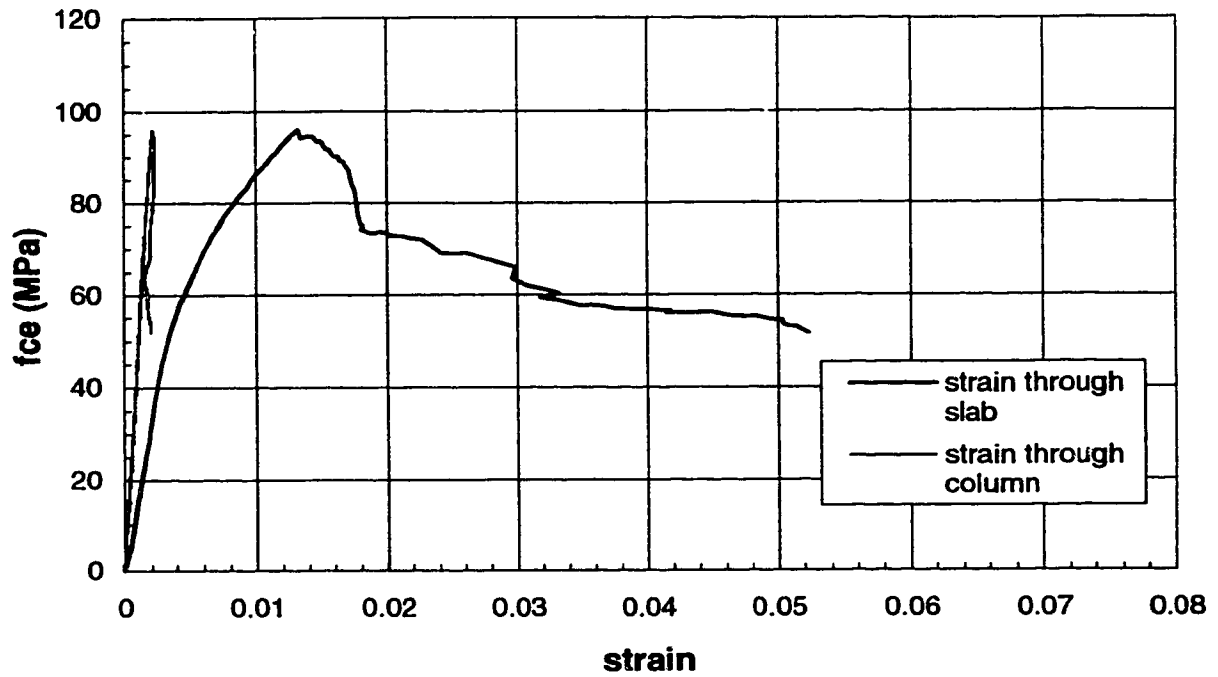


Figure B.29 Stress-strain behaviour (Specimen B-2)

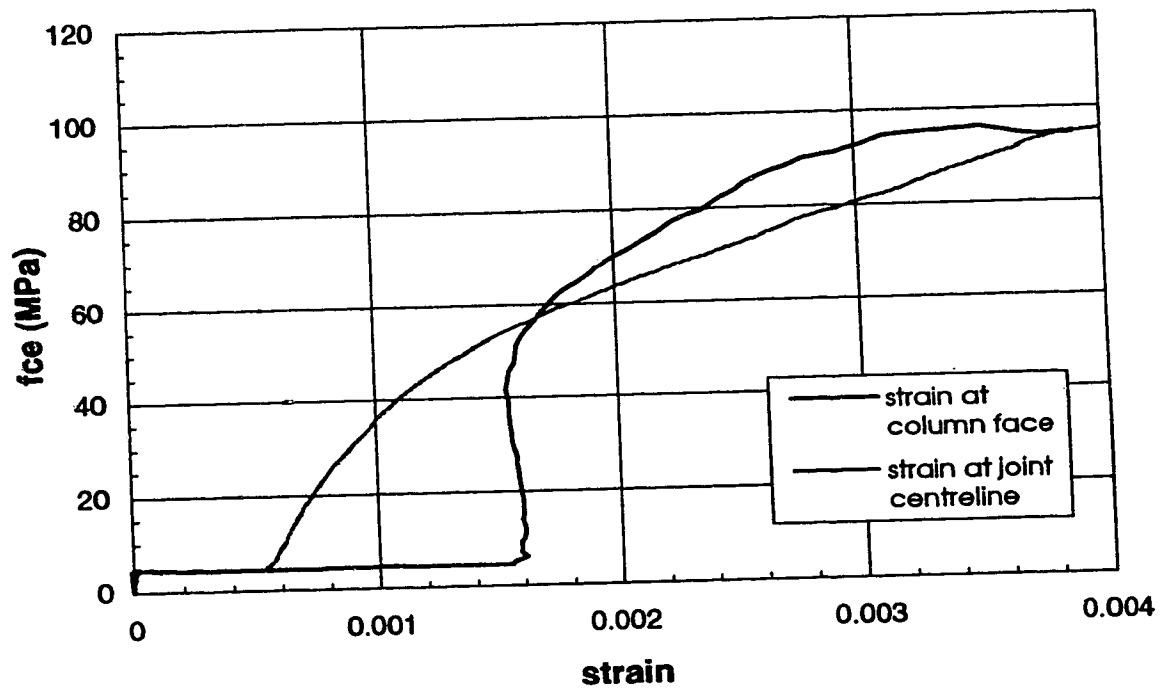


Figure B.30 Slab transverse strain (Specimen B-2)

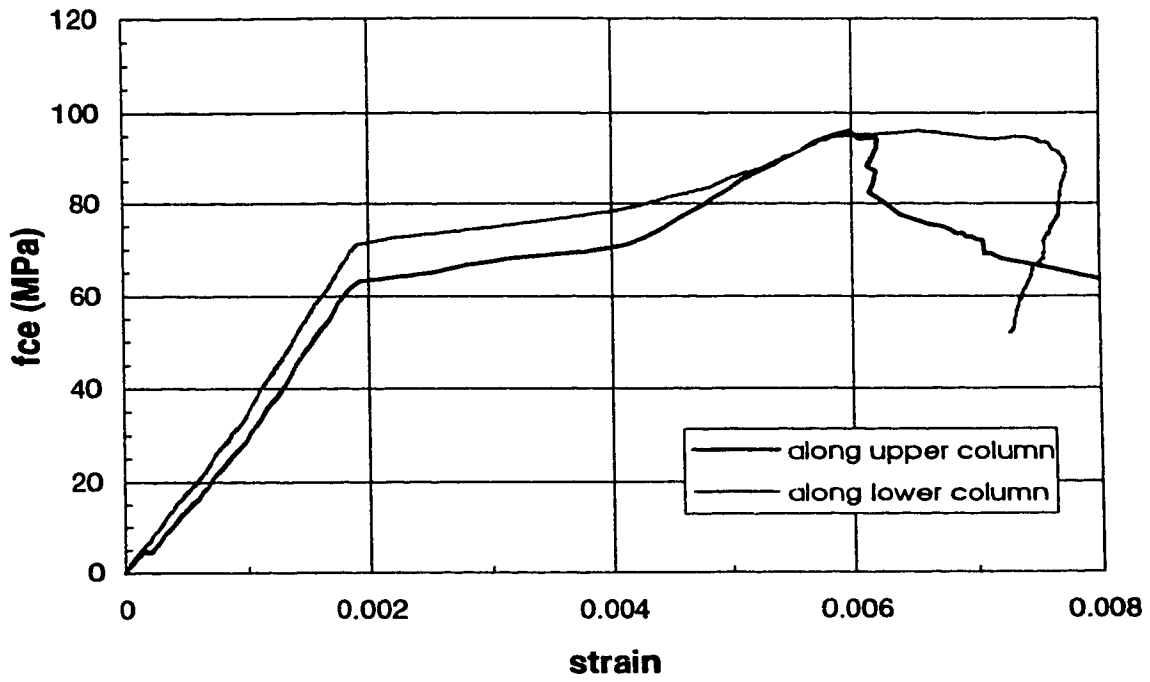


Figure B.31 Column longitudinal strain (Specimen B-2)

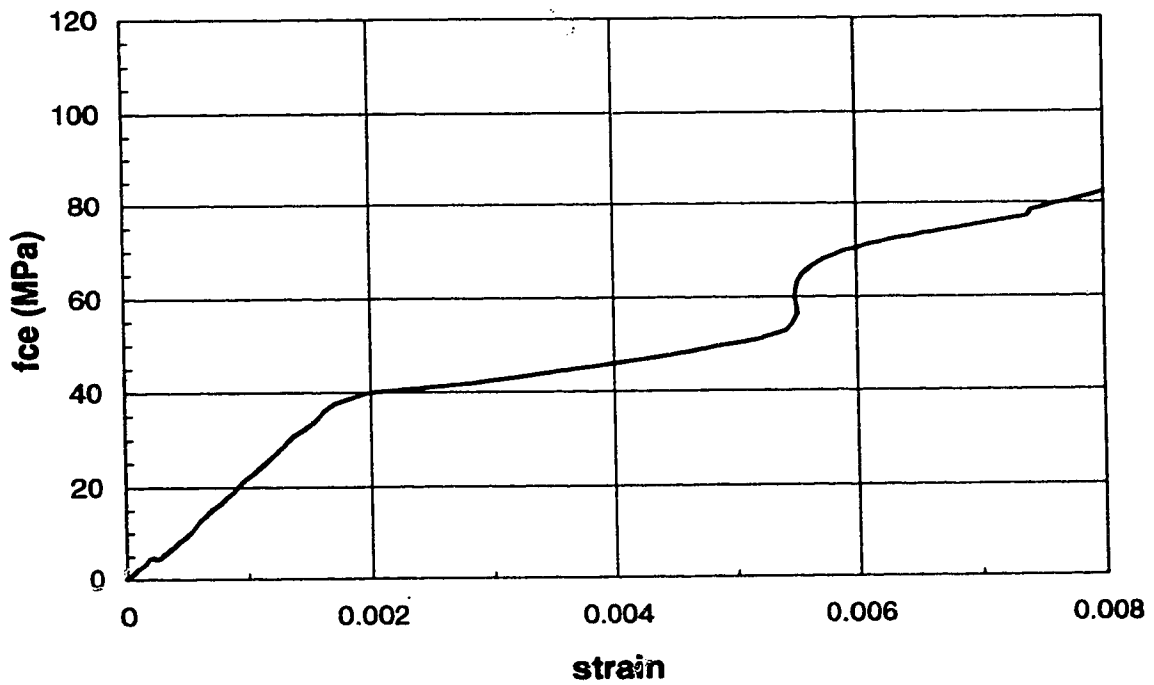


Figure B.32 Column strain through slab (Specimen B-2)

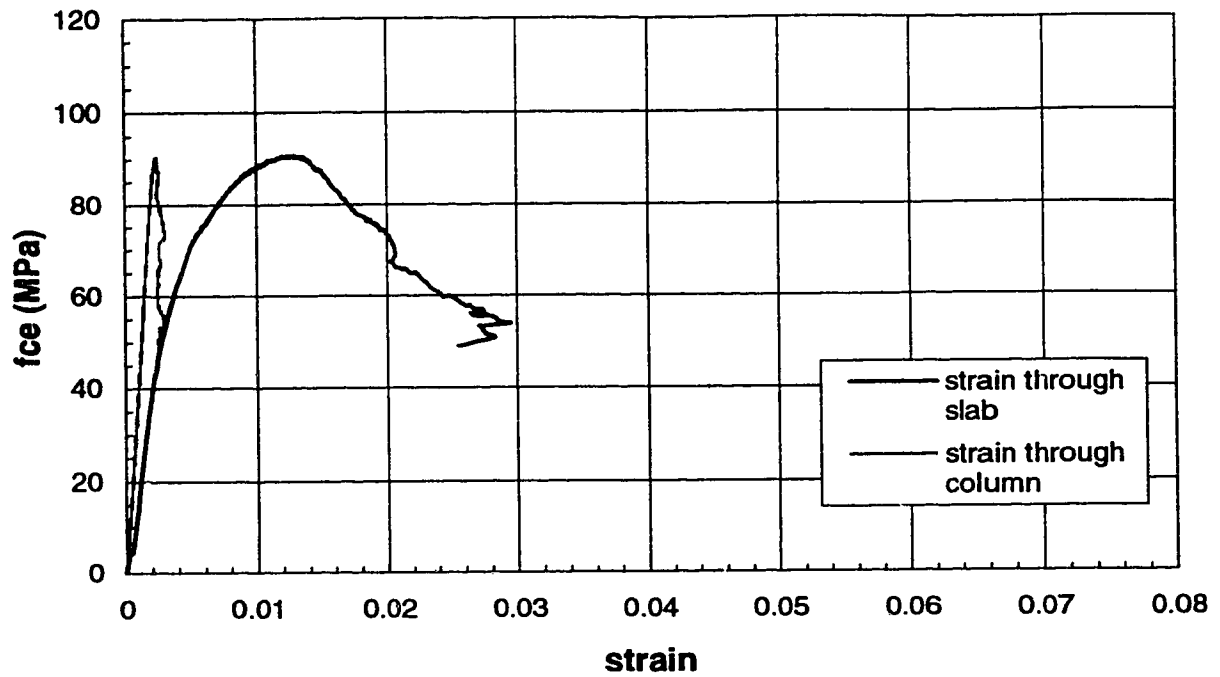


Figure B.33 Stress-strain behaviour (Specimen B-3)

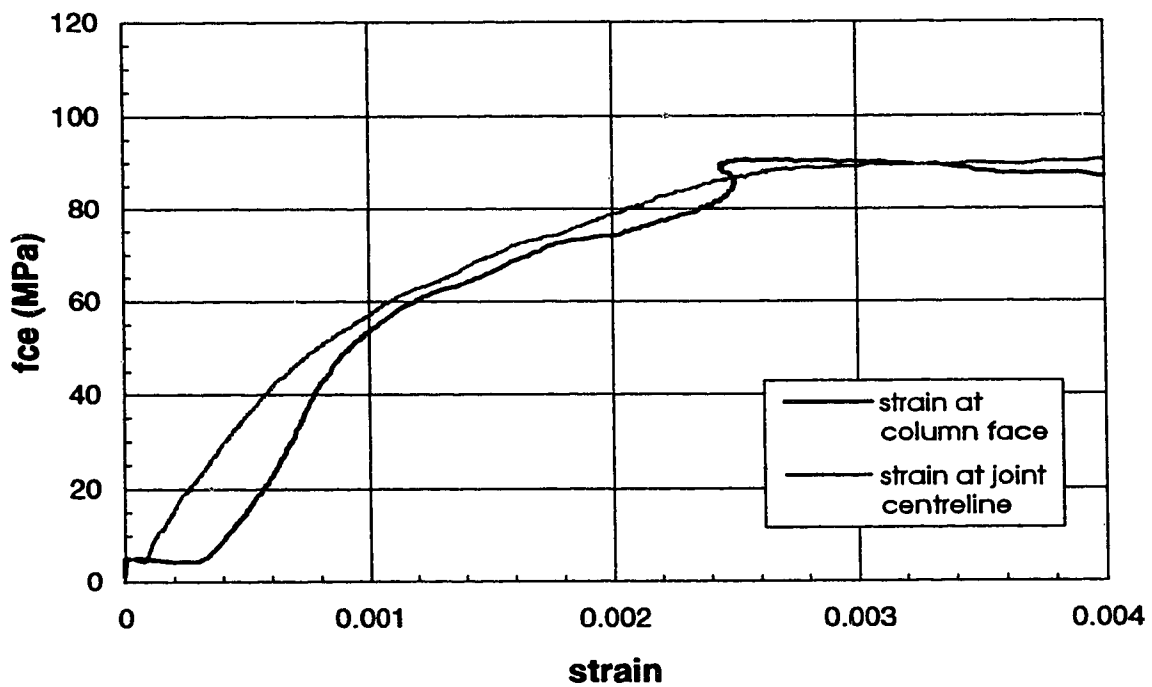


Figure B.34 Slab transverse strain (Specimen B-3)

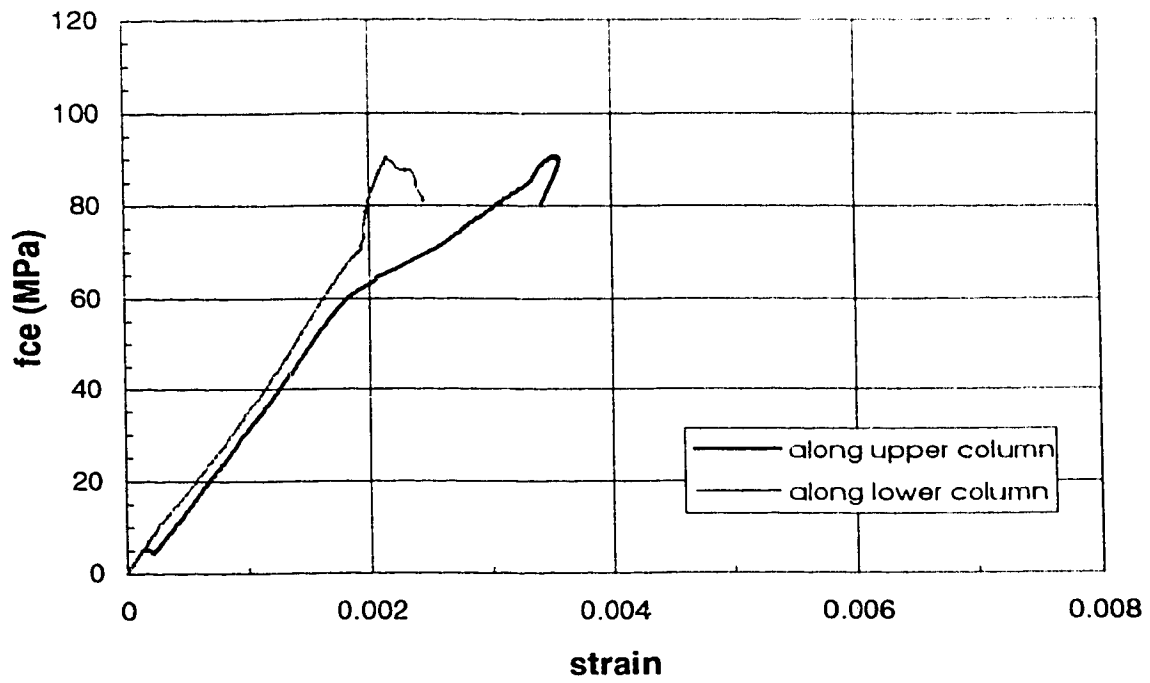


Figure B.35 Column longitudinal strain (Specimen B-3)

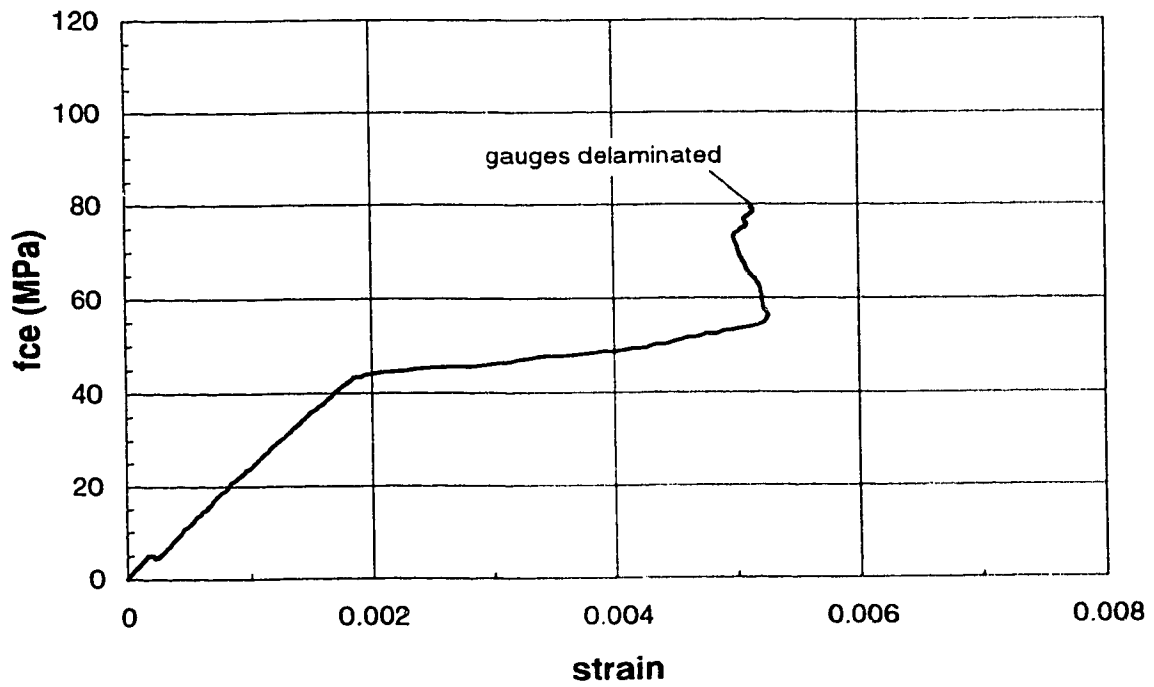


Figure B.36 Column strain through slab (Specimen B-3)

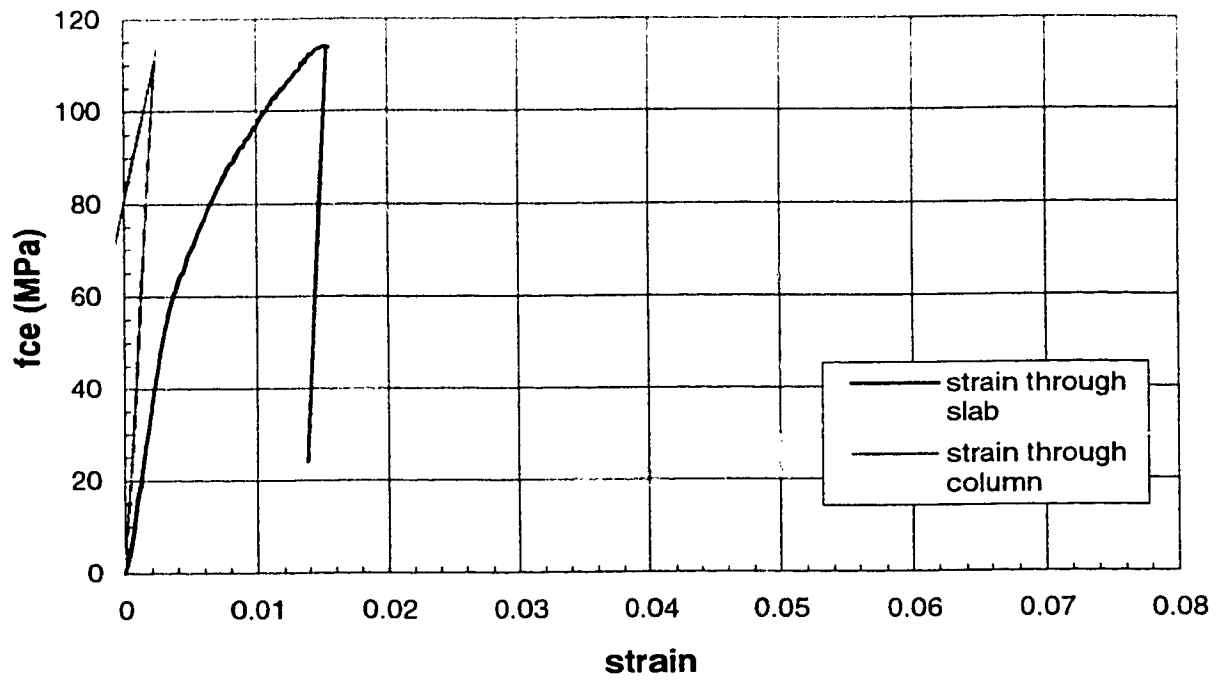


Figure B.37 Stress-strain behaviour (Specimen B-4)

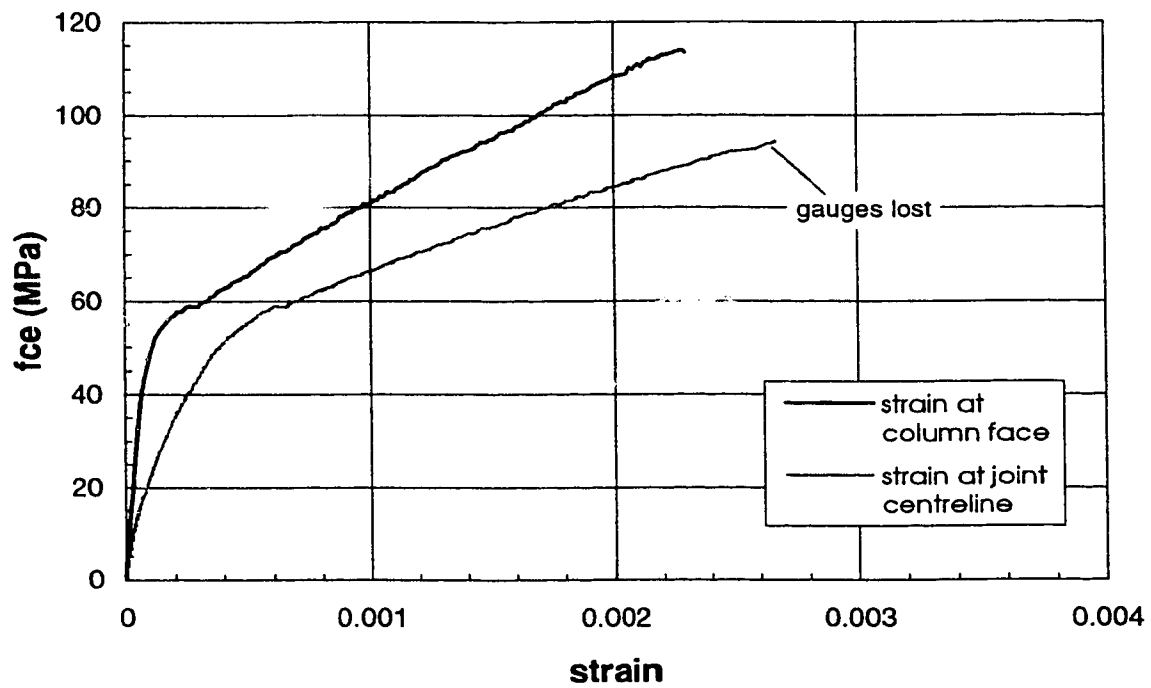


Figure B.38 Slab transverse strain (Specimen B-4)

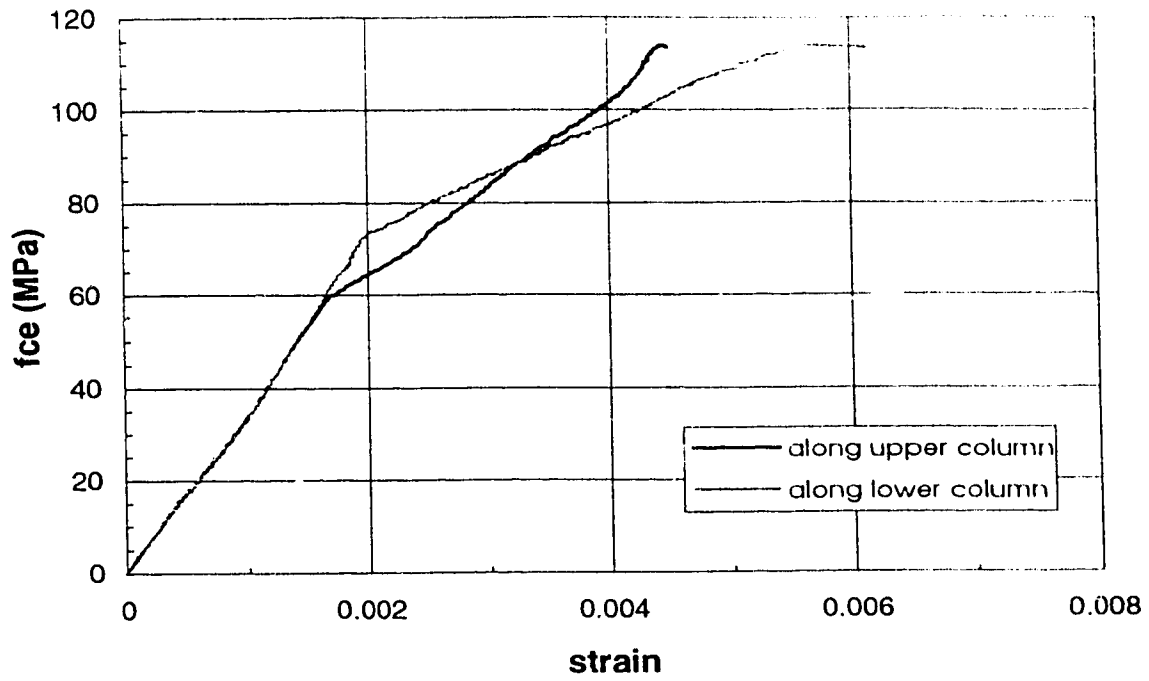


Figure B.39 Column longitudinal strain (Specimen B-4)

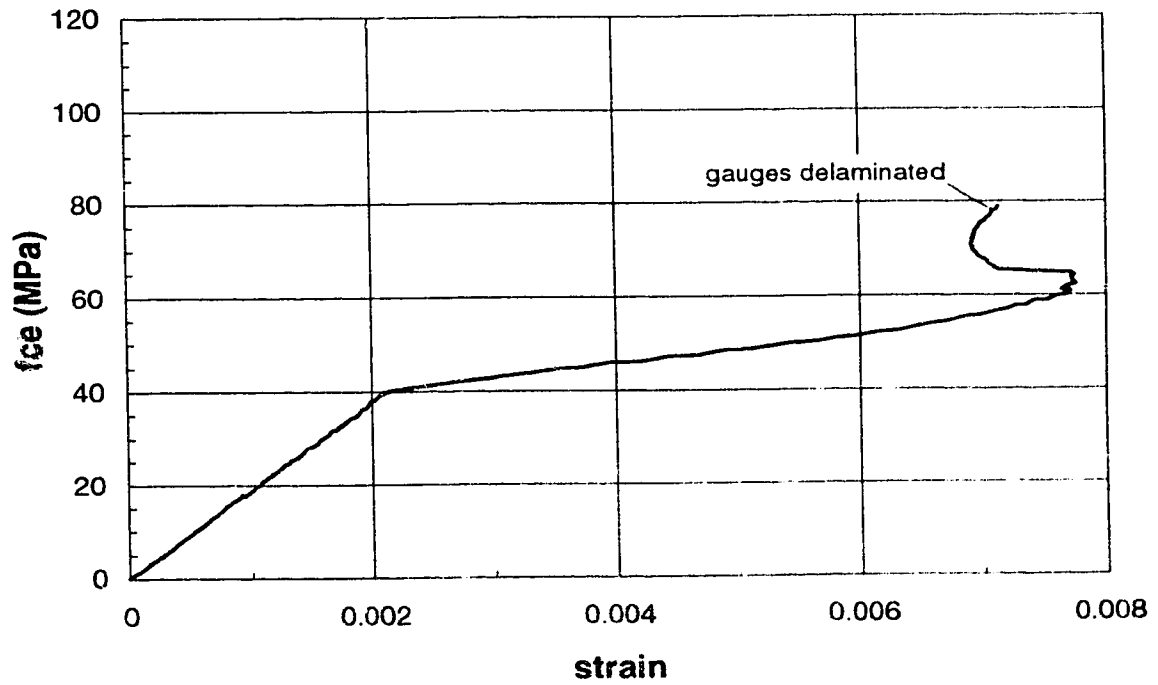


Figure B.40 Column strain through slab (Specimen B-4)

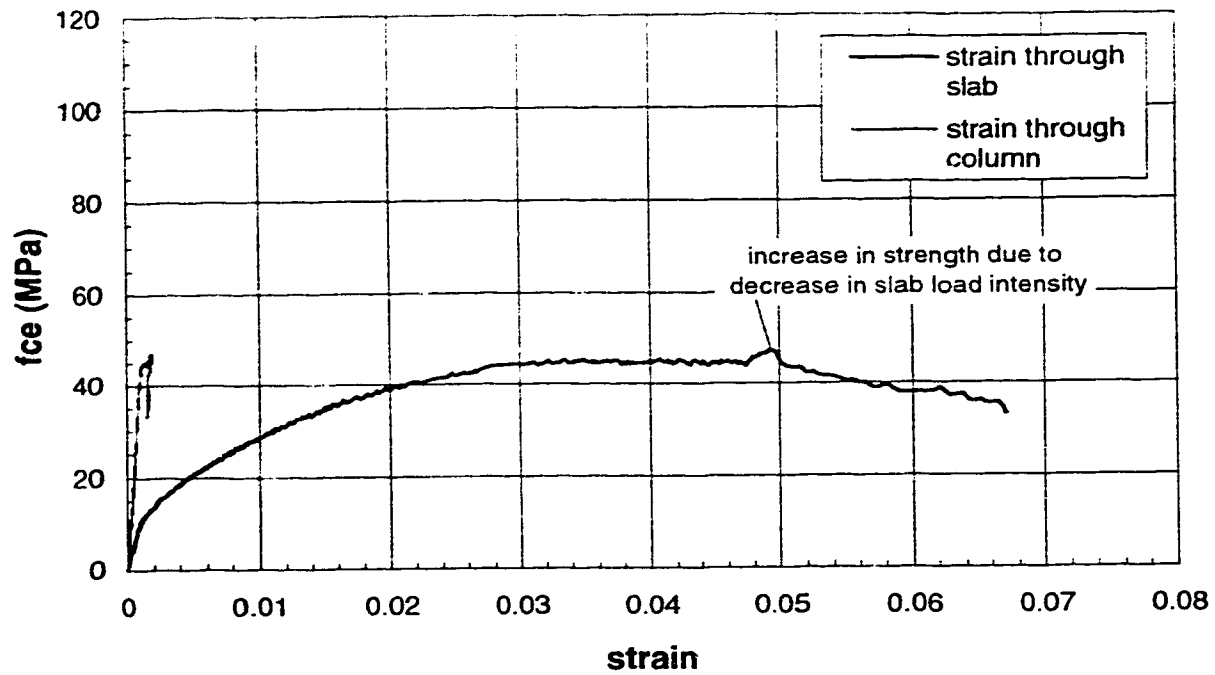


Figure B.41 Stress-strain behaviour (Specimen B-5)

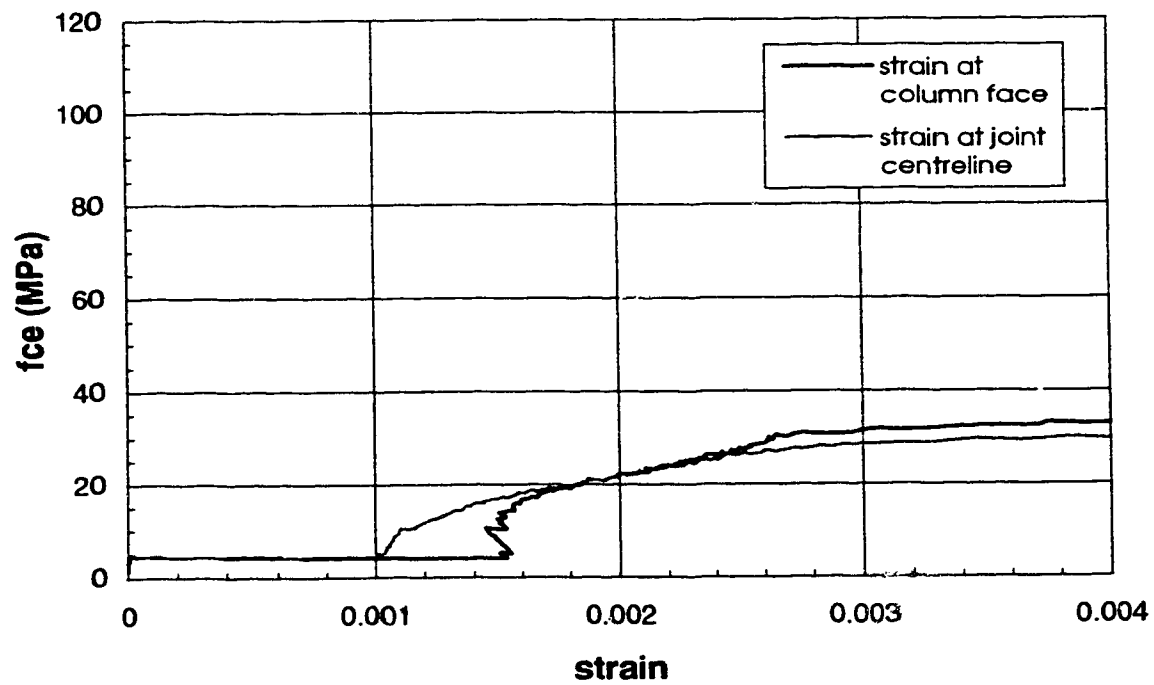


Figure B.42 Slab transverse strain (Specimen B-5)

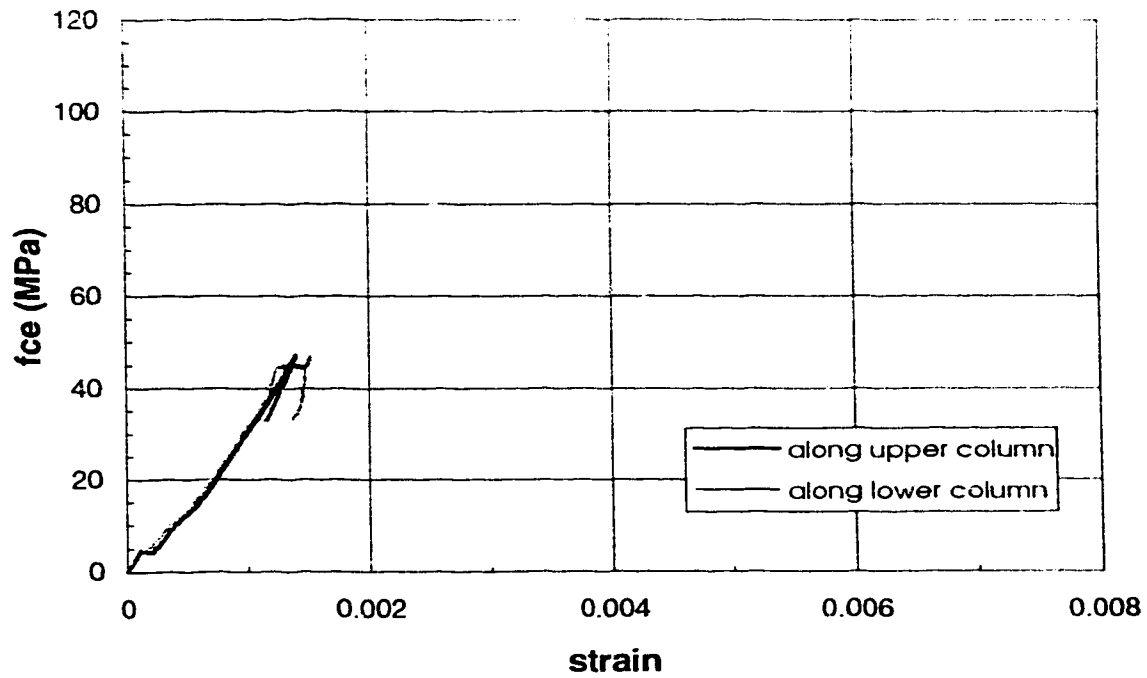


Figure B.43 Column longitudinal strain (Specimen B-5)

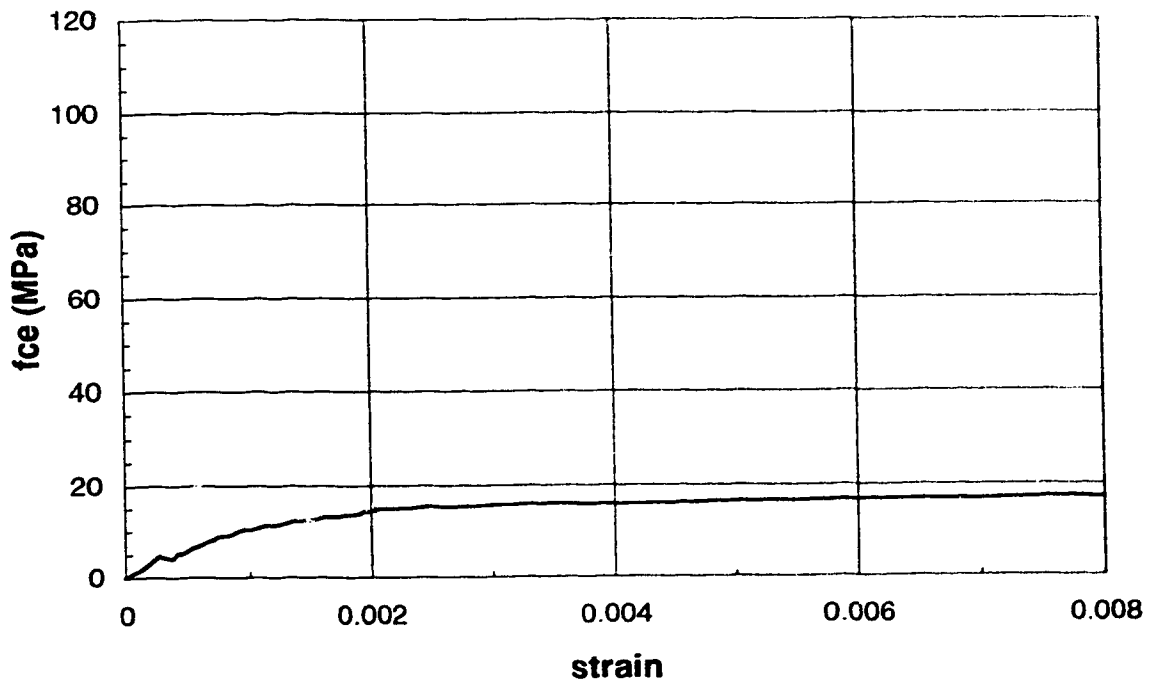


Figure B.44 Column strain through slab (Specimen B-5)

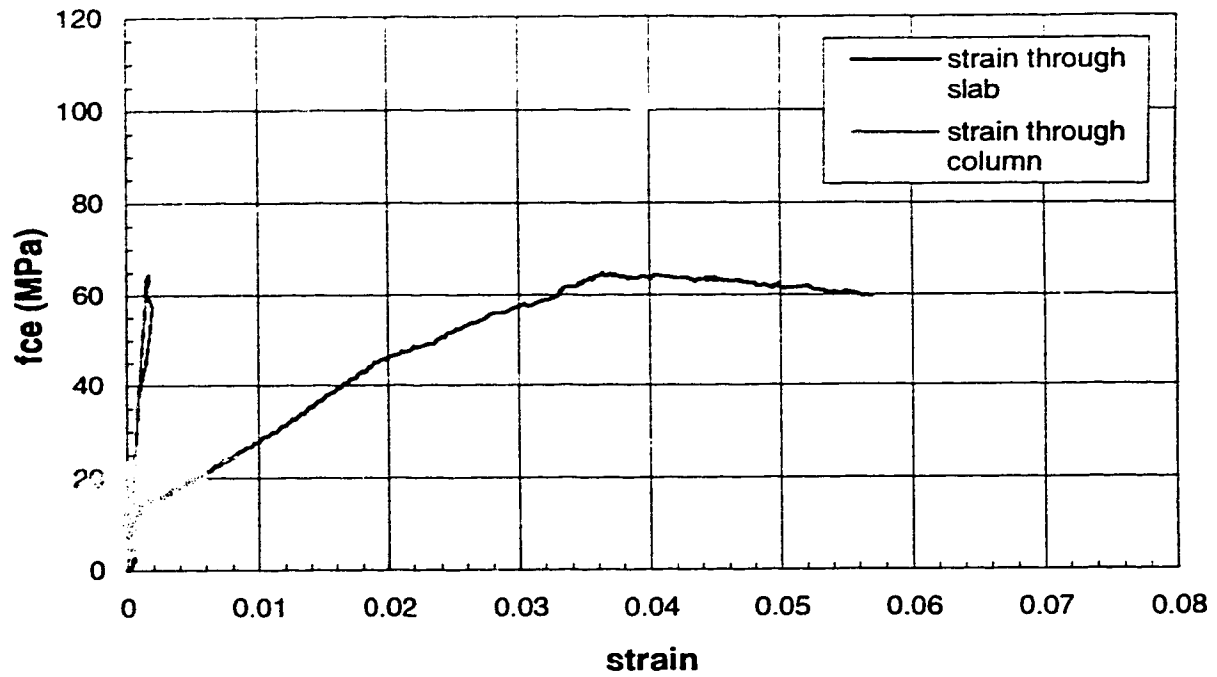


Figure B.45 Stress-strain behaviour (Specimen B-6)

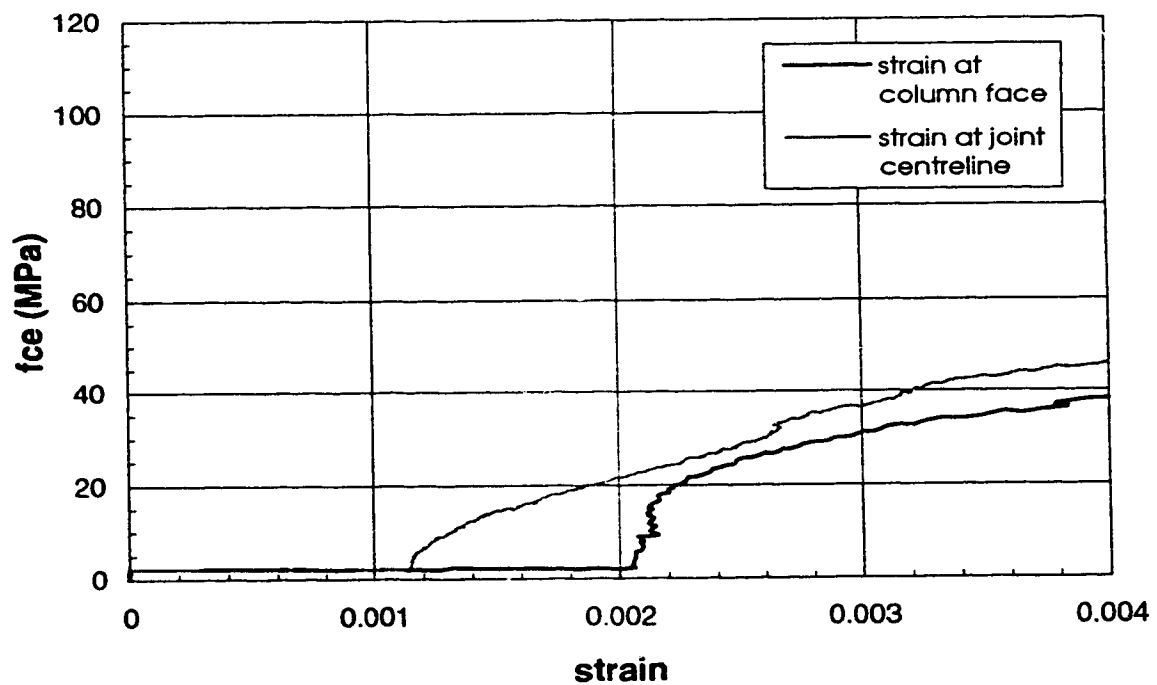


Figure B.46 Slab transverse strain (Specimen B-6)

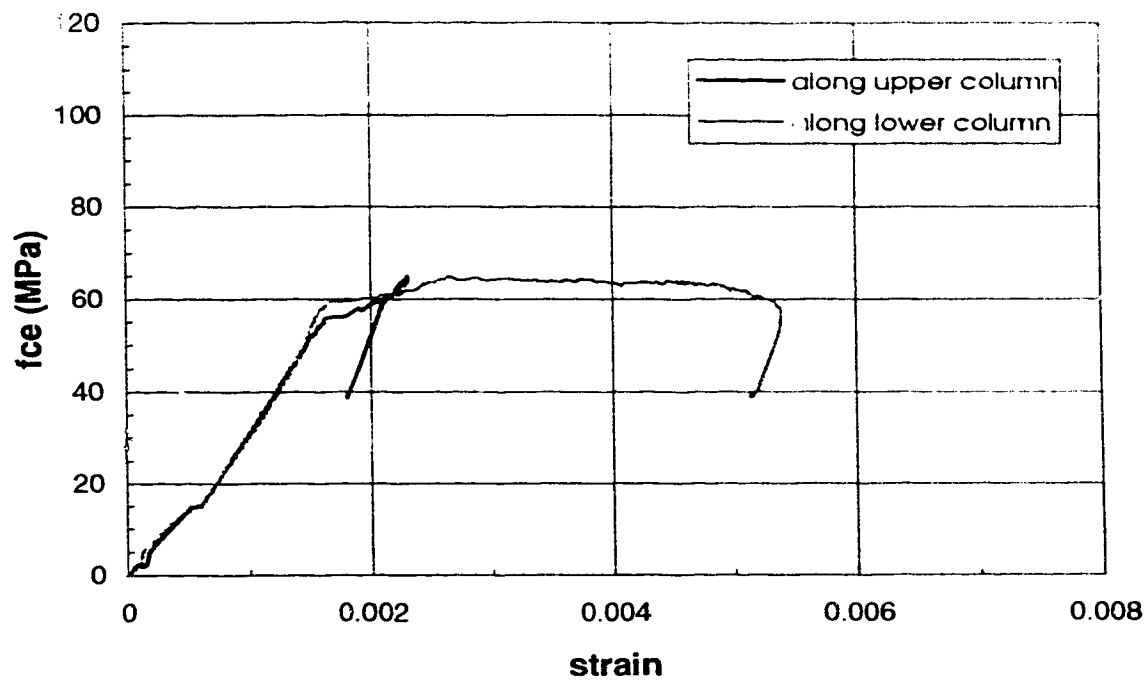


Figure B.47 Column longitudinal strain (Specimen B-6)

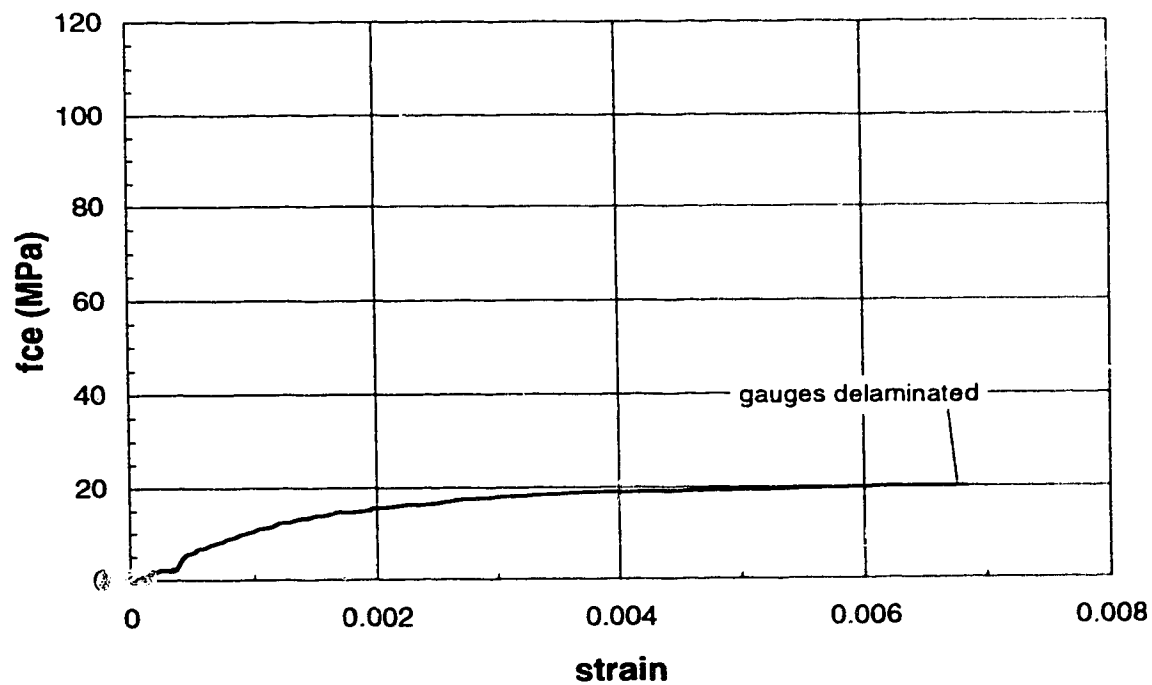


Figure B.48 Column strain through slab (Specimen B-6)

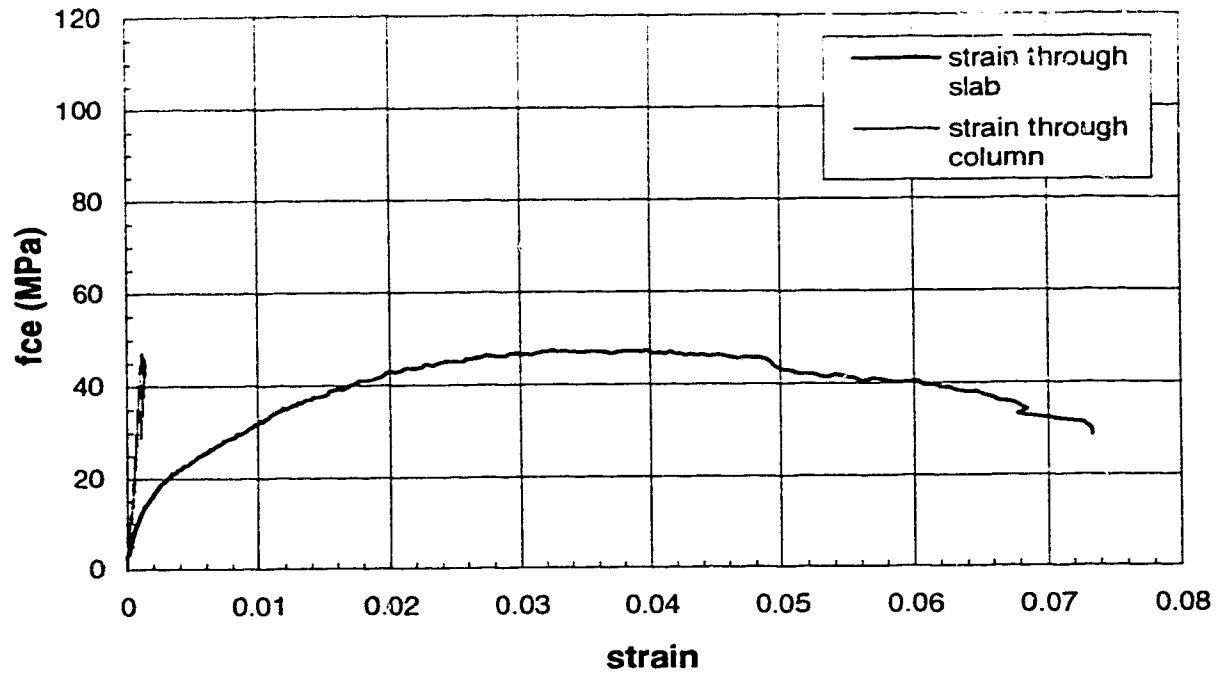


Figure B.49 Stress-strain behaviour (Specimen B-7)

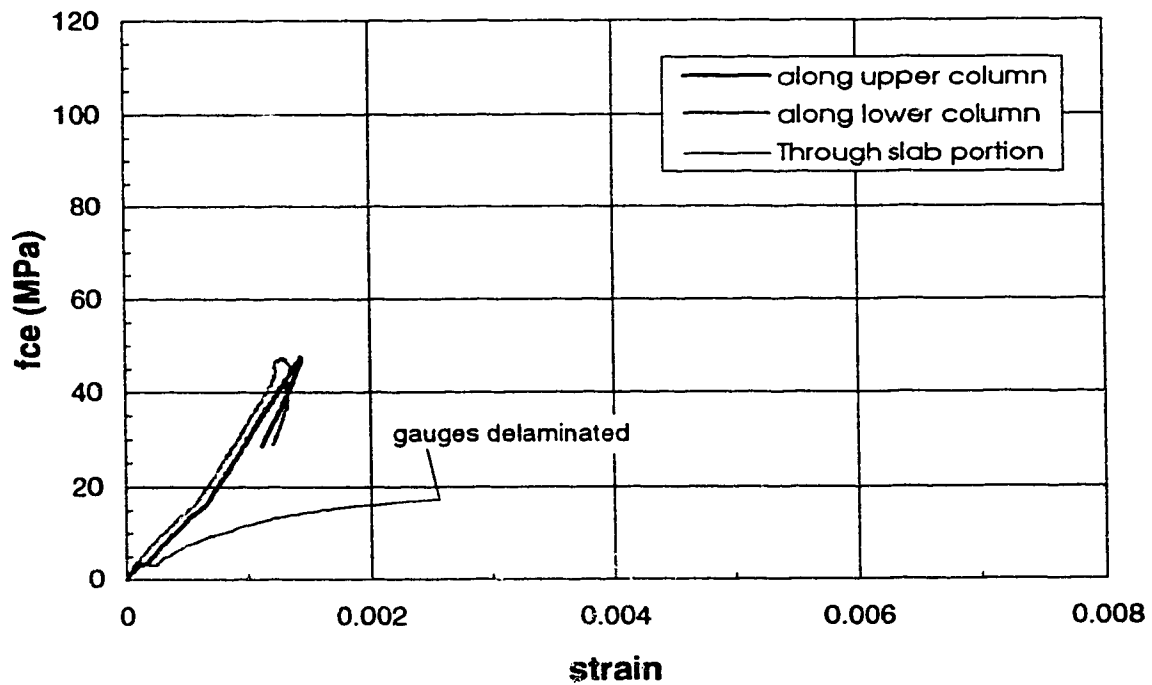


Figure B.50 Column longitudinal strain (Specimen B-7)

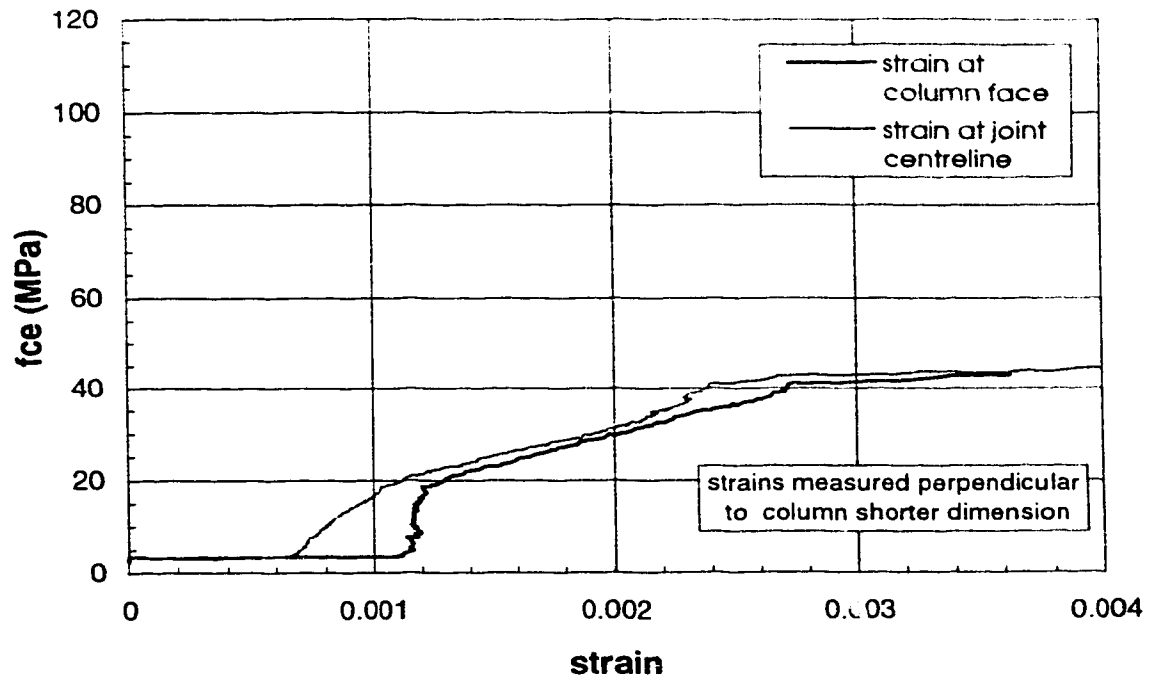


Figure B.51 Slab transverse strain (Specimen B-7)

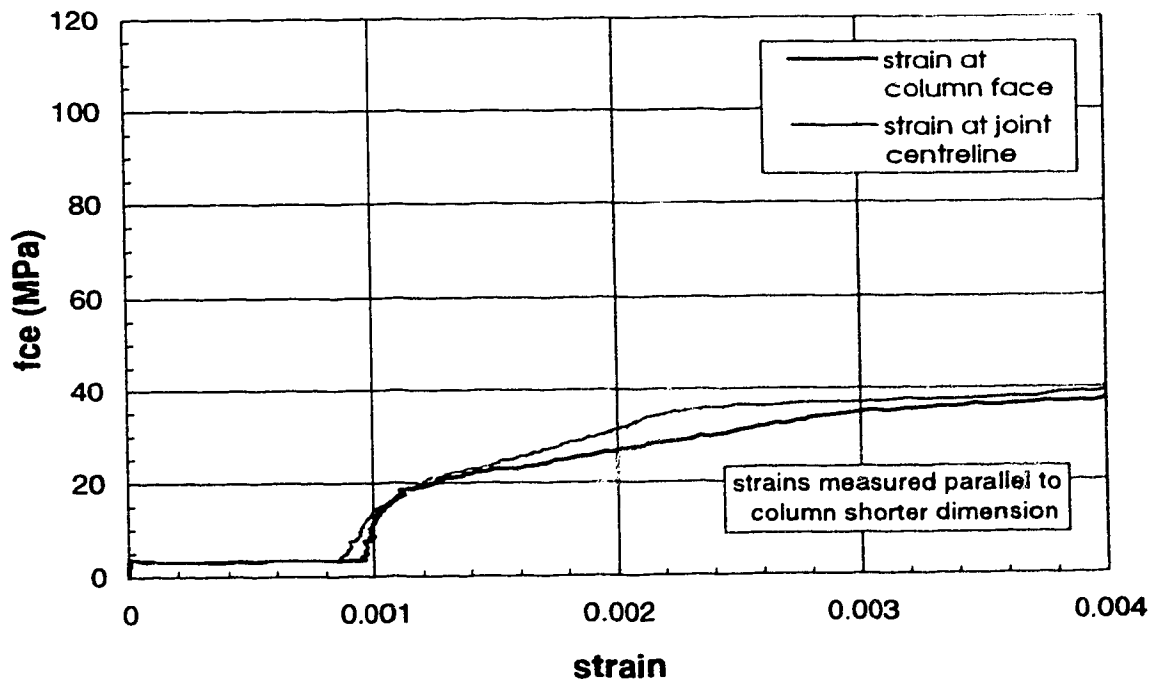


Figure B.52 Slab transverse strain (Specimen B-7)

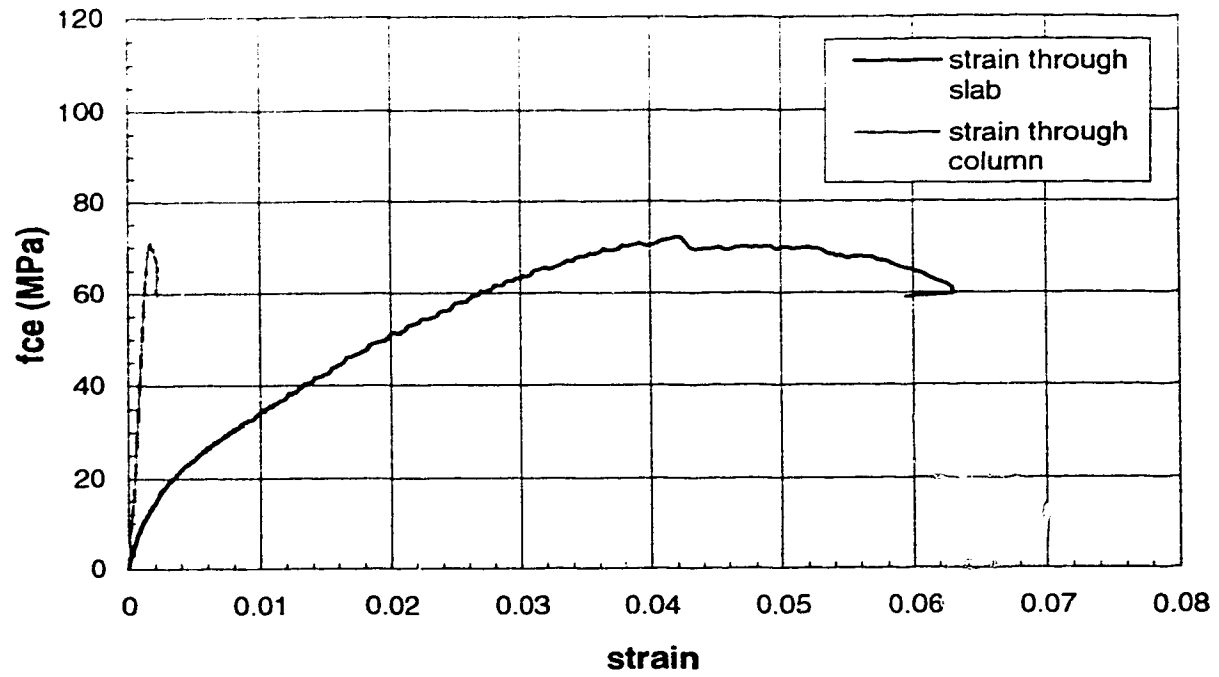


Figure B.53 Stress-strain behaviour (Specimen B-8)

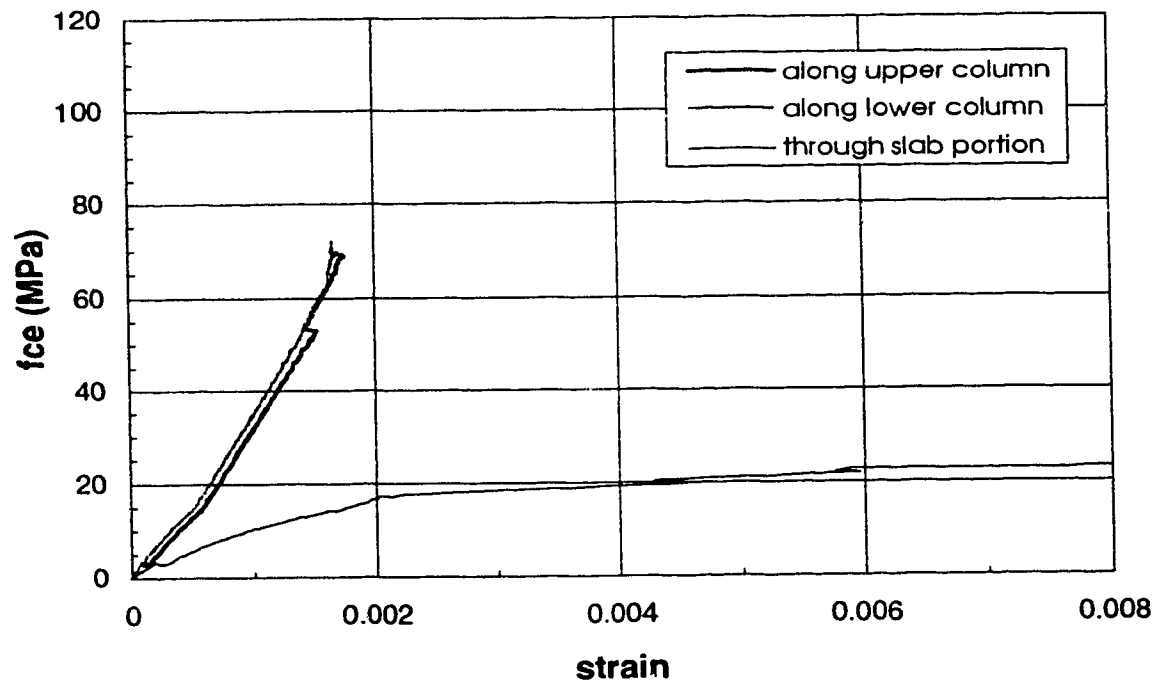


Figure B.54 Column longitudinal strain (Specimen B-8)

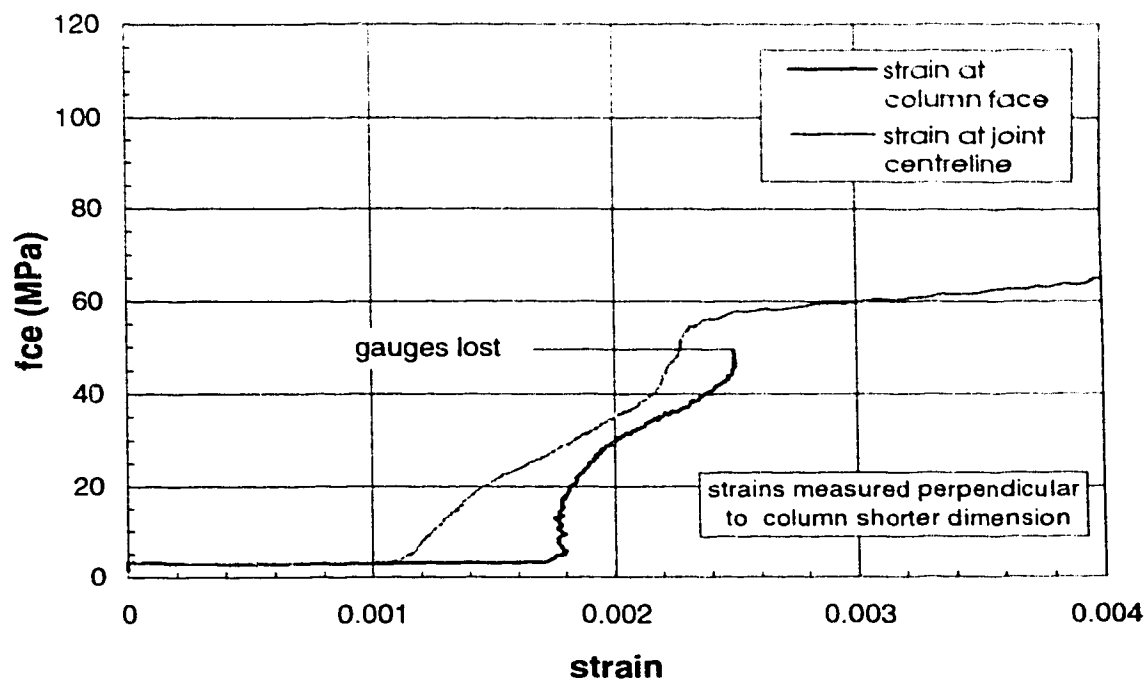


Figure B.55 Slab transverse strain (Specimen B-8)

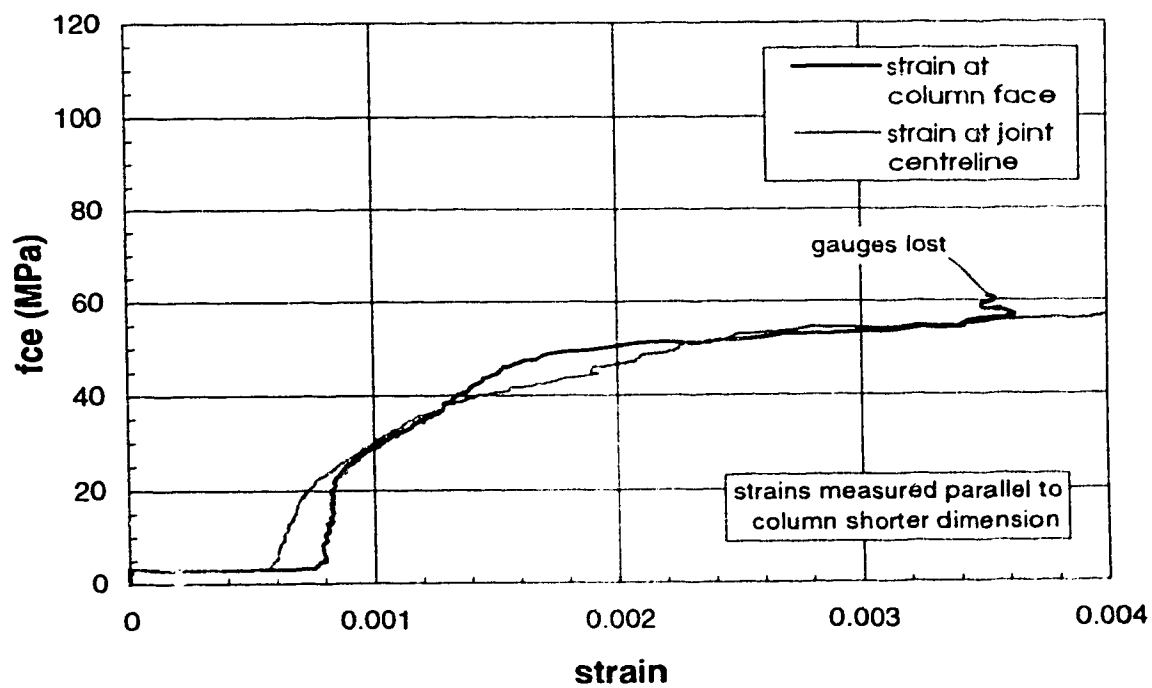


Figure B.56 Slab transverse strain (Specimen B-8)

Series C specimens

-Edge Sandwich Plates-

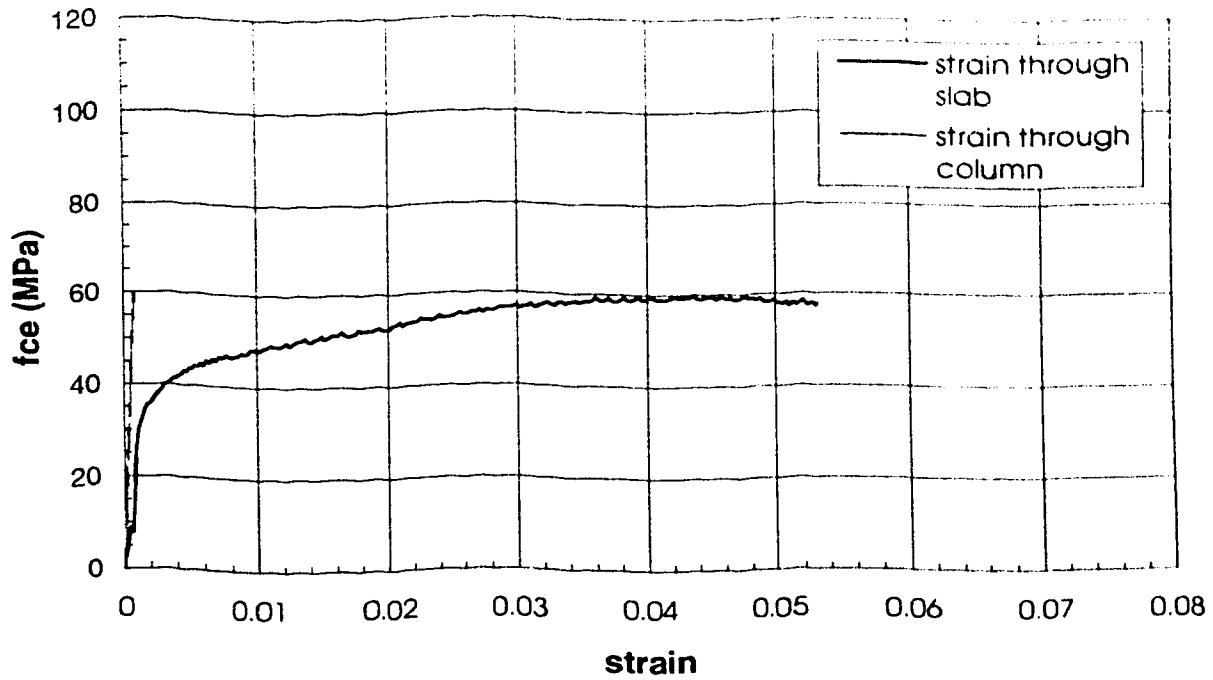


Figure B.57 Stress-strain behaviour (Specimen C1-A)

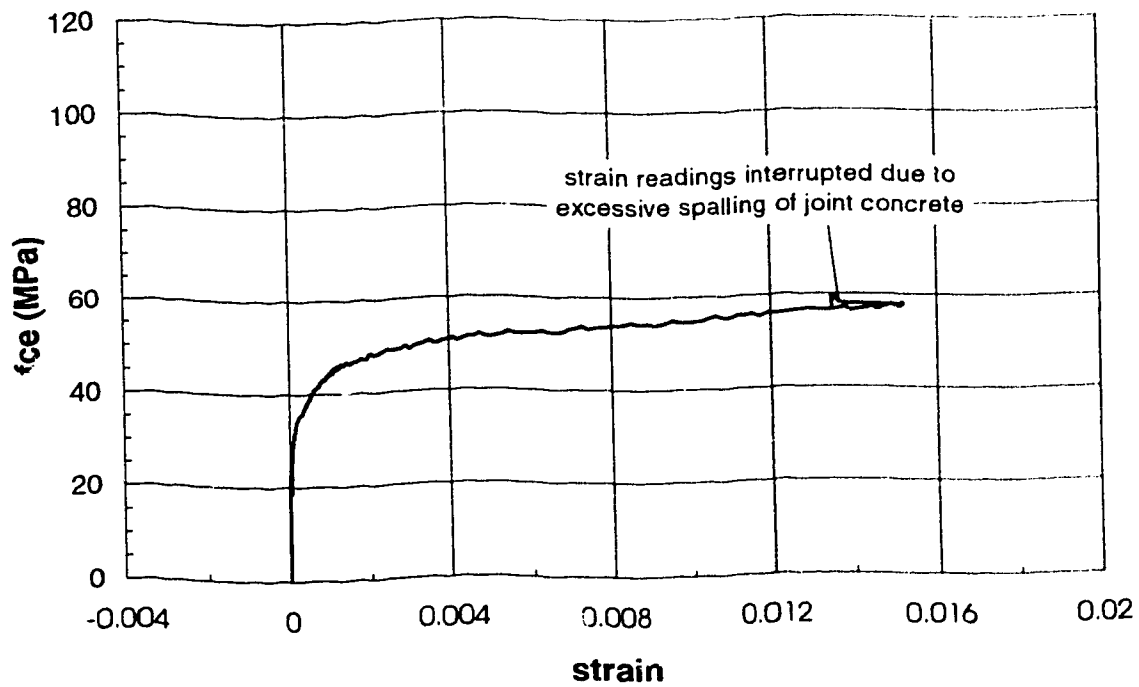


Figure B.58 Joint lateral expansion (Specimen C1-A)

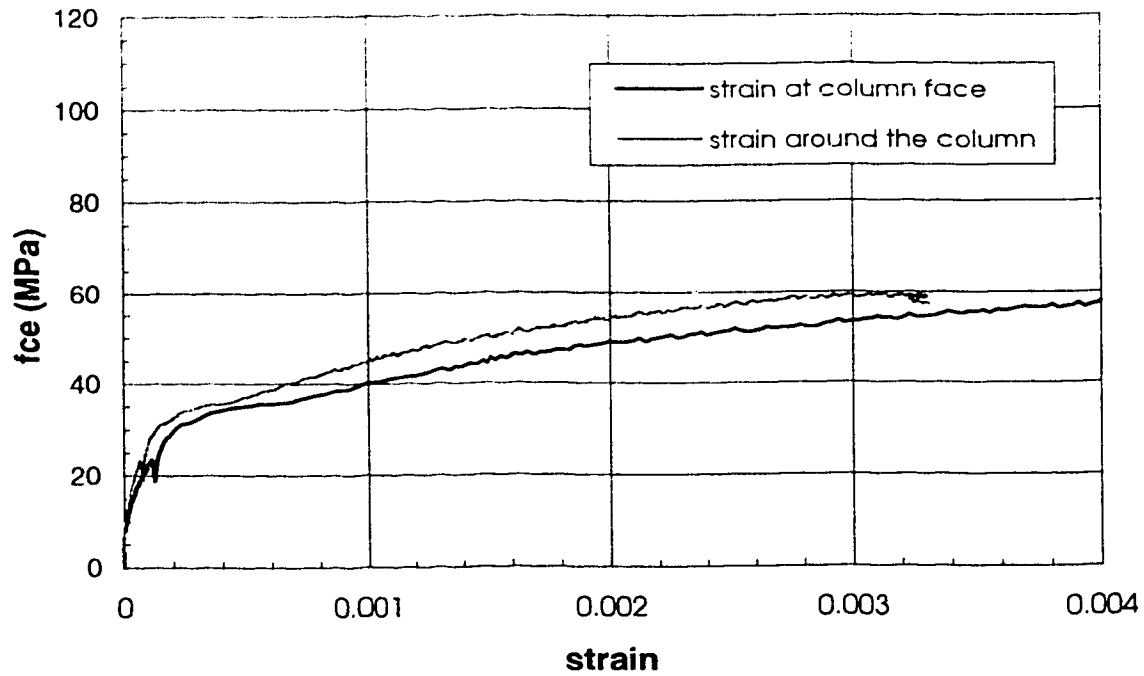


Figure B.59 Top slab transverse strain (Specimen C1-A)

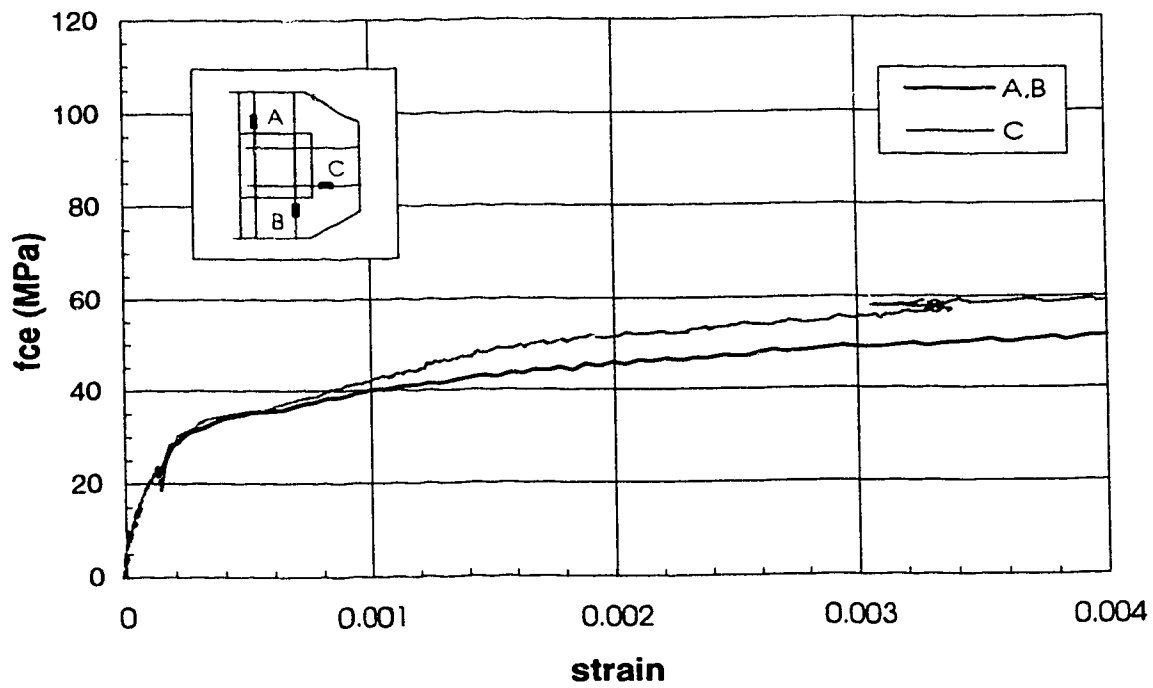


Figure B.60 Bottom slab transverse strain (Specimen C1-A)

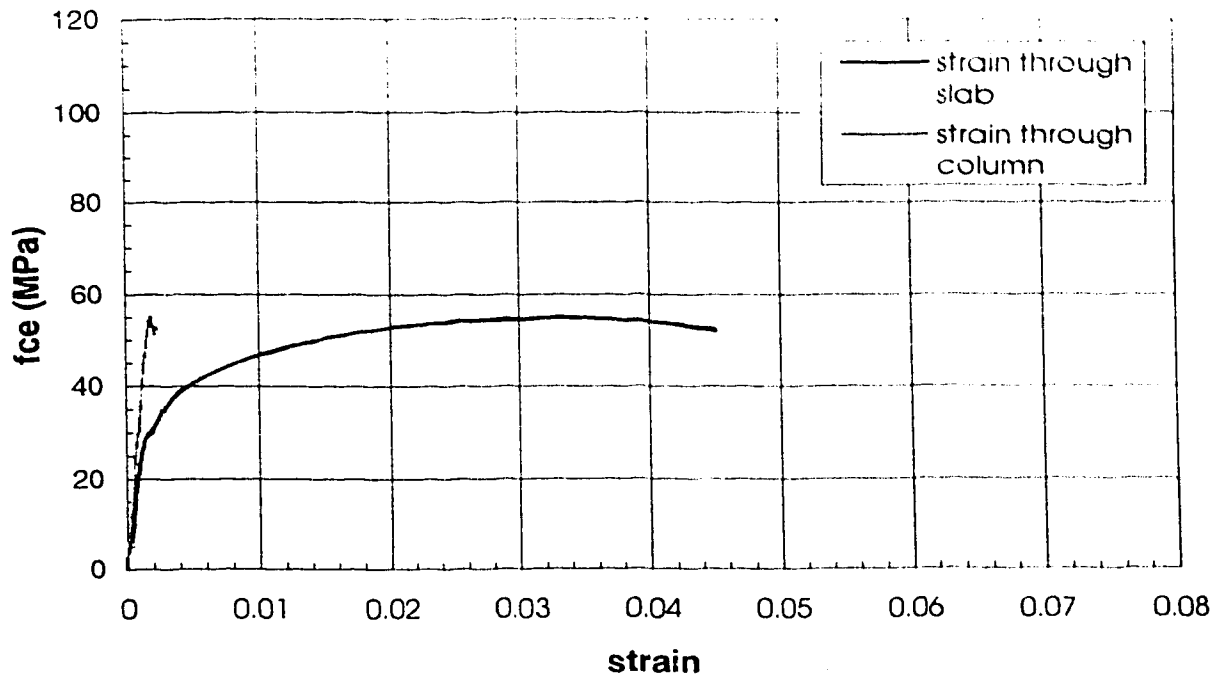


Figure B.61 Stress-strain behaviour (Specimen C1-B)

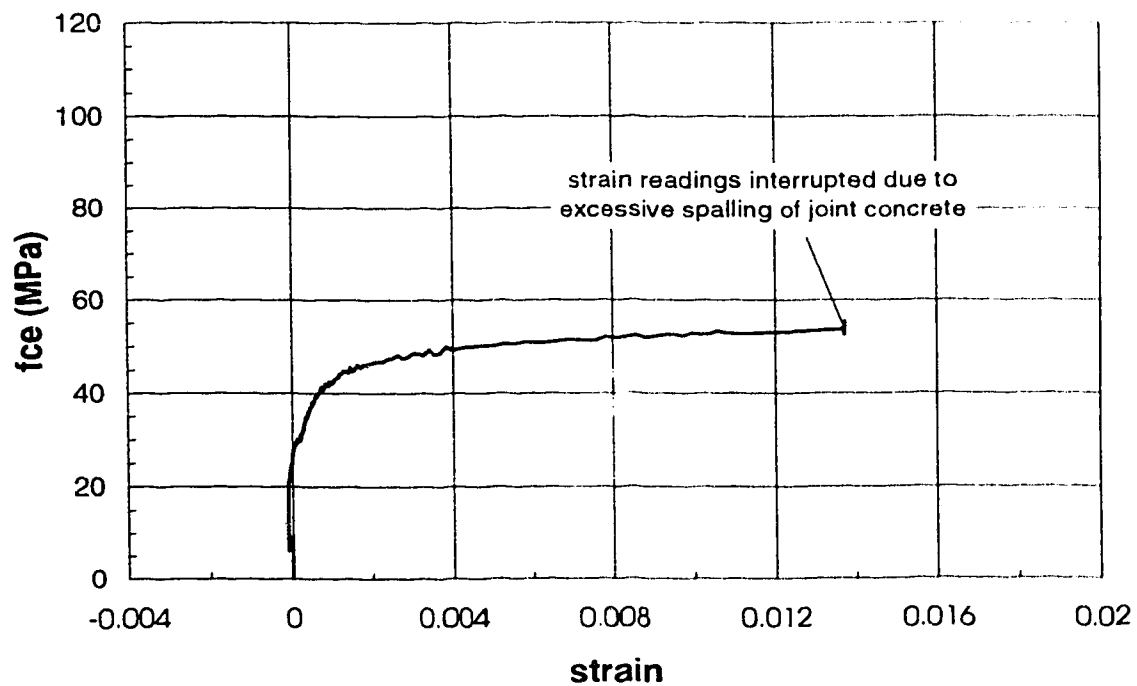


Figure B.62 Joint lateral expansion (Specimen C1-B)

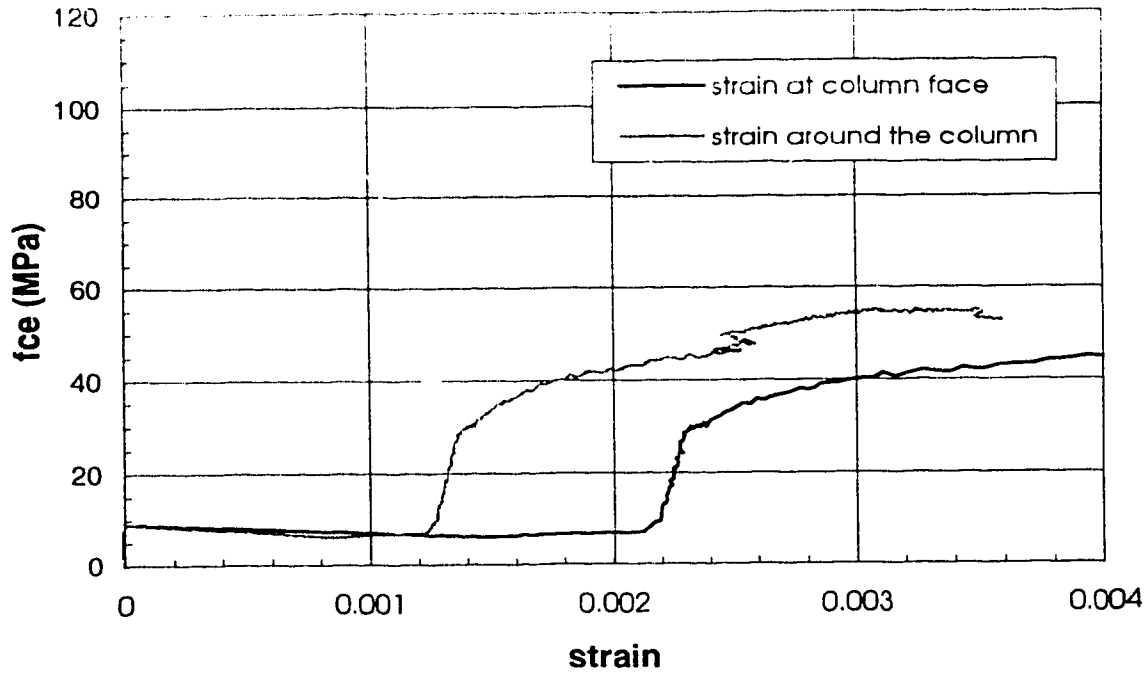


Figure B.63 Top slab transverse strain (Specimen C1-B)

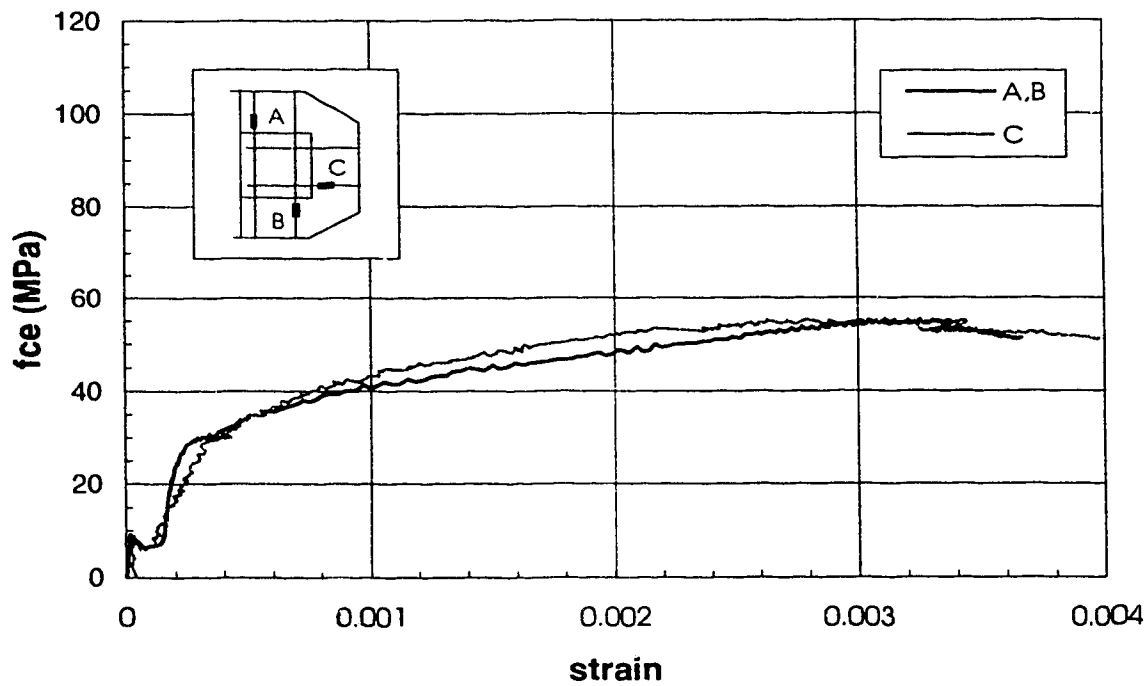


Figure B.64 Bottom slab transverse strain (Specimen C1-B)

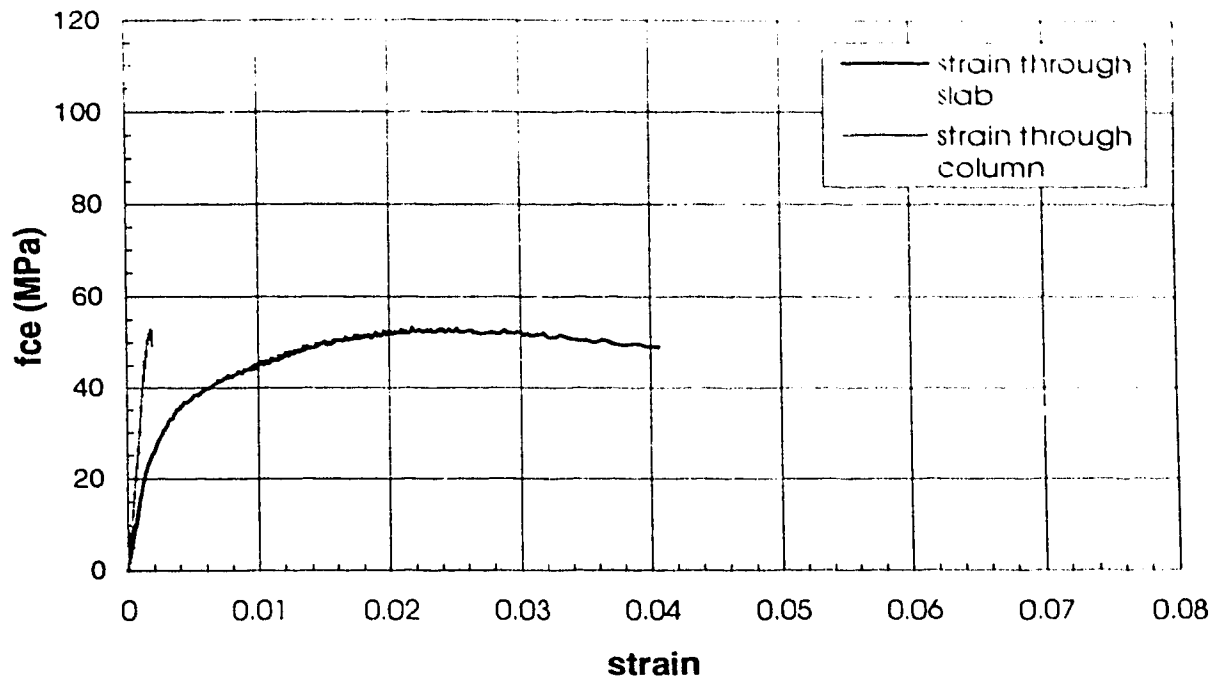


Figure B.65 Stress-strain behaviour (Specimen C1-C)

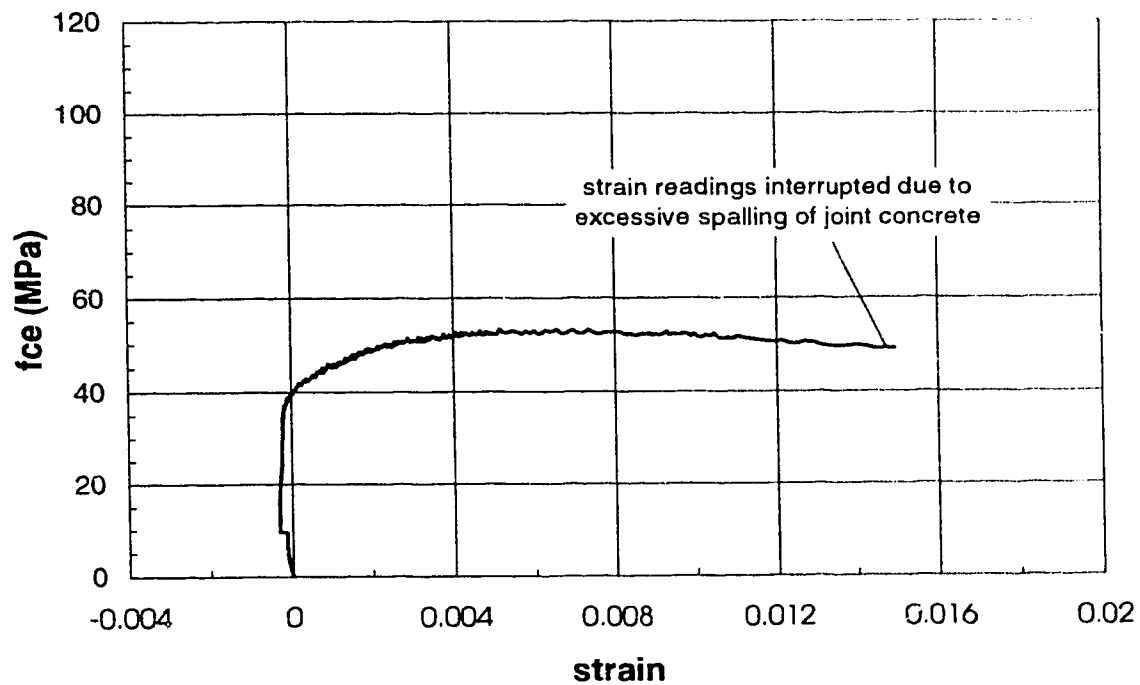


Figure B.66 Joint lateral expansion (Specimen C1-C)

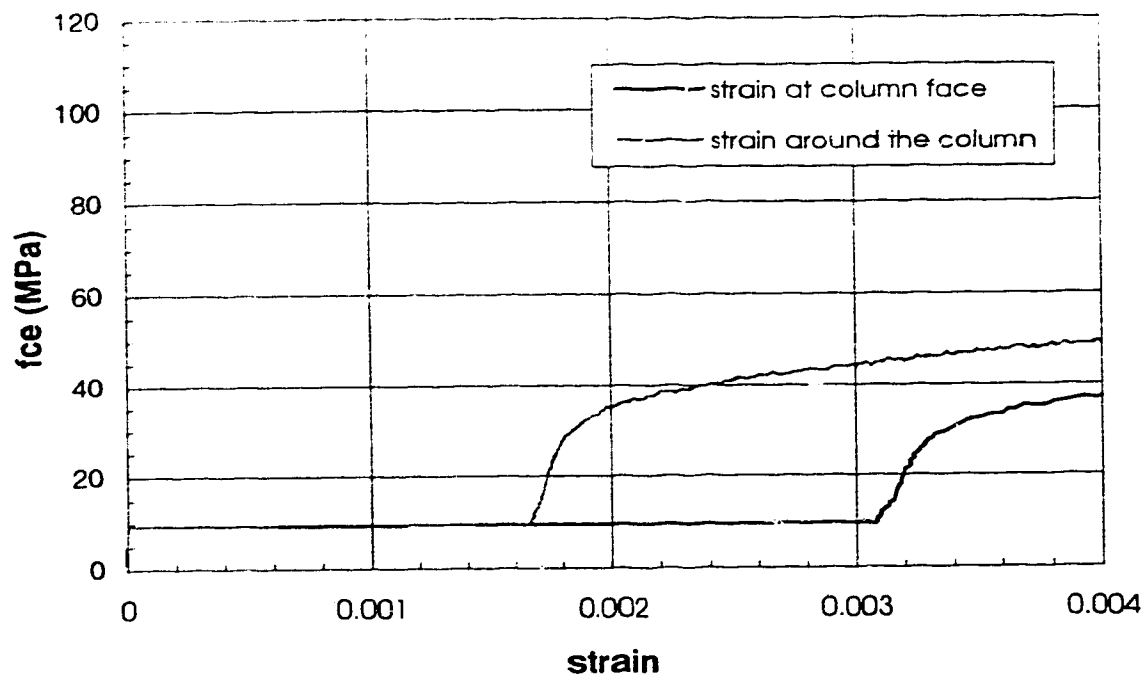


Figure B.67 Top slab transverse strain (Specimen C1-C)

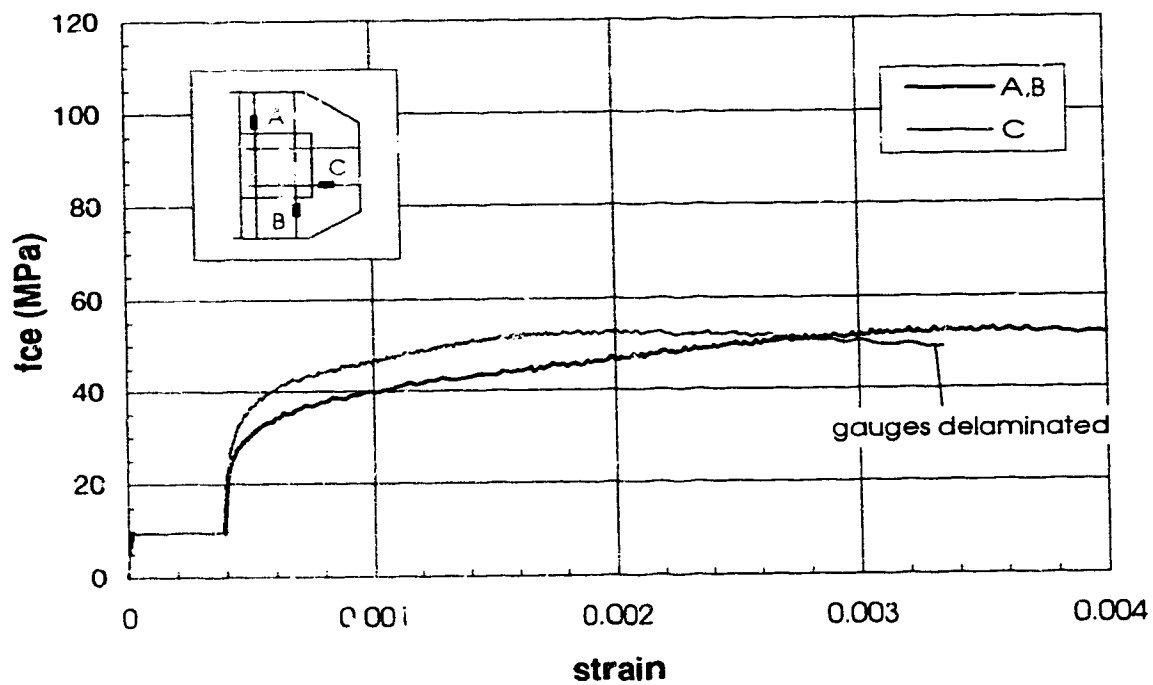


Figure B.68 Bottom slab transverse strain (Specimen C1-C)

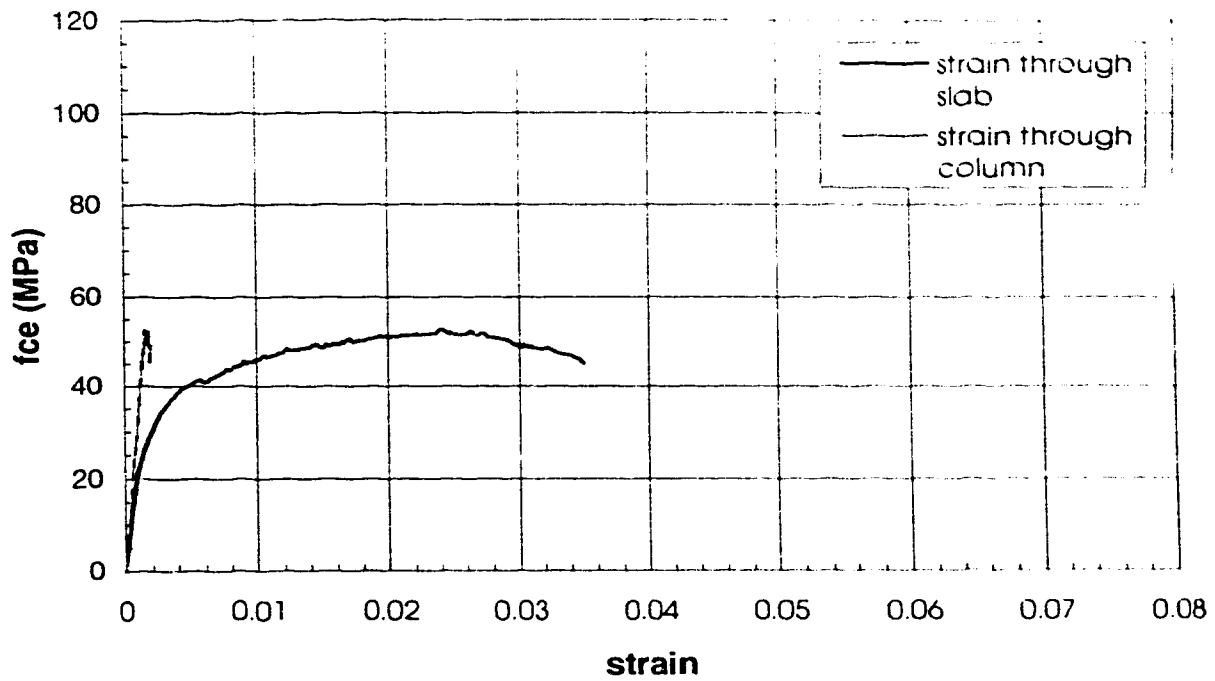


Figure B.69 Stress-strain behaviour (Specimen C2-A)

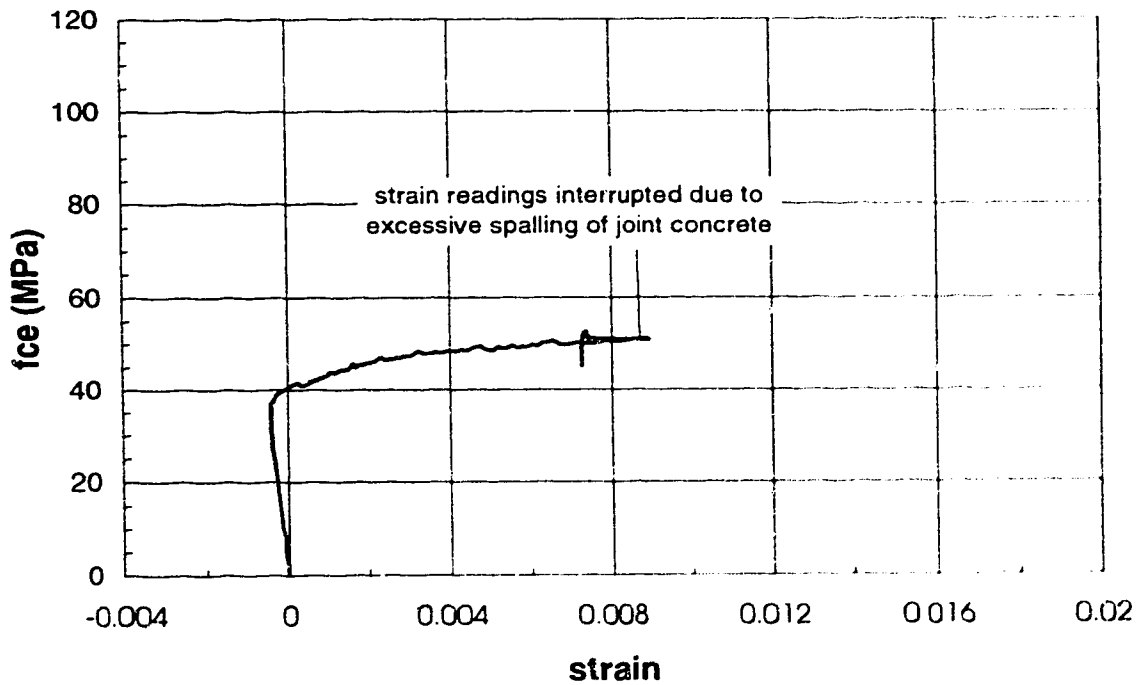


Figure B.70 Joint lateral expansion (Specimen C2-A)

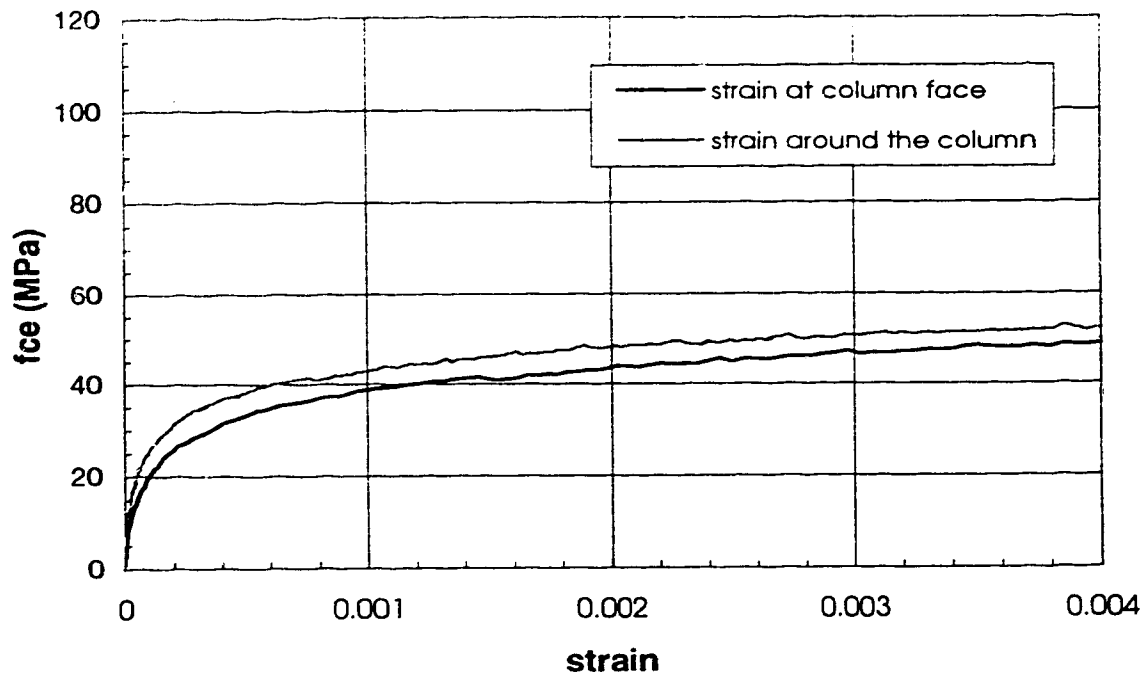


Figure B.71 Top slab transverse strain (Specimen C2-A)

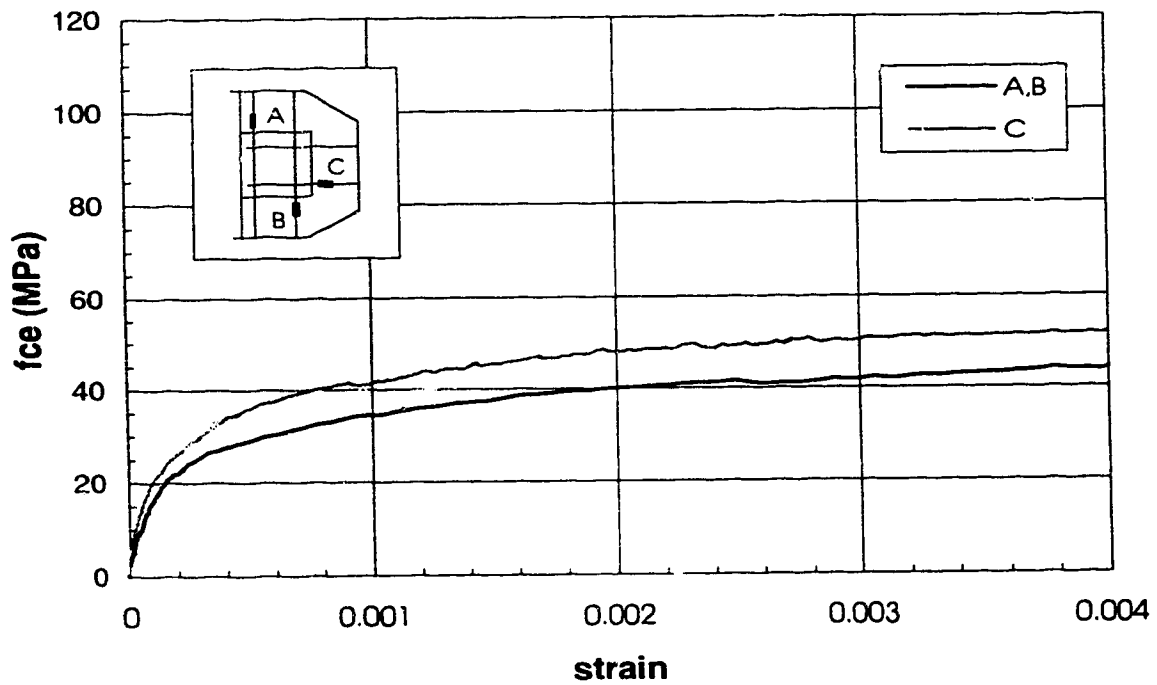


Figure B.72 Bottom slab transverse strain (Specimen C2-A)

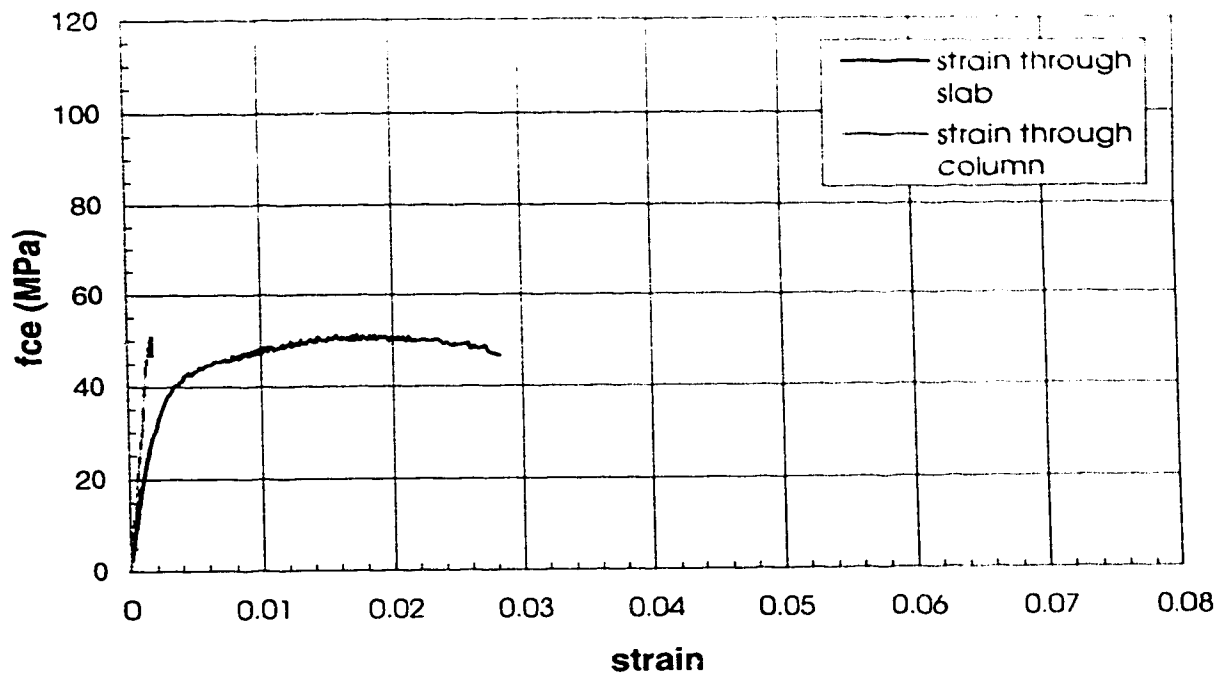


Figure B.73 Stress-strain behaviour (Specimen C2-B)

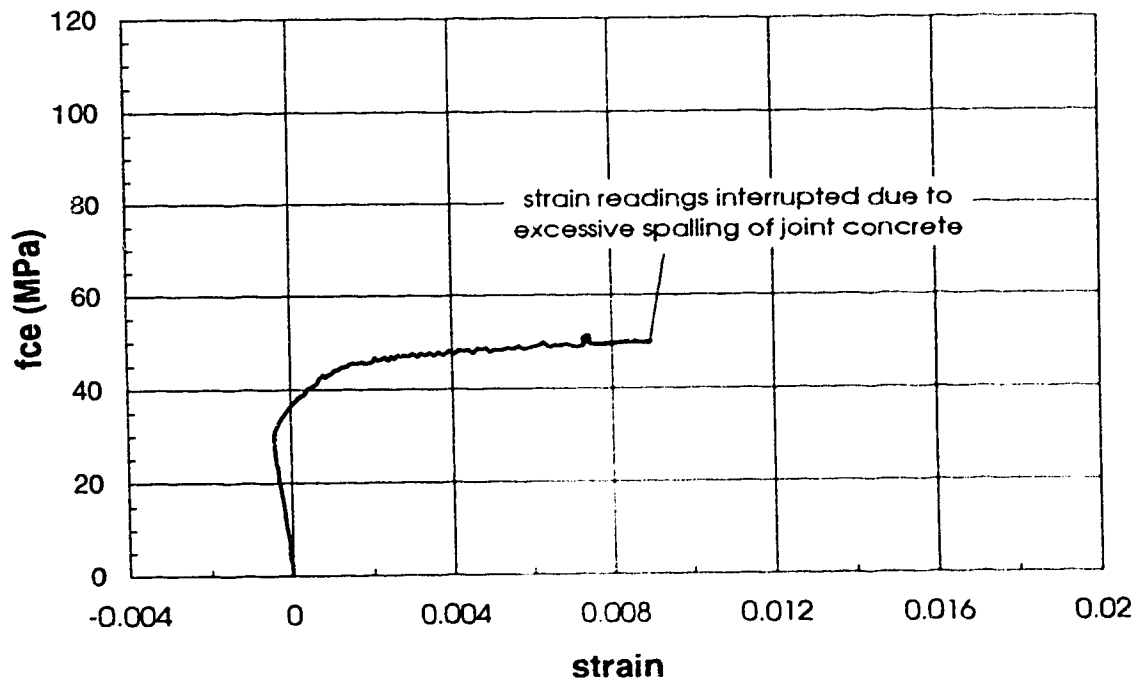


Figure B.74 Joint lateral expansion (Specimen C2-B)

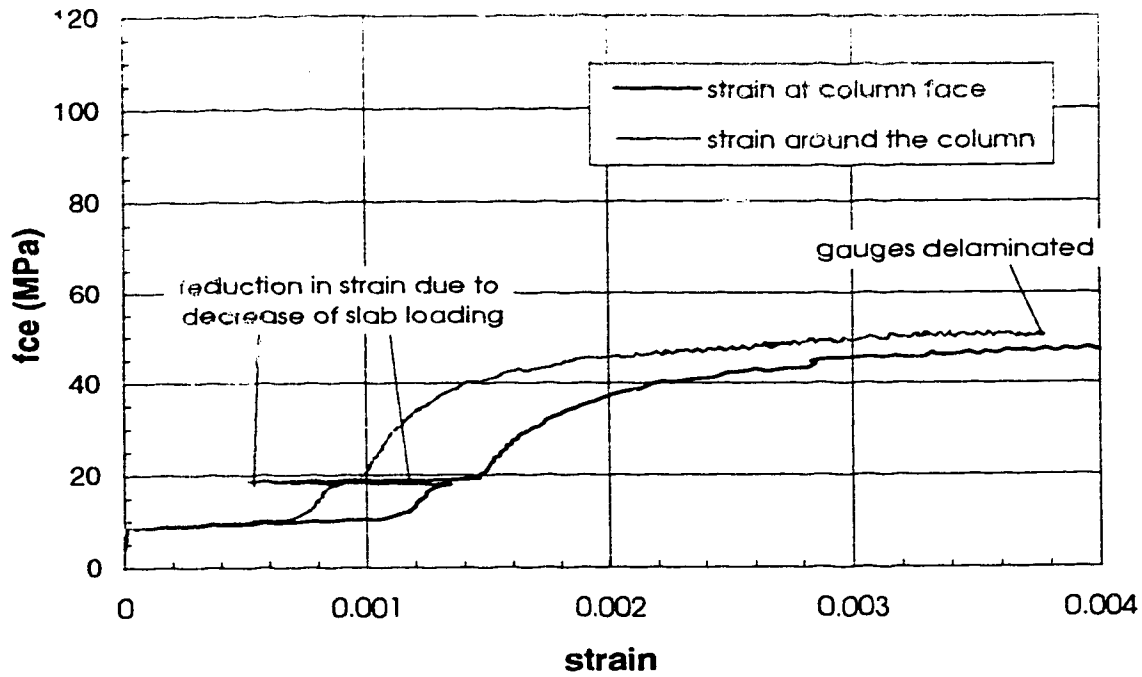


Figure B.75 Top slab transverse strain (Specimen C2-B)

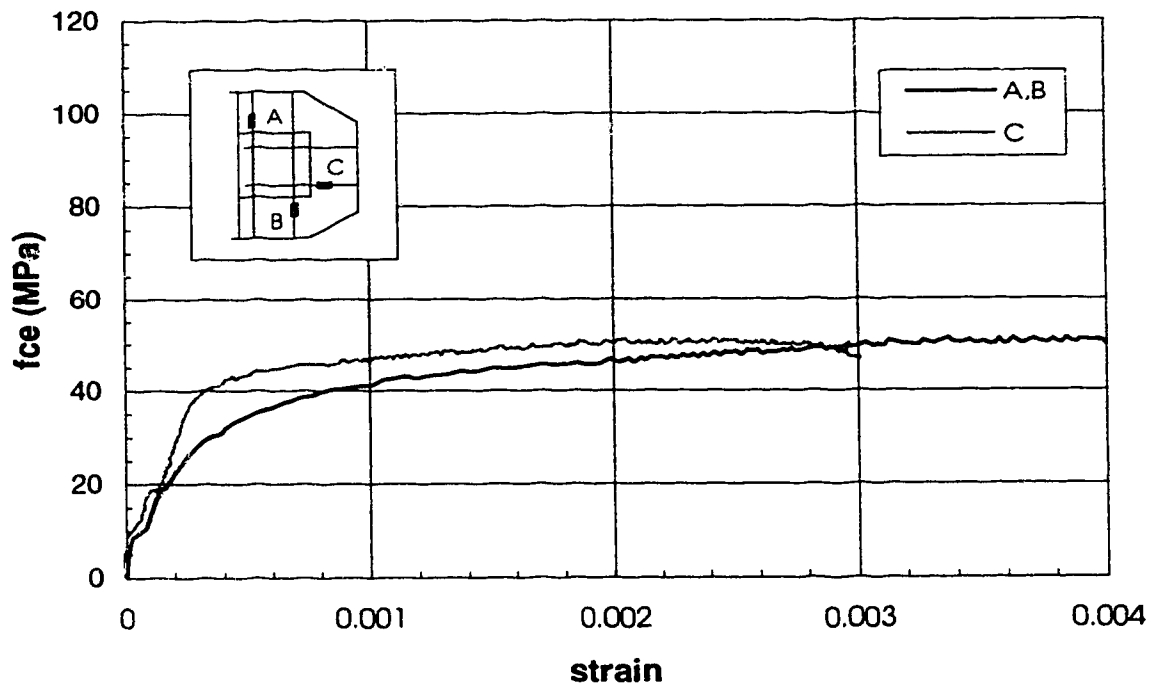


Figure B.76 Bottom slab transverse strain (Specimen C2-B)

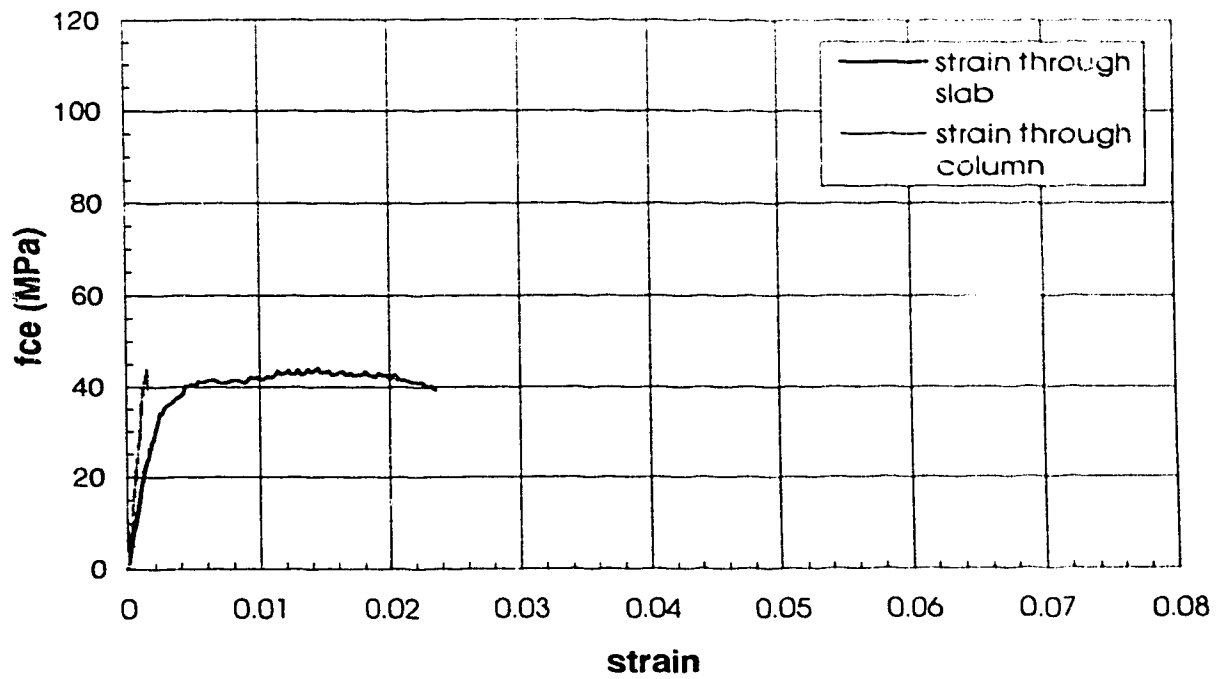


Figure B.77 Stress-strain behaviour (Specimen C2-C)

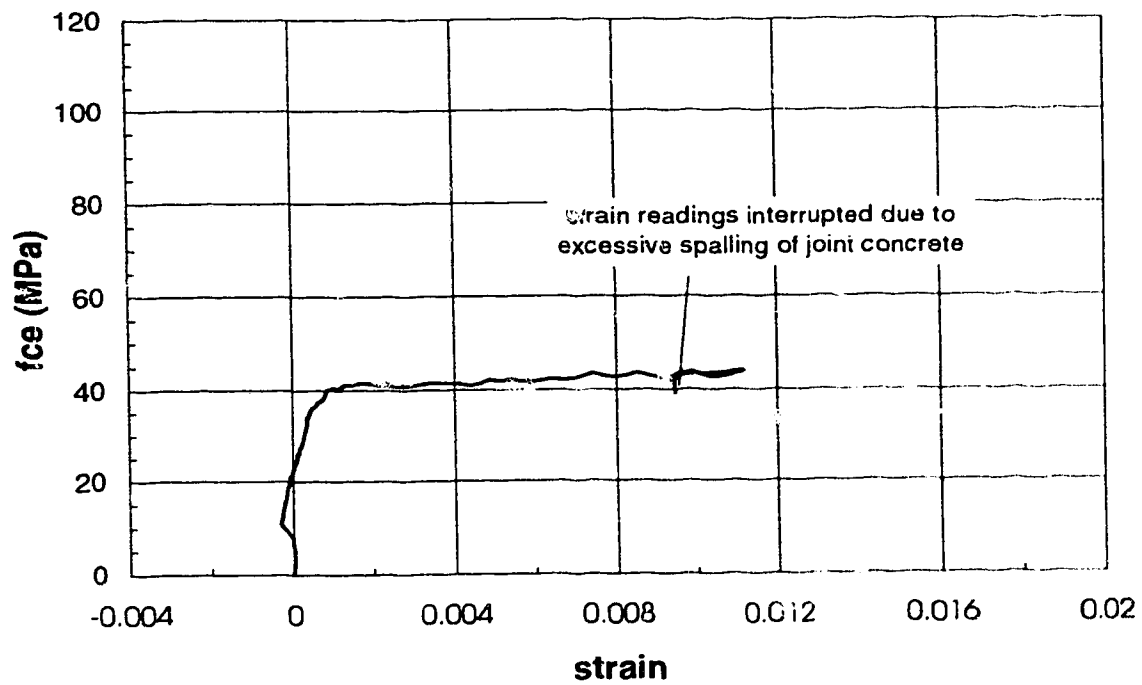


Figure B.78 Joint lateral expansion (Specimen C2-C)

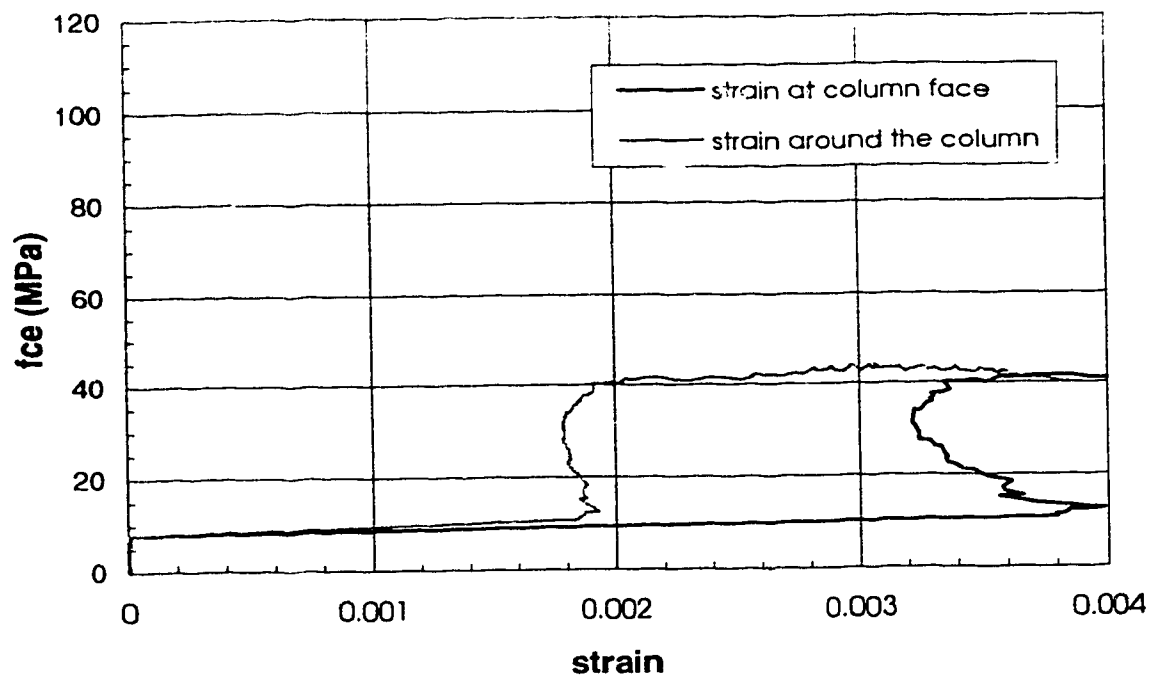


Figure B.79 Top slab transverse strain (Specimen C2-C)

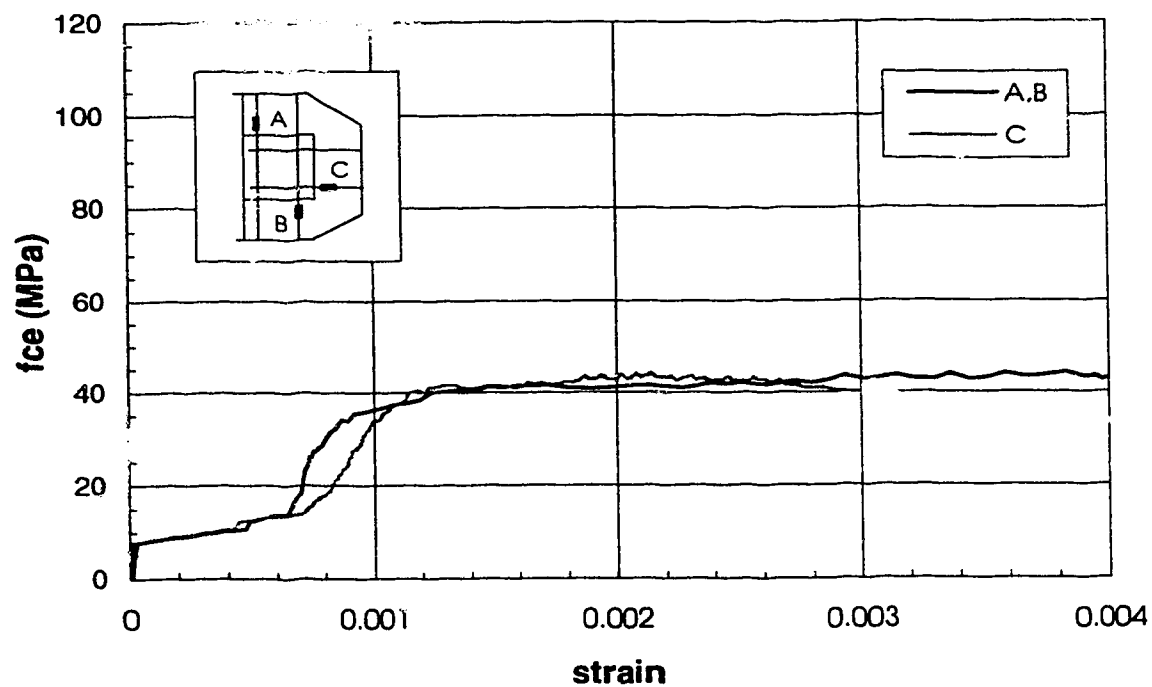


Figure B.80 Bottom slab transverse strain (Specimen C2-C)

Series D specimens

-Sandwich columns-

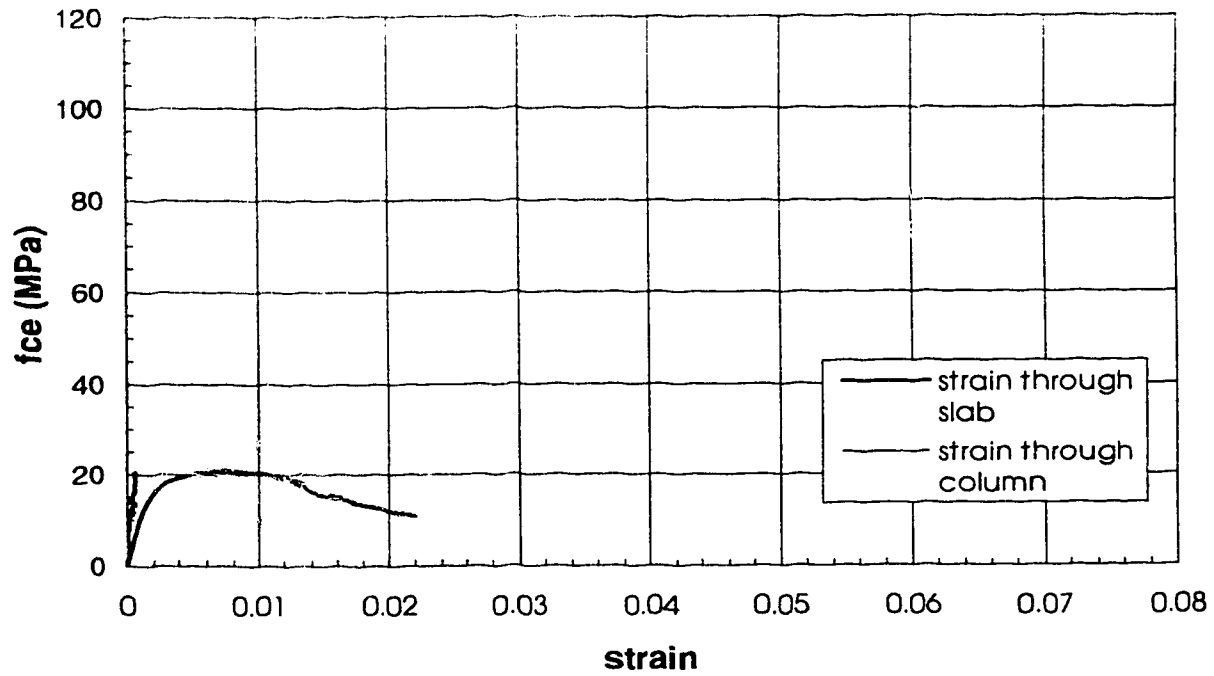


Figure B.81 Stress-strain behaviour (Specimen D-SC1)

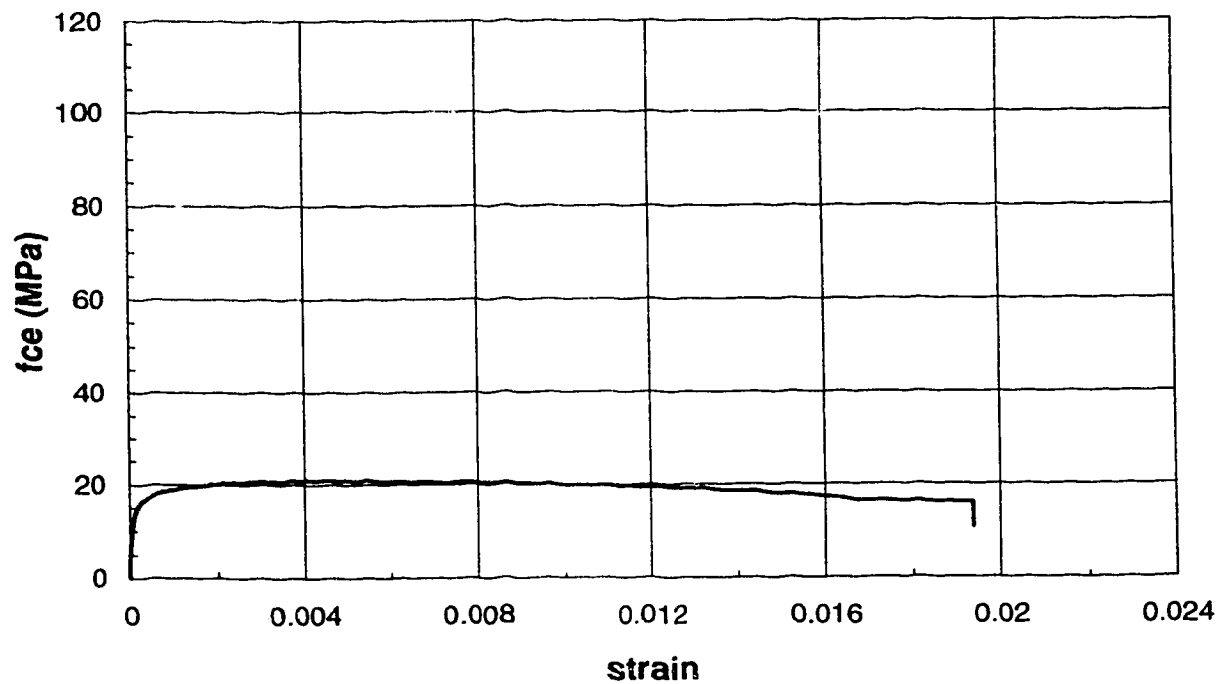


Figure B.82 Joint lateral expansion (Specimen D-SC1)

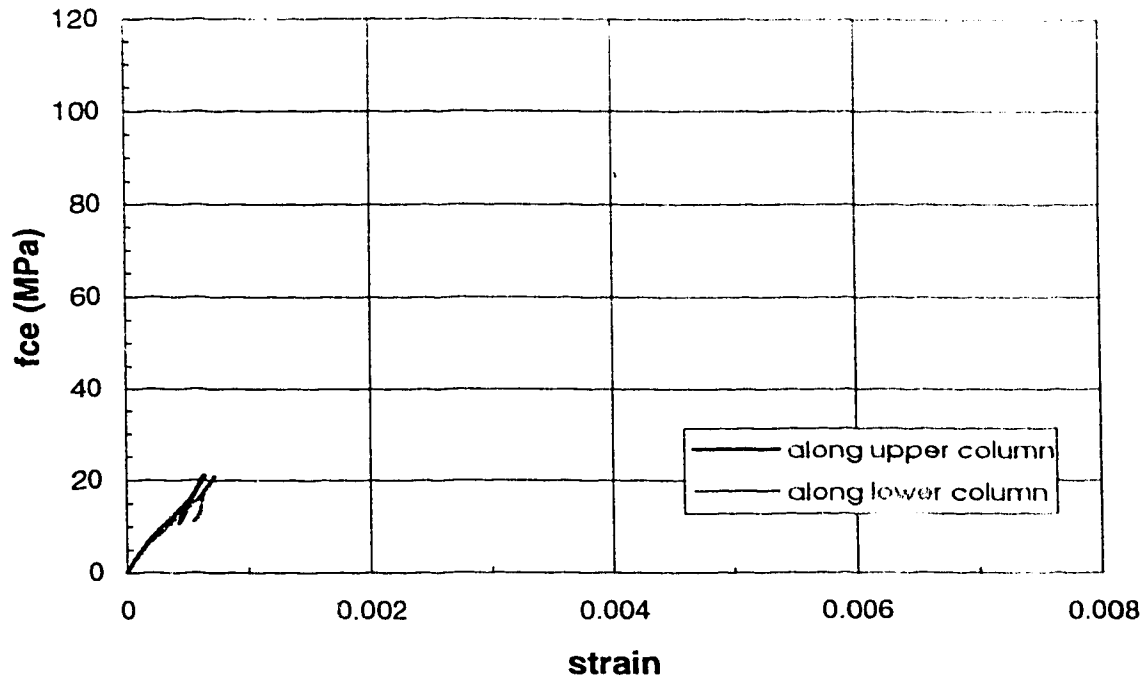


Figure B.83 Column longitudinal strain (Specimen D-SC1)

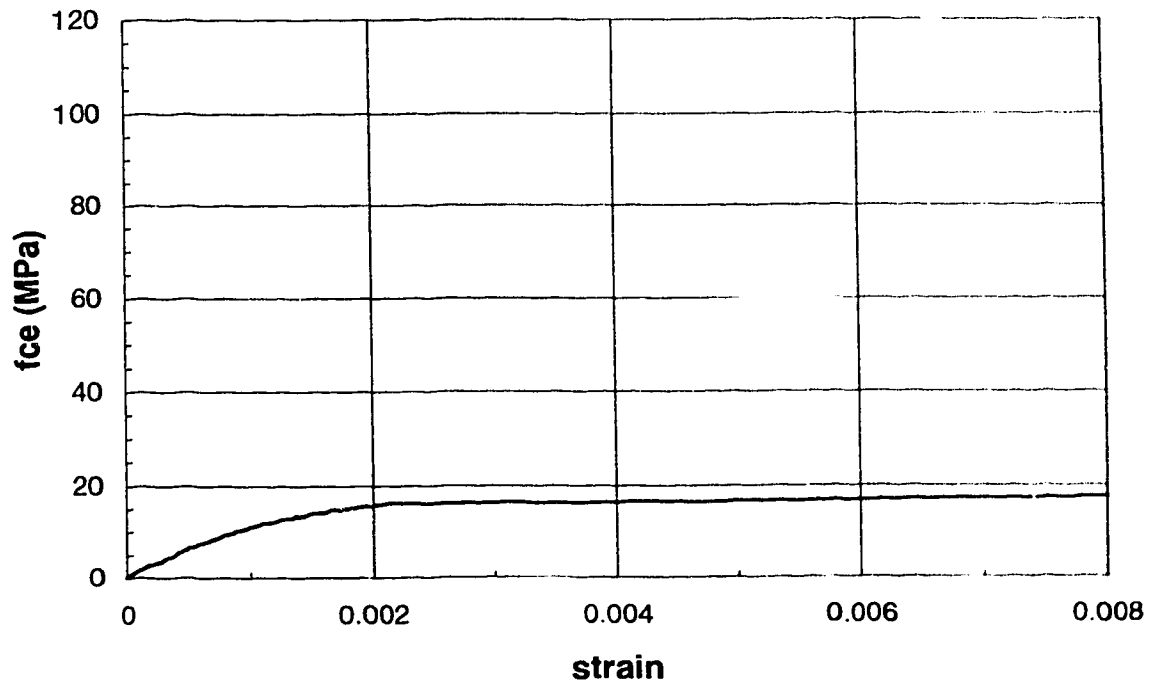


Figure B.84 Column strain through slab (Specimen D-SC1)

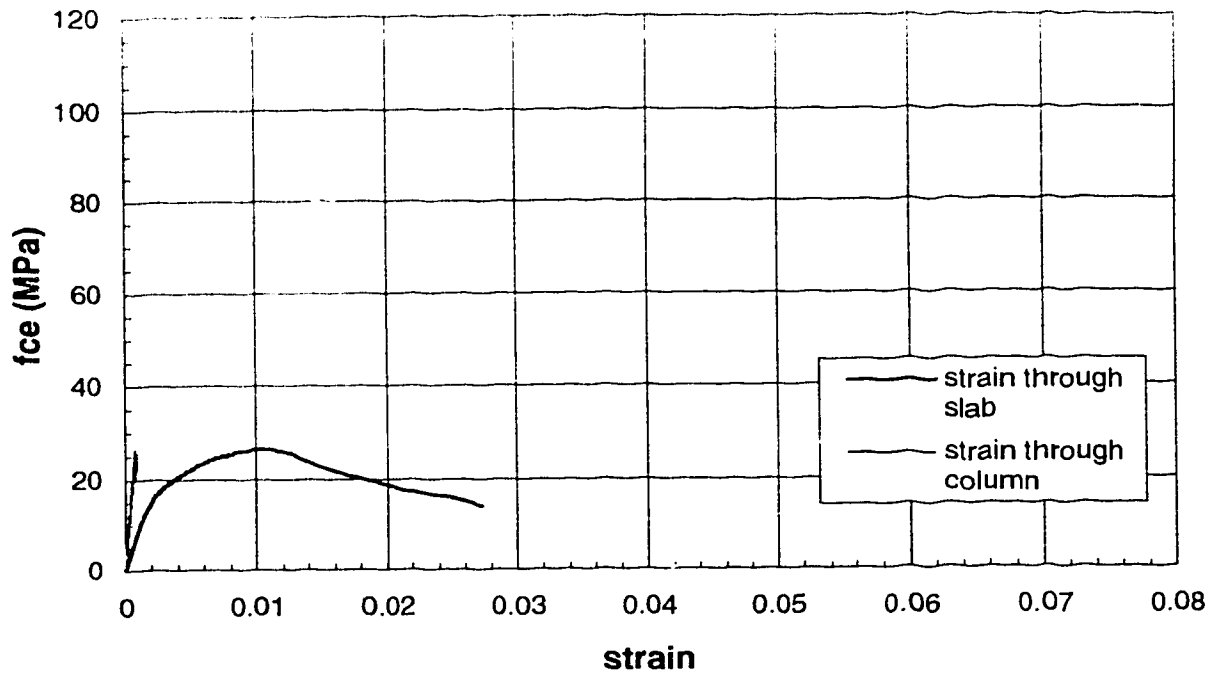


Figure B.85 Stress-strain behaviour (Specimen D-SC2)

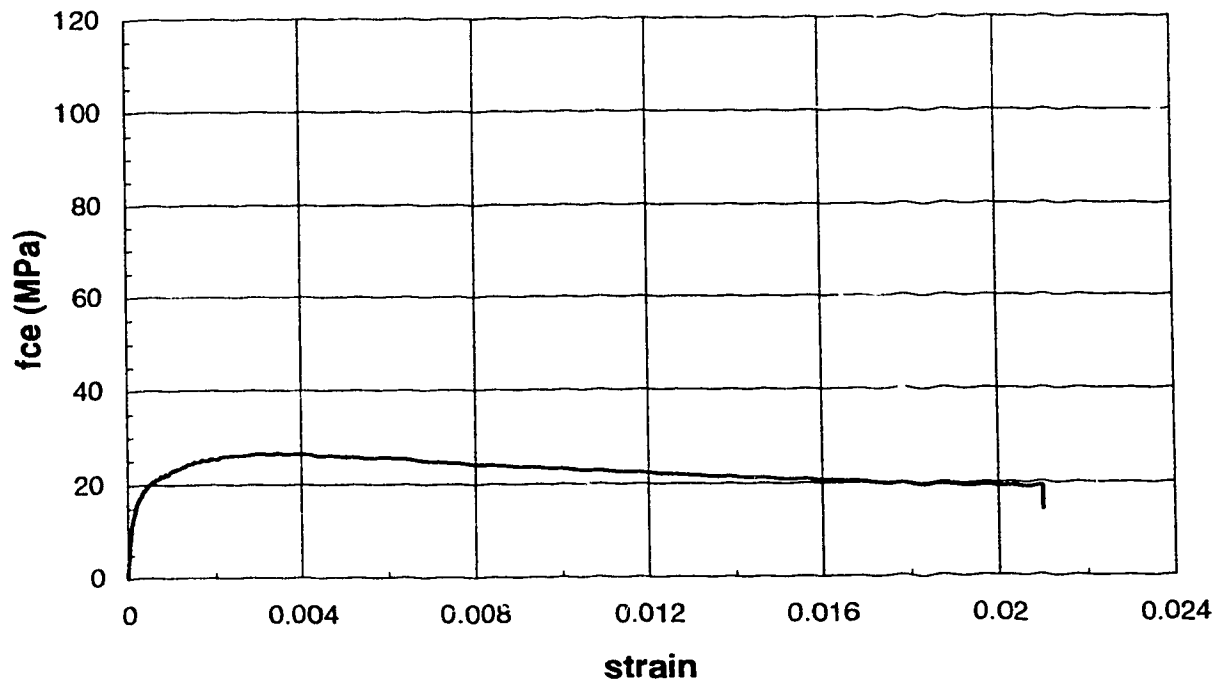


Figure B.86 Joint lateral expansion (Specimen D-SC2)

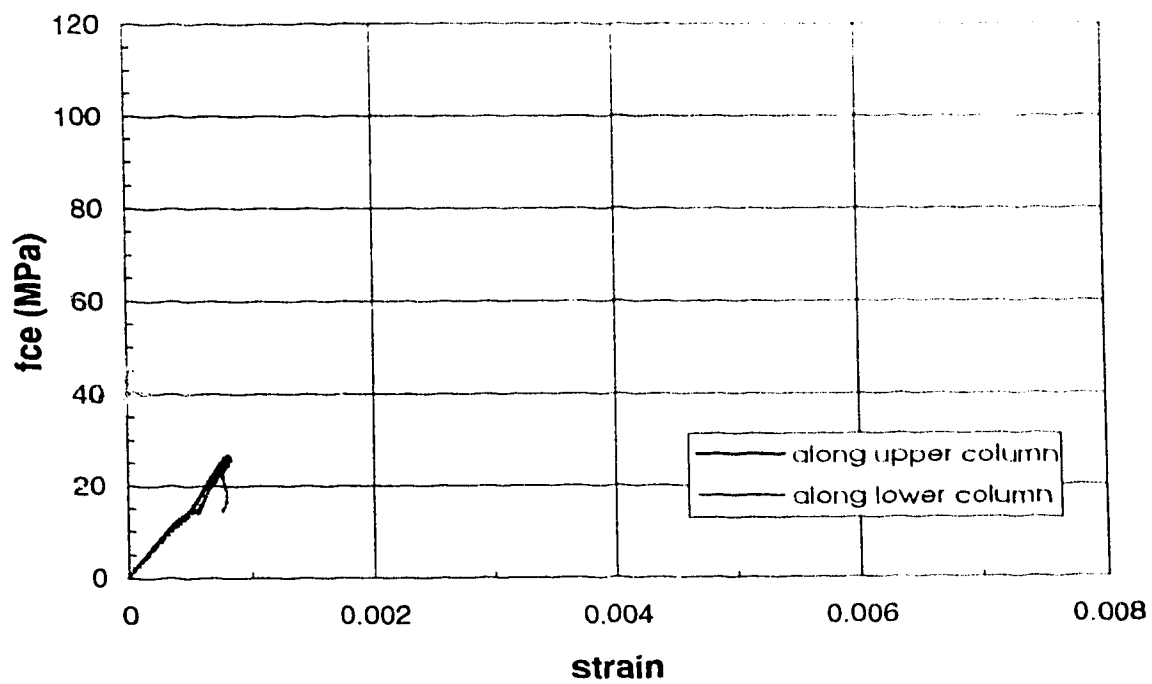


Figure B.87 Column longitudinal strain (Specimen D-SC2)

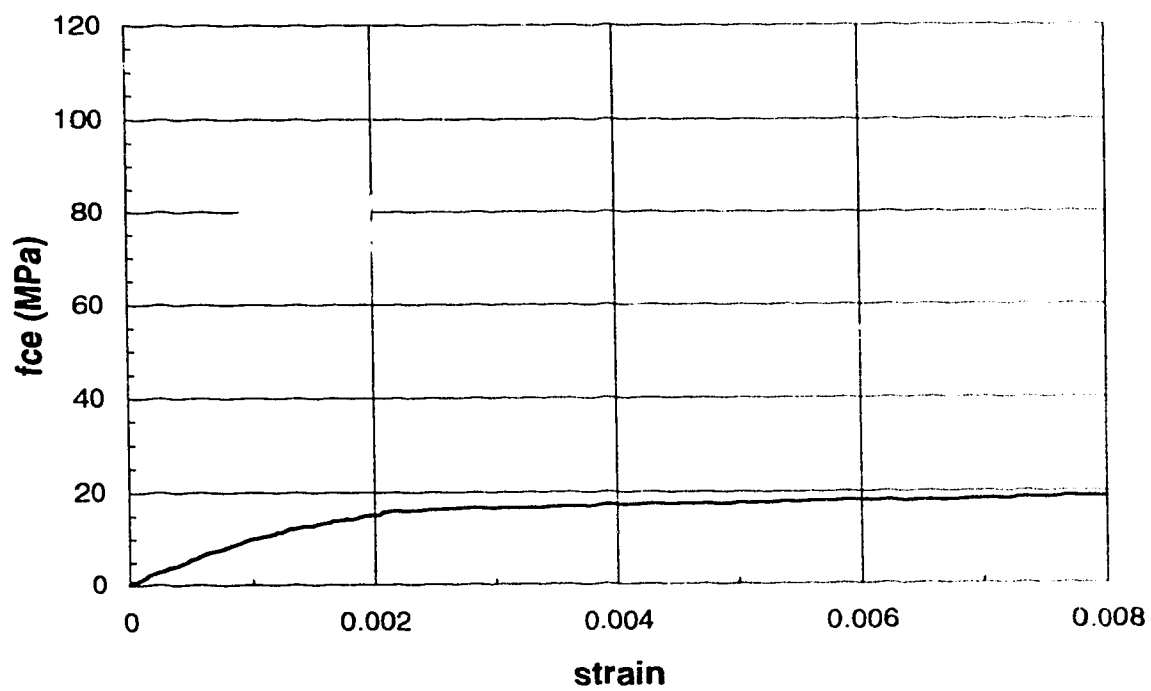


Figure B.88 Column strain through slab (Specimen D-SC2)

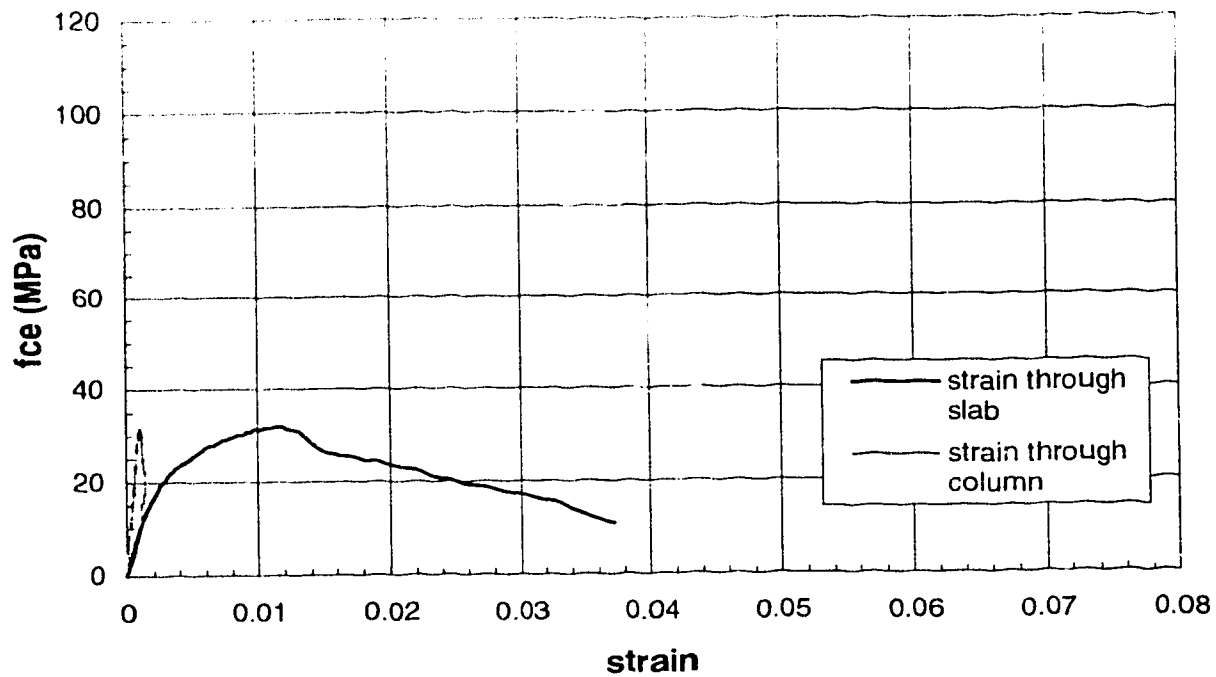


Figure B.89 Stress-strain behaviour (Specimen D-SC3)

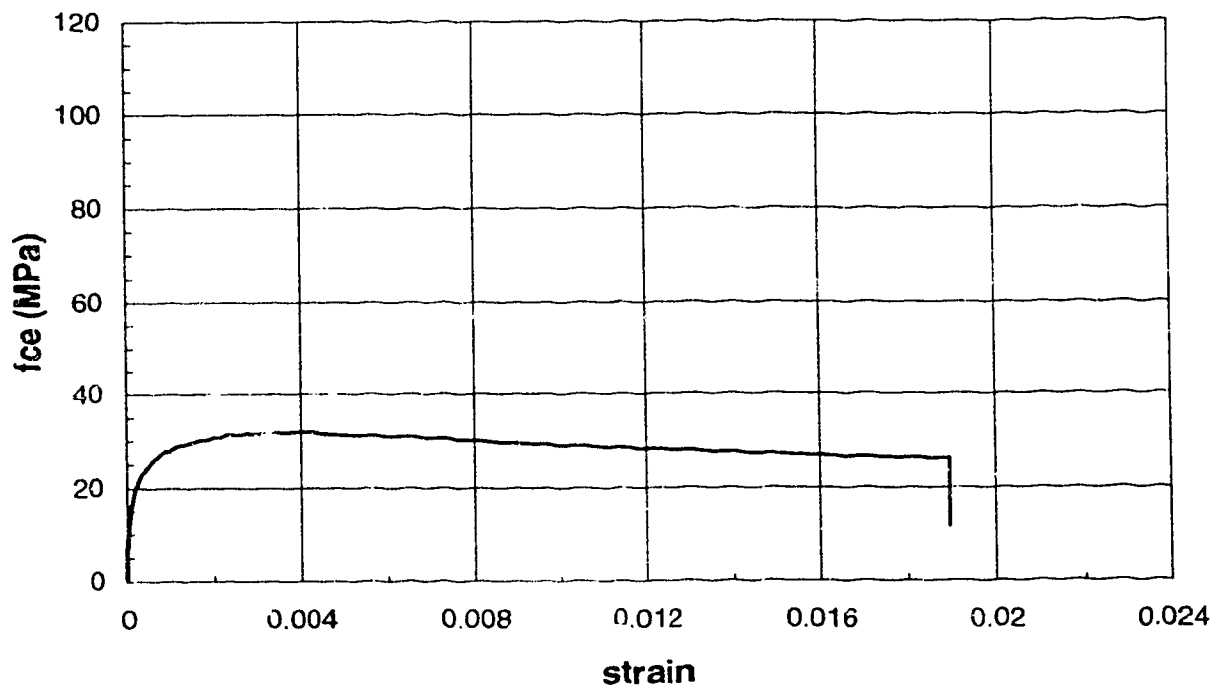


Figure B.90 Joint lateral expansion (Specimen D-SC3)

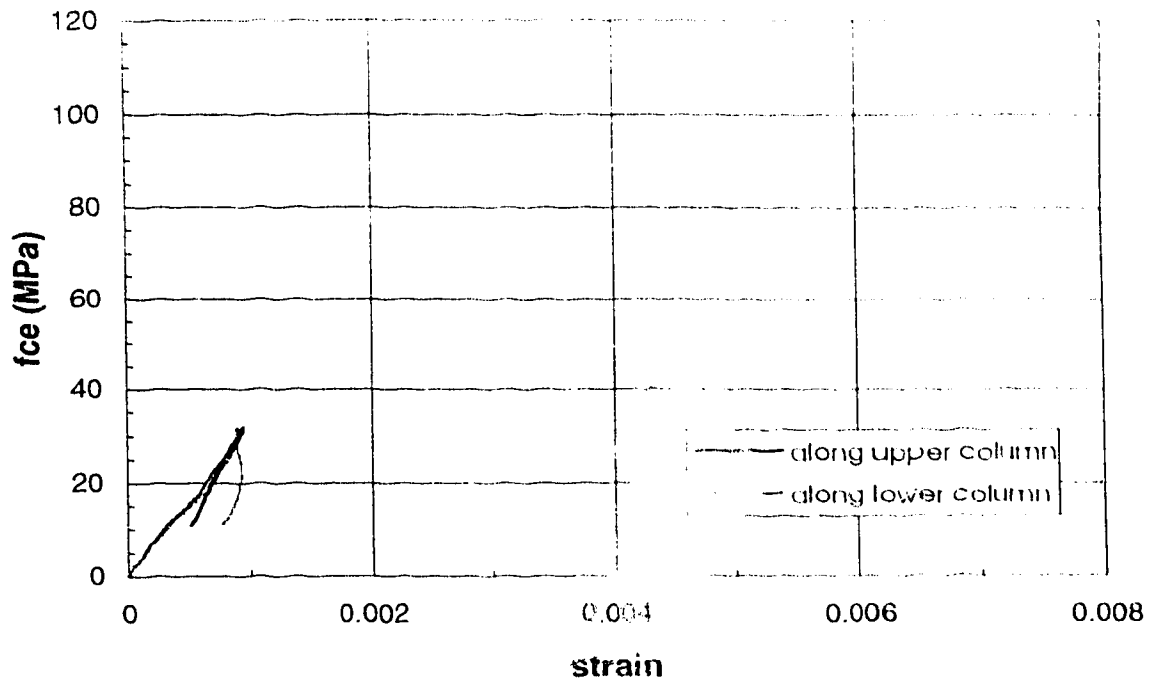


Figure B.91 Column longitudinal strain (Specimen D-SC3)

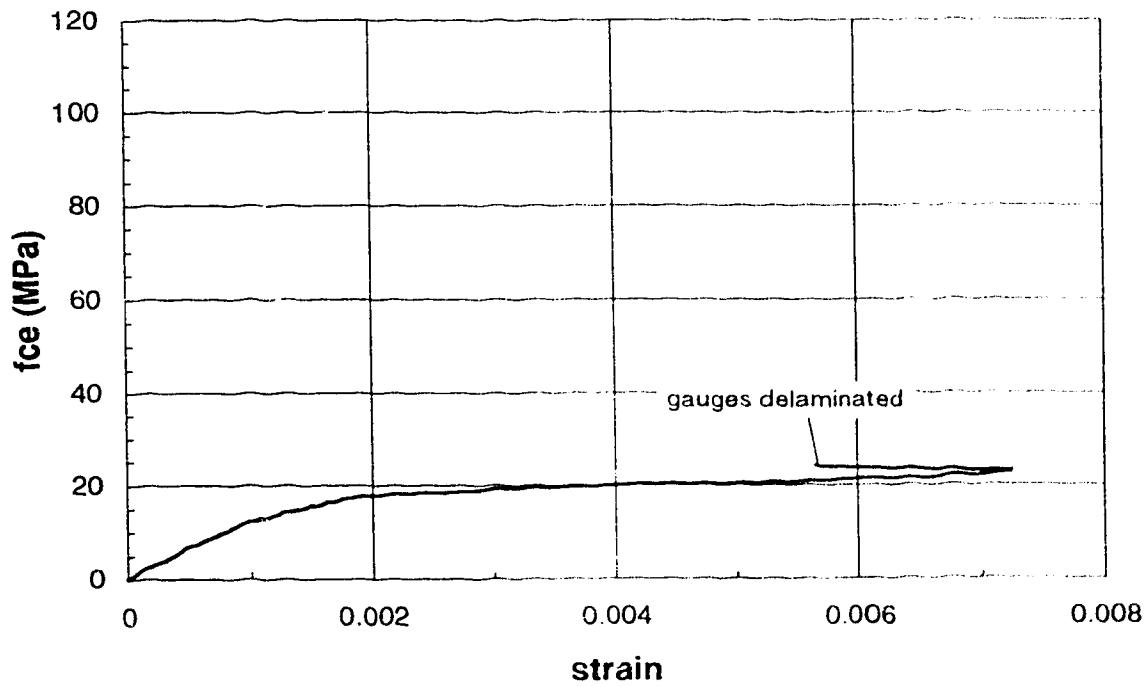


Figure B.92 Column strain through slab (Specimen D-SC3)

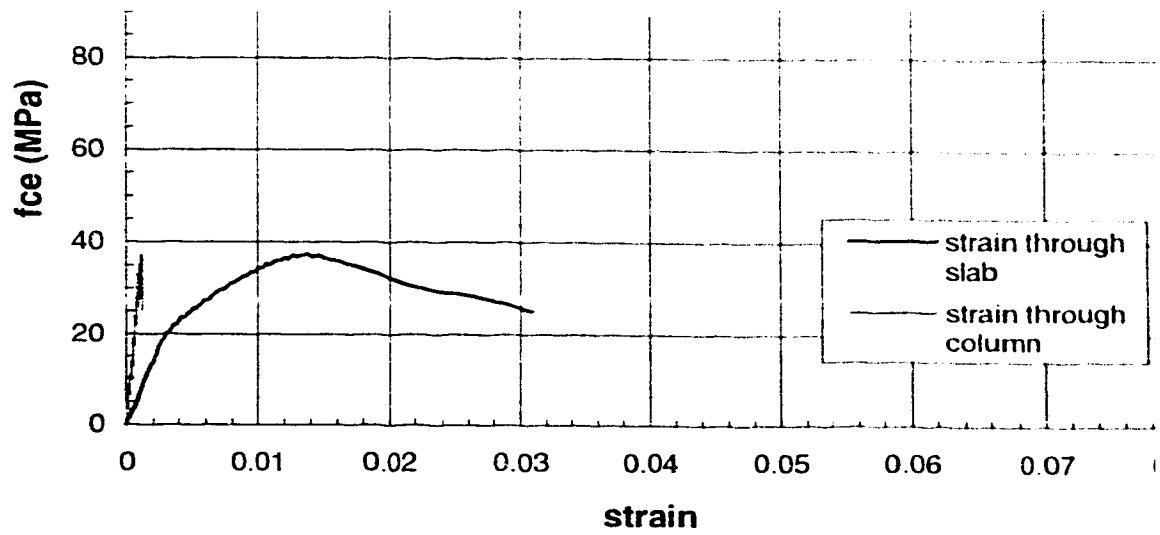


Figure B.93 Stress-strain behaviour (Specimen D-SC4)

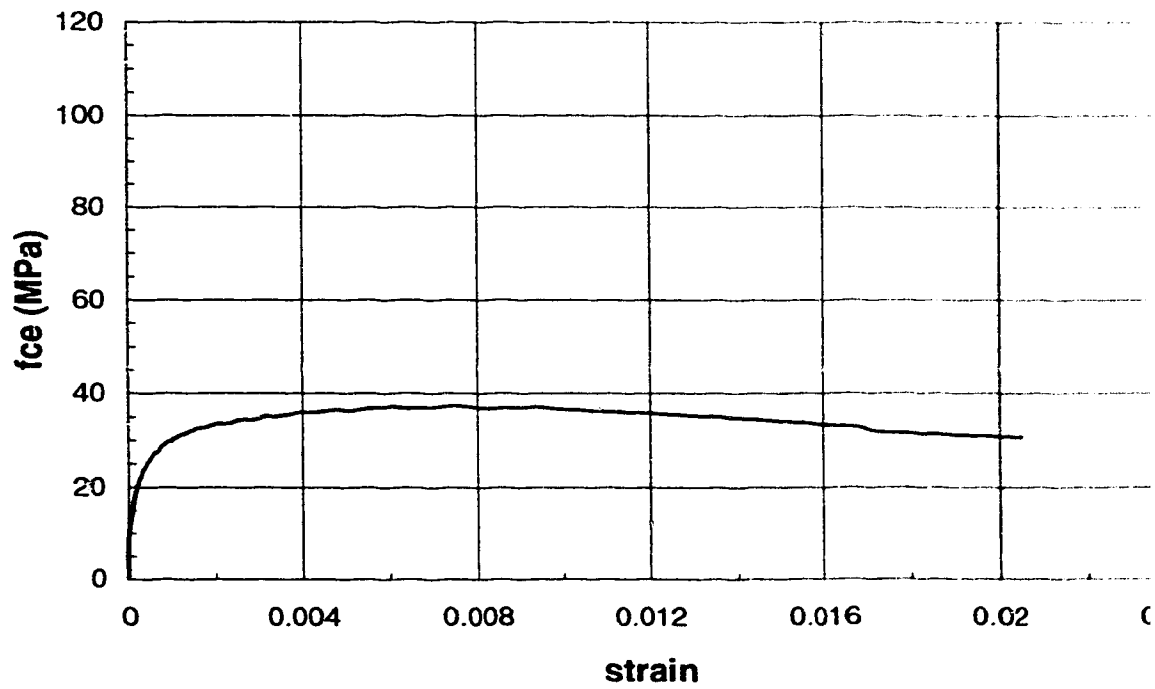


Figure B.94 Joint lateral expansion (Specimen D-SC4)

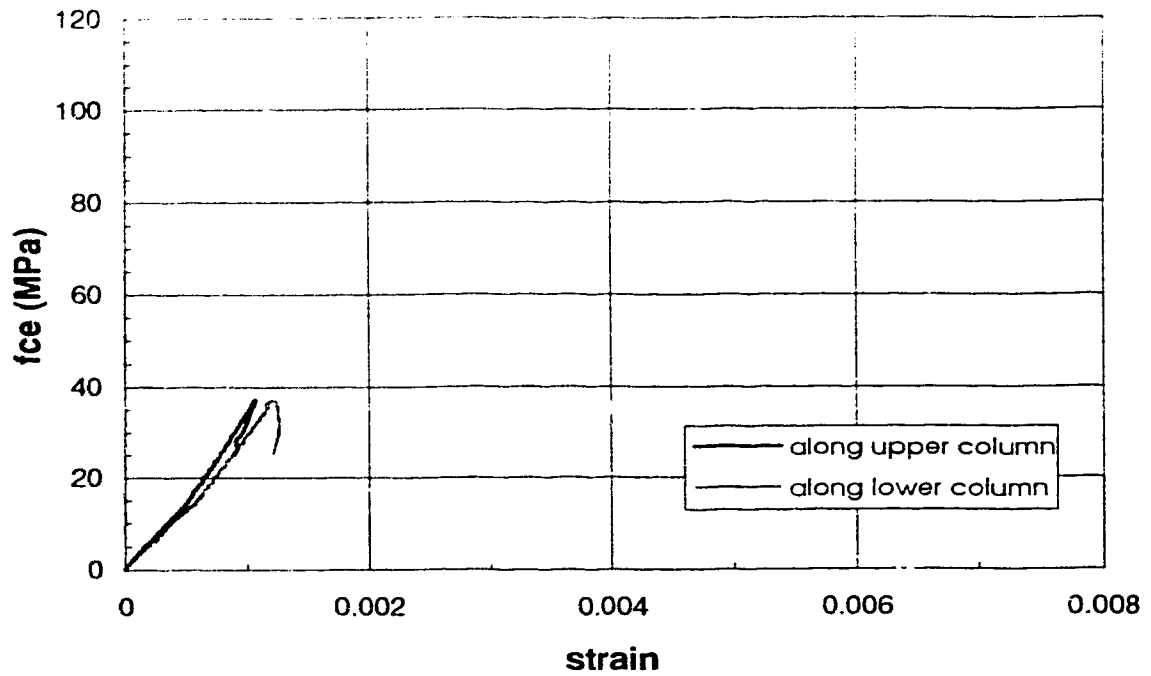


Figure B.95 Column longitudinal strain (Specimen D-SC4)

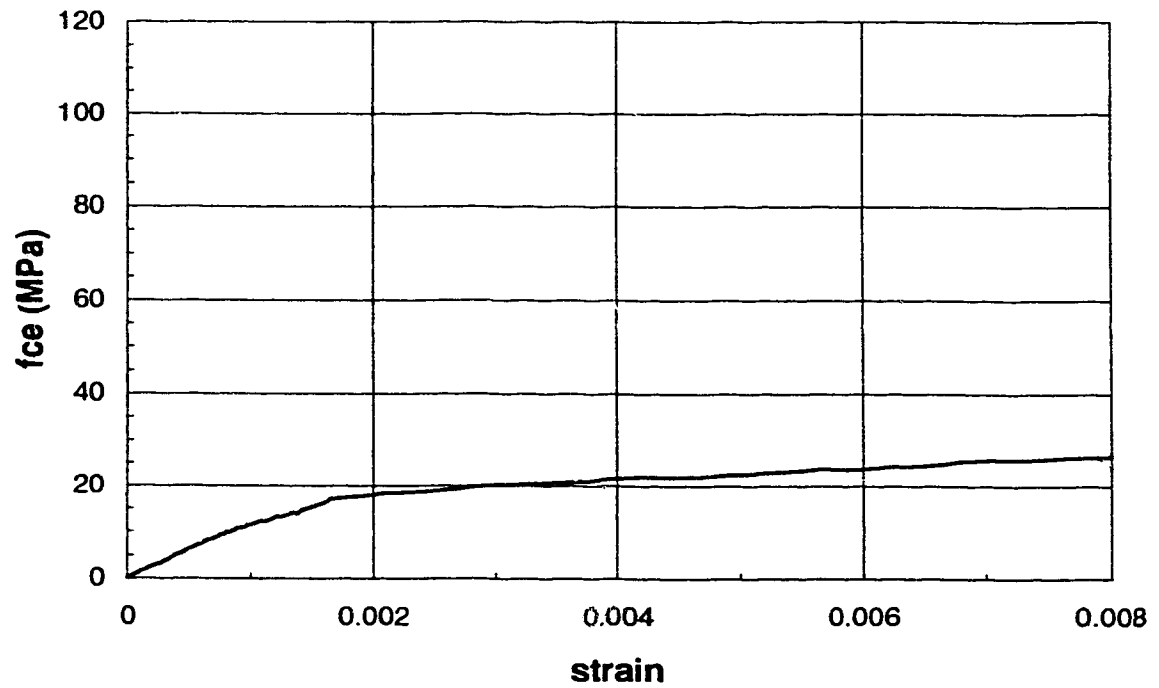


Figure B.96 Column strain through slab (Specimen D-SC4)